

**Biological function and clinical implication of
coagulation proteins during malignant transformation
of pancreatic cells**

Farzana Haque (MRCP)

PhD

The University of Hull and the University of York

Hull York Medical School

April 2023

Abstract

The premalignant pancreatic cellular genotype can remain stable for years before rapid malignant transformation, often associated with inflammation. Tissue factor (TF) is an inflammatory modulator regulated by factor VIIa (fVIIa) for its levels and activity. The presence of TF in PDAC and its role in cell proliferation, angiogenesis, and metastasis suggests that TF may be a marker of the inflammatory microenvironment driving precursor lesions of pancreatic cancer. This study examined the in vitro influence of TF on pancreatic epithelial cells and its clinical value in detecting malignant transformation within pancreatic cyst fluid (PCyF). PCyF from 27 patients with pancreatic cystic lesions was analysed in a blinded fashion. TF and fVIIa levels were measured (ELISA), and the fVIIa:TF ratios were calculated. A cut-off value for TF concentration was determined and compared to the conventional assessment parameters (radiological features, CEA and amylase). Patients were categorised into four groups based on cytopathology and two groups based on indication for resection ('resective'). Significant histological stage-dependent increases in TF levels were observed. Mean TF concentration was significantly higher ($p=0.006$) in the resective (high-grade dysplasia & malignant; 1.17 ng/ml, 95% CI 0.68, 1.67) vs non-resective group (benign & low-grade dysplasia; 0.27 ng/ml, 95% CI 0.1, 0.44), with a strong positive correlation ($r=0.746$, $p<0.001$, TF cut-off 0.75 ng/ml, AUC 0.877, $p=0.002$). The fVIIa:TF ratio did not add further value. Incubation of pancreatic cells with recombinant TF resulted in increased expression of a marker of epithelial to mesenchymal transition (Vimentin). This influence was moderated by supplementation with fVIIa in benign (hTERT-HPNE) but not overtly malignant pancreatic cells (AsPC-1). Cyst-associated TF levels appear to correlate with cytological progression to the malignant phenotype and may allow better discrimination (specificity 94%) of the 'resective' lesion, reduce healthcare costs and offer a more nuanced tool for monitoring indeterminate cystic lesions.

Contents

Abstract	2
Contents	3
List of figures.....	9
List of tables.....	14
Acknowledgements.....	16
Publication and conferences	17
1. General Introduction	18
1.1. Overview.....	19
1.2. Pancreatic cancer.....	19
1.2.1. Pathology of PC.....	20
1.2.2. Pancreatic ductal adenocarcinoma	22
1.3. Precursors of invasive ductal adenocarcinoma.....	27
1.3.1. Pathological features of precursor lesions.....	30
1.4. Evolution of pancreatic cancer	41
1.5. Inflammation and cancer- “the wound that never heals.”	44
1.5.1. The origins and triggers of inflammation in the process of cancer development 45	
1.5.2. Inflammation and Tumour Initiation	45
1.5.3. Inflammation and Tumour Promotion.....	47
1.5.4. Inflammation, Tumour Progression, and Metastasis	49
1.5.5. Inflammation and Cell Plasticity within the Tumour Microenvironment	50
1.6. Role of inflammation in the development of pancreatic cancer	51
1.6.1. Role of diabetes and obesity in the development of pancreatic cancer	51
1.6.2. Role of local inflammation in PDAC growth, development, and metastasis	51

1.6.3.	Role of cytokines in the inflammatory response to cancer cells.....	52
1.7.	Coagulation and cancer.....	55
1.7.1.	Coagulation proteins and pathways	57
1.7.2.	Role of coagulation proteins in cancer progression	57
1.7.3.	Tissue factor	57
1.7.4.	Factor VII	70
1.7.5.	FVIIa:TF ratio.....	71
1.8.	Pancreatic cystic lesion	72
1.8.1.	Diagnostic work-up for PCLs.....	73
1.8.2.	Characterisation of the cyst fluid.....	79
1.9.	Current NICE recommendation	90
1.10.	Aims	91
2.	General Methods	92
2.1.	Materials.....	93
2.2.	Equipment	95
2.3.	Cellular methods.....	96
2.3.1.	Cell lines used in this study	96
2.3.2.	Cell culture.....	100
2.3.3.	Maintenance and subculture of cancer cell lines.....	100
2.3.4.	Estimation of cell number using a haemocytometer	102
2.3.5.	Cryopreservation of cells.....	102
2.3.6.	Cell treatment.....	103
2.4.	Proteomic and immunological methods.....	103
2.4.1.	Estimation of protein concentration using Bradford Assay.....	103

2.4.2.	Quantification of TF antigen using Quantikine® enzyme-linked immunosorbent assay (ELISA) kit.....	105
2.4.3.	Quantification of fVII antigen using ELISA kit.....	109
2.4.4.	Separation of protein using sodium dodecyl sulphate-polyacrylamide gel electrophoresis (SDS-PAGE).....	113
2.4.5.	Western blot method.....	114
2.4.6.	Immunofluorescence microscopy	115
2.5.	Molecular methods.....	115
2.5.1.	Quantification of cDNA using RT-qPCR (reverse transcription-quantitative polymerase chain reaction)	115
2.5.2.	Preparation of purified RNA sample using Monarch® total RNA Miniprep Kit	115
2.5.3.	The 260:280 ratio was also calculated to determine the purity of the RNA. An RNA sample with a ratio of 1.8-2.1 was deemed sufficient purity for RT-qPCR reactions. All samples were stored at -80 °C and used within 20 days. RT-qPCR.....	117
2.6.	Statistical analysis	121
3.	Investigation of tissue factor as an early indicator of malignant transformation in pancreatic cystic lesions.....	122
3.1.	Introduction.....	123
3.2.	Aim	127
3.3.	Study Design	129
3.4.	Ethical Approval	129
3.5.	Materials and Methods.....	134
3.5.1.	Subject Selection.....	134
3.5.2.	Inclusion and Exclusion Criteria.....	134
3.5.3.	Subject recruitment	135

3.5.4.	Samples collection	139
3.5.5.	Data collection.....	139
3.5.6.	Enzyme-linked immunosorbent assay (ELISA)	141
3.5.7.	Statistical analysis methods	143
3.6.	Results	144
3.6.1.	Characteristics of the cyst cohort	144
3.6.2.	The physical appearance of the cyst fluid.....	144
3.6.3.	Pancreatic cyst patients stratification in risk groups.....	151
3.6.4.	Optimisation of the measurement of TF antigen with Quantikine® TF ELISA kit 151	
3.6.5.	Measurement of protein concentration in the cyst fluid	157
3.6.6.	Measurement of TF in the cyst fluid.....	161
3.6.7.	Analysis of TF concentration per unit of total protein (TP)	161
3.6.8.	Measurement of fVIIa in the cyst fluid	161
3.6.9.	Analysis of the ratio of fVII:TF in the cyst fluid.....	166
3.6.10.	Estimation of a cut-off value of TF as an indicator of malignancy.....	166
3.6.11.	Investigation of the diagnostic ability of fVIIa (ng/ml) concentration and fVIIa:TF	166
3.6.12.	Analysis of the association of high-risk cyst	171
3.6.13.	Measurement of TF in the serum samples.....	171
3.7.	Discussion	179
4.	Examination of the role of exogenous TF on EMT and pancreatic cancer progression	187
4.1.	Introduction	188
4.1.1.	Epithelial-mesenchymal transition	188
4.1.2.	EMT signalling pathways in PDAC.....	192

4.1.3.	Invasive behaviour precedes frank tumourigenesis in PDAC.....	192
4.1.4.	Inflammation promotes EMT in pre-malignant lesions.....	193
4.1.5.	Role of TF on EMT.....	193
4.1.6.	Ectopic synthesis of coagulation fVII influences cell migration and invasion .	194
4.2.	Aims.....	196
4.3.	Methods.....	197
4.3.1.	Optimisation of markers of EMT.....	197
4.3.2.	Optimisation of TGF β as a positive control to induce EMT.....	197
4.3.3.	Examination of TF in cell lysate and media.....	197
4.3.4.	Examination of the influence of TF and fVIIa on the expression of vimentin in cell lines	198
4.3.5.	Examination of the induction of vimentin expression on treatment with TF.	198
4.3.6.	Examination of the expression of fVII and HNF4 α in cells.....	198
4.3.7.	Examination of the influence of TF on the expression of HNF4 α in different cell lines	199
4.3.8.	Examination of the influence of different concentrations of TF on the mediators of cell proliferation and apoptosis.....	199
4.3.9.	Examination of the influence of TF on the expression of p16 protein.....	199
4.3.10.	Establish a spheroid model by co-culture of CAF and pancreatic cells.....	200
4.4.	Results.....	201
4.4.1.	Optimisation of detection of markers of EMT.....	201
4.4.2.	Utilisation of fluorescent microscopy for detection of E-cadherin and N-cadherin	201
4.4.3.	Determination of optimal concentration and duration of TGF β for induction of EMT	201
4.4.4.	Examination of TF concentration in cell lysate and media.....	207

4.4.5.	Examination of the influence of TF and fVIIa on the expression of vimentin in cell lines	207
4.4.6.	Examination of the influence of TF concentration on vimentin expression...	215
4.4.7.	Examination of the level of expression of fVII.....	215
4.4.8.	Examination of the level of expression of HNF4 α	225
4.4.9.	Examination of the influence of TF on the expression of HNF4 α in cell lines	225
4.4.10.	Examination of the influence of various concentrations of TF on cyclin D1225	
4.4.11.	Examination of the influence of various concentrations of TF on bax	231
4.4.12.	Examination of the influence of TF on the expression of p16 protein	231
4.4.13.	Establishing a spheroid model by the co-culture of CAF and the pancreatic cells	231
4.5.	Discussion	241
5.	General discussion.....	248
6.	References	256
	List of symbols and abbreviations.....	288
	Appendix 1.....	293
	Appendix 2.....	314

List of figures

Figure 1: Survival according to T category and the number of positive nodes for patients undergoing resection of exocrine pancreatic cancer	21
Figure 2: Computed tomography (CT) image and histologic appearance of PDAC.....	24
Figure 3: Radiological appearance of precursor lesions of pancreatic cancer.....	34
Figure 4: Histopathological features of the precursor lesions of pancreatic cancer.....	37
Figure 5: Histological stages in PDAC progression.....	38
Figure 6: Precursors of pancreatic cancer	42
Figure 7: Stepwise model versus punctuated model of PDAC progression.....	43
Figure 8: Mechanisms at play with inflammation that affect tumour growth	46
Figure 9: Pro-tumorigenic actions of inflammation in progression, metastasis, and growth	48
Figure 10: Types of inflammation in tumorigenesis and cancer	53
Figure 11: Coagulation pathways	59
Figure 12: The structure of TF	61
Figure 13: TF positive CTC propagate procoagulant activity.....	68
Figure 14: Types of pancreatic cystic lesions.....	74
Figure 15: Diagram of pancreatic cystic lesions	75
Figure 16: Algorithm for the management of suspected BD-IPMN	78
Figure 17: Scheme showing immortalisation and Ras transformation of human pancreatic duct cells.....	97
Figure 18: Diagram of histological progression of PC in parallel with mutations present in the cell lines	98
Figure 19: Diagram of sandwich ELISA technique used for TF ELISA.....	107
Figure 20: Diagram representing preparation of standards for TF ELISA	108

Figure 21: Diagram of sandwich ELISA technique used for fVII ELISA	111
Figure 22: Sample disruption and homogenisation.....	116
Figure 23: RNA binding and elution	118
Figure 24: Overview of the GoTaq® 1-Step RT-qPCR protocol.....	119
Figure 25: The interplay between cancer, coagulation and inflammation.....	125
Figure 26: Study design within the umbrella study ‘TEM-PAC’	130
Figure 27: Cyst study cohort.....	131
Figure 28: Cyst patient pathway.....	137
Figure 29: Pancreatic cancer patient pathway.....	138
Figure 30: Control patient pathway.....	140
Figure 31: Study design	145
Figure 32: Radiological appearance of PCLs.....	149
Figure 33: Appearance of the cyst fluids.....	152
Figure 34: Optimisation of TF ELISA in cyst fluid samples.....	154
Figure 35: Assessment of the presence of TF in patient samples	155
Figure 36: Standard curve for determining TF concentration using TF-ELISA	156
Figure 37: Bland-Altman plots assessing agreement in TF concentration measurements performed with and without Triton-X	158
Figure 38: Standard curve for determining protein concentrations using the Bradford assay	159
Figure 39: Assessment of protein concentration in the cyst fluid samples	160
Figure 40: Standard curve for determining TF concentration in the cyst cohort using TF-ELISA	162
Figure 41: Assessment of TF concentration in the cyst fluid samples.....	163
Figure 42: Analysis of cyst fluid TF/total protein ratio.....	164
Figure 43: Standard curve for determining fVIIa concentration using fVIIa-ELISA	165

Figure 44: Assessment of fVIIa concentration in the cyst fluid samples	167
Figure 45: Analysis of fVII:TF ratio	168
Figure 46: ROC curve of TF (ng/ml).....	169
Figure 47: ROC for fVIIa (ng/ml) and fVIIa:TF	172
Figure 48: Assessment of TF concentration in the cyst patients' serum samples	176
Figure 49: Assessment of serum TF concentration in the three cohorts of patients	178
Figure 50: Spectrum of EMT phenotypes in cancer.....	190
Figure 51: Detection of vimentin expression in cell line and conditioned media.....	202
Figure 52: Detection of cadherin 11 and Fibronectin expression in cell lines	203
Figure 53: Detection of cell surface N-cadherin by fluorescence microscopy	204
Figure 54: Determination of the duration of incubation with TGF β as a positive control in hTERT-HPNE cells	205
Figure 55: Determination of the duration of incubation with TGF β as a positive control in AsPC-1 cells.....	206
Figure 56: Determination of the optimal TGF β concentration as a positive control in hTERT-HPNE cells	208
Figure 57: Determination of the optimal TGF β concentration as a positive control in AsPC-1 cells.....	209
Figure 58: Standard curve for the determination of TF antigen concentration	210
Figure 59: Measurement of TF antigen in cells and corresponding media.....	211
Figure 60: Examination of expression of vimentin in hTERT-HPNE cells	212
Figure 61: Examination of expression of vimentin in hTERT-HPNE E6/E7/K-RasG12D cells	213
Figure 62: Examination of expression of vimentin in hTERT-HPNE E6/E7/K-RasG12D/st cells	214
Figure 63: Examination of expression of vimentin in AsPC-1.....	216
Figure 64: Examination of expression of vimentin mRNA in cell lines	217

Figure 65: Expression of vimentin following the incubation of hTERT-HPNE cells with TF ..	218
Figure 66: Expression of vimentin following the incubation of AsPC-1 cells with TF	219
Figure 67: Expression of vimentin mRNA following the incubation of hTERT-HPNE cells with TF.....	220
Figure 68: Expression of vimentin mRNA following the incubation of in AsPC-1 cells with TF	221
Figure 69: Examination of the presence of fVII and HNF4 α in hTERT-HPNE cells.....	222
Figure 70: Examination of the presence of fVII and HNF4 α in AsPC-1 cells.....	223
Figure 71: Assessment of fVII levels in hTERT-HPNE and AsPC-1 cells	224
Figure 72: Examination of the expression of fVII mRNA in hTERT-HPNE and AsPC-1 cells ..	226
Figure 73: Assessment HNF4 α levels in hTERT-HPNE and AsPC-1 cells.....	227
Figure 74: Examination of the influence of TF on HNF4 α expression in hTERT-HPNE cells .	228
Figure 75: Examination of the influence of TF on HNF4 α expression in AsPC-1 cells	229
Figure 76: Examination of the influence of TF on HNF4 α mRNA expression in hTERT-HPNE cells.....	230
Figure 77: Examination of the influence of different concentrations of TF on cyclin D1	232
Figure 78: Examination of the influence of different concentrations of TF on bax	233
Figure 79: Examination of the presence of p16 protein in hTERT-HPNE and AsPC-1 cells...	234
Figure 80: Examination of the influence of TF on the expression of p16 protein in hTERT-HPNE cells	235
Figure 81: Examination of the influence of TF on the expression of p16 protein in AsPC-1 cells.....	236
Figure 82: hTERT-HPNE and CAF cells for spheroid formation	237
Figure 83: hTERT-HPNE E6/E7/K-RasG12D and CAF cells for spheroid formation.....	239
Figure 84: hTERT-HPNE E6/E7/K-RasG12D/st and CAF cells for spheroid formation	240

Figure 85: Summary of advantages and limitation of currently available pre-clinical models
of PDAC..... 245

List of tables

Table 1: Overview of exocrine pancreatic neoplasm.....	23
Table 2: Exocrine PC TNM staging AJCC UICC 8th edition.....	25
Table 3: National cancer institute working group criteria for precursors to invasive cancer	29
Table 4: Common precursor lesions in the pancreas	31
Table 5: Radiology description	32
Table 6: Molecular features of precursor lesions of pancreatic cancer	33
Table 7: Proposed Revised Terminology of PanIN, IPMN and MCN.....	40
Table 8: Pro-inflammatory cytokines in pancreatic cancer.....	54
Table 9: Coagulation factors.....	58
Table 10: Overexpression of TF and progression of human malignancies	63
Table 11: Characteristics of the major types of cystic lesions of the pancreas	76
Table 12: Indication for EUS in PCLs	80
Table 13: Imaging features for diagnostic work-up.....	81
Table 14: Indications of surgical resection.....	82
Table 15: Cytologic features of low- and high-grade atypia in mucinous cyst.....	83
Table 16: Overview of reviewed studies regarding the use of cyst fluid for risk stratification of branch.....	86
Table 17: Cell line culturing conditions	99
Table 18: Genetic alteration present in the cell lines	101
Table 19: Preparation of standards	104
Table 20: Quantikine® ELISA kit Materials	106
Table 21: AssayPro Human Factor VII ELISA kit	110
Table 22: Preparing human fVII standard	112

Table 23: Standard thermocycling conditions for RT-qPCR	120
Table 24: Clinical characteristics of the cyst cohort (No=27)	146
Table 25: Radiographic characteristics of cyst cohort (No=27).....	147
Table 26: Pathological characteristics of cyst cohort (No=27)	148
Table 27: Physical appearance of the cyst fluid	150
Table 28: Clinical, biologic, radiographic, and pathologic characteristics with univariate analysis, stratified by non-resective and resective groups	153
Table 29: Coordinates of the ROC curve for TF	170
Table 30: Association of the high-risk cyst with current parameters	173
Table 31: Association of TF with resective cysts and current parameters	174
Table 32: Univariate analysis of factors associated with resective cysts.....	175
Table 33: Diagnostic performance of current cyst fluid markers used to identify a malignant cyst	183
Table 34: Diagnostic performance of predictors of malignancy in BD-IPMNs.....	184
Table 35: Markers of EMT in cancer	191

Acknowledgements

I would like to express my deepest gratitude to my clinical supervisor Prof Anthony Maraveyas, for recognising my ability and providing numerous opportunities throughout my PhD journey. I would also like to thank my lab supervisor Dr Camille Ettelaie, for her unwavering support and guidance, especially when I struggled to find direction.

I am also deeply grateful to my second lab supervisor Dr Leonid Nikitenko, whose valuable guidance has been instrumental in my success. I would like to extend my appreciation to Dr Sophie Featherby, who provided me with invaluable hands-on training and was there for me during some of my most challenging moments.

I extend my heartfelt thanks to all my colleagues Adenike Adekeye, Laura Broughton, Shirin Hasan, Mo Mohammad, Yahya Madkhali, Dimitrios Manolis, Eamon Faulkner and Mathew Morfitt, investigators of the TEM-PAC study, and especially the TEM-PAC nurses. Your contributions were vital to the success of my research, and I appreciate your unwavering support.

Lastly, I must express my gratitude to my family and friends, who have been my pillars of support throughout my academic journey. Your encouragement and support have been critical in helping me achieve my goals. Thank you for always believing in me.

Publication and conferences

Oral presentations

Haque F, Featherby S, Broughton L, Lykoudis P, Wedgwood K, Dasgupta D, Khulusi S, Buchanan A, Razack A, Huang C, Nikitenko L, Ettelaie C, Maraveyas A (2022) Tissue Factor (TF) as Potential Indicators of Malignancy in Pancreatic Cystic Lesions. HYMS post-graduate research conference, University of Hull, UK, July 14

Poster presentations

Haque F, Featherby S, Broughton L, Lykoudis P, Wedgwood K, Dasgupta D, Khulusi S, Buchanan A, Razack A, Huang C, Nikitenko L, Ettelaie C, Maraveyas A (2023) Tissue Factor (TF) and Factor VII/TF Ratio (fVIIa:TF) as Potential Indicators of Malignancy in Pancreatic Cystic Lesions. American Society of Clinical Oncology (ASCO) Gastrointestinal Cancer Symposium, San Francisco, USA 2023, January 20

Haque F, Featherby S, Broughton L, Lykoudis P, Wedgwood K, Dasgupta D, Khulusi S, Buchanan A, Razack A, Huang C, Nikitenko L, Ettelaie C, Maraveyas A (2023) Tissue Factor (TF) and factor VII modulate the cell phenotype and are potential indicators of malignancy in pancreatic cystic lesions. British Society for Haemostasis and Thrombosis (BSHT) Annual Scientific Meeting 2023, Birmingham, UK, January 26

Adekeye A, Haque F, Ettelaie C, Nikitenko L, Maraveyas A (2023) Establishing de novo platform for whole genome sequencing of pancreatic cyst fluid for early detection and diagnosis of pancreatic cancer. American association of cancer research (AACR) 2023, Orlando, USA April 14-19

Chapter 1

General Introduction

1.1. Overview

Pancreatic ductal adenocarcinoma (PDAC) is one of the deadliest epithelial malignancies, contributing to the overall increase in cancer deaths due to increased incidence and poor prognosis. Survival heavily depends on the disease stage (1, 2), warranting early detection. Hypothetically, there is an opportunity for screening within the window of malignant transformation of precursor lesions to pancreatic malignancy. It is recognised that the evolution of this malignant transformation results from genomic instability caused by somatic mutations, chromosomal rearrangements and epigenetic changes that dissociate the affected cells from regulatory cycles. Likewise, the strong connection between inflammation and pancreatic cancer (PC) development through tumour initiation, progression and metastases is also long-established (3). Both tumour-extrinsic and tumour-intrinsic inflammation can contribute to malignant transformation. Tissue factor (TF), which initiates the extrinsic blood coagulation cascade, is highly expressed in many cancer types, including PC (4-6). High TF expression is associated with an increased risk of venous thromboembolism (VTE) (7), where inflammation can both be a cause or a consequence of VTE (8-12). Inflammatory cytokines strongly induce the expression of TF, and simultaneously TF promotes pleiotropic inflammatory responses via protease-activated receptors (PARs) in concert with other coagulation factors. In addition, the TF-fVIIa complex plays an important role in intracellular non-haemostatic signalling pathways utilised by tumours to increase cell proliferation, angiogenesis, metastasis, and cancer stem-like cell maintenance (13, 14). This suggests that TF could serve as a diagnostic marker of the inflammatory microenvironment driving precursor lesions of pancreatic cancer. By examining the level of TF in fluid samples from precursor pancreatic cystic lesions (PCLs), this study aimed to investigate the potential of TF as an indicator of malignant transformation and compare it with current conventional assays. Furthermore, the study addressed the influence of TF in the modulation of cellular phenotype and the underlying mechanisms.

1.2. Pancreatic cancer

Cancer of the exocrine pancreas is a relatively rare, highly lethal malignancy; one person dies from the disease every hour in the UK (15). It is the 10th most common cancer in the UK, accounting for 3% of all new cancer cases. The crude incidence rate in the UK for 2016-2018

is 15.8 per 100,000 population (16). 79% of PC patients are diagnosed at stages III and IV, while 21% comprise early stages (stages I and II). The survival rate is relatively low and remains constant over time compared with other cancer types. Just 5% of males and females are predicted to survive for ten years or more. 5-year survival is 6.5% for men and 7.3% for women, which is the lowest of all common cancers and, unfortunately, has not shown much improvement since the early 1970s (17).

Most patients present late, which can be attributed to disease-specific signs and symptoms that are rarely apparent until the advanced stage. Potential curative surgery is possible for only 15-20% of patients. Most patients eventually relapse, even after potentially radical treatment. 30% of individuals who undergo complete (R0) resection of PC with limited nodal involvement are most likely to be long-term survivors (18) (Figure 1). An early diagnosis is essential for surgery for a favourable prognosis and improved chance of 5-year survival.

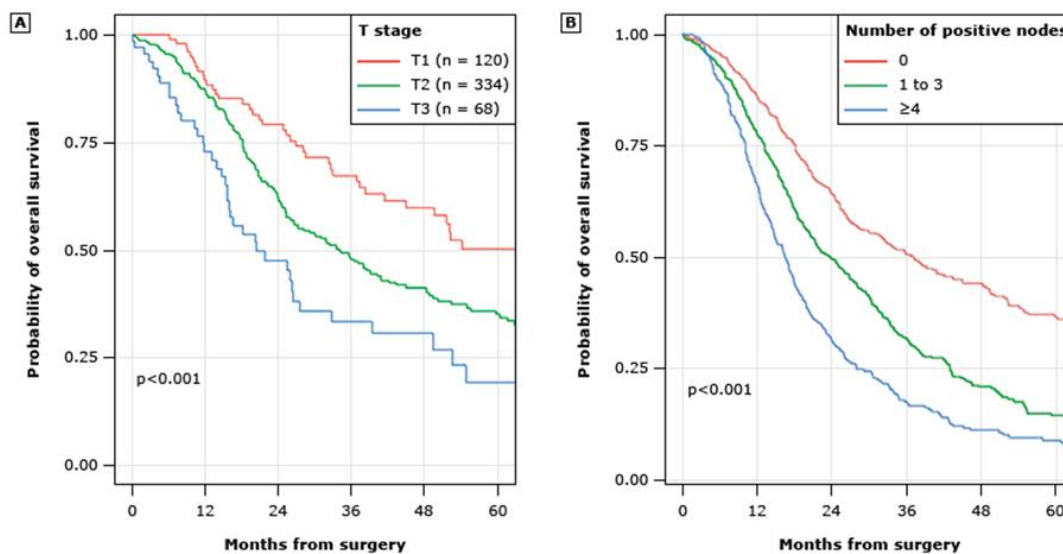
Epidemiological studies have found several environmental factors, including tobacco smoking (19), alcohol (20) and high body mass index (30 kg/m²) (21), to be high-risk factors in the development of PC (22). Abnormal metabolism of human micro-organisms (23), glucose (24) and lipid levels are also crucial in the development of pancreatic cancer. In addition to PC predisposition syndromes (e.g., Peutz-Jeghers syndrome, hereditary pancreatitis, familial atypical multiple mole melanoma, familial pancreatic cancer, Lynch syndrome, familial breast cancer and other Fanconi anaemia genes, familial adenomatous polyposis) (25), the ABO blood group (non-O blood group) (26) and cystic fibrosis (27) are among the hereditary risk factors. Patients with non-hereditary pancreatitis (28, 29) and pancreatic cysts (30) are also at risk of developing pancreatic cancer.

1.2.1. Pathology of PC

The normal pancreas contains exocrine and endocrine epithelial cells. Exocrine cells line the organised ductal network and converge into the main pancreatic duct, draining into the duodenum. The endocrine component comprises Islets of Langerhans and accounts for only 5% of the pancreas (31). Ductal Adenocarcinoma represents 85-90% of all pancreatic neoplasm and is commonly referred to as “pancreatic cancer” or “carcinoma of the pancreas.”

Exocrine pancreatic tumour classification by the World Health Organisation (WHO) and Armed Forces Institute of Pathology (AFIP) is based on the morphologic and histologic

Figure 1: Survival according to T category and the number of positive nodes for patients undergoing resection of exocrine pancreatic cancer



Survival stratified according to the revised AJCC 8th edition TNM staging criteria; T: tumour; AJCC: American Joint Committee on Cancer; TNM: tumour, node, metastasis; R0: no residual tumour. a- Overall survival by T stage of 525 patients who underwent resection for node-negative pancreatic cancer, stratified by proposed AJCC 8th edition criteria (training set only). b- Overall survival by the number of positive nodes for all patients who underwent an R0 resection (training set, n = 1551), stratified by proposed AJCC 8th edition criteria. Taken from (32)

features (33, 34). The classification broadly includes Benign (such as Cystadenoma), Premalignant lesions (low-grade dysplasia; LGD or high-grade dysplasia; HGD) and Malignant lesions (Table 1).

Malignant tumours of the pancreas include Ductal adenocarcinoma (85-90%), Intraductal Papillary Mucinous Neoplasm (IPMN) with associated invasive carcinoma (2-3%), Mucinous Cystic Neoplasm (MCN) with associated invasive carcinoma (1%). Other less common variants are solid pseudopapillary neoplasm, acinar cell carcinoma, pancreatoblastoma and serous cystadenocarcinoma (Table 1).

1.2.2. Pancreatic ductal adenocarcinoma

PDAC are sclerotic, yellow-white, ill-defined and infiltrative masses characterised histologically by invasive pancreatic epithelial neoplasm with glandular (ductal) differentiation, usually demonstrating luminal or intracellular mucin without a substantial component of any other histological type. They have intense stromal desmoplasia, variable necrosis, perineural invasion (both within and beyond the pancreas), and microscopic vessel and lymphatic invasion (Figure 2). Lymph node spread is present in most resection specimens with localised disease.

Nonneoplastic desmoplastic component (dense stromal fibrosis) accounts for more than 70% of the tumour mass and is a hallmark morphological feature of ductal adenocarcinomas, also known as fibroinflammatory tumour microenvironment (TME). The stroma, which consists of an extracellular matrix and numerous cell types, including inflammatory cells, pancreatic stellate cells (PSC), endothelial cells, nerve cells, fibroblasts and myofibroblasts, is hypovascular; this creates a barrier to effective drug delivery. The rigid TME also leads to aggressive tumour subclones resistant to nutrient deprivation.

The prognosis for individual patients depends on the extent of spread (Tumour, Node, Metastasis, TNM stage (Table 2, Figure 1) and histologic grade of the tumour. For patients with unresected PDAs, it is uniformly dismal; however, even in the setting of completely resected, node-negative PDAC, most patients still die of their disease (35). Pancreatic intraepithelial neoplasia (PanIN) -3 and Stage I disease are considered early PC as they are resectable. The development of PDAC is thought to result from a sequence of precursor lesions that evolve over time. The genetic timeline from initiation of malignant clone to

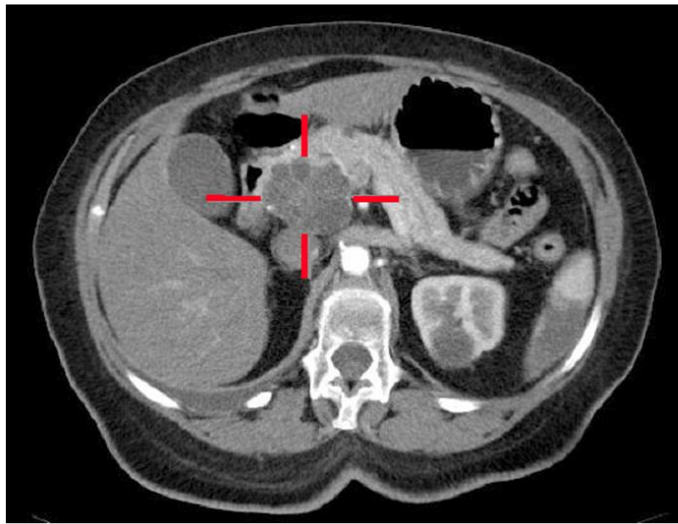
Table 1: Overview of exocrine pancreatic neoplasm

Exocrine neoplasm	Entity	Further subdivision
Benign	Acinar cell cystadenoma	
	Serous cystadenoma	
	Pyloric gland adenoma	
Pre-malignant	Pancreatic intraepithelial neoplasia, high grade	
	Intraductal papillary mucinous neoplasm	With low-grade dysplasia With high-grade dysplasia
	Mucinous cystic neoplasm	With low-grade dysplasia
		With high-grade dysplasia
Malignant	Acinar cell carcinoma	
	Acinar cell cystadenocarcinoma	
	Ductal adenocarcinoma	Adenosquamous carcinoma
		Colloid carcinoma
		Medullary carcinoma
		Signet ring cell carcinoma
		Undifferentiated carcinoma
		Undifferentiated carcinoma with osteoclast-like giant cells
		IPMN with an associated invasive carcinoma
	Intraductal tubulopapillary neoplasm with associated invasive carcinoma	
	Mixed acinar/ductal/neuroendocrine carcinoma	
	Pancreatoblastoma	
	Serous cystadenocarcinoma	
	Mucinous cystadenocarcinoma	
Solid-pseudopapillary neoplasm		

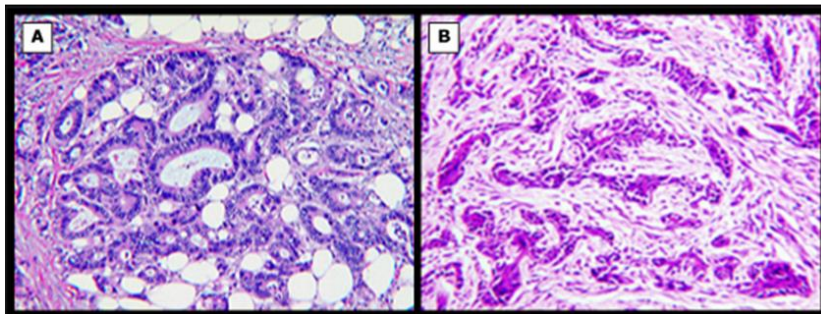
Taken from (36)

Figure 2: Computed tomography (CT) image and histologic appearance of PDAC

a



b



a- CT scanner section, after intravenous injection of a contrast medium, showing an adenocarcinoma cancer tumour at the head of the pancreas. Taken from (37)

b- Haematoxylin and Eosin stain sections. [A] Well-differentiated (grade 1) carcinoma invading fat. [B] Poorly differentiated (grade 3) carcinoma is desmoplastic and has a prominent fibrous stroma. Taken from (38)

Table 2: Exocrine PC TNM staging AJCC UICC 8th edition

Primary tumour (T)	
T category	T criteria
TX	Primary tumour cannot be assessed
T0	No evidence of primary tumour
Tis	Carcinoma in situ. This includes high-grade pancreatic intraepithelial neoplasia (PanIN-3), IPMN with high-grade dysplasia, intraductal tubule-papillary neoplasm with high-grade dysplasia, and MCN with high-grade dysplasia.
T1	Tumour ≤2 cm in greatest dimension
T1a	Tumour ≤0.5 cm in greatest dimension
T1b	Tumour >0.5 and <1 cm in greatest dimension
T1c	Tumour 1 to 2 cm in greatest dimension
T2	Tumour >2 and ≤4 cm in greatest dimension
T3	Tumour >4 cm in greatest dimension
T4	Tumour involves the celiac axis, superior mesenteric artery, and/or common hepatic artery, regardless of size
Regional lymph nodes (N)	
N category	N criteria
NX	Regional lymph nodes cannot be assessed
N0	No regional lymph node metastasis
N1	Metastasis in one to three regional lymph nodes
N2	Metastasis in four or more regional lymph nodes
Distant metastasis (M)	
M category	M criteria
M0	No distant metastasis
M1	Distant metastasis

Prognostic stage groups			
When T is...	And N is...	And M is...	Then the stage group is...
Tis	N0	M0	0
T1	N0	M0	IA
T1	N1	M0	IIB
T1	N2	M0	III
T2	N0	M0	IB
T2	N1	M0	IIB
T2	N2	M0	III
T3	N0	M0	IIA
T3	N1	M0	IIB
T3	N2	M0	III
T4	Any N	M0	III
Any T	Any N	M1	IV

Taken from (18).

metastatic disease is nearly two-decade, providing early detection opportunities. A specific and sensitive biomarker of these precursor lesions with malignant potential would be invaluable in detecting early malignancy, as current confirmatory PC diagnosis relies upon costly and invasive procedures.

Screening programmes like the European Registry of Hereditary Pancreatitis and Familial Pancreatic Cancer (EUROPAC) exist for individuals with a strong family history or genetic predisposition. However, an effective test is still required for those who develop sporadic disease.

1.3. Precursors of invasive ductal adenocarcinoma

PDAC, the most common type of cancer in the pancreas, accounts for over 90% of pancreatic cancers and has a distinct molecular profile. By combining early molecular profiling with histology, researchers have developed a hypothetical pathological progression model similar to the adenoma-carcinoma model in colon cancer (39). According to this model, intraductal precursors undergo a progression from low- to high-grade lesions, acquiring genetic abnormalities and increasing cytological atypia, ultimately leading to invasive adenocarcinomas. There are two recognised pathways to invasive pancreatic cancer, each with its own frequency, natural history, and genetic characteristics. The most commonly observed precursor lesions are pancreatic intraepithelial neoplasias (PanINs), which are microscopic and cannot be detected through abdominal imaging scans (40). On the other hand, cystic mucinous neoplasms of the pancreas, particularly intraductal papillary mucinous neoplasms (IPMNs), are macroscopic precursors that develop in the main pancreatic duct or its branches and can be monitored for progression using imaging techniques (41).

Approximately 85%–90% of PDAC cases are believed to arise from PanIN lesions, while the remaining 10%–15% originate from cystic precursors, including intraductal papillary mucinous neoplasms (IPMNs) and mucinous cystic neoplasms (MCNs) (42).

Among these cysts, IPMNs are the most common and can be classified broadly based on their location and extent within the pancreas as main-duct (MD-IPMN), branch-duct (BD-IPMN), or mixed type (MT-IPMN) (43). MD-IPMNs account for 15%–21% of all IPMNs and are often found in the pancreatic head. They are characterised by a segmental or diffuse dilation of the

main pancreatic duct (MPD) with a diameter greater than 5 mm after excluding other causes of ductal obstruction (44).

On the other hand, BD-IPMNs comprise 41%–64% of IPMNs and can occur throughout the pancreas, with a preference for the uncinata process. They are frequently multifocal and typically described as either unilocular or exhibiting a grape-like/multilobulated arrangement that communicates with the MPD. MT-IPMNs meet the criteria for both MD-IPMN and BD-IPMN and account for 22%–38% of all IPMNs. Unsurprisingly, the incidence of PDAC associated with IPMNs can vary depending on the subtype. PDAC is reported in 11%–80% of MD-IPMNs and 20%–65% of MT-IPMNs (45, 46).

Due to the high likelihood of malignancy, patients with MD-IPMNs or MT-IPMNs are often recommended to undergo surgical resection. However, malignant transformation of BD-IPMNs is observed in 1%–36% of surgical resections (44). It is important to note that these statistics are based on surgical data, which may overestimate the malignant potential of BD-IPMNs. Additionally, distinguishing BD-IPMNs from other pancreatic cysts based on preoperative clinical, radiographic, and pathological findings can be challenging. Benign neoplastic and non-neoplastic cysts, such as serous cystadenomas and lymphoepithelial cysts, can mimic BD-IPMNs before surgery (47, 48).

Consequently, accurate diagnosis of BD-IPMNs and identification of high-grade dysplasia and/or microscopic PDACs originating from BD-IPMNs have been key areas of focus for early detection efforts. Patients with an IPMN face an increased risk not only for IPMN-associated PDAC but also for PDAC unrelated to the IPMN (known as concomitant carcinomas). The reported incidence of concomitant carcinomas in IPMN patients ranges from 2% to 11.2% (44). Therefore, detecting concomitant carcinomas is also a crucial aspect of early detection strategies.

IPMN, MCN and PanIN fulfil the five criteria (Table 3) established to define a cancer precursor by the National Cancer Institute-sponsored consensus conference (49). For e.g., PCLs are associated with an increased incidence of pancreatic cancer, 22.5 times greater (50), identical gene mutations were demonstrated at the molecular level (49, 51, 52), the epithelium in all three lesions differs architecturally and cytologically from the normal ductal epithelium (49), the neoplastic epithelium has not penetrated through the basement membrane, and

Table 3: National cancer institute working group criteria for precursors to invasive cancer

1	The precursor to invasive cancer must be associated with an increased risk of the cancer
2	When a precursor to invasive cancer progresses to cancer, resulting cancer arises from cells within the precancer
3	A precursor to invasive cancer should differ from the normal tissue from which it arises
4	A precursor to invasive cancer should differ from the cancer into which it develops
5	There should be a method by which the precursor to invasive cancer can be diagnosed

Taken from (53)

they are all diagnosable by light microscopy (49). Table 4, Table 5 and Table 6 outline the features of these precursor lesions (53) (Figure 3).

1.3.1. Pathological features of precursor lesions

1.3.1.1. IPMN

IPMNs are neoplasms that originate in the main pancreatic duct or its branches and produce mucins (54). Noninvasive IPMNs can be classified into two clinical subtypes: those mainly involving the main duct and those predominantly affecting a branch duct (55). The terms "mixed-type" or "combined-type" IPMN are used when both the main and branch ducts are involved (56). Main duct IPMNs typically display more severe epithelial dysplasia and are more frequently associated with infiltrating adenocarcinoma than branch duct IPMNs (57, 58). However, there is a significant overlap between these two subtypes.

Based on the predominant direction of differentiation within the lining epithelium, IPMNs can also be categorised as gastric foveolar, intestinal, or pancreaticobiliary subtypes (58). Main duct IPMNs are often larger in size and exhibit an intestinal or pancreaticobiliary subtype in their lining epithelium. Branch duct IPMNs, on the other hand, are usually relatively small and predominantly of the gastric foveolar subtype. The intestinal subtype of IPMN typically shows increased expression of MUC2, while the pancreaticobiliary subtype expresses MUC1. The gastric foveolar subtype is characterised by MUC5AC expression and the absence of MUC1 or MUC2 expression (59, 60). CDX2, a crucial transcription factor in intestinal development, is expressed in the majority of IPMNs of the intestinal subtype, indicating the existence of an intestinal differentiation pathway for some IPMNs. In contrast, IPMNs of the pancreaticobiliary subtype, as well as pancreatic intraepithelial neoplasia (PanIN), which also tend to be MUC1 positive, lack CDX2 expression (61, 62).

The key pathological features of clinical relevance in IPMNs are the degree of dysplasia and the presence or absence of invasive carcinoma. The architectural and cytological atypia is used to subclassify IPMNs into low-grade, intermediate, and high-grade dysplasia; low and intermediate dysplasia are now both grouped as LGD, and HGD is characterised by complex architectural features (i.e. irregular branching, cribriforming) with loss of nuclear polarity along with increased nuclear hyperchromasia and nuclear irregularities. IPMNs are often associated with PanINs and chronic pancreatitis (63). Approximately one-third of IPMNs have a co-

Table 4: Common precursor lesions in the pancreas

Feature	IPMN	MCN	PanIN
Predominant Age	In the 60's	40-50 years	Increases with age
Gender	Male > female	Female >> male	Male = Female
Head vs body/tail	Head	Body/tail	Head >Body/Tail
Cyst Contents	Mucoid	Mucoid	N/A
Stroma Ovarian-type	Collagen-rich	Ovarian-type	Collagen-rich
Multifocal disease	In 20-30%	Very rare	Often

Adapted from (53)

Table 5: Radiology description

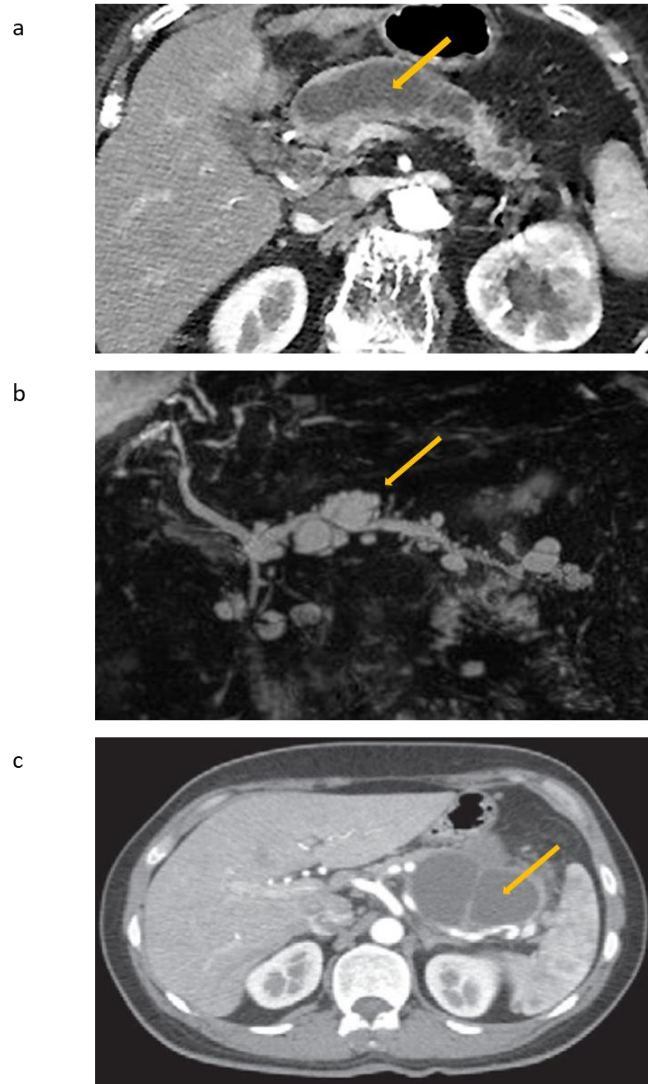
Radiographic features	MCN	IPMN
CT appearance	Well-demarcated thick-walled multilocular mass composed of large (1-3 cm) cysts	A dilated main pancreatic duct or a collection of multilocular grape-like cysts that represent dilated branch ducts
Mural nodules	Common with an associated invasive carcinoma, it may have calcification	May demonstrate on ERCP
Pancreatic ducts	Displaced or compressed pancreatic duct, and in the vast majority of cases	Dilated pancreatic duct and filling defects caused by intraluminal mucous plugs or papillary projections of the neoplasm itself
Relation of the cysts to large ducts	Do not communicate	Communicates
Mucin oozing from ampulla at endoscopy	No	Mucin extruding from a patulous ampulla of Vater is a classic, almost diagnostic feature

Table 6: Molecular features of precursor lesions of pancreatic cancer

Genetic alteration	IPMN	MCN	PanIN
<i>KRAS</i>	+ (more common in gastric subtype)	+ (in low and high-grade)	+ (in low and high-grade)
<i>GNAS</i>	+ (more common in intestinal subtype)	-	-
P16/<i>CDKN2A</i>	+ (in high-grade)	Aberrant methylation in minority	+ (high-grade)
<i>TP53</i>	+ (in high-grade)	+ (high-grade)	+ (high-grade)
<i>SMAD4</i>	+ associated with invasive carcinoma	+ (high-grade)	+ (high-grade)
<i>BRCA2</i>			+ (high-grade)
<i>LKB</i>	+ in 25%		
<i>PIK3CA</i>	+ 10%		

Taken from (36).

Figure 3: Radiological appearance of precursor lesions of pancreatic cancer



Example of imaging; a- CT scan of main duct IPMN, revealing a markedly dilated pancreatic duct with parenchymal atrophy; b- MRCP showing mixed-type IPMN. There are multiple dilated branch ducts and a moderately dilated main pancreatic duct in the pancreatic body region; c- CT scan of MCN. Taken from (64)

existing invasive adenocarcinoma (65), with colloid adenocarcinomas and ductal adenocarcinomas being the most common types. Colloid adenocarcinomas are characterised by abundant extracellular mucin pools containing floating neoplastic epithelium (66). They are typically associated with intestinal IPMNs expressing MUC2, while ductal adenocarcinomas are linked to pancreaticobiliary lesions expressing MUC1. Gastric IPMNs rarely progress to malignancy, which supports a conservative approach for most branch duct IPMNs where the neoplastic epithelium is typically present (62). However, considering the substantial difference in 5-year survival between patients with noninvasive and invasive IPMNs (90% versus 50%, respectively)(67), careful histopathological examination of the entire specimen is necessary to rule out the presence of invasive components.

1.3.1.2. MCN

MCNs are the least common among the three known precursor lesions of pancreatic cancer. For instance, low-grade PanINs are highly prevalent and can be found in up to 50% of pancreata in individuals over 65 years of age (68). The exact prevalence of mucinous cysts is challenging to determine, but some studies suggest that their prevalence is approximately half that of IPMNs (67). It is essential to note that MCNs are characterised by two components—an epithelium that produces mucin and a dense stroma similar to that of the ovary located beneath the lining epithelium. In fact, the presence of ovarian-like stroma is a requirement for diagnosing an MCN. The contents of an MCN cyst typically consist of fluid rich in mucin or haemorrhagic fluid.

Histologically, the lining epithelium of an MCN is composed of columnar cells that produce mucin and exhibit varying degrees of dysplasia (69). MCNs with low-grade dysplasia display minimal architectural and cytological changes. The lining cells contain abundant mucin, and their nuclei are basally oriented. These cells strongly express MUC5AC antibodies. In MCNs with intermediate (moderate) dysplasia, the nuclei lose polarity and exhibit variations in morphology and size. MCN lesions with high-grade dysplasia (carcinoma in situ) demonstrate significant architectural and cytological abnormalities. A notable feature that can be observed in the cyst lining is a sharp transition between areas of severe and mild dysplasia. As mentioned earlier, the presence of an ovarian-like stroma beneath the neoplastic epithelium is a diagnostic hallmark of MCNs (70). The stroma expresses progesterone and oestrogen receptors and can even undergo luteinisation, similar to the stroma found in the actual ovary.

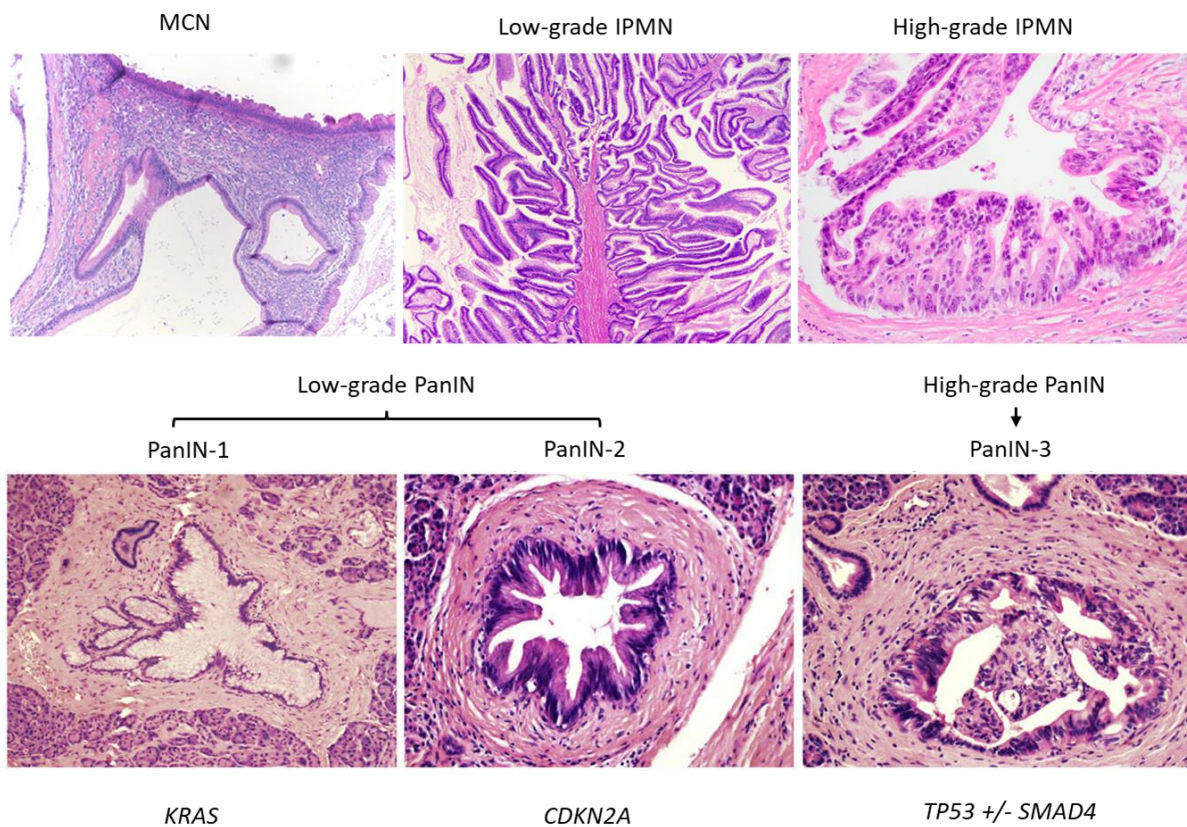
Similar to IPMNs, approximately one-third of reported MCNs are associated with invasive adenocarcinoma, usually of the ductal type (67). However, the percentage of MCNs associated with invasive cancer may be declining due to changing diagnostic criteria, particularly the strict requirement for the presence of an ovarian-like stroma. Patients who undergo resection for an MCN with associated invasive cancer have a 5-year survival rate of 50–60%. In contrast, patients who undergo resection for a noninvasive MCN typically have an excellent prognosis, with a disease-specific 5-year survival rate of nearly 100% (71, 72). The favourable survival outcome for surgically resected MCNs compared to surgically resected IPMNs is attributed to the fact that MCNs are usually unifocal lesions. Identifying the presence of an invasive component is crucial in the resection specimen since noninvasive MCNs, including those with severe dysplasia, are typically cured following surgical resection (69, 71, 72).

1.3.1.3. PanINs

PanINs are microscopic incidental lesions that cannot be clinically or radiologically visualised, making them unsuitable for fine needle aspiration biopsy. Typically measuring less than 0.5 cm, PanINs are too small to be detected through radiologic imaging. The earliest precursor lesion, PanIN 1A/low grade, consists of flat epithelium composed of tall columnar mucin-producing cells with small round to oval nuclei at the base. These cells exhibit minimal cytologic atypia. PanIN 1B/low grade is similar to PanIN 1A but exhibits papillary, micropapillary, or basally pseudostratified architecture. PanIN 2/low grade is characterised by flat to papillary mucinous epithelial proliferation with focal or mild nuclear abnormalities, including loss of polarity, nuclear enlargement, nuclear crowding, hyperchromatism, and pseudo stratification. Rare mitoses may be present, but they are not apical or atypical.

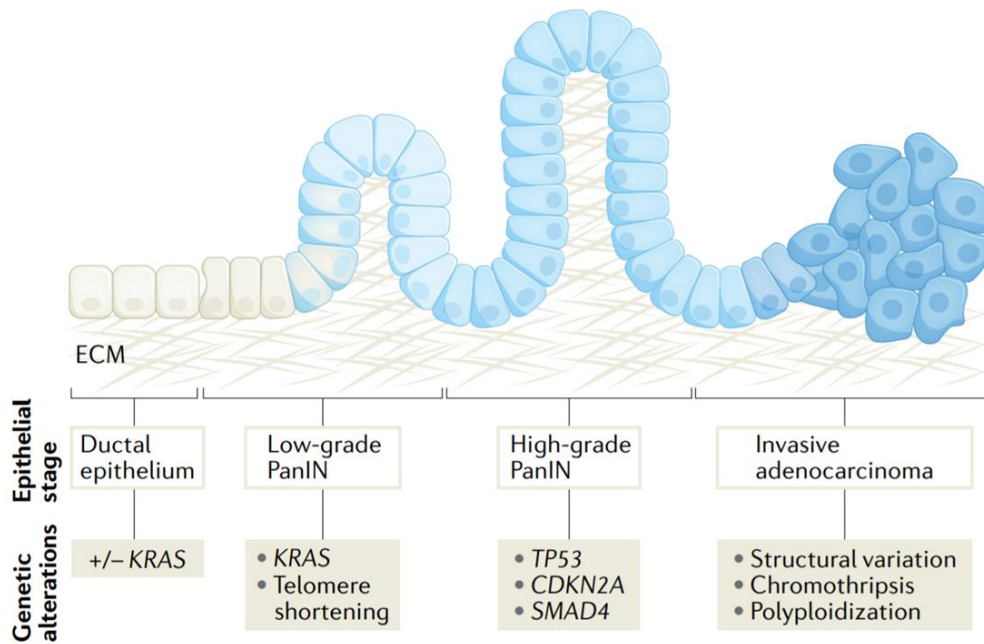
PanIN 3/high grade/carcinoma in situ predominantly displays a papillary or micropapillary architecture, rarely appearing flat. It exhibits cribiforming, tufting patterns, and luminal necrosis, which suggest PanIN 3. Cytologically, these lesions show a loss of polarity, dystrophic mucinous cells, enlarged irregular nuclei with prominent (macro) nucleoli, and an increased presence of mitotic figures, including atypical forms. Only lesions of the carcinoma in situ type are classified as PanIN 3/high grade (73). According to the WHO classification, PanIN 1A, 1B, and PanIN 2 are grouped as low-grade PanIN, while PanIN 3 is classified as high-grade PanIN (Figure 4, Figure 5).

Figure 4: Histopathological features of the precursor lesions of pancreatic cancer



Histopathological morphology of PDAC precursor lesions. Dysplasia increases with the accumulation of genetic drivers during precursor progression. Taken from (74)

Figure 5: Histological stages in PDAC progression



The progression from normal pancreatic ductal epithelium to low-grade, then high-grade dysplastic pancreatic intraepithelial neoplasias (PanINs) to invasive adenocarcinoma, with accompanying genetic alterations, is shown. Histologically normal ductal epithelium may bear *KRAS* activating mutations. Low-grade PanINs bear the earliest somatic changes of *KRAS* oncogene activation and telomere shortening. High-grade PanINs accumulate inactivation of the cell cycle regulatory tumour suppressor genes *TP53*, cyclin-dependent kinase inhibitor 2A (*CDKN2A*) and/or *SMAD4*. Invasive adenocarcinomas have more structural and copy number variants, including complex processes such as chromothripsis and polyploidisation. ECM, extracellular matrix. Taken from (75).

1.3.1.4. Recommended terminology for PCLs

- For PanIN:
 - Low-grade PanIN
 - High-grade PanIN (“carcinoma in situ”, according to local usage)
- For tumour-forming intraepithelial neoplasms (IPMN and MCN)
 - IPMN/MCN, low-grade
 - IPMN/MCN, high-grade
 - IPMN (and MCN), high-grade, may be further classified with the relevant local usage such as “carcinoma in situ” in parenthesis.
- For cases that also have an associated invasive carcinoma
 - IPMN/MCN, ___ grade, with an associated invasive carcinoma
 - Invasive carcinoma with an associated IPMN/MCN may also be used.

When reporting cases of IPMN and MCN, it is suggested to follow a specific order for consistent and clear documentation (Table 7). The reporting should begin with the entity name (IPMN or MCN), followed by the grade, and then the morphologic type (gastric, intestinal, pancreaticobiliary, or oncocytic) (58). If relevant, the involved portion of the ducts (main or branch) should be mentioned, along with the size of the lesion.

The determination and documentation of the presence or absence of an associated invasive carcinoma is of utmost importance. If an associated invasive carcinoma is present, the pathology report should provide separate and clear descriptions of the detailed characteristics of the precursor lesion (IPMN or MCN) and the invasive components (type, grade, size, and stage). While using the terminology "IPMN or MCN with associated invasive carcinoma" is recommended, it is also acceptable to use "Invasive carcinoma with associated IPMN/MCN" to prioritise reporting the biologically more significant lesion first.

Following the WHO 2010 recommendation, it is advised to avoid terms such as "invasive IPMN/MCN," "malignant IPMN/MCN," or "mucinous cystadenocarcinoma." The literature has used these terms to describe a wide range of neoplasms, from precursors with high-grade dysplasia to invasive carcinoma.

Table 7: Proposed Revised Terminology of PanIN, IPMN and MCN

Former terminology (based on the 2004 Classification and 2010 WHO)	Revised terminology (2015)
PanIN-1a	Low-grade PanIN
PanIN-1b	Low-grade PanIN
PanIN-2	Low-grade PanIN
PanIN-3 (carcinoma in-situ)	High-grade PanIN
IPMN with low-grade dysplasia	IPMN, low-grade
IPMN with intermediate-grade dysplasia	IPMN, low-grade
IPMN with high-grade dysplasia (carcinoma in situ)	IPMN, high-grade
IPMN with an associated invasive carcinoma	IPMN with an associated invasive carcinoma/invasive carcinoma with an associated IPMN (the latter may be used if the invasive component is substantial)
MCN with low-grade dysplasia	MCN, low-grade
MCN with intermediate-grade dysplasia	MCN, low-grade
IPMN with high-grade dysplasia (carcinoma in situ)	MCN, high-grade
MCN with an associated invasive carcinoma	MCN with an associated invasive carcinoma/invasive carcinoma with an associated MCN (the latter may be used if the invasive component is substantial)

Taken from (73)

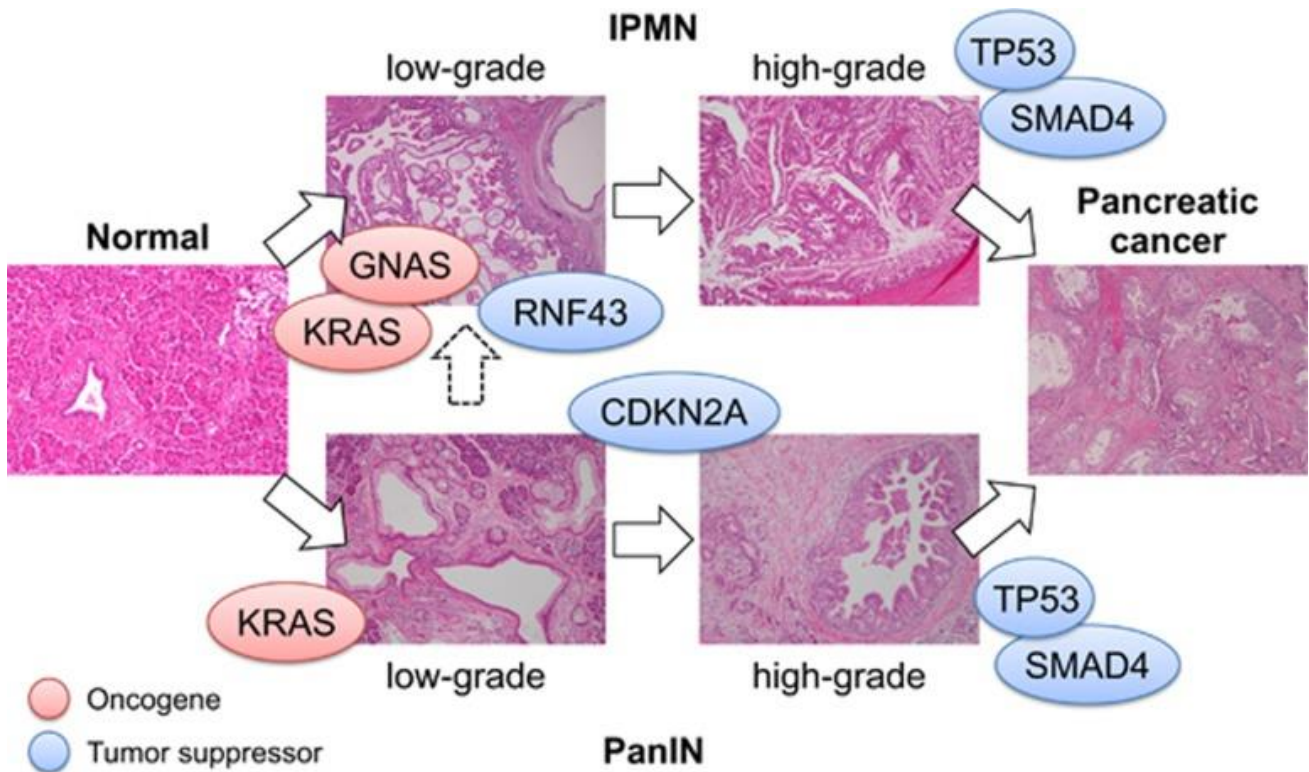
However, they are non-specific and can lead to clarity and help accurate data comparison across different medical centres.

1.4. Evolution of pancreatic cancer

PDAC evolves through specific steps of progression within a hostile fibroinflammatory microenvironment (Figure 6). Two evolution models have been proposed; first, a stepwise progression model (76), where malignancy develops over the years; here, a higher degree of precursor dysplasia is associated with a higher accumulation of genetic alterations. Second is the punctuated evolution progression model (77) (Figure 7), characterised by rapid tumour development and dissemination due to simultaneous driver gene inactivation and complex chromosomal rearrangements. PDAC is driven by activation of the rat sarcoma (RAS) (*KRAS* mutation (78)) and transforming growth factor (TGF) β (*SMAD4* mutation (79)) signalling pathways; cancer growth is subsequently facilitated by the disruption of the G1/S cell cycle checkpoint machinery with *CDKN2A* and *TP53* (80) deletions and, in a few cases, by disruption of deoxyribonucleic acid (DNA) repair through homologous recombination deficiency (HRD) or mismatch repair deficiency (MMRD). The oncogenic point mutations can be aggregated in 13 canonical molecular pathways that include RAS signalling, regulation of the G1/S cell cycle phase transition, TGF β signalling, JUN amino-terminal kinase (JNK) signalling, integrin signalling, Wntless/Integrated (WNT)–Notch signalling, hedgehog signalling, apoptosis, DNA damage control, small guanosine triphosphate (GTP)ase dependent signalling, invasion and homophilic cell adhesion (81) and embryonic regulators of axon guidance (82). Time from the first somatic mutation to the origin of the parental invasive cell is estimated to be 10-12 years (83), and from then to the origin of index metastatic cell 6-7 years (84).

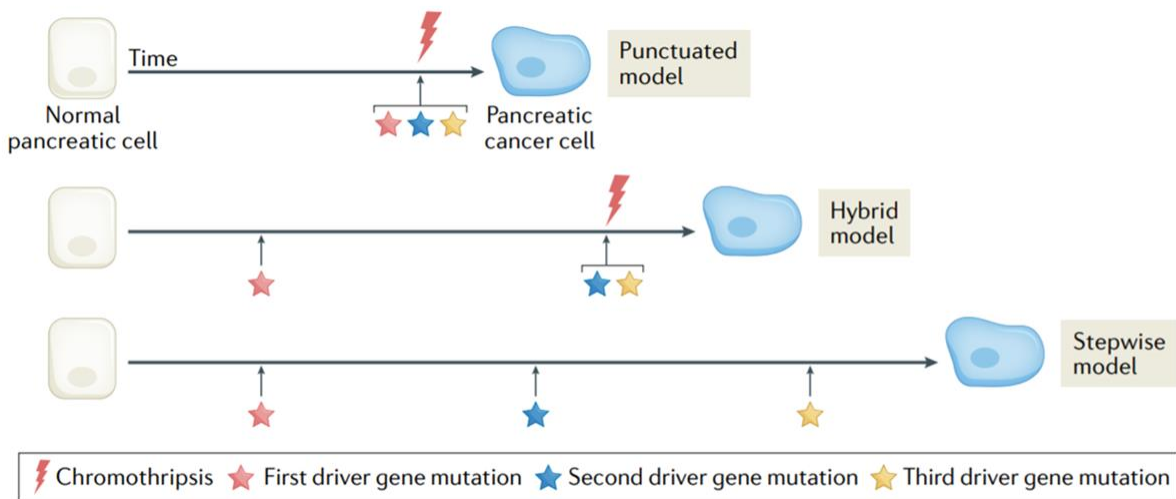
Activating Kirsten rat sarcoma virus (*KRAS*) mutations represent one of the earliest genetic events during neoplastic transformation and are present in approximately 90% of PDACs (85). The *KRAS* gene product participates in the signal transduction pathways to help epithelial cells cope during stressful conditions (86, 87); the *KRAS* signalling activates several adaptations that promote growth, survival and neoplastic transformation of both native and metaplastic ductal epithelial cells. These cells often persist as microscopic in situ PanIN or undergo neoplastic cytogenesis in IPMN in association with guanine nucleotide binding protein (*GNAS*) (88, 89). In PanINs that persist, the mutated epithelial cells secrete protective fibroinflammatory cytokines and construct a localised rim of fibroinflammatory tissue around mutated epithelial cells that allows the mutated cells to persist even

Figure 6: Precursors of pancreatic cancer



PDAC can arise from the progression of IPMN (top) or PanIN (bottom). It is not known whether early IPMNs (incipient IPMNs) originate from low-grade PanIN or develop independently from normal pancreatic ducts or other pancreatic cell lineages. Red and blue circles indicate oncogenes and tumour-suppressor genes, respectively. The precise timing of *RNF43* mutations and the order of *GNAS* and *KRAS* mutations have not been fully established. IPMN, intraductal papillary mucinous neoplasm; PanIN, pancreatic intraepithelial neoplasia. Taken from (90).

Figure 7: Stepwise model versus punctuated model of PDAC progression



The hypothetical accumulation of somatic events over time as a pancreatic cell undergoes dysplasia, including structural (chromothripsis) and simple somatic mutations under a punctuated model (top), a stepwise model (bottom) or a hybrid model (middle). Adapted from (75)

without inflammation (91). This fibroinflammatory rim favours the survival of epithelial cells with mutant *KRAS*; the mutated cells also secrete paracrine signals to maintain this rim. *KRAS* mutation is weakly oncogenic and displays morphological features of LGD (73). However, it acts as a portal for stepwise (86) or punctuated acquisition (77) of additional driver gene alterations in precursors, including mutations and/or allelic losses targeting specific tumour suppressor genes (most commonly *CDKN2A* (92, 93), *TP53* (94), and *SMAD4* (95)). Inactivation of *CDKN2A* and *TP53* eliminates cell cycle checkpoints that defend against genome instability. Mutation and/or loss of *SMAD4* (40-55%) favours survival from the lethal aspects of stromal TGF β when neoplastic cells undergo epithelial-to-mesenchymal transition (EMT) and/or migrate through stromal matrix barriers (96, 97). Thus, the inactivation of cell cycle checkpoints, induction of epigenetic instability and enhanced mobility produce the features of HGD and subsequent malignant transformation.

The invasion of the primary tumour is initiated through the parental clone (84). On invasion, they activate the resident PSCs, secrete extracellular matrix and recruit inflammatory cells (98). This constitutes the desmoplastic stroma. The activated PSCs proliferate and differentiate into two distinct types of cancer-associated fibroblasts, including myofibroblast-type fibroblasts (myCAFs) that secrete densely collagenous extracellular matrix and inflammatory-type fibroblasts (iCAFs) (99). iCAFs enhance the fitness of the PDAC cells by secreting growth factors and immunosuppressive cytokines (100). Myeloid-derived suppressor cells (101), immunosuppressive cytokines (102, 103), stromal matrix deposition (104) and endocytosis of PDAC neoantigens (105, 106) all contribute to the tumour defence and PC progression.

1.5. Inflammation and cancer- “the wound that never heals.”

Inflammation is a process that involves the activation, recruitment, and action of cells of innate and adaptive immunity (107). While its primary function is to protect the host from pathogens, it also plays a role in tissue repair, regeneration, and remodelling. In recent years, the contribution of the immune system and inflammation to cancer development, progression, and therapy has gained significant interest. Cancer biology has shifted from focusing on cancer cells to a more inclusive view that considers the entire TME, which includes stromal cells, fibroblasts, and inflammatory immune cells. Inflammation has a significant effect on the composition of the TME and can shape the TME toward a more tumour-permissive state. The immune system can play both pro- and anti-tumorigenic roles at all stages of tumorigenesis (108-110). The pro-tumorigenic role of the immune system in

cancer plays a distinct role during tumour initiation, promotion, and progression, referred to as "cancer-promoting inflammation."

Inflammation that occurs before or during tumour development is influenced by a range of environmental factors, which can contribute to the onset and progression of cancer. 15-20% of all cancers are preceded by infection, chronic inflammation or autoimmunity at the same tissue or organ site (111). Even non-inflammatory cancers can alter the TME and promote tumour growth by recruiting immune cells and increasing the expression of inflammatory mediators, a process called tumour-elicited inflammation (Figure 8) (111, 112).

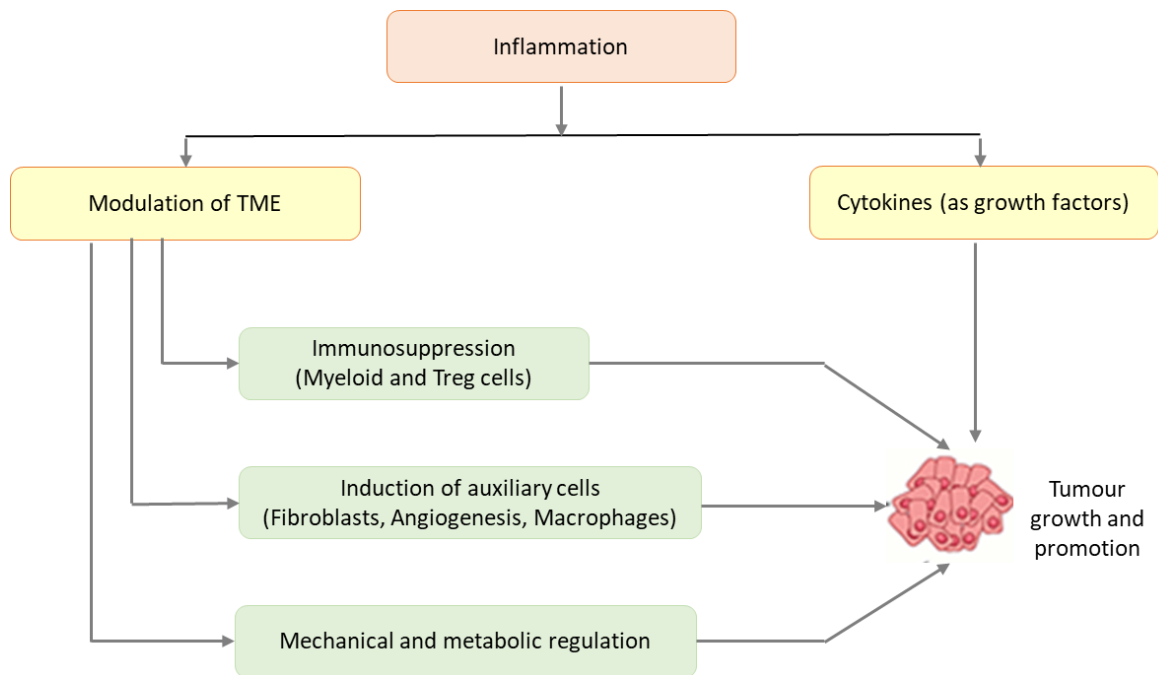
1.5.1. The origins and triggers of inflammation in the process of cancer development

Ground zero inflammatory responses in cancer can be induced by various causes and stimuli. Loss of tumour suppressors, such as *TP53*, can lead to increased expression of nuclear factor (NF)- κ B-dependent inflammatory genes (113) and trigger DNA-damage-induced inflammatory pathways (114). Oncogene activation (*KRAS*) can also lead to excessive production of inflammatory cytokines, chemokines and recruitment of myeloid cells (115). Recognition of cancer-inducing pathogens (e.g., *H. pylori*, Hepatitis B and virus, human papillomavirus) (116), commensal microbiota (e.g., Th17 responses in chronic pancreatitis (117)), and cell death (118) can also trigger innate inflammatory responses. These mechanisms all contribute to tumour progression and metastasis. As inflammation is often wired to be induced during oncogenic transformation, it is often pre-encoded in the genetic and transcriptional programs necessary for cancer.

1.5.2. Inflammation and Tumour Initiation

The initiation of tumours requires two main interdependent events. The first event leads to the accumulation of mutations and/or epigenetic changes in genes and signalling pathways involved in tumour suppression (inactivation) and oncogenic pathways (activation). This process can be caused by environmental factors and inherent errors in DNA repair and replication. Inflammatory responses can also lead to increased mutagenesis, accumulating mutations in normal tissue (119). Inflammatory cytokines such as interleukin (IL)-22 can trigger the expression of DNA damage response (DDR) genes that protect against potential genotoxic harm caused by inflammation. This mechanism is believed to be an evolutionary adaptation to the mutagenic effects of inflammation (120). The second event involves the creation of transformed and/or malignant clones, which should be followed by their outgrowth into a tumour. Inflammatory mechanisms can contribute to this process, such as cytokine

Figure 8: Mechanisms at play with inflammation that affect tumour growth



Inflammatory entities, such as cytokines and growth factors, released by immune cells within the TME can directly affect pre-malignant and cancer cells by increasing their proliferation and resistance to cell death and stresses, thereby directly promoting tumour growth and progression. This can be caused at different time points of cancer development. In addition, inflammatory signals can shape TME to induce immunosuppression via the action of regulatory T-lymphocytes (Treg), immature myeloid cells and other suppressive players; to enhance recruitment, proliferation, and distinct functions of other pro-tumorigenic auxiliary cells within the TME (such as fibroblasts, myeloid cells, and endothelium of new blood vessels); and to alter mechanical and metabolic functions of TME. Altogether, these inflammation-driven changes also significantly contribute to tumour growth and progression. Adapted from (3)

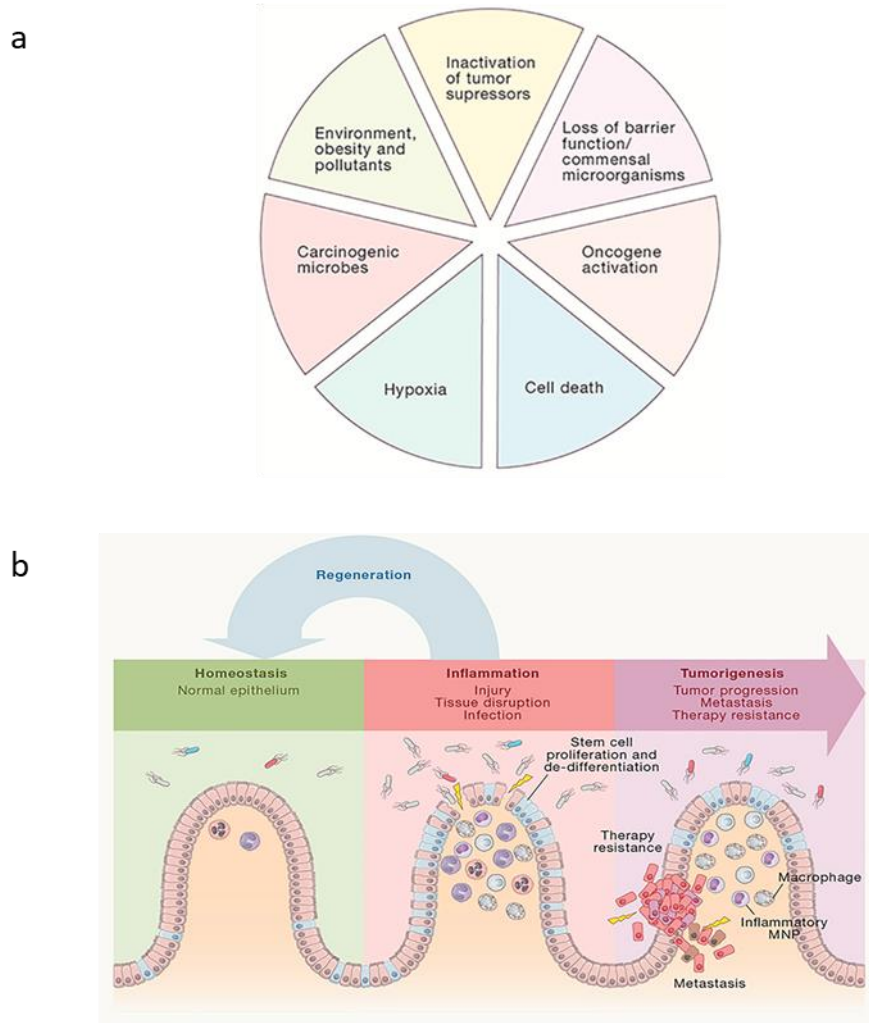
receptor signalling in mutated cells that might converge at the induction of pro-survival pathways, particularly mediated by NF- κ B, signal transducer and activator of transcription (STAT) 3, and other types of signalling (121, 122), thereby increasing the survival probability of transformed clones or enabling proliferation. Inflammation and injury trigger cell turnover in tissues, creating space for malignant clones' outgrowth (118). This is especially evident in liver and skin cancer, where the death of normal cells is required for compensatory proliferation of neighbouring transformed clones, thereby creating a scenario where inflammation-induced tissue injury and cell death are necessary for tumour outgrowth (Figure 9).

Chronic inflammation can trigger tissue damage, weaken barrier function, expose the stem cell compartment to environmental carcinogens, or bring stem cells to close proximity to active inflammatory cells producing genotoxic compounds. In microbial-rich cancer, such as colon cancer, enhanced inflammation can shape the qualitative characteristics of epithelial-adhesive microbiota, enriching the content of species harbouring genotoxic gene products, such as colibactin in some strains of *Escherichia coli* (*E.coli*), capable of inflicting mutations in host cells. Inflammatory signals might increase fitness and reduce the expression of "stress ligands" on cancer cells, which is required to recognise and eliminate the tumour cells (91) properly. The issue of inflammation-driven cell survival might also be important in the context of cancer immunosurveillance and the tumour elimination phase of mutated and stressed cells. Signals activating STAT3 protect epithelial cells from cluster of differentiation (CD)8 T cytotoxic cell attack (123), and signalling by interferon (IFN) γ , albeit a typically anti-tumorigenic cytokine, upregulates the expression of T cell exhaustion-inducing molecule programmed death ligand 1 (PD-L1) on the transformed epithelium, which is recognised by T cells.

1.5.3. Inflammation and Tumour Promotion

The relationship between inflammation and cancer has been extensively studied, and it is widely recognised that inflammation can promote tumour growth. The molecular and cellular mechanisms underlying this process have been identified through preclinical animal models of inflammation and cancer. Inflammation can serve as a direct growth factor for tumours, and inflammatory factors also shape cell plasticity within the TME, affecting tumour growth in at least three distinct ways. Inflammatory signals can antagonise anti-tumour immunity and promote tumour auxiliary functions such as angiogenesis and recruitment of stromal cells, which exert tumour-supporting functions.

Figure 9: Pro-tumorigenic actions of inflammation in progression, metastasis, and growth



a- Various cell intrinsic, host-dependent or environmental factors can cause tumour-associated inflammation in different tumour types. b- Activation of inflammatory responses due to injury, infection or tissue disruption can lead to the expansion of the stem cell pool via stem cell proliferation or epithelial cell de-differentiation into stem cells. This process, called “Regeneration,” is designed to normalise epithelium and its barrier function. However, if stem cells already have oncogenic mutations, expanding the stem cell pool can lead to enhanced metastasis and therapy resistance. Inflammatory stimuli regulate the emergence of these stem cells, affecting tumour progression, metastasis, and resistance. Here the case of colon cancer is used as an example, but the concept can apply to other cancers with activated inflammatory pathways. Adapted from (3).

Additionally, through modulation of TME, inflammatory signals alter mechanical and metabolic properties of stromal and tumour cells, affecting the availability of key metabolites involved in amino acid and redox metabolism.

NF- κ B, a master regulator of cytokine expression, plays a significant role in inflammation-induced tumour growth by promoting survival and proliferation in epithelial and cancer cells and chemokine expression, which is essential for cell recruitment and reshaping TME. NF- κ B-dependent cytokines confer unique and non-redundant roles in tumour growth, and their inactivation reduces tumour growth (124). Inflammatory cytokines such as IL-6, IL-17, and IL-11 can cause signalling that promotes the growth of tumour cells, particularly in the suboptimal conditions that exist in the body, including hypoxia, lack of nutrients, absence of growth factors, and the suppression of anti-tumour immunity. Insights into how inflammation drives tumour growth are important for the development of new therapies for cancer. Inhibition of inflammation can stall tumour growth and further progression, widening the opportunity for early detection of cancers.

1.5.4. Inflammation, Tumour Progression, and Metastasis

Inflammation plays a critical role in the regulation of metastasis, the spread of cancer cells from the primary tumour to distant organs. Prolonged use of aspirin reduces overall mortality, especially of gastrointestinal cancers and distant metastasis (125). Mechanisms showing how inflammation might affect the metastatic process have recently emerged. The method of metastasis starts with the invasion of cancerous cells away from the epithelial layer into the neighbouring tissues and acquiring the EMT phenotype (126). Cancer stem cells (CSC), as opposed to bulk tumour cells, are more efficient in their capacity to serve as metastatic seeds (127). Inflammation influences cancer invasion, EMT, and cell migration on several levels. Cytokines can directly affect the expression of EMT-inducing transcription factors (EMT-TFs) (128, 129). Increased accumulation of cytotoxic T and natural killer cells at the invasive margin of the primary tumour and decreased presence of myeloid cells correlate with better prognosis (130). It becomes increasingly clear that the number and proportion of CSC in the tumour are not constant. Instead, various stimuli, including prominent inflammatory signalling via transcription factors (NF- κ B and STAT3) in cancer cells, can drive their stemness and elevate the invasive potential (131). Inflammatory cells such as monocytes and neutrophils play a key role in the process of adhesion and extravasation of metastatic cancer cells, forming complexes with the cancer cells and aiding their passage throughout the vessel wall. Inflammatory cytokines are potent inducers

of integrins, selectins, and adhesion molecules such as vascular cell adhesion molecule (VCAM)-1 and intercellular adhesion molecule (ICAM)-1. Furthermore, specific inflammatory signals, such as those produced by obesity, microbes or tobacco smoke, can increase the rate of metastasis via induction of neutrophil activation and increased neutrophil-cancer cell interactions mediated by neutrophil extracellular traps (NETs) (132). Thus, the inflammatory response is an essential mediator of tumour development, promoting cancer progression and providing novel therapeutic targets for cancer treatment.

1.5.5. Inflammation and Cell Plasticity within the Tumour Microenvironment

The plasticity of cells in the TME is a relatively new concept in cancer research. Cells within the TME exhibit cell polarisation driven by different transcriptional programs, which allows them to acquire the functions necessary for tissue regeneration and tumour development. Plasticity allows the transition of cells from one state to another, such as the EMT and mesenchymal-to-epithelial transition (MET) during metastasis. Cancer cells are not the only cells subject to plasticity. Other cell types in the TME also engage in reciprocal signals of activation, inhibition, and differentiation to drive plasticity. Cancer-associated fibroblasts (CAF) can be both pro- and anti-tumorigenic (133), depending on their proximity to cancer cells and their response to different signals to IL-1R or TGF β (99). They can provide differentiation, growth factor, survival, and metabolic cues to cancer cells, maintain cancer stem cell niche (134-136), and drive immunosuppressive phenotypes (137, 138). Myeloid cells also present a high degree of plasticity regulated by the TME. Tumour-cell-derived factors can polarise macrophages towards a tissue-repair type, characterised by enhanced tissue-protective factors and decreased expression of genes involved in antigen presentation and induction of antigen-dependent immune responses (139, 140). Inflammation, cytokines, and growth factors can regulate tumour cell plasticity. This new understanding of the plasticity of cells in the TME offers unique opportunities for cancer research.

As inflammation is significant in all stages of tumour progression, further research is expected to reveal the molecular and cellular mechanisms through which inflammation and immune cells operate, particularly during the early stages of tumour formation and the spread of metastatic cells.

1.6. Role of inflammation in the development of pancreatic cancer

Several studies have investigated the role of inflammation in PC and identified various cellular and molecular mechanisms that contribute to this link. For instance, cytokines, chemokines, and immune cells have been shown to play a significant role in the development of pancreatic cancer.

1.6.1. Role of diabetes and obesity in the development of pancreatic cancer

Diabetes and obesity are known risk factors for PDAC (141, 142), and the tumour itself can cause diabetes by reducing insulin release and causing insulin resistance (143). The state of hyperadiposity or diabetes mellitus is associated with chronic subclinical inflammation, known as "metaflammation," which suggests a link between chronic inflammation and cancer (144). Obese patients typically have lower levels of the anti-inflammatory adipokine adiponectin and higher levels of the pro-inflammatory adipokine leptin. This leads to a shift from M2 anti-inflammatory to M1 pro-inflammatory macrophages, causing the release of pro-inflammatory cytokines, such as tumour necrosis factor (TNF) α and IL-6 (145). In addition, metabolic syndrome may increase cancer risk by promoting the release of pro-angiogenic cytokine vascular endothelial growth factor (VEGF) and the pro-proliferative effects of insulin. Inflammatory cells play a primary role in cancer development and evolution and may help tumour cells escape immune control. Cytokines produced by tumour and inflammatory cells, including IL-1 β , IL-6, TGF β and TNF α , are key players in the inflammatory and immunomodulatory scenario (145). Patients with metabolic syndrome might be at higher risk of PDAC due to the underlying metaflammation, activating oncogenic pathways in epithelial cells while reducing immune cell response to cancer. Overeating and an unhealthy diet may also increase the risk of PDAC by incurring an excessive intake of potential carcinogens. The role of the gut microbiota is also crucial. It may be influenced by diet, impacting the immune response and favouring dysbiosis and over-representation of bacterial species producing pro-carcinogenic metabolites. Lipopolysaccharide (LPS) is a key element found in the cell wall of Gram-negative bacteria that can cause inflammation and insulin resistance by binding to immune cells' TLR4 and activating the NF- κ B signalling pathway.

1.6.2. Role of local inflammation in PDAC growth, development, and metastasis

Pancreatic cancer is a model of a "cold" tumour and "immune privilege" where only a moderate range of mutated PC cells are associated with neoepitopes, making it difficult for cancer cells to activate an

effective adaptive immune response. The number of neoepitopes and CD8+ T cell infiltrates are predictive of patients with the longest survival (146).

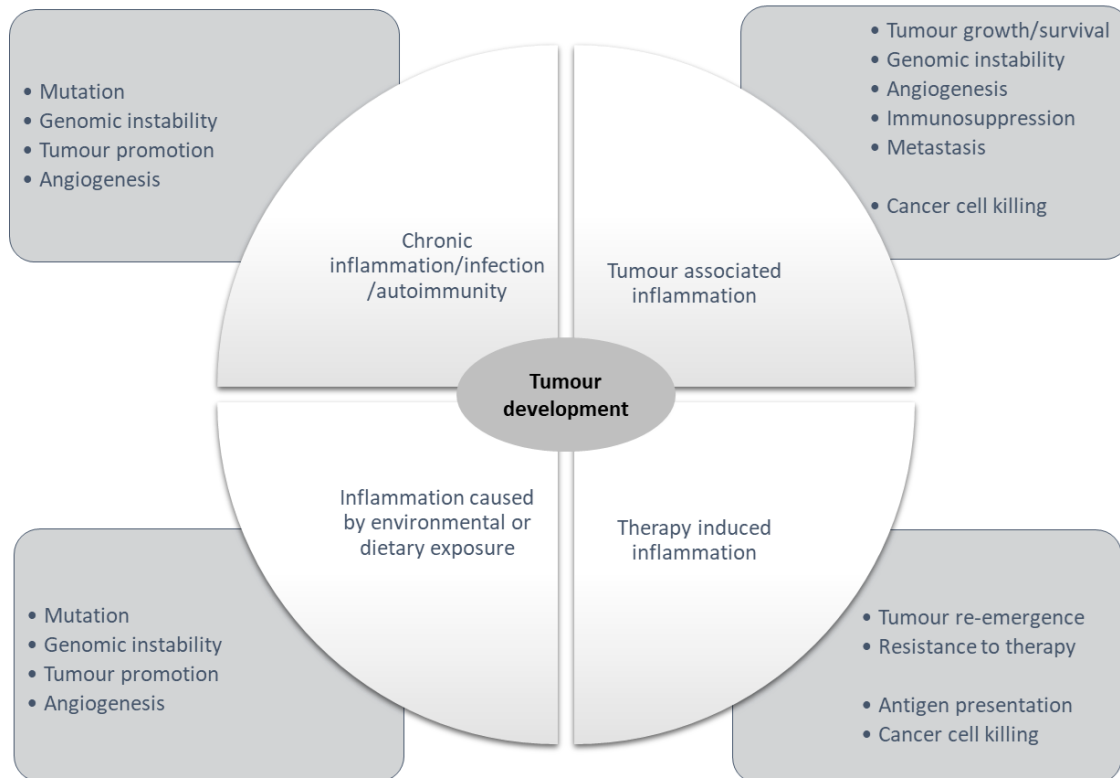
The mechanisms underlying the ability of the immune system to protect a host from tumour growth and subsequent cancer progression reside mainly within the tumour and the surrounding stroma, which includes fibroblasts, PSC, and infiltrating immune cells. The local immune response primes local inflammation generated and maintained mainly by cytokines, chemokines, and other reactive molecules like reactive oxygen species (ROS) and small peptides. Despite several inflammatory immune cell types being found in the PDAC dense stromal tissue, the microenvironment remains immunosuppressive in nature. This can be explained by the fact that the PDAC microenvironment restricts the infiltration of anti-tumour T-cells, whose role may be further attenuated by the co-infiltrating immune suppressive Treg, myeloid-derived suppressor cells (MDSC), and M2 macrophages. The recruitment of mast cells by tumour stimuli further contributes to immune suppression by downregulating the immune response and promoting the expansion and activation of Treg, leading to immune tolerance (147) (Figure 10).

The genetic profile of PDAC and the type of immune cells in the tumour stroma contribute to the high incidence of metastasis and poor survival. Inflammatory mediators, particularly S100A8 and S100A9, may play a crucial role in the link between PDAC genetics and inflammatory cells, leading to metastasis. In the presence of the *SMAD4* tumour suppressor gene, S100A8 and S100A9 are produced by inflammatory cells infiltrating the tumour, whereas in homozygous *SMAD4* deletion, the cancer cells themselves produce these molecules (148, 149). The distant sites like the liver and lungs may be affected by S100A8 and S100A9, which can alter the microenvironment, resulting in a "pre-metastatic niche" that facilitates metastatic cell adhesion and growth (150, 151).

1.6.3. Role of cytokines in the inflammatory response to cancer cells

Inflammatory cells within the TME, including immune cells, fibroblasts, and endothelial cells, produce and secrete various cytokines (Table 8), such as IL-6, IL-10, IL-13, VEGF, and TGF β (152). The balance between pro- and anti-inflammatory cytokines constantly changes in response to interactions between cancer and inflammatory cells. Cytokines such as TGF β , IL-10, IL-1 β , IL-6, IL-17, and TNF α play a major role in PDAC. CAF, which originates from mesenchymal stem cells, quiescent resident fibroblasts, and PSC, produce pro-inflammatory cytokines and develop into an activated phenotype via cytokines such as Sonic Hedgehog, TGF β , TNF α , IL-1, IL-6, and IL-10. In addition to producing most

Figure 10: Types of inflammation in tumorigenesis and cancer



Chronic inflammation associated with infections or autoimmune disease precedes tumour development and can contribute to it through the induction of oncogenic mutations, genomic instability, early tumour promotion, and enhanced angiogenesis. Prolonged exposure to environmental irritants or obesity can also result in low-grade chronic inflammation that precedes tumour development and contributes to it through the mechanisms mentioned above. Tumour-associated inflammation goes hand in hand with tumour development. This inflammatory response can enhance neoangiogenesis, promote tumour progression and metastatic spread, cause local immunosuppression, and further augment genomic instability. Cancer therapy can also trigger an inflammatory response by causing trauma, necrosis, and tissue injury that stimulate tumour re-emergence and resistance to therapy. However, in some cases, therapy-induced inflammation can enhance antigen presentation, leading to immune-mediated tumour eradication. Adapted from (111)

Table 8: Pro-inflammatory cytokines in pancreatic cancer

Cytokine	Cell sources	Effects on immune cells	Effects on PDAC initiation and EMT
TGFβ	M2 macrophages, Th2 lymphocytes, and TAM	Promotes immune evasion and tolerogenic DC	Inhibits cell cycle progression in early stages, enhances invasion and metastasis by inducing EMT in advanced stages
IL-10	M2 macrophages, Mast cells, and TAM	Promotes immune evasion	PDAC-associated TAM have a mixed M1 and M2 phenotype, produce high amounts of IL-10, IL-1β, IL-6 and TNFα and induce EMT in early tumorigenesis
IL-6	CAFs and TAM	Promotes Th2-type cytokine production	Promotes oncogenesis through JAK2-STAT3 activation, angiogenesis through the induction of VEGF, cancer cell migration and EMT
IL-1β	DC, M1 macrophages, and TAM	Recruitment of MDSC and T-cell activation by inducing the production of IL-2 and IL-2R	Promotes cancer growth, invasion, and metastases
IL-17	Th 17 CD4+ cells	Recruitment of MDSC	Induces stemness, tumour initiation, and progression, not complete EMT. The expression of the IL-17 receptor is evident on cancer cells undergoing EMT and depends on oncogenic <i>KRAS</i> .
TNFα	M1 macrophages, TAM, neutrophils, mast cells, and PSC	Antagonizes M2 macrophages polarisation	Associated with PDAC initiation. Promotes angiogenesis by inducing VEGF production by fibroblasts and metastases by activating NF-β signalling

CAFs-cancer associated fibroblasts; DC-dendritic cells; EMT-epithelial to mesenchymal transition; MDSC-myeloid derived suppressor cells; PSCs-pancreatic stellate cells; TAM-tumour-associated macrophages. VEGF-vascular endothelial growth factor; TGFβ-transforming growth factor beta; IL-interleukin; TNF-tumour necrosis factor; PDAC-pancreatic ductal adenocarcinoma. Taken from (152)

of the extracellular matrix, CAF promotes tumour growth and metastases by secreting inflammatory cytokines like IL-6, chemokines, and chemokine ligands, specifically chemokines C–C motif chemokine ligand 2 (CCL2) and C-X-C motif chemokine ligand 12 (CXCL12) (153, 154).

Thus, systemic and local inflammation may increase the likelihood of developing PDAC, and once present, the inflammatory infiltrates in the TME encourage tumour growth and spread. Communication between cancer and inflammatory cells occurs through soluble and exosome-carried cytokines, which can contribute to PDAC risk and development.

1.7. Coagulation and cancer

The relationship between cancer and excessive blood coagulation was first noticed in the 1800s by Jean-Baptiste Bouillaud and Armand Trousseau (Trousseau, 1867). Thrombotic complications are common in patients with cancer (155) and are one of the leading causes of death and illness (156-158). The regulation of haemostasis involves plasmatic coagulation, circulating platelets, and the vascular endothelium. It is crucial to maintain a delicate balance between clot formation and bleeding. Evidence suggests that cancer cells can disrupt this equilibrium by activating blood clotting.

Thrombotic events can range from VTE to more widespread changes in the clotting system that may not show clinical symptoms (159, 160). It can indicate the presence of underlying cancer and is also linked to cancer progression and prognosis. The underlying cause of cancer-associated thrombosis (CAT) is complex. It includes direct factors such as procoagulant proteins released into the bloodstream from the tumour (156, 161) and indirect factors such as vascular damage from chemotherapy or surgery (162). These procoagulant proteins include haemostatic proteins (TF, fVIIa) (163, 164), inflammatory cytokines (TNF α , IL-1 β) and proangiogenic factors (VEGF, basic fibroblast growth factor (bFGF)) (165, 166).

TF expressed on the malignant cell surface plays a central role in cancer-associated coagulation (167). The expression of TF and/or fVIIa by cancer cells is thought to be the main promoter of CAT, as they are responsible for initiating coagulation (168). Oncogenic mutations, EMT, tumour hypoxia, inflammatory cytokines and alterations in tumour cell metabolism can lead to the induction of TF expression in cancer cells (169). The oncogenic mutations that can influence TF expression include dysregulation of *p53*, *KRAS* and *PTEN* (170-173).

Elevated TF expression on tumour cells has been associated with tumour progression, worse prognosis, and thrombosis in cancer patients (174). When exposed to blood, TF interacts with plasmatic coagulation factors and facilitates the formation of thrombin, which has various cellular effects. Hence, the expression of TF on cancer cells can serve as a potential link between haemostasis and tumour progression. In addition to TF, fVIIa expression has been found in hypoxic areas of tumours and under normoxic conditions (175, 176). The procoagulant activity of TF and fVIIa can be further increased when they are packaged into microvesicles (MV) and released into the bloodstream (175, 177). This causes systemic activation of the coagulation system (178, 179).

Thrombin induces thrombotic effects through the cleavage of fibrinogen and mediates pleiotropic cellular responses through PARs expressed on different cells, including platelets, neurons, immune cells, fibroblasts, and endothelial cells (EC) (167). In mouse models, cancer cells that overexpress PARs have shown increased metastatic potential (180). In addition, thrombin can activate human platelets by interacting with PAR1 and PAR4, leading to the secretion of various molecules (181). Since platelets secrete multiple factors like VEGF, platelet factor 4, and matrix metalloproteinases, tumours could use their proangiogenic properties to develop new blood vessels, promoting the migration and activation of EC (167, 181). Thrombin-mediated PAR activation can also induce a range of cellular alterations in endothelial cells, including migration and upregulation of VEGF-A, which are essential for angiogenesis.

Cancer cells can also activate platelets, either directly through the expression of adhesion molecules and receptors on their surface (182, 183) or by secreting platelet-activating molecules, such as adenosine diphosphate (ADP) and thromboxane A₂ (184). Cancer cells can indirectly affect coagulability by releasing growth factors, cytokines and proangiogenic factors that alter the properties of vascular EC (166, 185, 186). For example, the expression of IL-6 and TNF α by cancer cells can cause the expression of adhesion molecules, like P- and E-selectin, on the surface of EC and the release of von Willebrand factor (vWF) into the bloodstream (156, 182), which facilitate the binding and activation of platelets (182, 187).

The activation of EC by tumour cells converts their non-thrombotic and anti-inflammatory surface to an adhesive and procoagulant one (188). This conversion occurs through tumour cell-generated thrombin or the secretion of VEGF-A by the tumour cells. The endothelial cell activation is characterised by the secretion of several factors stored in endothelial Weibel-Palade bodies, including IL-8, angiopoietin-2 (Ang2), P-selectin, and vWF (188, 189). Upon secretion, the vWF is

stretched in the blood flow, exposing binding sites for circulating platelets, thus promoting its procoagulant activity (190). Therefore, molecules adjacent to vWF and stored in EC have also been investigated to predict CAT.

It is clear that coagulation plays a role in the advancement of tumours, and components of the coagulation cascade have been identified as potential biomarkers for malignancy. However, the connection between thrombotic events and inflammatory processes has yet to be determined.

1.7.1. Coagulation proteins and pathways

Coagulation proteins are a series of proteases which, together with their co-factors, initiate the coagulation cascade following vascular injury (Table 9). The coagulation pathway can be divided into intrinsic, extrinsic, and common pathways, which involve the sequential activation and interaction of different coagulation factors. The pathways converge at the activation of prothrombin to thrombin, which then converts fibrinogen into fibrin, forming a stable blood clot (Figure 11). The coagulation system is tightly controlled by anticoagulant proteins and the fibrinolytic system. Activation of the coagulation system has been linked to other biological processes involved in wound healing, such as angiogenesis. However, the dysregulation of these processes can significantly contribute to the development of chronic diseases like cancer and cardiovascular disease.

1.7.2. Role of coagulation proteins in cancer progression

There is a close association between coagulation activation and tumour progression. Different components of the haemostatic system, including thrombin, TF and fVIIa, factor Xa (fXa), fibrinogen and vascular cells, contribute to tumour growth and aggressiveness through both clotting-dependent and clotting-independent properties.

1.7.3. Tissue factor

TF, also referred to as thromboplastin, coagulation factor III, or CD142, is a transmembrane glycoprotein with a molecular weight of 47 kDa (191). It is classified as a type I integral membrane protein and is made up of three domains: an extracellular domain (residues 1-219), a transmembrane domain (residues 220-242), and a cytoplasmic domain (residues 243-263) (192, 193). The extracellular domain consists of two fibronectin type III domains connected at an angle of 125 degrees, irrespective of whether the protein is bound to fVIIa or in a free state (194, 195). TF plays a critical role in haemostasis as it is the primary initiator of the coagulation cascade. It functions as a

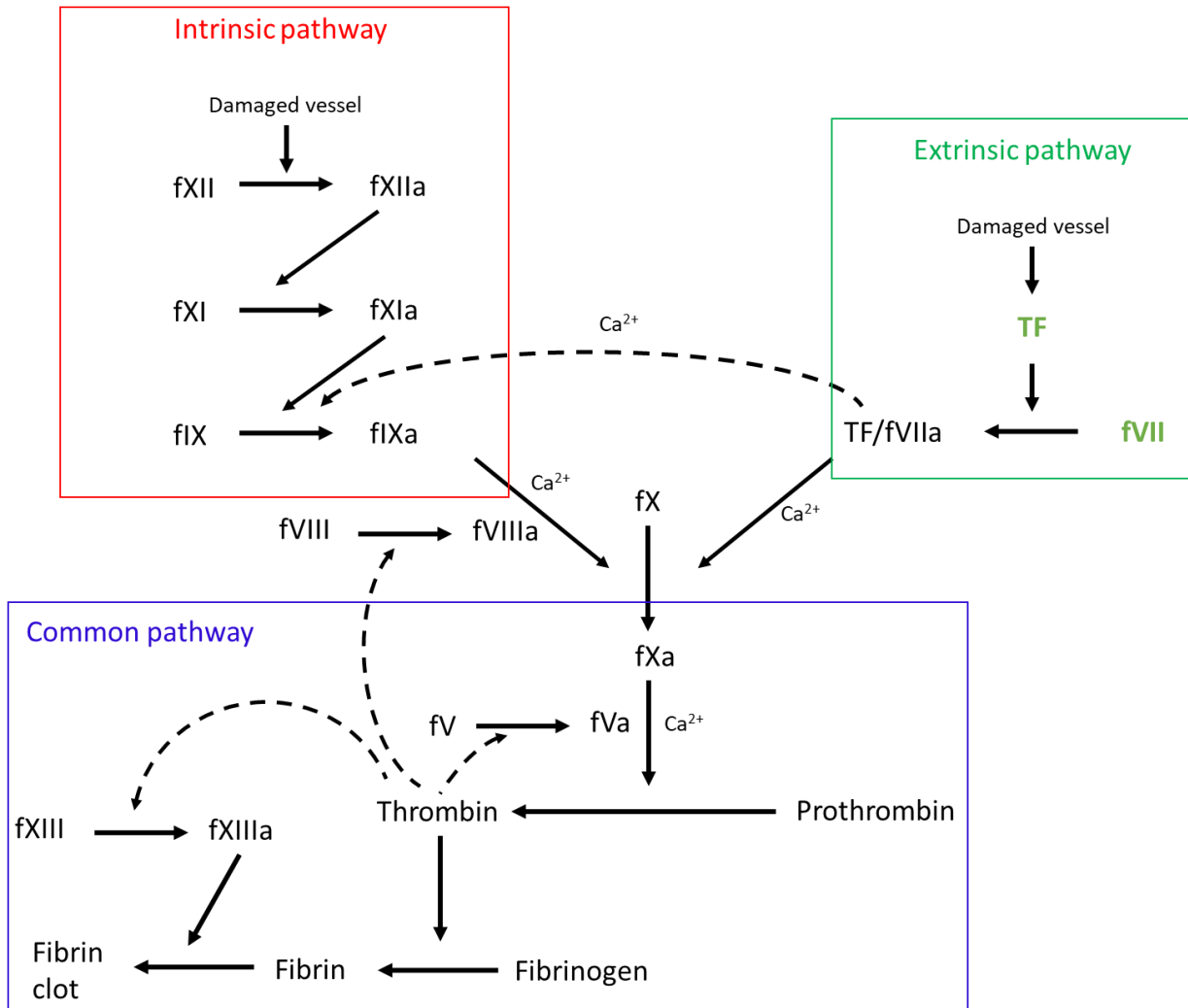
Table 9: Coagulation factors

Clotting factor number	Clotting factor name	Function	Plasma half-life (h)	Plasma concentration (mg/L)
I	Fibrinogen	Clot formation	90	3000
II	Prothrombin	Activation of I, V, VII, VIII, XI, XIII, protein C, platelets	65	100
III	TF	Co factor of VIIa	-	-
IV	Calcium	Facilitates coagulation factor binding to phospholipids	-	-
V	Proacclerin, labile factor	Co-factor of X-prothrombinase complex	15	10
VI	Unassigned			
VII	Stable factor, proconvertin	Activates factors IX, X	5	0.5
VIII	Antihaemophilic factor A	Co-factor of IX-tenase complex	10	0.1
IX	Antihaemophilic factor B or Christmas factor	Activates X: Forms tenase complex with factor VIII	25	5
X	Stuart-Prower factor	Prothrombinase complex with factor V: Activates factor II	40	10
XI	Plasma thromboplastin antecedent	Activates factor IX	45	5
XII	Hageman factor	Activates factor XI, VII and prekallikrein		-
XIII	Fibrin-stabilising factor	Crosslinks fibrin	200	30
XIV	Prekallikerin (F Fletcher)	Serine protease zymogen	35	
XV	HMWK- (F Fitzgerald)	Co factor	150	
XVI	vWf	Binds to VIII, mediates platelet adhesion	12	10 µg/mL
XVII	Antithrombin III	Inhibits IIa, Xa, and other proteases	72	0.15-0.2 mg/mL
XVIII	Heparin cofactor II	Inhibits IIa	60	-
XIX	Protein C	Inactivates Va and VIIIa	0.4	-
XX	Protein S	Cofactor for activated protein C		-

HMWK – High molecular weight kininogen; vWf – Von Willebrand factor; TF – Tissue factor

Proteases highlighted by the blue boxes are of particular interest for the current study. Taken from (196)

Figure 11: Coagulation pathways



The coagulation cascades in the blood can be categorised into extrinsic, intrinsic, and common pathways. The extrinsic pathway is activated by the exposure of TF on the surface of injured tissue following vascular injury. On the other hand, the intrinsic pathway is activated by the exposure of negatively charged molecules such as collagen and ADP, leading to the activation of factor XII. These two pathways merge at the common pathway to initiate the final steps of blood clot formation.

receptor and co-factor for coagulation factor fVII(a), which leads to fVIIa cleavage of fX and fXI. The fibronectin-like domain's upper region (residues 1-107) is where the amino acid residues responsible for the interaction with fVII(a) are located, while the lower region (residues 108-219) contains the residues responsible for the interaction with fX or fXI (197). Two disulphide bridges, Cys49-Cys57 and Cys186-Cys209, are present in each fibronectin type III domain (191). Changes in the reduction status of the Cys186-Cys209 disulphide bonds have been found to decrease the binding affinity for fVIIa and completely abolish the interaction of TF with fX or fXI (198). TF is glycosylated and contains three glycosylation sites in the extracellular domain at Asp11, Asp124, and Asp137 (191, 199). However, TF's glycosylation is not essential for its function (200).

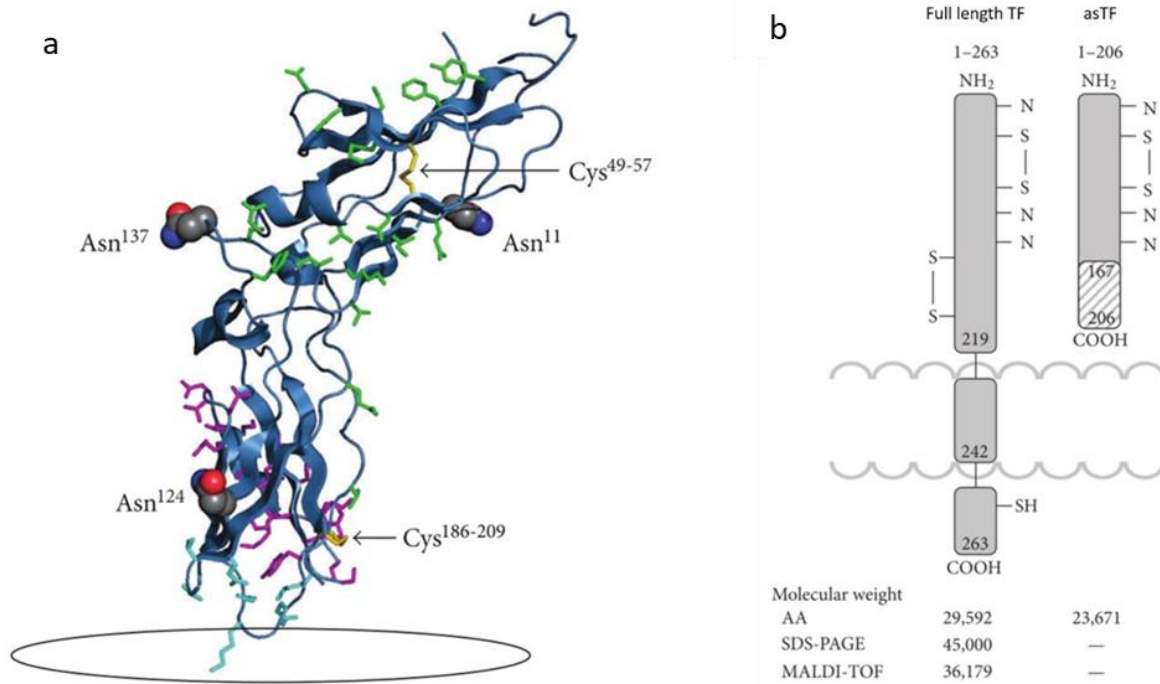
Besides its role in coagulation, TF also acts as a signalling receptor capable of regulating cellular functions. For instance, the cleavage of PAR by TF/fVIIa has been found to impact cell migration, proliferation and apoptosis (201). Moreover, the interaction of TF with integrin adhesion molecules can induce cell migration and promote angiogenesis (202). TF signals are suggested to be triggered and/or controlled by the cytoplasmic domain of the protein (203, 204). Although this domain does not possess any enzymatic activity (204, 205), it contains a palmitoylation site (Cys245), two phosphorylation sites (Ser253 and Ser258), and an ubiquitination site (Lys255). The modification of these sites has been shown to affect TF signalling.

An isoform of TF called alternatively-spliced TF (asTF), produced from a splice variant of TF pre-messenger ribonucleic acid (mRNA) that excludes exon 5, has been discovered. Unlike full-length TF (flTF), asTF is a 26 kDa isoform that does not contain the usual transmembrane and cytoplasmic domains but instead has a unique c-terminus (206) that is not similar to any other known protein sequence (207). This unique c-terminus contains a cluster of five positively charged residues that allow asTF to interact with cell membranes, even though it does not have a transmembrane domain (13) (Figure 12). Although asTF can bind fVII(a), it lacks large portions of the fX and fXI binding site and therefore has no procoagulant activity. However, despite lacking procoagulant activity, asTF has been reported to have the ability to induce cellular signalling (206-208).

1.7.3.1. Role of TF in tumour progression

Aside from its involvement in thrombosis, TF plays a vital role in the progression of tumours. TF is highly expressed in cancer tissues and circulating tumour cells (CTCs). It is the activation of fVII to fVIIa which leads to increased tumour cell proliferation, angiogenesis, EMT, and activity of CSC.

Figure 12: The structure of TF



a- The extracellular domain of TF has specific residues that enable it to bind with both fVII(a) (green) and fX or fXI (magenta). Furthermore, the C-terminal end of the TF extracellular domain interacts with the cell membrane (aqua). TF also has three potential glycosylation sites (red) and two disulfide bridges (yellow) (Adapted from (197))

b- The structures of TF and asTF are compared, where asTF lacks the transmembrane or cytoplasmic domains and instead has a unique C-terminus. (Adapted from (191)).

Additionally, TF and TF-positive microvesicles (TF+MVs) activate the coagulation system to promote the formation of clots that include non-tumour cell components such as platelets, leukocytes, and fibrin. These clots cause tumour cells to adhere to them and form CTC clusters. The tumour cells then utilise the clots to reduce fluid shear stress, resist anoikis, escape the immune system, and facilitate adhesion, extravasation, and colonisation.

1.7.3.2. TF expression in cancer cells and stroma

TF expression is upregulated in human malignancies (Table 10) and can be found in three different compartments; cancer cells, their adjacent stroma, and the circulating blood (209-212). This increase in expression can be up to 1000-fold greater than normal cells and is consistent across various types of human cancers with a few exceptions. While some attribute this consistency to non-specific micro-environmental conditions, such as inflammation, thrombosis, and hypoxia, the increased expression of TF is also observed *ex vivo*, suggesting intrinsic factors involved in the malignant process. Recently, evidence has emerged linking TF expression to oncogenic pathways, changes in cellular differentiation status, and the formation of the CSC hierarchy (213).

Several pro-oncogenic events can activate TF expression in cancer, such as mutations in the tumour suppressor *TP53* and proto-oncogene *KRAS*, which activate mitogen-activated protein kinases (MAPK) and PI3K/AKT signalling pathways (170, 212). Amplification of the epidermal growth factor receptor (EGFR) or its mutant form, EGFRvIII, in glioma cells also increases TF-mediated signalling, resulting in increased TF expression, PARs, and fVII production (214). Blocking EGFR signalling in cancer cells reduces TF expression (215), while loss of tumour suppressor *PTEN* (216, 217) or E-cadherin leads to TF upregulation. *MYCN* amplification is associated with high levels of TF in neuroblastoma (218). Hypoxia can also stimulate TF expression via hypoxia-associated signalling molecules, such as hypoxia-inducible factor 1-alpha, Egr-1, Cyr61, and VEGF (219, 220).

1.7.3.3. Role of TF in cancer cell proliferation

TF is strongly linked to the proliferation of tumour cells. Both fITF and asTF have been shown to increase the proliferation of various types of cancer, possibly via different mechanisms (221). In an experiment involving the transplantation of PC cells into nude mice, the tumour volume of TF-positive cells was larger than that of TF-negative cells (222). In colon cancer cells, fITF:fVIIa activates PAR2, which leads to increased proliferation via the protein kinase C (PKC) α and extracellular signal-regulated kinase (ERK)1/2 pathways (223, 224). In breast cancer cells, the pro-proliferative effect of

Table 10: Overexpression of TF and progression of human malignancies

Cancer	TF overexpression and correlates
Bladder	TF in urine of patients with bladder cancer (225)
	TF expression and bladder cancer progression (226)
	TF in bladder cancer N0 and patient survival (227)
Brain	TF in high-grade tumours and blood vessels (228)
	TFPI and low TF in haemorrhagic GBM (229)
	TF levels correlate with tumour progression (230)
	TF staining increases with tumour grade (231)
	Proposed linkage between TF, vaso-occlusive events and Pseudopalisades in GBM (232)
Colon	Increase in TF+MV in blood of cancer patients (233)
	TF and VEGF levels correlate in tumours (234)
	TF levels correlate with angiogenesis, VEGF expression and disease progression (235)
	TF levels correlate with poor prognosis and liver metastasis (236)
	TF overexpression correlates with an increase in angiogenesis and metastasis (237)
	Increased TF levels in metastatic cell lines (238)
	FVII dependence of tumour-induced coagulation (239)
Gastric	TF levels correlate with venous invasion and lymphatic metastasis in intestinal-type tumours (240)
Leukaemia	TF predominates in M3 and M4–M5 blasts (241)
	Increased TF levels in leukaemic cells (242)

	TF overexpression in leukaemic blasts (243)
	Overexpression of TF in AML and ALL (244)
	TF overexpression in AML (245)
Other	No increase in TF levels in haematopoietic malignancies (246)
haematopoietic malignancies	TF upregulation in paediatric lymphoma (247)
Lung	Overexpression of full-length and variant TF (asTF) in NSCLC (248)
	Hypercoagulability and disease progression in NSCLC in association with the presence of TF and asTF in tumours and in circulation (249)
	TF+MV in blood accompany Trousseau's syndrome (250)
	Microparticle-associated TF accompanies DIC (251)
	Association of high TF expression with metastasis (252)
	TF levels correlate with tumour angiogenesis (253)
Melanoma	Unchanged levels of TF with a decrease in TF pathway inhibitor (254)
Ovary	Increase in TF expression and associated thrombosis (255)
	TF in serum is associated with poor prognosis (256)
	Increased expression of TF and coagulation intermediates are detectable in ovarian cancer (257)
Pancreas	Circulating TF+MV parallel disseminated disease (210)
	TF expression correlates with VEGF production, angiogenesis and thrombosis (5)
	Expression of cell-associated and soluble TF correlate with the onset of coagulation (258)

	Involvement of TF in tumour invasiveness, metastasis and progression (6)
	Increasing TF levels parallel tumour progression (259)
Liver	TF expression correlates with progression and angiogenesis in hepatocellular carcinoma (260)
Prostate	TF levels correlate with Gleason score (261)
	TF is present on prothrombotic MV (prostasomes) from cancer patients and contributes to coagulopathy (262)
	Plasma MV TF levels correlate with cancer coagulopathy and risk of recurrence (263)
	TF expression correlates with poor survival (264)
	TF expression is associated with tumour angiogenesis and metastasis (265)
	TF expression correlates with tumour progression and angiogenesis (266)

Taken from (213)

asTF is dependent on β 1 integrin (267). TF in cancer cells has several anti-apoptotic properties, including activating signalling pathways such as phosphoinositide 3-kinases (PI3K), AKT, and janus kinase (JAK)/STAT5, suppressing death-associated protein kinase-1, and enhancing Bcl_{XL} expression (268-272). These properties help prevent a type of apoptosis called anoikis, which is triggered by the loss of anchorage-dependent survival signalling due to the absence of the extracellular matrix (207, 270, 273).

Role of TF on stem cell activity in cancer

CSC are a specific subpopulation of cells in tumours that can self-renew and contribute to therapy resistance, recurrence, and distal metastasis (274). TF has been found to contribute to the CSC phenotype (275). TF expression positively correlates with well-known CSC markers such as CD44 and CD133 and is enriched on CSC compared to non-self-renewing cancer cells (276-280). TF expression has been linked to CSC activity in human squamous cell carcinoma and breast cancer carcinoma (13). Several studies have demonstrated that high expression of TF increases the sphere-forming ability and the expression of stem cell markers in breast cancer and A431 cells (277, 280). Conversely, TF depletion in mice can inhibit the formation of the vascular niche for tumour-initiating CSC (281). Conditional knockdown experiments have shown that the lack of TF can prevent the growth of some xenografted cancers for prolonged periods, followed by abrupt and rapid growth when TF expression is restored. These studies suggest that TF expression increases the activity of CSC, which enables them to resist radiotherapy, chemotherapy, and targeted therapy in some types of tumours. However, in colon cancer cells, it was found that the expression of TF was increased while the activity of CSC was decreased (282), indicating that the relationship between TF and CSC needs further verification in different types of tumours.

1.7.3.4. Role of TF on tumour invasion and metastasis

TF is highly expressed at the invasive edges of various tumours, and its expression is positively correlated with invasiveness (252, 259, 260, 283). The expression of TF is much higher in metastatic cells than in non-metastatic cells (284, 285). The cytoplasmic domain of fITF promotes invasion by activating Rac1 and p38 MAPK, causing the extension of filopodia and lamellipodia (286). fITF-mediated PAR2 activation recruits actin-binding proteins, leading to cytoskeletal reorganisation and cell motility through MAPK and cofilin pathways (287-289).

The interaction between fITF and β 1 integrin promotes cell migration when the fITF cytoplasmic domain is phosphorylated (290), but this interaction requires PAR2 activation. In contrast, asTF enhances cell motility by directly activating β 1 integrins through binding (291). Tumours release fITF-MVs, which can facilitate metastasis through paracrine signalling locally and in distant sites (179, 292). Elevated levels of fITF-MVs have been observed in the plasma of cancer patients, and they can activate PAR1 and PAR2 in noncancerous cells (293, 294). EC stimulated with fITF-MVs express more adhesion molecules and secrete pro-inflammatory molecules that can attract protumour monocytes, creating a pre-metastatic environment for circulating cancer cells (293, 295).

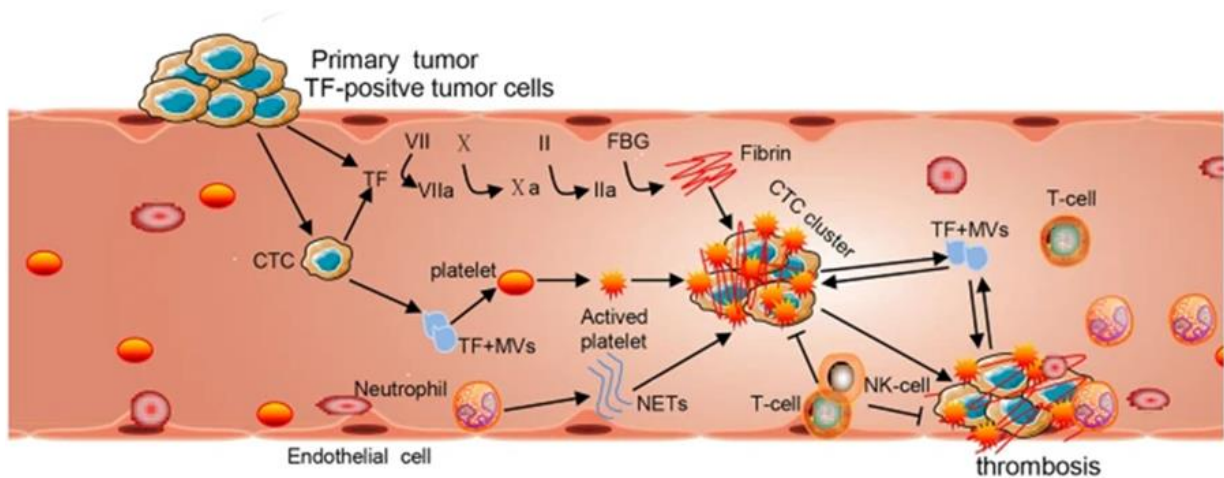
1.7.3.5. Role of TF on CTCs

TF is also highly expressed on the surface of CTCs and is associated with poor patient prognosis (296). EMT-positive CTCs have a stronger ability to metastasise and resist chemoradiotherapy and targeted therapy (297, 298). EMT-positive CTCs express higher levels of TF and exhibit higher metastasis rates and worse survival than EMT-negative CTCs in breast cancer (298). TF is also linked to the procoagulant activity of EMT-positive CTCs (298)(Figure 13). These findings suggest that TF plays an important role in the characteristics of EMT-positive CTCs metastasis.

CTC clusters are formed when two or more CTCs come together during tumour metastasis. They are composed of tumour cells, platelets, leukocytes, and other plasma components. TF-induced coagulation promotes fibrin generation from fibrinogen, which then covers the surface of CTCs along with platelets, leukocytes, and red blood cells to form a clot, ultimately forming a CTC cluster (299-301). TF+MV also have a procoagulant effect and activates platelets, facilitating clot formation (302-304). When tumour cells are covered by platelets, their TF may be less exposed, as platelets per se have no significant TF expression. In addition to the endothelial source, there is an interaction between platelets and leukocytes or leukocyte-derived TF+MVs that may further propagate cancer-induced thrombosis (303, 304).

Leukocytes that express the P-selectin glycoprotein ligand-1 (PSGL-1) and their TF+MVs can interact with platelets that express P-selectin and release NET. This interaction can lead to the recruitment of platelets more efficiently, promoting cancer-induced thrombosis (305, 306). Additionally, the presence of neutrophils elastase (NE) can increase pro-coagulant

Figure 13: TF positive CTC propagate procoagulant activity



Tumour cells that express TF can detach from the primary tumour and form Circulating CTCs. These CTCs can activate coagulation in the blood by releasing TF and TF-positive microvesicles, which leads to the formation of clots that adhere to CTCs and form clusters. This cluster formation can prevent natural killer and T cells from killing the CTCs. When platelets cover the tumour cells, the exposure of their TF may decrease because platelets do not express significant levels of TF. The interaction between activated platelets and leukocytes or leukocyte-derived TF+MVs may further enhance cancer-induced thrombosis. Taken from (307)

activity by inactivating tissue factor pathway inhibitor (TFPI), which can further favour thrombosis (308, 309).

Platelets activated by TF play an important role in CTC cluster formation, as they can form clots to capture tumour cells for survival and protect CTCs from fluid shear stress and anoikis (310-312). Overall, TF plays an important role in the formation and survival of CTC clusters, particularly EMT-positive CTC clusters.

1.7.3.6. Inflammation enhances TF expression

During an inflammatory state, anti-thrombotic factors are downregulated, and the activated EC and blood cells promote increased coagulability. ECs are known to upregulate TF expression in response to various inflammatory cytokines, such as TNF α , LPS, IL-1, c-reactive protein (CRP), and IFN I β , as well as inflammatory coagulation factors Xa and thrombin *in vitro* (313-316). However, factor Xa inhibition, but not thrombin inhibition, has been shown to reduce TF-mediated pro coagulability *in vivo*, highlighting the complex interplay of coagulation proteases that can activate TF (317). Inflammatory conditions in ECs can also induce TF transcription through the action of vasoactive mediators, such as histamine (318) and serotonin (319), VEGF (320), and atherogenic oxidised low-density lipoprotein (321). Monocytes can be induced to express TF via LPS, TNF α , CD40 ligand, CRP, advanced glycosylation end products, and the peptide hormone angiotensin II through its specific receptor (220, 322-324). Other stimuli, such as hypoxia or radiation, were shown to raise TF expression in monocytes and smooth muscle cells (220, 325), and hypoxia-induced TF in mononuclear cells via early growth response-1 leads to vascular fibrin deposition (326). Various signal transduction pathways downstream of vascular inflammation, such as the MAPK, ERK1/2, c-jun terminal NH₂-kinase (JNK), and p38 or the PKC, transmit signals that elicit TF expression in ECs (327-330). Activator protein-1 (AP-1), early growth-response gene product (ERG)-1, and NF- κ B are transcription factors that initiate TF gene transcription by synergistic activation, as demonstrated by reporter gene studies (331).

fITF is responsible for generating thrombin and depositing fibrin in the local area. Once thrombin is produced, it can cleave complement component C5 directly, creating C5a and C5b (332). C5a, also referred to as anaphylatoxin, has a pro-tumorigenic effect by attracting MDSCs to the tumour microenvironment, leading to an immunosuppressive environment

(333). At the same time, TF-induced thrombosis within the TME may result in local ischemia and hypoxia, triggering a local inflammatory response and necrosis of tumour tissue. Hypoxia induced by TF could, in turn, increase flTF, Clk1, and Clk4, producing asTF (220). This potential positive feedback loop may contribute to tumour cell proliferation and angiogenesis and increase MDSC infiltration within the tumour microenvironment. Tumour cell-clot formation caused by TF induces the expression of VCAM-1 and the recruitment of myeloid cells, which promotes tumour invasion and metastasis (334). Overall, TF aids tumour cells to metastasise and evade the host immune system by modifying the tumour microenvironment.

The interplay between inflammation, coagulation and cancer progression makes coagulation proteins, like TF, a potential biomarker of malignant transformation.

1.7.4. Factor VII

FVII is a vitamin K-dependent coagulation factor and forms a complex with TF to initiate the extrinsic pathway of the coagulation system. The human fVII gene is located on chromosome 13 and encodes a 406-amino acid single-chain protein with a mature form that weighs 50 kDa (335). FVII circulates in the plasma as a zymogen with a concentration of approximately 500 ng/ml, and about 1% of the protein is in its active form, fVIIa (336, 337). The protein has a half-life of 2-3 hours and comprises a gamma-carboxyglutamic acid-rich (Gla) domain, two epidermal growth factor (EGF) domains, and a C-terminal catalytic domain. The Gla domain binds Ca^{2+} ions, enabling fVII to associate with the negatively charged phospholipids on the membrane surface of activated cells, while the EGF domains serve as the binding site for TF (337-339). Proteases such as fXa, fIXa, and fXIIa activate fVIIa, and fVII can also activate itself by coming into contact with other TF-fVIIa complexes (340, 341). The activation of fVIIa occurs by cleaving a single peptide bond between Arg152 and Ile153, resulting in a light chain (152 amino acids) and a heavy chain (254 amino acids) held together by a disulphide bond (340-342).

Elevated plasma levels of fVII/fVIIa have been observed in patients with liver cirrhosis (343) and heart disease (344). Although liver cells are the primary source of fVII, other cells, such as monocytes, express the protein in response to inflammatory modulators (345, 346). *In vitro* studies have shown that monocytes and macrophages express fVII/fVIIa on their surfaces in response to lipopolysaccharide stimulation. Additionally, fVII has been found in human

keratinocytes, coronary artery smooth muscle cells, and fibroblasts (347). Various cancers, including ovarian, lung, liver, thyroid, prostate, and stomach cancer, express the ectopic form of fVII/fVIIa protein, which is regulated by hypoxic conditions (163, 348). Ectopic fVII expression has been found to drive the migration and invasion of breast and ovarian cancer cells. It may sensitise tumour cells to respond to promigratory and pro-invasive cues, such as extravasated fX, representing a key factor of malignant tumour progression and metastasis.

1.7.5. FVIIa:TF ratio

A novel study demonstrated that different ratios of fVIIa to TF within microvesicles (MV) could lead to varying outcomes in cultured primary endothelial cells. Results showed that when combinations of purified fVIIa and recombinant TF were incubated with human coronary artery endothelial cells (HCAEC), the ratio of fVIIa to TF determined whether the cells underwent apoptosis or proliferation. The transition from pro-apoptotic to proliferative properties occurred at an estimated fVIIa to TF molar ratio of 15:1, which was consistent with the ratios found in the MV purified from cell lines. For instance, the fVIIa:TF ratio in the 786-O renal carcinoma cell line was 10:1, which induced cellular apoptosis in HCAEC. In contrast, this ratio was 17:1 in MV obtained from the BxPC-3 pancreatic cell line, which was largely ineffective. In addition, higher molar ratios of 54:1 and 38:1 observed in HepG2 hepatocellular and MCF-7 breast cancer lines were concurrent with increased cell proliferation. The change in cell numbers was significantly proportional to the observed fVIIa:TF ratio, with a Pearson correlation of 0.956. However, the concentration of TF with which the cells came into contact was also a critical factor in determining the outcome, in addition to the fVIIa:TF ratio. This was evidenced by the fact that TF-rich MV derived from the MDA-MB-231 cell line (34:1) were significantly less proliferative than those derived from the MCF-7 cell line (38:1), despite the similar fVIIa:TF molar ratios. Therefore, the proliferative/pro-apoptotic property may also be regulated by the higher TF content of MV from MDA-MB-231 cells.

It is important to note that endogenous cellular fVII levels will alter the true ratios obtained, and the level for the transition from pro-apoptotic to proliferative form is likely to be higher than reported here (15:1). Previous studies have also shown the proliferation response by a number of TF-expressing cells following supplementation with exogenous fVIIa (349, 350).

The study also found that the activation of PAR2 is necessary for the pro-apoptotic function of MV, but inhibition of PAR2 prevents this function. Interestingly, simultaneous activation of PAR2 using the activating peptide at the time of MV addition also inhibits the pro-apoptotic effect of 786-O cell-derived MV. The researchers observed that maximal apoptosis in HCAECs was induced at 0.05 nM of MV, and higher concentrations were less effective. This could be due to the endocytosis of PAR2 after rapid activation with fVIIa:TF or with PAR2-activating peptide (AP), which leads to the desensitisation of HCAECs to further stimuli. Therefore, inducing apoptosis in endothelial cells requires controlled activation of PAR2.

The study showed that fVIIa is essential for both the proliferative and pro-apoptotic influence of MV and blocking fVIIa with an inhibitory polyclonal antibody against fVIIa blocked these effects. Moreover, TF is obligatory since the addition of purified fVIIa alone to HCAECs did not promote proliferation or apoptosis. Blocking TF signalling with an antibody did not prevent the pro-apoptotic effect of 786-O cell-derived MV, indicating that TF induces cellular apoptosis through pro-coagulant signalling, which requires the binding of fVIIa with TF.

Incubating HCAECs with higher concentrations of TF alone also promoted cell apoptosis, indicating that fVII is needed to induce apoptosis, and this fVII should be derived from another source. The study found that approximately 20% of the fVII antigen was present on the surface of resting endothelial cells, and incubation of HCAECs with recombinant TF or activation of PAR2 increased the amount of the cell-surface fVII antigen. Thus, endothelial cells may respond to injury/trauma by altering the fVIIa:TF ratio to counter the pro-apoptotic influence that arises from the presence of excessive levels of TF. However, repeated exposure of HCAECs to recombinant TF resulted in the depletion of cellular fVII reserves. The study concluded that the ratio of fVIIa:TF determines the outcome in endothelial cells, resulting in either proliferation or apoptosis, and the pro-coagulant activity of TF is a pre-requisite for both proliferative and pro-apoptotic activities, requiring interaction with fVII.

1.8. Pancreatic cystic lesion

With the widespread use of cross-sectional imaging such as computed tomography (CT), magnetic resonance imaging (MRI), and magnetic resonance cholangiopancreatography (MRCP), there is an increase in the frequency of incidental findings of PCL. Pancreatic cysts may be detected in up to 45% of patients (351-355). Pathologically, PCLs can be classified into

inflammatory fluid collections, non-neoplastic pancreatic cysts, and pancreatic cystic neoplasms (PCNs) (Figure 14, Figure 15). PCNs account for more than half of the PCLs (356). The four subtypes of PCNs are categorised using the WHO histological classification that includes serous neoplasms, MCN, IPMNs and solid pseudopapillary neoplasms (SPNs).

The incidence and prevalence rates of mucinous cystic pancreatic neoplasms are 2.4% and 2.6%, respectively. However, other studies conducted in the past have reported a higher prevalence rate of up to 17.5% (357). MCNs are present in 10% to 20% of resected pancreatic tumours, and the majority of them are benign (72%), while a smaller percentage are borderline (10.5%), in situ carcinoma (5.5%), or invasive carcinoma (12%) (358). Around one-third of IPMNs are discovered to have an invasive adenocarcinoma associated with them (359); however, the association is 60% with main duct (MD)-IPMNs (360). According to a large long-term study involving 1,404 patients with branch duct (BD)-IPMNs, the occurrence of PC within five years of IPMN diagnosis was 3.3%. The incidence rate increased to 15% after 15 years (361). A retrospective study examined the relative frequencies of various PCNs in a series of 851 patients who underwent surgical resection between 1978 and 2011 (362). The study found that IPMN accounted for 38% of the lesions, while MCN, serous cystic tumours, and SPNs accounted for 23%, 16%, and 3%, respectively. Of the 376 patients who underwent surgery between 2005 and 2011, 49% were diagnosed with IPMN, 16% with MCN, 12% with serous cystic tumours, and 5% with solid pseudopapillary neoplasms.

1.8.1. Diagnostic work-up for PCLs

Achieving a precise method of accurate diagnosis and identifying dependable and consistent ways of categorising the risk of cancer in patients with PCLs challenging (Table 11). Several groups have proposed management recommendations or algorithms for patients with suspected cystic neoplasm of the pancreas. Fukuoka guidelines, also known as International Consensus Guidelines (ICG), were published in 2012 and were updated again in 2017 (46) (Figure 16).

Patients who are asymptomatic and have cysts less than 5 mm in size are unlikely to have a cyst with invasive carcinoma and may not need further workup; however, follow-up is still recommended (356, 363). However, if the cyst size is greater than 5 mm, it is recommended to undergo a pancreatic protocol CT or gadolinium-enhanced MRI with MRCP for a better

Figure 14: Types of pancreatic cystic lesions

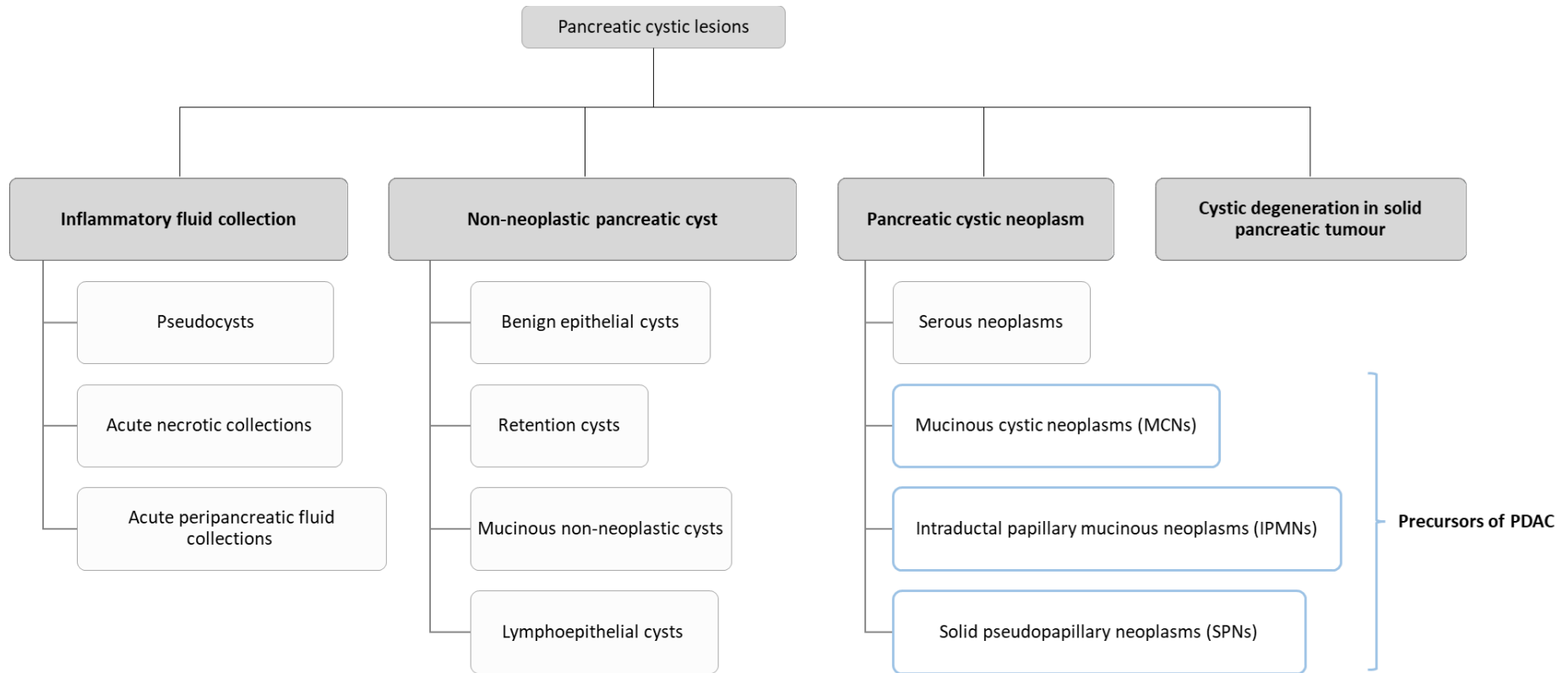
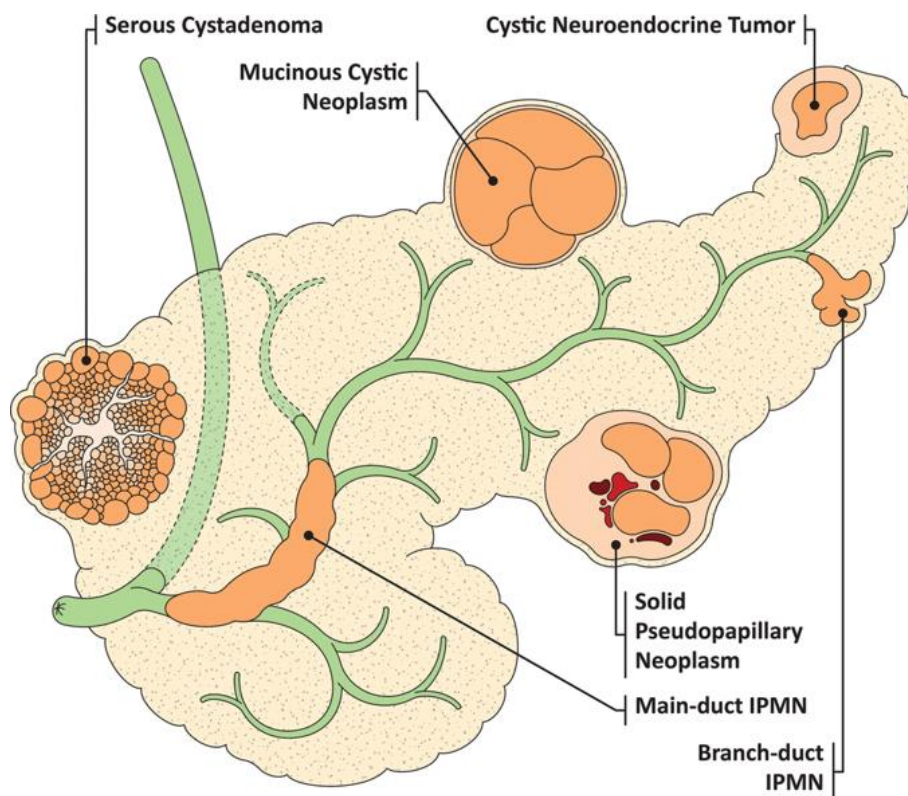


Figure 15: Diagram of pancreatic cystic lesions



Pancreatic cystic lesions, including serous cystadenoma, MCN, IPMN, SPN, and cystic neuroendocrine tumour. Taken from (364)

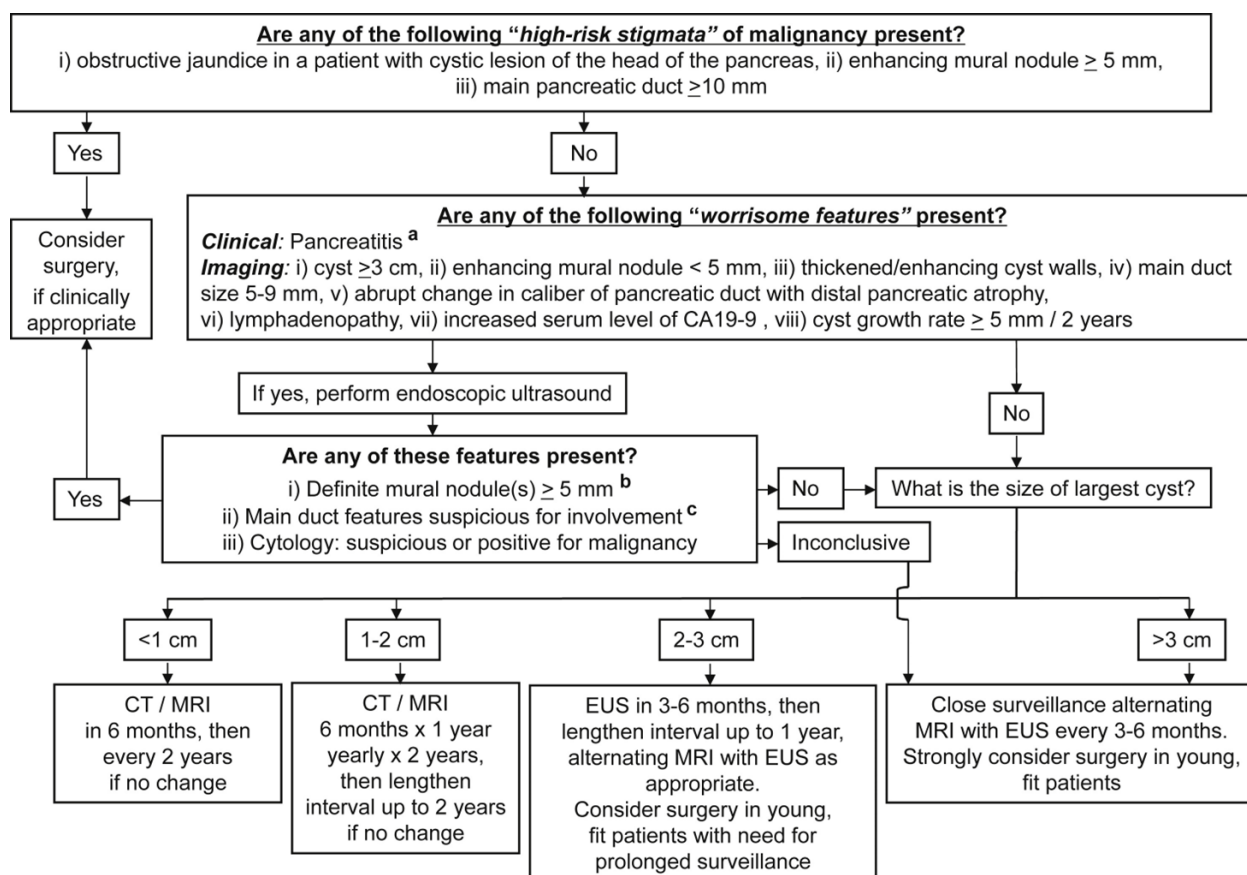
Table 11: Characteristics of the major types of cystic lesions of the pancreas

Type of PCL	Age at diagnosis (years)	Gender distribution	Connection to main duct	Characteristics on imaging	Fluid CEA	Fluid amylase	Solitary or multifocal	Malignancy rate
Pseudocyst	Any	Equal	Some	Well-circumscribed, oval, or round, anechoic on EUS, low attenuation on CT	Low	High	Either	None
Serous cystic neoplasm	40s–60s	75% female	No	Microcystic/honeycomb, 30% have a central scar	Low	Low	Solitary	None
Solid-pseudopapillary neoplasms	20s	90% female	No	Well-demarcated mixed solid-cystic tumours. Occur anywhere in the pancreas	Low	Low	Solitary	High

Type of PCL	Age at diagnosis (years)	Gender distribution	Connection to main duct	Characteristics on imaging	Fluid CEA	Fluid amylase	Solitary or multifocal	Malignancy rate
Cystic pancreatic neuroendocrine tumour	30s–50s	Equal	No	Well-circumscribed cystic lesion with peripheral rim enhancement	Low	Low	Typically solitary	<2 cm in size: Low >2 cm in size: Moderate
Mucinous cystic neoplasm	40s–60s	Almost exclusively females	No	May be unilocular or septated, some have peripheral calcifications, most located in the tail of the pancreas	High	Low	Solitary	<3 cm in size: <5% >3 cm in size: high
Main duct IPMN	40s–60s	Equal	Yes	Dilation of PD	High	High	Either	Very high
Branch duct IPMN	40s–60s	Equal	Yes	Dilation of side branches of PD; grape-like cystic lesion	High	High	Either	Variable (depending on high-risk features)

Taken from (365)

Figure 16: Algorithm for the management of suspected BD-IPMN



Algorithm for the management of suspected BD-IPMN. a. Pancreatitis may be an indication for surgery for the relief of symptoms. b. Differential diagnosis includes mucin. Mucin can move with a change in patient position, may be dislodged on cyst lavage and does not have Doppler flow. Features of true tumour nodules include lack of mobility, presence of Doppler flow and FNA of nodule showing tumour tissue. c. The presence of any one of thickened walls, intraductal mucin or mural nodules is suggestive of main duct involvement. In their absence, main duct involvement is inconclusive. Abbreviations: BD-IPMN, branch duct - intraductal papillary mucinous neoplasm; FNA, fine needle aspiration. Taken from (46).

assessment (366). Based on better contrast resolution, allowing identification of septae, nodules, and duct communication, a consensus of radiologists has suggested that dedicated MRCP is the preferred method for evaluating a pancreatic cyst (366). Furthermore, since patients may require frequent follow-up imaging, MRI can help avoid radiation exposure. Cysts that cause symptoms are more likely to develop invasive carcinoma and HGD. Further evaluation or resection should be conducted depending on the clinical circumstances. Patients with worrisome features (367-372) on imaging should be evaluated with endoscopic ultrasonography (EUS) (Table 12) to further stratify the lesion. The cysts with obvious high-risk stigmata should undergo resection without further testing in surgically fit patients (373) (Table 13, Table 14).

1.8.2. Characterisation of the cyst fluid

1.8.2.1. Cytology

Cytology depends on MUC-containing cells (for IPMN and MCN), malignant cells, glycogen-rich cuboid cells for serous cystic tumour (SCT), branching papillae with myxoid stroma in the case of a SPN, and abundant anucleate squamous cells and debris in lymphoepithelial cysts. Fluids from the mucinous cysts are frequently acellular in the absence of solid components. A systematic review of cytology revealed that the sensitivity of detecting benign mucinous cysts was 45%, while the sensitivity of detecting malignant cysts was 48% (374). The results were even worse for diagnosing SCT; out of 60 cases, only 23 (38%) yielded a positive result based on 11 studies that had confirmed histopathology, the pooled sensitivity and specificity for differentiating mucinous from nonmucinous lesions was 63% (95% CI, 0.56- 0.70) and 88% (95% CI, 0.83–0.93), respectively (375). According to a meta-analysis of four studies involving 96 patients, cytology demonstrated a relatively low sensitivity (64.8% with 95% CI of 0.44-0.82) but a high specificity (90.6% with 95% CI of 0.81-0.96) for pancreatic cancer. While negative results do not necessarily exclude the possibility of a high-risk lesion, positive results are an indication for surgical resection according to all of the guidelines. As negative cytology has a poor negative predictive value, it is reasonable to perform FNA in cysts associated with a solid lesion to determine the presence of malignancy. However, a two-tier system (Table 15) for grading epithelial atypia recommended by the Papanicolaou Society of Cytopathology,

Table 12: Indication for EUS in PCLs

	Indications for endoscopic ultrasound
2015 AGA	<p>≥2 high-risk features</p> <p>Cyst size ≥3 cm</p> <p>Dilated PD</p> <p>Presence of a solid component</p>
2017 International Consensus	<p>If any of the following present</p> <p>Pancreatitis due to cyst</p> <p>Cyst size ≥3 cm</p> <p>Enhancing mural nodule <5 mm</p> <p>Thickened/enhancing cyst walls</p> <p>PD 5–9 mm</p> <p>Abrupt change in diameter of PD with distal pancreatic atrophy</p> <p>Lymphadenopathy</p> <p>Elevated CA-19-9</p> <p>Rapid growth of cyst (>5 mm/2 years)</p>
2018 ACG	<p>If any of the following present</p> <p>PD ≥5 mm</p> <p>IPMN or MCN ≥3 cm</p> <p>Change in PD calibre with upstream atrophy</p> <p>Size increase of ≥3 mm/year during surveillance</p> <p>Jaundice due to cyst</p> <p>Pancreatitis due to cyst</p> <p>Presence of a mural nodule or solid component</p>
2018 European	<p>Clinical or radiological features of concern for malignancy Can be alternated or done in conjunction with MRI during surveillance</p>

ACG, American College of Gastroenterology; AGA, American Gastroenterological Association; CA-19-9, carbohydrate antigen 19-9; MRI, magnetic resonance imaging; PCN, pancreatic cystic neoplasm; PD, main pancreatic duct. Adapted from (365).

Table 13: Imaging features for diagnostic work-up

Worrisome features	High-risk stigmata
Cyst of ≥ 3 cm	Obstructive jaundice in a patient with a cystic lesion of the pancreatic head
Enhancing mural nodule < 5 mm	Enhanced mural nodule
Thickened enhanced cyst walls	MPD size ≥ 10 mm
MPD size of 5-9 mm	
Abrupt change in the MPD calibre with distal pancreatic atrophy	
An elevated serum level of carbohydrate antigen (CA) 19-9	
A rapid rate of cyst growth > 5 mm/2 years	

Table 14: Indications of surgical resection

Indications for surgical resection	
2015 AGA	Positive cytology on EUS-guided FNA, both a solid component and dilated PD
	both a solid component and dilated PD
2017 International Consensus	Obstructive jaundice with PCN in the head of the pancreas
	Enhancing mural nodule ≥ 5 mm
	PD ≥ 10 mm
	Cytology suspicious or positive for malignancy
2018 ACG	All MD-IPMNs
	Cytology with HGD or malignancy
	Mural nodule
	Concerning features on EUS
2018 European	Absolute indications
	Cytology suspicious or positive for malignancy or HGD
	Solid component
	Obstructive jaundice with PCN in the head of the pancreas
	Enhancing mural nodule > 5 mm
	PD ≥ 10 mm
	Symptoms due to PCN
	Relative indications
	PCN growth rate ≥ 5 mm/year
	Elevated CA-19-9 level;
	PD 5–9.9 mm
	PCN size ≥ 40 mm
	New-onset diabetes mellitus; acute pancreatitis (due to PCN)
	Enhancing mural nodule < 5 mm

ACG, American College of Gastroenterology; AGA, American Gastroenterological Association; BD-IPMN, branch duct intraductal papillary mucinous neoplasm; CA-19-9 carbohydrate antigen 19-9; EUS, endoscopic ultrasound; FNA, fine needle aspiration; IPMN, intraductal

papillary mucinous neoplasm; MCN, mucinous cystic neoplasm; PCN, pancreatic cystic neoplasm; PD, main pancreatic duct; High-grade dysplasia (HGD). Taken from (365).

Table 15: Cytologic features of low- and high-grade atypia in mucinous cyst

Cytological feature	Low-grade atypia	High-grade atypia
Cellularity	Low	Low to high
Architecture	Single cells, small groups or flat sheets of bland-appearing glandular epithelial cells ($\geq 12\text{-}\mu\text{m}$ duodenal enterocyte)	Single cells, small to large three-dimensional crowded cluster ($< 12\text{ }\mu\text{m}$ duodenal enterocyte, papillary architecture)
Nucleus	Round and regular with even chromatin and inconspicuous to occasional discernible nucleoli	Nuclear hypochromasia or hyperchromasia, with or without prominent nucleoli, and nuclear membrane irregularity
Nuclear/cytoplasmic ratio	Low	High
Mucin	Apical cytoplasmic mucin and basally located nuclei; the cells may be indistinguishable from gastric contamination	A variable amount of cytoplasm with or without visible mucin or vacuoles
Background	Muciphages, no necrosis	Variable cellular necrosis

which includes low-grade atypia (low- and intermediate-grade dysplasia) and high-grade atypia (HGD) is useful once the presence of a mucinous cyst is determined (376).

1.8.2.2. Chemical analysis of cyst fluid

1.8.2.2.1. Tumour markers

Tumour markers, carcinoembryonic antigen (CEA) and carbohydrate antigen 19-9 (CA19-9), and biochemical markers like amylase and mucin are used to diagnose the premalignant lesion. Of all the tests available, CEA has the highest diagnostic accuracy when distinguishing premalignant mucinous cysts from nonmucinous ones (377, 378). However, CEA cannot differentiate between a premalignant cyst and a malignant lesion (379, 380). CEA analysis requires up to 1 ml of cyst fluid (381, 382). The drawback of this test is that in cases of small cysts or viscous aspirates, an insufficient volume may be obtained.

A >192 ng/ml CEA level captures 79% of the mucinous cyst (356). The cooperative pancreatic cyst showed this as the optimum level for distinguishing mucinous cysts from nonmucinous cysts, with 75% sensitivity and 84% specificity. At this cut-off value, the PANDA study found a sensitivity of 64% and specificity of 83% for diagnosing a mucinous cyst (382). Van der Waaij et al. demonstrated that using a cut-off level of >800 ng/mL for CEA testing could yield higher specificity (98%) but at the cost of low sensitivity (48%) (374). However, elevated levels of CEA alone cannot definitively differentiate between a benign or neoplastic cyst fluid cancer antigen 19-9 is rarely used. CA19-9 at a <37 U/ml level in the fluid may indicate the presence of a pseudocyst or a serous lesion, with a sensitivity of 19% and specificity of 98% (374).

1.8.2.2.2. Amylase

The presence of amylase in the cyst fluid is consistent with ductal communication. The cut-off value for the cyst fluid amylase is selected as the upper limit of normal serum amylase values, which is set at 250 U/L. Cyst with amylase <250 U/L excludes pseudocyst (374) and also indicates a lack of ductal communication with a specificity of 98% (374, 383). However, low amylase does not exclude malignancy (384). The highest level of amylase is observed in pseudocysts. The sensitivity (62.5%) and specificity (69.4%) for diagnosis of premalignant or malignant lesions with amylase are lower than those of CEA and CA19-9 (385).

1.8.2.2.3. Mucin (MUCs)

Mucins are heavily glycosylated glycoproteins commonly expressed in epithelial cells lining the MCNs. The subtypes of MUCs vary depending on the histopathological subtypes of IPMNs, including gastric, intestinal, pancreaticobiliary, and oncocytic subtypes. MUC staining has reported a PPV of 83%, but sensitivity was poor (386). A large series of mucinous cysts reported a sensitivity of 80% and a specificity of 40% (387). Maker et al. investigated the ability of mucin to determine the degree of IPMN dysplasia, as the different IPMN subtypes also correlate with specific degrees of dysplasia (388). They found a significant increase in MUC2 and MUC4 among cysts with HGD and increased MUC2 in intestinal-type IPMNs with a higher degree of malignant transformation. Recent studies have demonstrated that mucins can carry abnormal glycoforms, including oligosaccharide linkages α GlcNAc and β GlcNAc associated with MUC5AC, which were found to be associated with malignancy (389). However, the diagnostic utility of cyst fluid levels of mucins in determining the degree of dysplasia is limited, as one study did not show variation in the degree of dysplasia.

1.8.2.3. Molecular analysis

The addition of molecular analysis to other diagnostic tests can provide significant value. Kadayifci et al. investigated the usefulness of GNAS testing in conjunction with KRAS and CEA testing of pancreatic cyst fluid. The combination of these three markers resulted in improved accuracy in diagnosing BD-IPMN when compared to single tests ($p < 0.05$) (390). However, KRAS and/or GNAS detection alone in pancreatic cyst fluid (PCyF) are highly sensitive and specific (100% and 96%, respectively) for diagnosing BD-IPMN (391). Singhi et al. discovered this in their 2018 study, where molecular analysis outperformed fluid viscosity and elevated CEA levels as diagnostic tools. Other mutations have been identified that contribute to BD-IPMN carcinogenesis. Ren et al. revealed that in mucinous PCLs without KRAS mutations, BRAF mutations with concurrent GNAS mutations supported an alternate mechanism of activation in the Ras pathway (392). Over the years, many studies have been performed to risk-stratify PCLs, especially branch-duct (BD)-IPMNs, to avoid unnecessary surgeries. These studies describe various options for BD-IPMN to risk stratification into LGD or HGD/invasive carcinoma (Table 16).

Table 16: Overview of reviewed studies regarding the use of cyst fluid for risk stratification of branch

Author	Molecular Marker(s)	Key Findings	Diagnostic Parameters	Conclusions
Singhi (2018)	<i>TP53, PIK3CA, PTEN, KRAS, GNAS</i>	Combination of <i>KRAS/GNAS</i> and <i>TP53/PTEN/CDKN2A</i> indicates advanced neoplasia	Analysis of <i>KRAS/GNAS</i> and <i>TP53/PTEN/CDKN2A</i> was 100% specific and 89% sensitive for advanced neoplasia	The integration of molecular testing in pre-operative patients can be useful in predicting future risk of malignancy.
Hata (2018)	Telomere fusions	Branch duct IPMN cyst fluid aspirates revealed no telomere fusions in low-grade lesions, however, prevalence increased with advancing histologic grade	Prevalence of telomere fusions: Low grade 0% Intermediate 15.4% High 26.9% Cancer 42.9% p = 0.025	Telomere fusions can be readily detected in cyst fluid and help predict the grade of dysplasia
Shirakami (2021)	miR-711, miR-3679-5p, miR-6126, miR-6780b-5p, miR-6798-5p, and miR-6879-5p	Six miRNAs were significantly elevated in the cyst fluid of branch duct IPMN with carcinoma when compared to benign branch duct IPMNs	Differences in miRNA levels between low-grade and high-grade lesions were all statistically significant (p < 0.05)	Certain miRNAs are elevated in the cyst fluid of cancerous lesions thus offering the potential to predict high-risk lesions requiring surgical resection

Author	Molecular Marker(s)	Key Findings	Diagnostic Parameters	Conclusions
Hata (2017)	<i>SOX17, PTCHD2, BNIP3, FOXE1, SLIT2, EYA4, and SFRP1</i>	Gene methylation patterns can accurately distinguish between advanced neoplasia and low-grade lesions (all but <i>BNIP3</i>)	Single marker: <i>SOX17</i> sensitivity 83%, specificity 82% Two gene: <i>SOX17/FOXE1</i> or <i>EYA4</i> accuracy 86% Four gene: <i>FOXE1/SLIT2/EYA4/SFRP1</i> accuracy 88%, 84% sensitivity, and 89% specificity	Cyst fluid analysis of gene methylation patterns, whether a single gene or in combination, can accurately distinguish between advanced neoplasia and low-grade lesions
Majumder (2019)	<i>TBX15</i> and <i>BMP3</i>	Two gene methylation analysis can discriminate between advanced neoplasia and low-grade lesions	Combination of methylated <i>TBX15</i> and <i>BMP3</i> had sensitivity 90% and specificity of 92% for detecting advanced neoplasia	Methylation analysis of this two gene combination can be useful in predicting the grade of dysplasia
Singhi (2016)	<i>TP53, PIK3CA, PTEN</i>	Molecular analysis of cyst fluid was able to detect advanced neoplasia via mutations in <i>TP53, PIK3CA, and/or PTEN</i>	Detected branch duct IPMN harbouring advanced neoplasia with 91% sensitivity and 97% specificity	Integration of molecular analysis in PCLs can better detect cysts with advanced neoplasia than AGA guidelines

Author	Molecular Marker(s)	Key Findings	Diagnostic Parameters	Conclusions
Khalid (2009)	<i>KRAS</i> , allelic loss, DNA quantity	10/40 malignant cysts had negative cytology, all of which could be diagnosed as malignant with high amplitude <i>KRAS</i> mutation in conjunction with high amplitude allelic loss	High amplitude <i>KRAS</i> mutation followed by allelic loss: 96% specific and 37% sensitive for malignancy in the cyst	Increased cyst fluid DNA quantity, high-amplitude mutations, and allelic loss can be used to predict malignancy, especially when cytology is negative
Springer (2015)	<i>SMAD4</i> , LOH in <i>RNF43</i> and <i>TP53</i> , Chromosomal aneuploidy	Analysis for <i>SMAD4</i> , <i>TP53</i> , LOH in chromosome 17, or aneuploidy of 5p, 8p, 13q, or 18q could correctly identify HGD or invasive cancer. This could reduce unnecessary operations by 91%	The panel could identify patients requiring surgery with 75% sensitivity and 92% specificity	Molecular analysis of cyst fluid can be used to risk-stratify cysts with malignant potential and can reduce the amount of unnecessary operations
Rosenbaum (2017)	<i>TP53</i> , <i>SMAD4</i> , <i>CDKN2A</i> , <i>NOTCH1</i>	NGS revealed mutations in <i>TP53</i> , <i>SMAD4</i> , <i>CDKN2A</i> , and <i>NOTCH1</i> to only be present within malignant cysts.	These mutations had 100% specificity and 46% sensitivity for carcinoma	Variants in <i>TP53</i> , <i>SMAD4</i> , <i>CDKN2A</i> , and <i>NOTCH1</i> favour the diagnosis of high-risk cysts and warrant surgery or further investigation

Author	Molecular Marker(s)	Key Findings	Diagnostic Parameters	Conclusions
Fujikura (2021)	<i>KLF4</i>	<i>KLF4</i> mutations detected in cyst fluid samples were significantly more prevalent in cysts with low-grade dysplasia	<i>KLF4</i> prevalence: Low grade 50% Intermediate 39% High 15%	High and low grade IPMNs have distinct molecular pathways with <i>KLF4</i> mutations being enriched in the low grade pathway
Simpson (2018)	DNA quantity, LOH in tumour suppressor	High DNA quantity in conjunction with high clonality LOH in tumour suppressor genes could detect advanced neoplasia	High quantity DNA and LOH had specificity of 99%, PPV 60%, and diagnostic accuracy of 91% for advanced lesions	Increased DNA quantity along with LOH in tumour suppressors can be predictive of high-risk lesions

Taken from (393)

While molecular analysis of PCyF has shown to be useful when used along with existing clinical management to improve classification and risk stratification of branch-duct IPMNs, it has yet to be established as a reliable standalone diagnostic method. The need for widespread access to the technology needed to perform molecular analysis is a current issue hindering its clinical implementation. However, advancements in technology and decreasing costs may make it more accessible for wider testing in the future.

1.9. Current NICE recommendation

The current National Institute of Health and Care Excellence (NICE) recommendation (NG85) for people with pancreatic cysts was published on 17th February 2018. The guideline includes the following;

1.1.7 Offer a pancreatic protocol CT scan or MRI/MRCP to people with pancreatic cysts. If more information is needed after these tests, offer the other one.

1.1.8 Refer people with any of these high-risk features for resection:

- obstructive jaundice with cystic lesions in the head of the pancreas
- a main pancreatic duct that is 10 mm in diameter or larger.

1.1.9 Offer EUS after CT and MRI/MRCP if more information on the likelihood of malignancy is needed or if it is not clear whether surgery is needed.

1.1.10 Consider fine-needle aspiration during EUS if more information on the likelihood of malignancy is needed.

1.1.11 When using fine-needle aspiration, perform CEA assay in addition to cytology if there is a sufficient sample.

1.1.12 For people with cysts that are thought to be malignant, follow the recommendations on staging.

Resection of HGD provides an opportunity to cure a lesion before it progresses to an incurable invasive disease. However, previous recommendations for routine resection of IPMN or MCN have resulted in overtreatment, as high-risk pathology is identified in less than half of all patients who have undergone pancreatectomy. The ability of current laboratory, radiographic,

and endoscopic tests to distinguish between low-risk (LGD) and high-risk (HGD) diseases is limited. Therefore, identifying a suitable biomarker that can reliably differentiate HGD and LGD could prevent the morbidity and mortality associated with unnecessary surgery.

1.10. Aims

The role of TF in malignancy and its impact beyond thrombosis on cell proliferation, angiogenesis, and metastasis is well established. Elevated levels of TF have been detected in various cancers, including pancreatic cancer.

In this study, a novel approach was taken to examine the potential of measuring TF and fVIIa levels in the pancreatic cyst fluids as an indicator of the malignant transformation of precursor cystic lesions. The data was compared to the current parameters used during the diagnostic work-up of PCLs. The study also explored the mechanisms by which TF promotes a more invasive phenotype, including EMT, through in vitro experiments with various cell lines. The impact of TF on the regulation of fVII expression and cell proliferation was also examined.

Chapter 2

General Methods

2.1. Materials

Company	Material
Abcam, Cambridge, UK	
American Type Cell Collection, Manassas, USA	AsPC-1, BxPC-3, hTERT-HPNE, hTERT-HPNE E6/E7/K-RasG12D, hTERT-HPNE E6/E7/K-RasG12D/st; Pancreatic cell lines
AssayPro/Universal Biologicals Cambridge, UK	Human Factor VII ELISA Kit
Bio-Rad Laboratories, Watford, UK	TGFβ
Corning – supplied by Scientific Laboratory Supplies Ltd	96-well TC-treated Microplate
Dade Behring, Deerfield, USA	Recombinant relipidated human TF (Innovin®)
eBiosciences/ThermoFisher, Paisley, UK	Mouse anti-TF antibody (HTF-1)
Eurofins, Wolverhampton, UK	Bax & cyclinD1 PCR primers
Fisher Scientific, Loughborough, UK	Butanol, Methanol, Tris base, Glycine, SDS, Mr Frosty Freezing container, Isopropanol, 25 ml Steralin tubes
GE Healthcare illustra/Fisher Scientific, Loughborough, UK	Nitrocellulose membrane
Gibco - supplied by ThermoFisher, Paisley, UK	Foetal calf serum (FCS)
Greiner -	T25 & T75 cell culture flasks, 6-, 12- & 24-well plates
INCELL corporation LLC, San Antonio, USA	M3 Base Medium
New England Biolabs, Hitchin, UK	Monrach® Total RNA Miniprep Kit
Promega, Southampton, UK	Go Taq 1-step RT-qPCR system
Qiagen, Manchester, UK	β-Actin, vimentin primers
R&D systems, Abingdon, UK	Quantikine Human Tissue Factor ELISA, Mouse anti-vimentin monoclonal antibody, Rabbit anti-

	fVII(a) polyclonal antibody, AF488-conjugated mouse monoclonal anti-N-cadherin antibody, mouse anti-cadherin-11 monoclonal antibody, mouse anti-fibronectin monoclonal antibody, mouse anti-HNF4 α monoclonal antibody, PE-conjugated mouse monoclonal anti-E-cadherin antibody, goat polyclonal anti-p16 antibody
Santa Cruz Biotechnology- supplied by Insight Biotechnology, Wembley, UK	AP-conjugated mouse anti-rabbit IgG antibody, AP-conjugated mouse anti-goat IgG antibody, AP-conjugated goat anti-mouse IgG antibody, goat anti-GAPDH antibody
Sarstedt, Leicester, UK	5 ml & 10 ml cell culture pipette
Sigma-Aldrich, Poole, UK	Formaldehyde (37%), PAR2-AP peptide, DMSO, Tween-20, Triton-X100, RNase-free ethanol, BSA, Purified fVIIa, Ammonium persulfate, Laemmli buffer (2x), Bradford reagent, TEMED, DAPI, Puromycin
Sino Biological- supplied by Fisher Scientific	EGF
Scientific Laboratory Supplies (SLS) Limited, Wilford, Nottingham, UK	DMEM media, RPMI-1640 media, PBS buffer (10x), Trypsin/EDTA solution (10x), Penicillin-streptomycin, ProtoFLOWGel 30 % acrylamide bis-acrylamide solution
Star labs, Milton Keynes, UK	200 μ l gel loading tips, 5 ml bedu tubes, 96-well PCR plates, PCR plate covers, Filter pipette tips
ThermoFisher, Paisley, UK	Spectra™ Multicolor Broad Range Protein Ladder, Nunclon Sphera 96-well plate

2.2. Equipment

Equipment Name	Manufacturer	Model
Automated microplate washer and Shaker	Thermo Fisher Scientific, Paisley, UK	Wellwash™ Microplate Washer
Cell Culture cabinet	Telstar, Birstall, Batley, UK	AV100
Cell culture incubator	Heraeus – supplied by ThermoFisher scientific	
Fluorescent Microscope	Carl Zeiss Microscopy, Cambridge, UK	AXIO Vert.A1
Light Microscope	Nikon, Kingston Upon Thames, UK	TMS
pH meter	SevenCompact – supplied by Fisher scientific	pH/ion S220
pH meter probe	SLS, Nottingham, UK	X18470
Plate reader	BMG labtech, Aylesbury, UK	PolarStar Optima
RT-PCR machine	BIORAD, Watford, UK	iCycler Real-Time
Refrigerated microfuge	Sigma, Poole, UK	1 - 14 K

2.3. Cellular methods

2.3.1. Cell lines used in this study

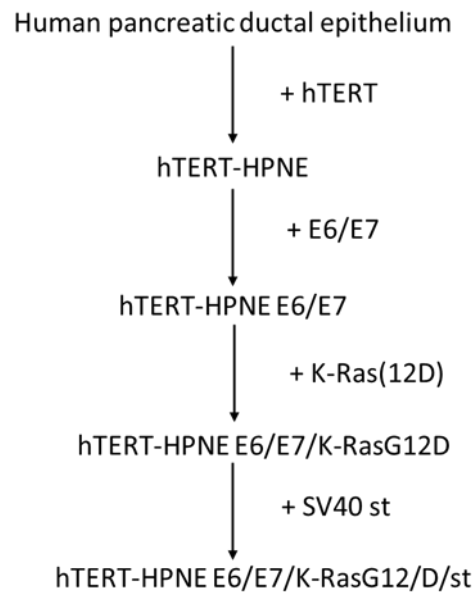
Five cell lines were used during this study which were human telomerase reverse transcriptase (hTERT)- human pancreatic nestin-expressing ductal cells (HPNE), hTERT-HPNE E6/E7/K-RasG12D, hTERT-HPNE E6/E7/K-RasG12D/st, AsPC-1 and BxPC-3.

The telomerase-immortalized hTERT-HPNE, hTERT-HPNE E6/E7/K-RasG12D and its oncogenic KRAS variant, hTERT-HPNE E6/E7/K-RasG12D/st (HPNE-mut-KRAS), were obtained from the American Type Culture Collection (ATCC). The hTERT-HPNE cells were generated from primary human cells derived from the pancreatic ducts that were transfected with hTERT (catalytic subunit of human telomerase) complementary DNA (cDNA) (394). These transfected cells express Nestin (neuronal stem cell marker) and do not possess any cancer-associated alterations. These cells represent normal human pancreatic epithelial cells. The hTERT-HPNE cells were also transformed through the stepwise introduction of oncogenes, designed to mimic PDAC progression, including oncogenic *KRAS* (carrying the G12D mutation), human papillomavirus (HPV) 16 E6 and E7 proteins (to block the function of p53 and Rb tumour suppressors respectively). A separate set of cells were transfected to express the SV40 small-t antigen to allow mutant K-Ras (12D) mediated tumourigenic growth transformation (Figure 17) (395). This additional genetic alteration is required for full malignant transformation of the hTERT-HPNE cells. In this study, experiments were performed using the telomerase-immortalized hTERT-HPNE and its oncogenic variant, which exhibit genetic alterations commonly observed in the stepwise progression of the histological stages of PDAC (Figure 18).

Cell lines were cultured in the recommended complete growth medium, which included 5% foetal calf serum, 75% Dulbecco's modified essential medium (DMEM) without glucose, 25% Medium M3 Base, 10 ng/mL of human recombinant EGF, 5.5 mmol/L of D-glucose (1 g/L) and 750 ng/mL of puromycin in the presence of 5% CO₂ at 37°C (Table 17).

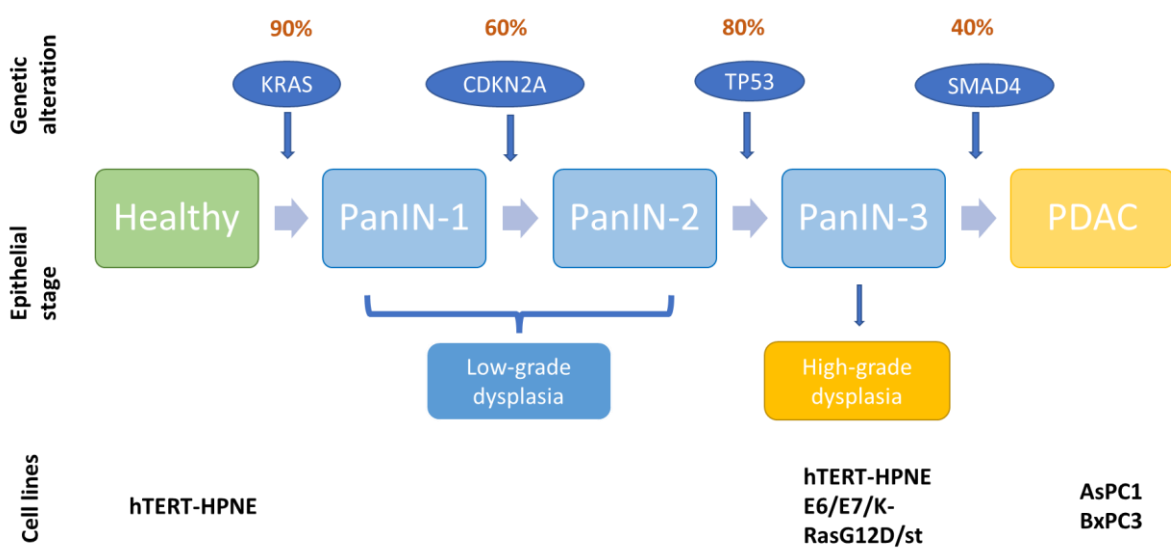
The AsPC-1 cell line was derived from nude mouse xenografts initiated with cells from the ascites of a 62-year-old white female patient with pancreatic cancer. These cells express mutant *KRAS*, *CDKN2A*, *TP53*, *FBXW7* and *MAP2K4*. The BxPC-3 cell line was derived from the pancreatic tissue of a 61-year-old female patient with pancreatic adenocarcinoma. The

Figure 17: Scheme showing immortalisation and Ras transformation of human pancreatic duct cells



hTERT is used to immortalise a primary pancreatic duct cell culture to generate hTERT-HPNE cells. These cells are then sequentially transfected with retroviral constructs to first express the HPV proteins E6 and E7 (E6/E7) and then constitutively active K-Ras (12D). Subsequently, the resultant E6/E7/Ras cells are transfected with retrovirus encoding SV40 st to establish E6/E7/Ras/st cells.

Figure 18: Diagram of histological progression of PC in parallel with mutations present in the cell lines



Scheme showing the histological progression from normal pancreatic epithelium to pancreatic adenocarcinoma with accompanying genetic alteration that corresponds to the cell lines used in this study

Table 17: Cell line culturing conditions

Cell name	Origin/Cancer type	Media	Supplements	Subcultivation ratio
AsPC-1	Pancreatic cancer	RPMI-1640	<ul style="list-style-type: none"> • 2mM Glutamine • 1mM Sodium Pyruvate • 10% FCS 	1:3 - 1:8
BxPC-3	Pancreatic cancer	RPMI-1640	<ul style="list-style-type: none"> • 2mM Glutamine • 10% FCS 	1:3 - 1:6
hTERT-HPNE	Pancreatic epithelial cell	75% DMEM	<ul style="list-style-type: none"> • 2 mM L-glutamine • 1.5 g/L sodium bicarbonate • 5% FCS • 10 ng/ml human recombinant EGF • 5.5 mM D-glucose (1g/L) + 750 ng/ml puromycin 	1:8 - 1:12
hTERT-HPNE E6/E7/K-RasG12D	Epithelial like	25% Medium M3 Base		1:8 - 1:12
hTERT-HPNE E6/E7/K-RasG12D/st	Epithelial like			1:8 - 1:12

cell line has mutant *CDKN2A*, *TP53*, *SMAD4* and *MAP2K4* (Table 18). Both the cell lines were obtained from the ATCC. The culture media used for the cell lines are listed in (Table 17). Utilising the different cell lines for experiments in this study allowed a comparison of the behaviour of benign and malignant cells in response to external influence or stimulus.

2.3.2. Cell culture

All cell culture procedures were carried out in a class II biological safety laminar flow cabinet in a sterile environment. Before commencing any work inside the culture cabinet, diluted Dettol and industrial methylated spirit (70% v/v) were used for cleaning all surfaces. Various volumes of sterile plasticware were used to transfer liquids, including sterile pipettes, micropipettes and tips. All media were prewarmed by placing them in a 37°C water bath for 15 min before use. The cell contained within cryovials were collected from liquid nitrogen and were immediately placed in a 37°C water bath with constant agitation for 1-2 min. Cells were washed with fresh pre-warmed medium to remove dimethyl sulphoxide (DMSO), centrifuged at 168 x *g* for 5 mins. The cells were re-suspended in a pre-warmed medium and added to a T25 cell culture flask. All cells were maintained in a humidified incubator at 37°C under 5% (v/v) CO₂ atmosphere. Cells were checked after 24 hours using an inverted microscope. Every 2-3 days, the culture media was replaced to ensure sufficient nutrition and prevent the accumulation of waste products.

2.3.3. Maintenance and subculture of cancer cell lines

Cell lines were cultures in appropriate media (Table 17) according to the supplier's instructions. Essential supplements, including foetal calf serum (FCS; 10% v/v), were added to the culture media. Cancer cells were propagated as monolayers until almost 90% confluent. The medium was then removed from the flask, and the cells were washed with 5 ml of sterile phosphate buffer saline (PBS, pH 7.2) to remove any traces of serum. To detach the cells, approximately 2-3 ml of Trypsin-ethylenediaminetetraacetic acid (EDTA) solution (0.25% w/v Trypsin, 0.02% w/v EDTA) was pipetted into the flask and then incubated for 4-5 min at 37°C.

Table 18: Genetic alteration present in the cell lines

Cell Line	Altered Gene				
	<i>KRAS</i>	<i>CDKN2A</i>	<i>TP53</i>	<i>SMAD4</i>	Others
hTERT-HPNE	-	-	-	-	-
hTERT-HPNE E6/E7/KRASG12D/st	+	-	+	-	-
AsPC-1	+	+	+	-	<i>MAP2K4, FBXW7</i>
BxPC-3	-	+	+	+	<i>MAP2K4</i>

The flasks were tapped gently to release the cells from the surface. The serum-containing complete medium (2-3 ml) was then added to deactivate the trypsin enzyme. The cell suspension was then transferred into a fresh 20 ml tube and centrifuged at 168 x *g* for 5 min. The supernatant was discarded, and the cells were re-suspended in a fresh medium. The cell density was determined using a haemocytometer, and the cell suspension was diluted to the desired density for experimental work, freezing or subculture. The cells were subcultured into new culture flasks at the ratios shown in the table.

2.3.4. Estimation of cell number using a haemocytometer

The cell suspension (20 μ l) was loaded into a haemocytometer to calculate the cell density, and the number of cells in each 1 mm² area was counted. The average was taken, and the number of cells was calculated using the following formula.

$$\begin{aligned} & \text{Total number of cells in the flask} \\ & = \text{number of cells counted per mm}^2 \times \text{volume cell suspension} \times 10^4 \end{aligned}$$

2.3.5. Cryopreservation of cells

For long-term freezing, cells were harvested at the logarithmic phase of growth. The cells were centrifuged at 168 x *g* for 5 min, and the supernatant was discarded. The cell pellet was then resuspended in an appropriate cryopreservation medium (containing 10% v/v DMSO and methylcellulose for AsPC-1, BxPC-3; and 95% FBS and 5% DMSO (v/v) for hTERT-HPNE, hTERT-HPNE E6/E7/K-RasG12D, hTERT-HPNE E6/E7/K-RasG12D/st) at a concentration of 10⁶ cells/ml. 500 μ l aliquots were transferred to cryovials and labelled with cell type, cell numbers, passage number and date of freezing. The vials were transferred to a freezing chamber (Mr Frosty) and placed in a -80°C freezer overnight. This chamber contains 100% isopropanol and ensures that the cells are cooled at a rate of -1°C/min to maintain cell viability throughout cryopreservation and recovery. After 24 hours, the cryovials containing the cells were placed in a liquid nitrogen container for long-term storage.

2.3.6. Cell treatment

Cells were harvested for experimentation while sub-confluent and seeded into 6/12-well plates. At a density of 1×10^5 cells/well when using a 6-well plate and 5×10^4 cells/well when using a 12-well plate. Plates were then placed into an incubator, and the cells were allowed to adhere for 24 hours. Generally, the media was refreshed before treatment with the test reagents and for the desired durations. When required, the medium in each well was discarded, and the cells were washed three times, each with 1 ml of PBS. The cells were then detached using 500 μ l of trypsin/EDTA for 6-well plates and 250 μ l for 12-well plates. The cells were transferred into 1.5 ml microcentrifuge tubes and centrifuged at 4°C, 8000 x *g* for 5 min. The supernatant was discarded, and cells were washed using PBS and put on ice or stored at -20°C for further analysis.

2.4. Proteomic and immunological methods

2.4.1. Estimation of protein concentration using Bradford Assay

The Bradford protein assay was used to measure the protein concentration of the samples to be used for enzyme-linked immunosorbent assay (ELISA) experiments. A series of standards were prepared by diluting lipid-free bovine serum albumin (BSA) stock solution (10 mg/ml) to a range of varying concentrations (10-1000 μ g/ml) (Table 19). A standard curve was created with concentration plotted on the x-axis and absorbance plotted on the y-axis. 20 μ l of the standards and protein samples were pipetted into a 96-well plate, and 200 μ l of Bradford reagent (Coomassie brilliant blue 39 G-250) stock was added. The Bradford reagent was prepared by diluting it in distilled water (60% v/v or 1:1 v/v). The plate was incubated in a dark room for 15 min at room temperature. The absorption values were measured at 584 nm using a plate reader. The protein concentrations of the samples were computed using the standard curve.

Table 19: Preparation of standards

Standard	Volume of diluent Distilled water (μl)	Volume of BSA (μl) (5000 $\mu\text{g}/\text{ml}$)	Final BSA concentration ($\mu\text{g}/\text{ml}$)
A	800	200	1000
B	850	150	750
C	900	100	500
D	950	50	250
E	980	20	100
F	990	10	50
G	998	2	10
H	1000	0	0

2.4.2. Quantification of TF antigen using Quantikine® enzyme-linked immunosorbent assay (ELISA) kit

The Quantikine® ELISA kit (Table 20) was used to measure the concentration of TF antigen in the patient's samples. This assay employs the quantitative Sandwich enzyme immunoassay technique (Figure 19). The manufacturer's protocol (396) was followed for steps including sample and reagent preparation, assay procedure and calculation of results. The patients' samples were 2-fold diluted with Calibrator Diluent RD5-20 (150 µl of sample + 150 µl of Calibrator Diluent RD5-20). Before preparing, all reagents were allowed to reach room temperature. Recombinant Human Coagulation Factor III provided with the kit was reconstituted with distilled water to produce a stock solution and then diluted to concentrations of 7.8-500 pg/ml in the Calibrator Diluent to prepare standards (Figure 20). The standards were tested alongside the samples to generate a standard curve.

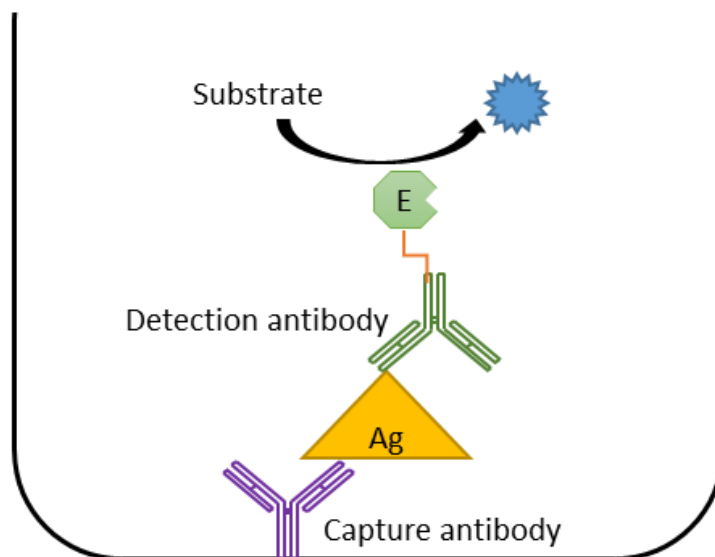
100 µl of Assay Diluent RD1-89 was added to each well of the human monoclonal TF antibody-coated 96-well plate, followed by the addition of 100 µl of standards and patient samples. The plate was sealed with an adhesive film and incubated for 2 hours at room temperature on a microplate shaker. The wells were aspirated and washed four times with the provided wash buffer (400 µl). 200 µl of polyclonal antibody specific for Human Coagulation Factor III conjugated to horseradish peroxidase was added to each well. The plate was covered and incubated for another 2 hours at room temperature on the shaker. The wells were washed four times with wash buffer following incubation.

The substrate solution was prepared within 15 min of use by mixing an equal volume of two color reagents (Color Reagent A – stabilised hydrogen peroxide, Color Reagent B – stabilised chromogen, tetramethyl benzidine). 200 µl of the resultant mixture was added to each well. The plate was incubated at room temperature in the dark for 30 min. 50 µl of stop solution (2 N sulfuric acid; H₂SO₄) was added to stop the reaction. The absorption of the samples was measured at 450 nm using a microplate reader. The concentration of the TF antigen in the samples was calculated using the generated standard curve.

Table 20: Quantikine® ELISA kit Materials

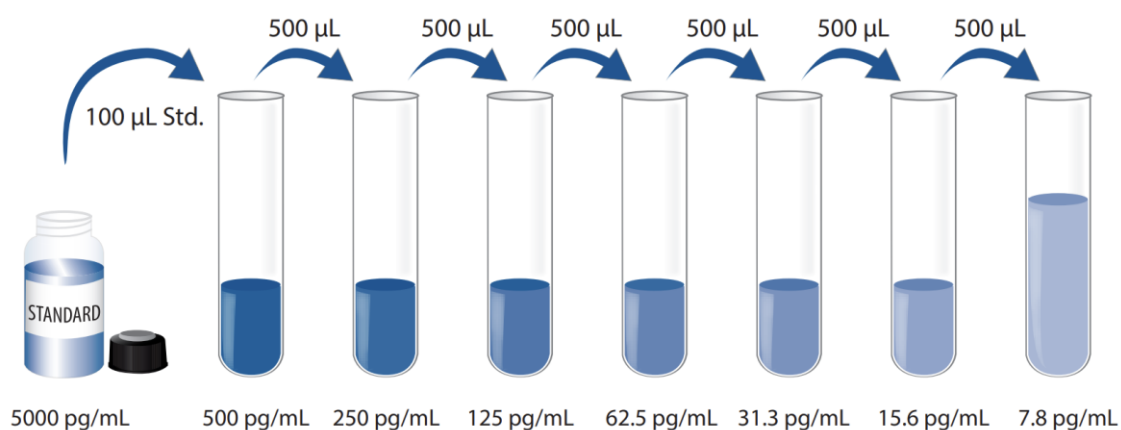
Material	Description
Human coagulation factor III microplate	96-well polystyrene microplate (12 strips of 8 wells) coated with a monoclonal antibody specific for human coagulation factor III
Human coagulation factor III conjugate	21 mL of a polyclonal antibody specific for human coagulation factor III conjugated to horseradish peroxidase with preservatives
Human coagulation factor III standard	Recombinant human coagulation factor III in a buffered protein base with preservatives; lyophilised.
Assay diluent RD1-89	11 mL of a buffered protein base with preservatives
Calibrator diluent RD5-20	21 mL of a buffered protein base with preservatives
Wash buffer concentrate	21 mL of a 25-fold concentrated solution of buffered surfactant with preservative
Colour reagent A	12 mL of stabilised hydrogen peroxide
Colour reagent B	12 mL of stabilized chromogen (tetramethylbenzidine)
Stop solution	6 mL of 2 N sulfuric acid
Plate sealers	4 adhesive strips

Figure 19: Diagram of sandwich ELISA technique used for TF ELISA



The 96-well plate was coated with the human monoclonal TF antibody (purple). Any TF present (yellow) is bound by the immobilised antibody. The antigens then bind to the HRP-conjugated human factor III antibody (green). An HRP substrate is then added, and the colour (blue) develops in proportion to the amount of TF antigen bound in the initial step.

Figure 20: Diagram representing preparation of standards for TF ELISA



The Human Coagulation Factor III Standard was reconstituted with deionised or distilled water. This reconstitution produced a stock solution of 5000 pg/mL. The standard was mixed to ensure complete reconstitution and allowed to sit for a minimum of 5 min with gentle agitation before diluting. 900 µL of Calibrator Diluent RD5-20 was pipetted into the 500 pg/mL tube; 500 µL into the remaining tubes. The stock solution was used to produce a dilution series. Each tube was mixed thoroughly before the next transfer. The 500 pg/mL standard serves as the high standard. Calibrator Diluent RD-20 serves as the zero standard (0 pg/mL). (Adapted from R & D Systems, 2016)

2.4.3. Quantification of fVII antigen using ELISA kit

The AssayPro Human Factor VII ELISA kit (Table 21) was used to determine the concentration of fVII antigen in the patient's samples. This assay employs the quantitative sandwich enzyme immunoassay technique (Figure 21). The manufacturer's recommendation (397) was followed for steps including sample and reagent preparation, assay procedure and calculation of results.

All reagents were freshly diluted and brought to room temperature before use. Human coagulation fVII provided with the kit was reconstituted with MIX diluent to generate a standard stock solution of 200 ng/ml and then diluted to concentrations of 3.125 - 200 ng/ml in the MIX diluent to prepare standards (Table 22). The MIX diluent was the zero standards (0 ng/ml). The standards were tested alongside the samples to generate a standard curve.

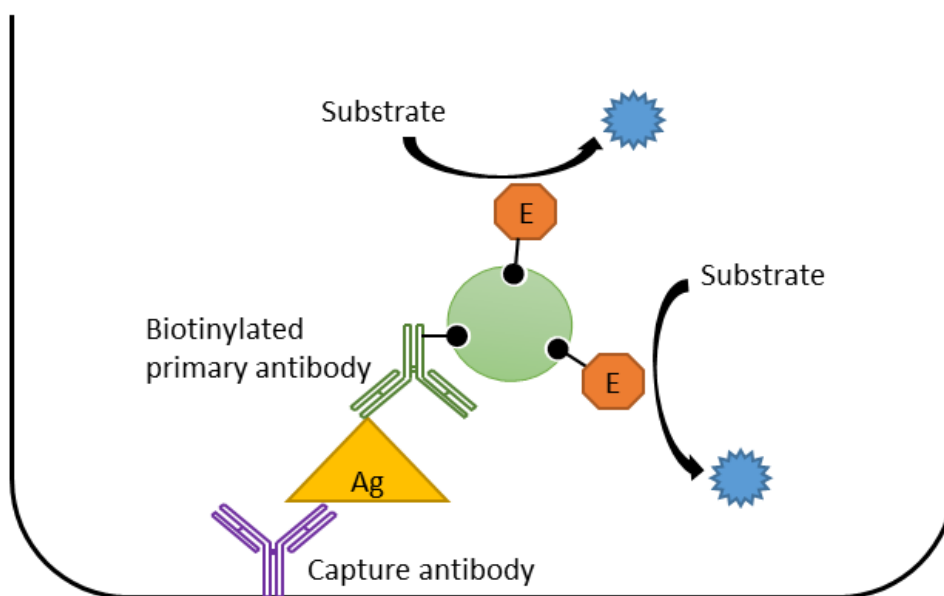
50 µl of Human fVII standards and patient samples were added to each well of the human monoclonal fVII antibody-coated 96-well plate. The plate was sealed with an adhesive film and incubated for 2 hours at room temperature on a microplate shaker. The wells were aspirated and washed five times with the provided wash buffer (300 µl). 50 µl of Biotinylated polyclonal human fVII antibody was added to each well. The plate was covered with sealing tape and incubated for 1 hour at room temperature on the shaker. The wells were washed five times with wash buffer following incubation.

50 µl of streptavidin-peroxidase (SP) conjugate was added to each well; the plate was covered with a sealing tape and incubated at room temperature for 30 min in the dark. The wells were again washed five times with wash buffer. After this, 50 µl of Chromogenic substrate (a stabilised peroxidase chromogen substrate tetramethylbenzidine) was added to each well to coat the wells thoroughly and incubated in ambient light for 25 min or till optimal blue colour density developed. Then 50 µl of stop solution (0.5 N hydrochloric acid; HCl) was added to stop the reaction. The absorption of the samples was measured at 450 nm using a microplate reader. The concentration of the fVII antigen in the samples was calculated using the generated standard curve.

Table 21: AssayPro Human Factor VII ELISA kit

Material	Description
Human factor VII microplate	A 96-well polystyrene microplate (12 strips of 8 wells) coated with a monoclonal antibody against human factor VII.
Human factor VII standard	Human factor VII in a buffered protein base (640 ng, lyophilised)
Biotinylated human factor VII antibody (50x)	A 50-fold concentrated biotinylated polyclonal antibody against human factor VII (120 µl)
MIX diluent concentrate (10x)	A 10-fold concentrated buffered protein base (30 ml)
Wash buffer concentrate (20x)	A 20-fold concentrated buffered surfactant (30 ml, 2 bottles)
SP conjugate (100x):	A 100-fold concentrate (80 µl)
Chromogen substrate (1x)	A stabilised peroxidase chromogen substrate tetramethyl benzidine (7 ml)
Stop solution (1x)	A 0.5 N hydrochloric acid solution to stop the chromogen substrate reaction (11 ml)
Sealing tapes	3 pre-cut, pressure-sensitive sealing tapes that can be cut to fit the format of the individual assay

Figure 21: Diagram of sandwich ELISA technique used for fVII ELISA



The 96-well plate is pre-coated with a monoclonal antibody (purple) specific for human fVII. FVII (yellow) in standards and samples is sandwiched by the immobilised antibody. A biotinylated polyclonal antibody specific for human fVII (green) is recognised by the SP conjugate (green circle). Peroxidase enzyme substrate (orange) is added, and colour (blue) develops in proportion to the amount of fVII antigen bound in the initial step.

Table 22: Preparing human fVII standard

Standard Point	Dilution	FVII (ng/ml)
P1	1 part Standard (200 ng/ml)	200
P2	1 part P1 + 1 part MIX Diluent	100
P3	1 part P2 + 1 part MIX Diluent	50
P4	1 part P3 + 1 part MIX Diluent	25
P5	1 part P4 + 1 part MIX Diluent	12.5
P6	1 part P5 + 1 part MIX Diluent	6.25
P7	1 part P6 + 1 part MIX Diluent	3.125
P8	MIX Diluent	0.0

2.4.4. Separation of protein using sodium dodecyl sulphate-polyacrylamide gel electrophoresis (SDS-PAGE)

Prepare samples: To prepare the samples for SDS-PAGE, Laemmli buffer (2% w/v SDS, 10% v/v glycerol, 5% v/v 2-mercaptoethanol, 0.002% w/v bromphenol blue and 62.5 mM Tris-HCl, pH 6.8) was used to lyse the cells. The samples were transferred to microfuge tubes and boiled in a dry heating block for 10 min at 95°C to denature the proteins. They were allowed to cool down at room temperature for 2 min and then centrifuged at 12,225 x g for 1 minute.

Prepare separating gel: For most experiments, 12% (w/v) separating gel was used. It was prepared by mixing 4 ml acrylamide solution (30% w/v acrylamide, 0.8% w/v bis-acrylamide), 2.6 ml resolving buffer (1.5 M Tris-HCl pH 8.8, 0.4% w/v SDS), 3.3 ml de-ionised water and 100 µl ammonium persulphate (10% w/v). The solution was then gently and thoroughly mixed, and 10 µl of N, N, N', N'-tetramethylethylenediamine (TEMED) was added to initiate polymerisation.

The solution was poured between the glass electrophoresis plates in a gel caster and covered with a layer of butanol (100%). The gel was kept for 1 hour at room temperature to complete polymerisation. Butanol was removed once the gel was set.

Prepare stacking gel: A 4% (w/v) stacking gel was prepared by mixing 0.65 ml of the acrylamide solution, 1.3 ml stacking buffer (0.5 M Tris-HCl pH 6.8, 0.4% w/v SDS), 3 ml de-ionised water and 100 µl ammonium persulphate (10% w/v). The solution was gently mixed, and 10 µl of TEMED was added.

The solution was poured on top of the separating gel, an appropriate comb was inserted, and the gel was allowed to polymerise for about 1 hour at room temperature.

Electrophoresis: The comb was removed, and the gel was transferred to an electrophoresis tank (BioRad Mini-PROTEAN TETRE Cell). 10 - 15 µl of samples were loaded into the wells. 6 µl of pre-stained protein molecular weight markers (10 - 260 kDa) were loaded into an adjacent well. The gel was covered with electrophoresis buffer (25 mM Tris-HCl pH 8.3, 192 mM glycine, 0.1% w/v SDS), and electrophoresis was carried out at 100 V for 120 min.

2.4.5. Western blot method

Once electrophoresis was complete, the gel was removed from the glass plate to transfer the separated proteins onto a nitrocellulose membrane. The blotting (filter) papers and nitrocellulose membrane were soaked in transfer buffer (20 mM Tris-HCl, 150 mM glycine, 20% (v/v) methanol, pH 8.3). The gel sandwich was set up by placing the gel over the nitrocellulose membrane between the blotting papers and sponges on either side and then placed in a gel cassette holder.

The holder was transferred to a transfer tank containing a transfer buffer. The proteins were allowed to transfer at 70 V for 1 hour at 4° C.

Once the proteins were transferred, the nitrocellulose membrane was blocked with TBST (150 mM NaCl, 10 mM Tris-HCl pH 8, 0.05% Tween 20 (w/v)) for 2 hours at room temperature with shaking to avoid non-specific binding. The membrane was then incubated overnight at 4°C with an appropriate primary antibody diluted in TBST against the protein of interest (specific for each chapter). For every experiment, one membrane was incubated with an antibody against the housekeeping gene glyceraldehyde-3-phosphate dehydrogenase (GAPDH) to ensure equal protein loading in each lane and establish the successful transfer of proteins from gel to membrane.

On the following day, the membranes were washed three times (10 min each time) with TBST and once with distilled water. They were subsequently incubated with appropriate alkaline phosphatase (AP) conjugated secondary antibodies against mouse, rabbit or goat (specific for each chapter) in 10 ml of TBST in a shaker for 60 min at room temperature. The membranes were rinsed thrice with TBST and once with distilled water.

The protein bands were developed using Western Blue stabilised substrate for alkaline phosphatase. Images of the membranes were taken with a digital camera and analysed using ImageJ v1.48 software.

2.4.6. Immunofluorescence microscopy

hTERT-HPNE cells (5×10^4) were seeded in a 96-well plate and allowed to adhere overnight. Selected wells were incubated with TGF β (5 ng/ml) or PAR2-AP (20 μ M) at 37°C for 1 day. The cells were then fixed for 20 mins with 4% (v/v) formaldehyde at room temperature and washed three times with PBST (PBS containing 0.1% v/v Tween-20; 100 μ l). The cells were blocked with 3% BSA solution (100 μ l) for 30 mins at room temperature. Samples were incubated with either R-phycoerythrin (PE)-conjugated anti-E-cadherin antibody or Alexa Fluor (AF) 488-conjugated anti-N-cadherin antibody (100 μ l; diluted 1:200 in 3% FBS solution) at 4°C overnight. The samples were washed three times with PBST (100 μ l). The nuclei were stained with 4',6-diamidino-2-phenylindole (DAPI; 0.4 μ g/ml diluted in PBST) for 20 min at room temperature. The samples were then washed twice in PBST and images were captured using a fluorescence microscope controlled by the Zen 2012 SP1v8.1 software (Carl Zeiss Microscopy). The amount of fluorescence in each sample was quantified using the ImageJ program.

2.5. Molecular methods

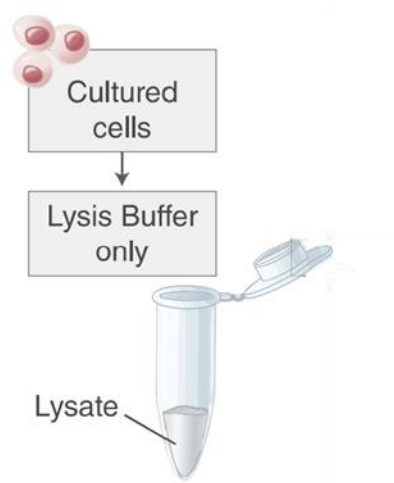
2.5.1. Quantification of cDNA using RT-qPCR (reverse transcription-quantitative polymerase chain reaction)

Real-time RT-qPCR was used for relative quantification of mRNA for detection and observation of variation of gene expression by measuring cDNA. Monarch[®] total RNA Miniprep Kit was used to purify RNA samples. GoTaq[®] 1-Step RT-qPCR System and iCycler Real-Time PCR machine (BioRad) were used for the PCR reaction according to the manufacturer's protocols (398).

2.5.2. Preparation of purified RNA sample using Monarch[®] total RNA Miniprep Kit

Cell pellets from cultured cell lines were resuspended in RNA lysis buffer (300 μ l) (Figure 22). The sample was transferred to the genomic DNA (gDNA) removal column and centrifuged for 30 seconds to remove most of the gDNA. An equal volume of ethanol ($\geq 95\%$) was added to

Figure 22: Sample disruption and homogenisation



Disruption and lysis cultured cells using RNA lysis buffer (Adapted from New England Biolabs, 2020).

the follow-through and mixed thoroughly by pipetting. After that, the mixture was transferred to an RNA purification column and centrifuged for 30 seconds. The column matrix was then incubated with DNase (5 μ l DNase with 75 μ l DNase reaction buffer) for 15 min. 500 μ l of RNA priming buffer was added, centrifuged for 30 seconds, and the follow-through was discarded. The column was washed twice with RNA wash buffer and centrifugation for 30 seconds at 12,225 $\times g$ followed by 2 min at 12,225 $\times g$. RNA was eluded by adding 50 μ l of nuclease-free water to the centre of the column matrix and centrifuging for 30 seconds (Figure 23). Purified RNA was collected in an RNase-free microfuge tube. All centrifugation steps were performed at 12,225 $\times g$.

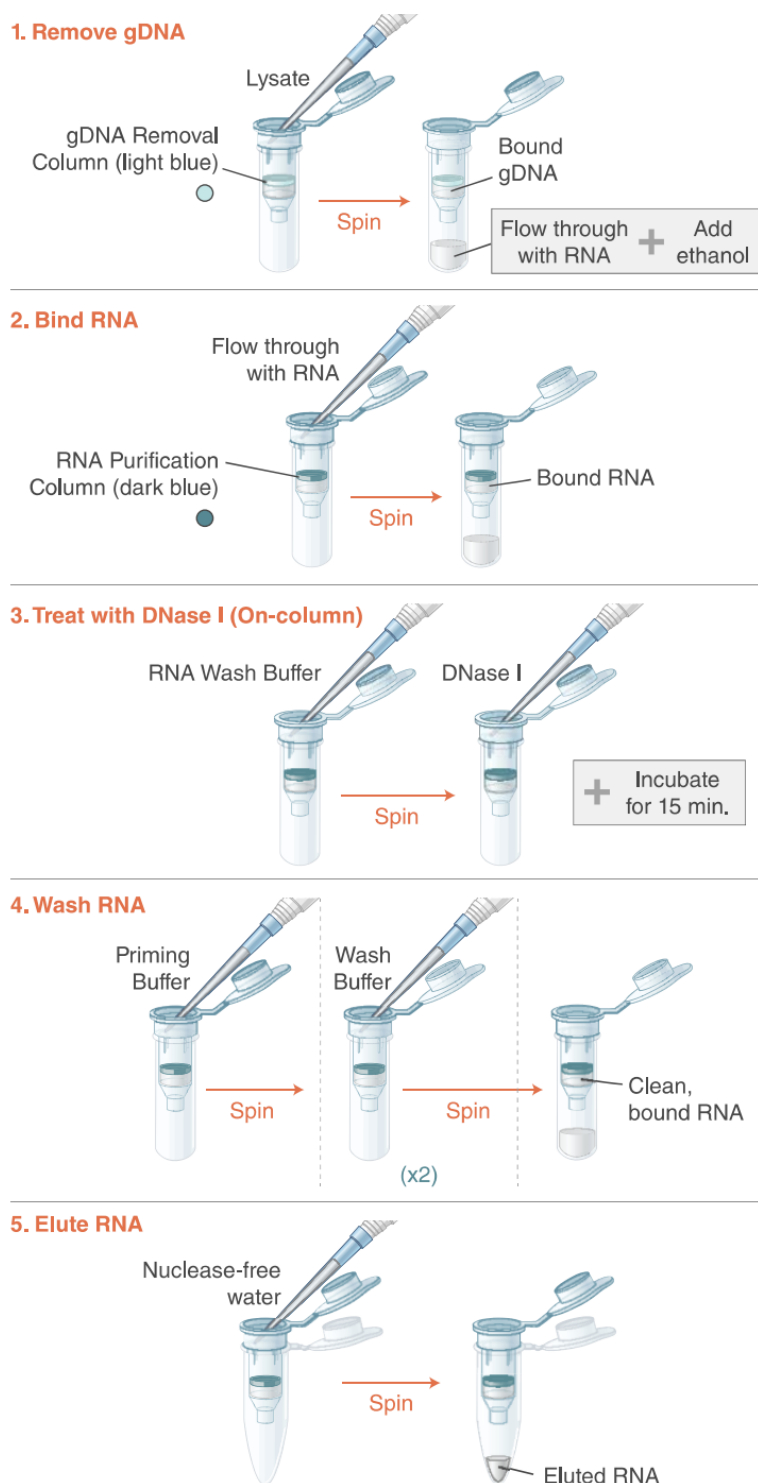
To determine the concentration of the isolated RNA, the absorption of the RNA sample was measured at 260 nm using a spectrometer. The RNA concentration (μ g/ml) was calculated according to the Beer-Lambert law using the equation:

$$\text{RNA concentration } (\mu\text{g/ml}) = \text{Absorption (260 nm)} \times 40$$

The 260:280 ratio was also calculated to determine the purity of the RNA. An RNA sample with a ratio of 1.8-2.1 was deemed sufficient purity for RT-qPCR reactions. All samples were stored at -80 $^{\circ}$ C and used within 20 days of RT-qPCR.

The RT-qPCR reaction was prepared by combining the GoTaq[®] qPCR Master Mix (10 μ l), GoScript[™] RT Mix (0.4 μ l), specific primer (1 μ l, 0.5 μ M final concentration) and nuclease-free water (7.6 μ l). The final reaction volume for this protocol is 20 μ l. Following a brief vortex of the mixture, an appropriate volume of reaction mix was added to each PCR tube or well of an optical grade PCR plate. A purified RNA sample template (1 μ l; 7.5-10 ng/ μ l final concentration) or water for no template control reaction was added to the appropriate wells of the reaction plate (Figure 24). A reaction without the GoScript[™] RT Mix was performed in order to test for the presence of contamination or foreign DNA. Each reaction was divided between 2 wells in a 96-well PCR plate. The plate was sealed, centrifuged briefly to collect the content of the wells at the bottom and placed in the iCycler Real-Time PCR machine. The cycling parameters in Table 23 were used as a guideline for amplification.

Figure 23: RNA binding and elution



Workflow for RNA Purification using the Monarch Total RNA MiniPrep Kit (Adapted from New England Biolabs, 2020).

Figure 24: Overview of the GoTaq® 1-Step RT-qPCR protocol

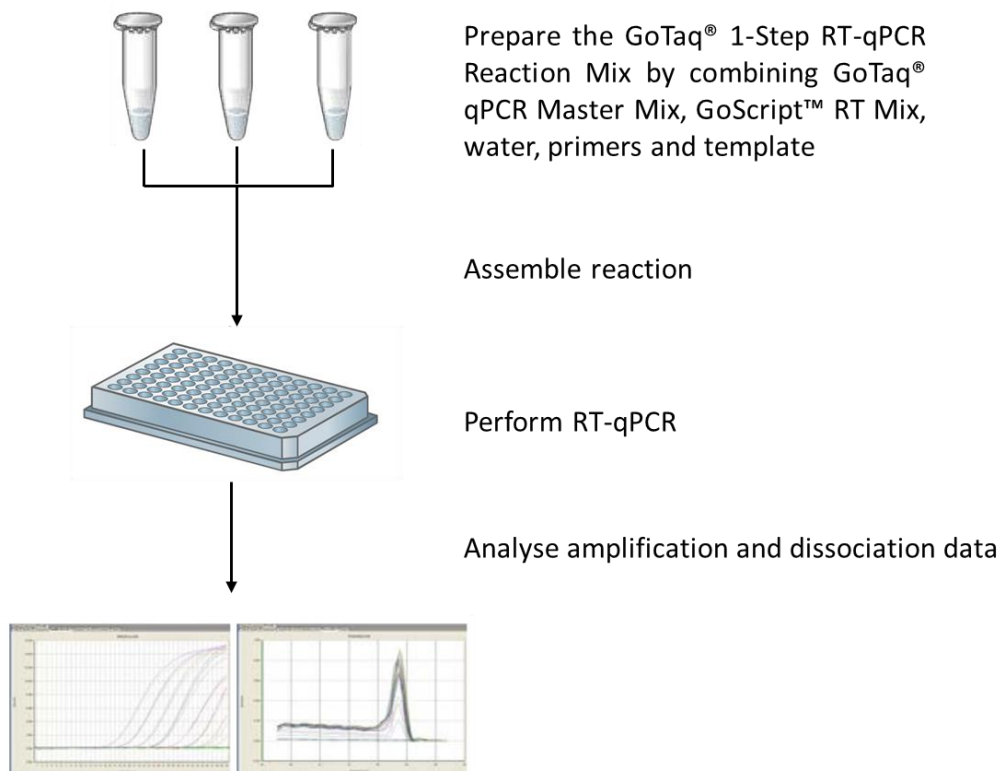


Table 23: Standard thermocycling conditions for RT-qPCR

Step	Cycles	Temperature	Time
Reverse transcription	1	≥ 37°C	15 min
Reverse transcriptase inactivation and GoTaq® DNA Polymerase activation	1	95°C	10 min

Protocol for qPCR

Cycle	Step	Number of cycles	Temperature	Time (min)
1	Step 1	X 1	50°C	02:00
2	Step 1	X 1	95°C	02:00
3	Step 1 Denaturation	X 40	95°C	00:15
	Step 2 Annealing		60°C	01:00
Data collection				
4	Step 1	X 1	95°C	01:00
5	Step 1	X 1	50°C	01:00
6	Step 1	X 60	60°C	00:05
Increase setpoint temperature after cycle 2 by 0.5°C				
Melt curve data collection				
7	Step 1	X 1	4°C	HOLD

The iCycler iQ v3.1 software was used to calculate the cycle threshold (Ct) for each sample, and the relative gene expression levels were calculated using the following equation (399):

$$2^{-((Ct(TE)-Ct(HE)) - (Ct(TC)-Ct(HC)))}$$

TE = Test gene experimental sample

HE = Housekeeping gene experimental sample

TC = Test gene control sample

HE = Housekeeping gene control sample

For all PCR experiments in this study, β -actin was used as the housekeeping gene. A melt curve was performed to ensure the presence of a single amplicon for each primer set. The Ct value of a well was not used if the melt curve peak temperature varied more than 0.5°C on either side of the predicted melt curve peak value, as this will indicate that an incorrect sequence was amplified.

In all RT-qPCR experiments the MIQE guidelines (400) were adhered to the best of our ability covering experimental design, sample quality and extraction, use of appropriate controls, normalisation, data analysis and reporting.

2.6. Statistical analysis

The graphical figures show the mean value of the experiments with the standard error of the mean (SEM) or standard deviation (SD) as stated in the legends. Statistical analysis was performed using the Statistical Package for the Social Sciences (SPSS) program v28 (IBM). Kolmogorov-Smirnov test was used to check for normal distribution, and a reading of $p > 0.05$ indicated normal distribution. Levene's Test of Equality of Variance was used to check if the variances of the two groups were equal, and a reading of $p > 0.05$ indicated they could be treated as equal. For comparing two normally distributed groups with equal variables, the independent sample t-test was used, and a p-value of < 0.05 was considered significant. For experiments with multiple variables, a one-way ANOVA test was used, and a p-value of < 0.05 was considered significant.

Chapter 3

Investigation of tissue factor as an early indicator of malignant transformation in pancreatic cystic lesions

3.1. Introduction

The Study of Tumour Regulatory Molecules as Markers of Malignancy in Pancreatic Cystic Lesions (TEM-PAC) is an umbrella study of tumour regulatory molecules in the context of malignant pancreatic transformation (REC reference number 18/LO/0736). The aim of this study is to identify novel regulatory molecules and genetic changes associated with PC development. The study employs conventional techniques and platform technologies to measure the levels of these molecules in pancreatic cysts of patients who are strongly suspected of having PC and have undergone EUS or surgery. The study aims to determine if these molecules can serve as markers for the early detection of pancreatic cancer.

TF/ fVIIa tumour-regulatory signalling molecules were investigated under the umbrella of the TEM-PAC study and are the subject of the study of this thesis. A detailed review of these pathways and their signalling has been discussed in section 1.7.3. Briefly, TF can influence pathological processes through its ability to initiate intracellular signalling. It plays a central role in the coagulation cascade. It is consistently upregulated in a large spectrum of human malignancies, including pancreas, liver, brain, colon, gastric, bladder, prostate, melanoma, ovary, leukaemia and other haematopoietic malignancies (Table 10)(4).

On tumour cells, fITF binds to an inactive precursor, fVII, leading to the formation of a complex, fITF:fVII. This complex rapidly converts fVII into an active enzyme, fVIIa. The fITF:fVIIa complex then activates another enzyme, Factor X, leading to the formation of a ternary complex called fITF:fVIIa:fXa. These complexes (fITF:fVIIa, fITF:fVII:fXa) cleave several PARs belonging to the seven-transmembrane G protein-coupled receptor family, which initiate a diverse array of functions via coagulation-dependent and independent mechanisms (section 1.7).

Pre-clinical studies have revealed the impact of TF on gene expression and cell phenotype, tumour growth, angiogenesis, metastases and formation of cancer stem cell niches (13, 14). Likewise, the role of oncogenic transformation and TME as regulators of TF is also well recognised. TF serves as the primary initiator of the blood coagulation cascade due to its receptor activity for fVII, which helps in rapid haemostasis during organ damage.

Inflammatory cytokines, such as TNF α or ILs, can induce the expression of both fITF and asTF in endothelial and blood cells. Aside from its haemostatic function, TF has signalling activity and can stimulate various inflammatory responses via PARs with other coagulation factors. Activation of PARs can lead to the release of pro-inflammatory cytokines, chemokines, and growth factors, contributing to the amplification of the inflammatory response. Overall, TF and fVII play crucial roles in the complex interplay between coagulation, inflammation, immunity and cancer (Figure 25).

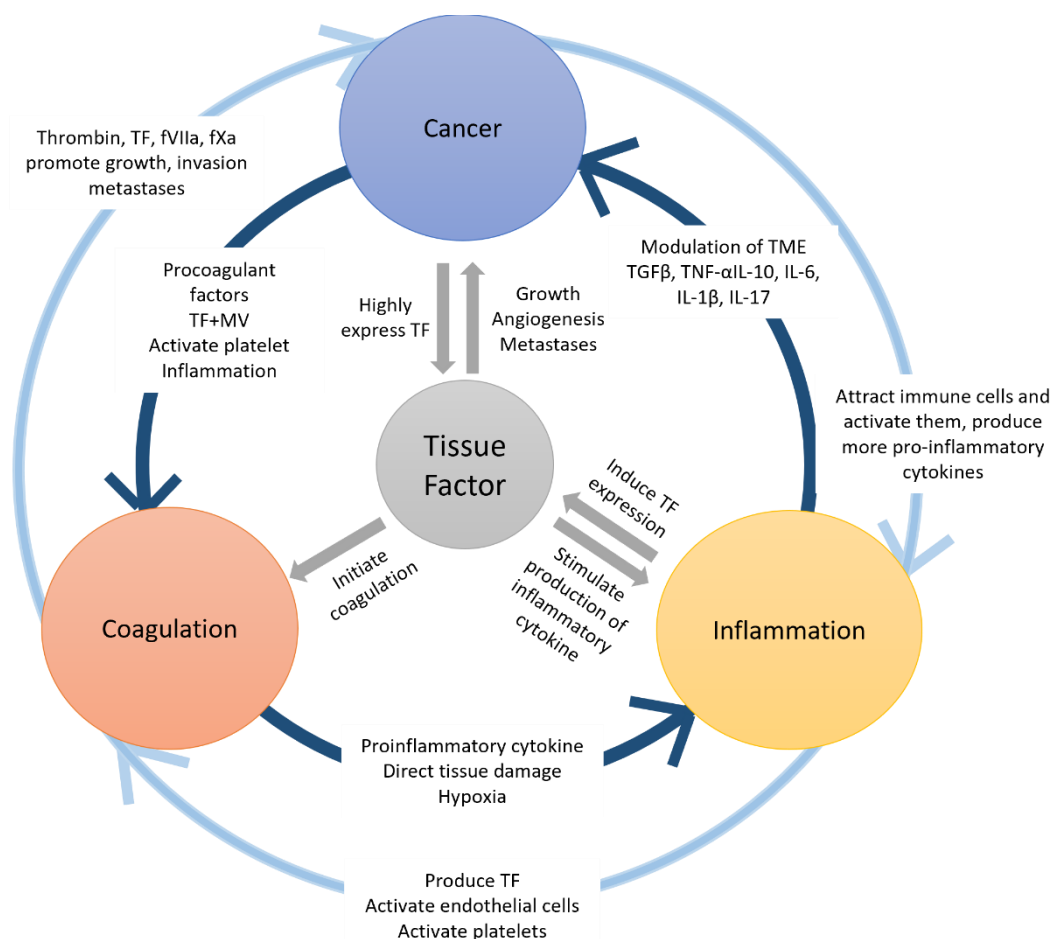
This suggests that TF is either an epiphenomenon associated with some common pathological occurrence during the malignant process or contributes to this process as an integral part or both (401). The elevated expression of TF in cancer may involve cancer cells, adjacent stroma (blood vessels, fibroblastic and inflammatory cells) and circulating blood (211, 402). The shedding of TF+MV from cancer cells, their entry into the circulation and their role in the intercellular transfer of TF activity, cancer coagulopathy and other processes are of growing interest (403).

Our team and others have already shown the relationship of TF+MV and TF expression in PC (404, 405), with a substantial reduction in circulating TF+MV levels being observed post resective surgery in pancreatic cancers with positive TF expression (404).

Cancer cell TF expression and level in plasma have been correlated with histological grade, aggressiveness and poor prognosis. They can reach up to 1000-fold in pro-metastatic cells compared to their normal counterparts (4-6, 259, 406). Pro-oncogenic events, such as mutations in the tumour suppressor *TP53* and proto-oncogene *KRAS* activate MAPK and PI3K/AKT signalling pathways, stimulating TF expression (212, 407). Amplification of EGFR or its constitutively active form, EGFRvIII (214, 408), loss of tumour suppressor Pten or E-cadherin (216, 217, 408) leads to TF upregulation. Cancer-associated hypoxia also stimulates TF expression via hypoxia-associated signalling molecules (219, 220).

Likewise, there is considerable evidence of an association between TF expression and tumour invasiveness (283), metastatic properties (409) and malignant phenotype (211), which

Figure 25: The interplay between cancer, coagulation and inflammation



TF impacts various aspects of cancer biology, such as gene expression, cell phenotype, tumour growth, angiogenesis, metastasis, and cancer stem cell niches. TF is primarily involved in the blood coagulation cascade, leading to rapid haemostasis during organ damage. Inflammatory cytokines such as TNF α or ILs induce the expression of TF in endothelial and blood cells. TF also has signalling activity and can stimulate various inflammatory responses via PARs, leading to the amplification of the inflammatory response. TF and fVII play crucial roles in the complex interplay between coagulation, inflammation, immunity, and cancer.

suggests that TF is a major contributor to phenotypic alterations that induce cancer invasiveness as well as angiogenesis which is necessary for tumour growth (211, 410).

In addition, the involvement of the coagulation system has been identified as a generic enabling mechanism for cancer progression affecting early, mid and late stages of cancer. There is evidence of early involvement of the coagulation system with the notion that tumour initiation could be blocked by TF-neutralizing antibodies (411). Blockade of TF-dependent signalling in colorectal, brain and breast cancer models resulted in reduced tumour growth and angiogenesis, thereby influencing early and intermediate stages of cancer (173, 412).

Furthermore, there is evidence of the role of TF as a switch that may promote the transition from a dormant (non-tumourigenic) or latent (delayed-tumourigenic) state of cancer progression (413). The presence of TF at a biologically relevant level in the tumour microenvironments may lead to the cessation of dormancy by modifying the functional state and molecular evolution of tumour cells and driving the dynamic formation of growth-promoting functional units. TF is well-known as a pro-inflammatory mediator (Section 1.7.3.6). During injury or other events that lead to a procoagulant or proinflammatory response, an enforced expression of TF can interrupt the state of cell dormancy (e.g. damaged endothelial cells) and induce mechanisms of angiogenesis, invasion and propagation which, when dysregulated, typically characterise the cancer cell state. The exact drivers for the malignant transformation from low-grade to HGD or invasive phenotype are not known in pancreatic cancer. A pro-inflammatory and pro-proliferative mediator like TF may play a crucial role in the initiation of early events of tumourigenesis.

TF expression is high in localised pancreatic cancer. Its appearance in the early stages of pancreatic neoplastic transformation is confirmed by increased expression in pancreatic precursor lesions, including PanINs and IPMNs (5, 6, 259).

The interaction between TF and fVIIa has been linked to the potential for cell proliferation. High levels of TF exposure can lead to cell cycle arrest at the G1/S checkpoint and induce cell apoptosis (414-416). EC and eosinophils lacking fVIIa have been shown to be more susceptible

to apoptosis when exposed to TF+MV (417, 418). During inflammation, disease, or injury, TF is released within MV, which interacts with EC and can be cleared by endocytosis. The inability of cells to effectively process TF is harmful to EC (419). A novel study from our lab (420) investigated the effects of different ratios of fVIIa to TF within MV on cultured primary endothelial cells. The researchers found that the fVIIa:TF ratio determined whether the cells underwent apoptosis or proliferation, with a transition from pro-apoptotic to proliferative properties occurring at an estimated ratio of 15:1. The study also showed that the concentration of TF with which the cells came into contact was a critical factor in determining the outcome, in addition to the fVIIa:TF ratio. The activation of PAR2 was necessary for the pro-apoptotic function of MV, and inhibition of PAR2 prevented this function. The study concluded that the ratio of fVIIa:TF determines the outcome in endothelial cells, resulting in either proliferation or apoptosis, and the pro-coagulant activity of TF is a pre-requisite for both proliferative and pro-apoptotic activities, requiring interaction with fVII. Higher molar ratios of 54:1 and 38:1 were observed in the HepG2 hepatocellular line and MCF-7 breast cancer, whereas the ratio was lower in the BxPC-3 pancreatic cancer cell line. However, the reported ratios may not accurately represent the real ratios for the transition from the proapoptotic to proliferative form since the study only used exogenous fVIIa and TF in calculating the ratios. Repeated exposure of EC to TF+MV resulted in the depletion of cellular fVII reserves, suggesting that chronic exposure to such MV may exhaust the ability of EC to counteract the proapoptotic property of TF.

In this context, we examined the potential of TF and fVII concentrations within the pancreatic cystic fluid as an indicator of malignant cellular transformation from benign to malignant, with particular emphasis on distinguishing LGD from HGD/already malignant lesions.

3.2. Aim

The primary aim of this TEM-PAC sub-study was to assess the accuracy of TF and fVIIa as markers classifying resective (malignant and HGD requiring resection) vs non-resective (benign and LGD, not requiring resection).

The objectives were to:

- a) Assess cyst TF and fVIIa as co-markers of malignancy
- b) Compare cyst TF and (or) fVIIa with the conventional markers/criteria (radiological and pathological) currently in use
- c) Explore whether the levels of serum TF levels in patients reflected those detected in the cysts and had any diagnostic value compared to a control cohort as well as known locally advanced cancers

3.3. Study Design

This is a sub-study of the TEM-PAC umbrella study.

TEM-PAC is a prospective feasibility study. The main study aim is to collect samples from 50 patients with a pancreatic cyst, 50 patients with localised PC (resectable and non-resectable) and 80 patients with benign hepatobiliary conditions and normal controls (age and gender matched, Appendix 1 & 2). The control population would comprise 20 patients with acute pancreatitis with non-resolving pseudocysts, 20 patients undergoing cholecystectomy for stones, 20 undergoing cholecystectomy for inflammation, and 20 undergoing endoscopy for dyspepsia. The dyspepsia group was classified as “normal controls” (Figure 26).

Samples, including cyst fluids, serum and urine from the index cases, were collected before the commencement of any anti-cancer treatment.

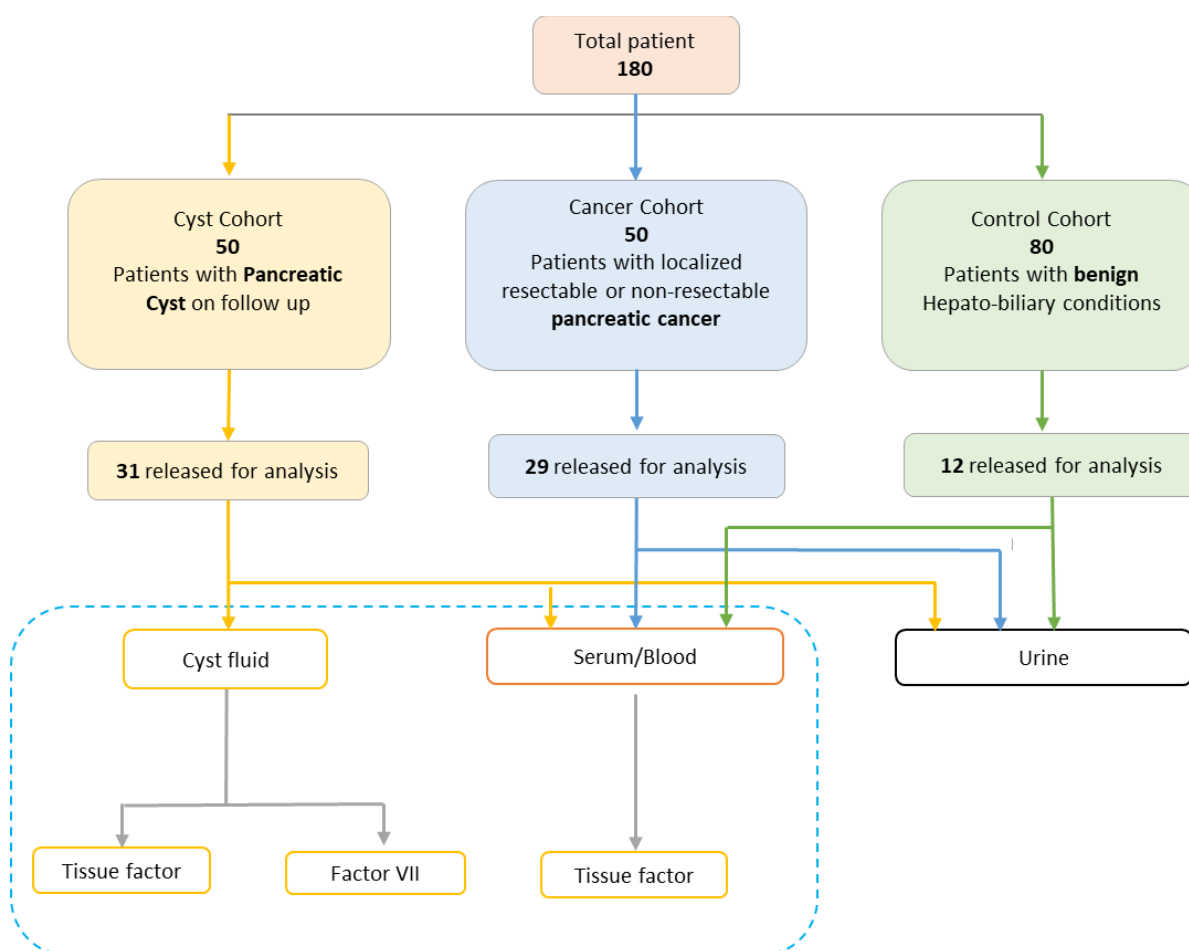
The present study focused on the analysis of cyst fluid to identify an indicator of malignant transformation from benign to an invasive phenotype. The profile of the available samples for this study can be seen in Figure 27.

3.4. Ethical Approval

The TEM-PAC study has approval from Research Ethics Committee (REC) and Health Research Authority (HRA) and had confirmation from the trust R&D capacity and capability. The REC reference number is 18/LO/0736, and the R&D reference number is R2224 with the amendments (Appendix 2)

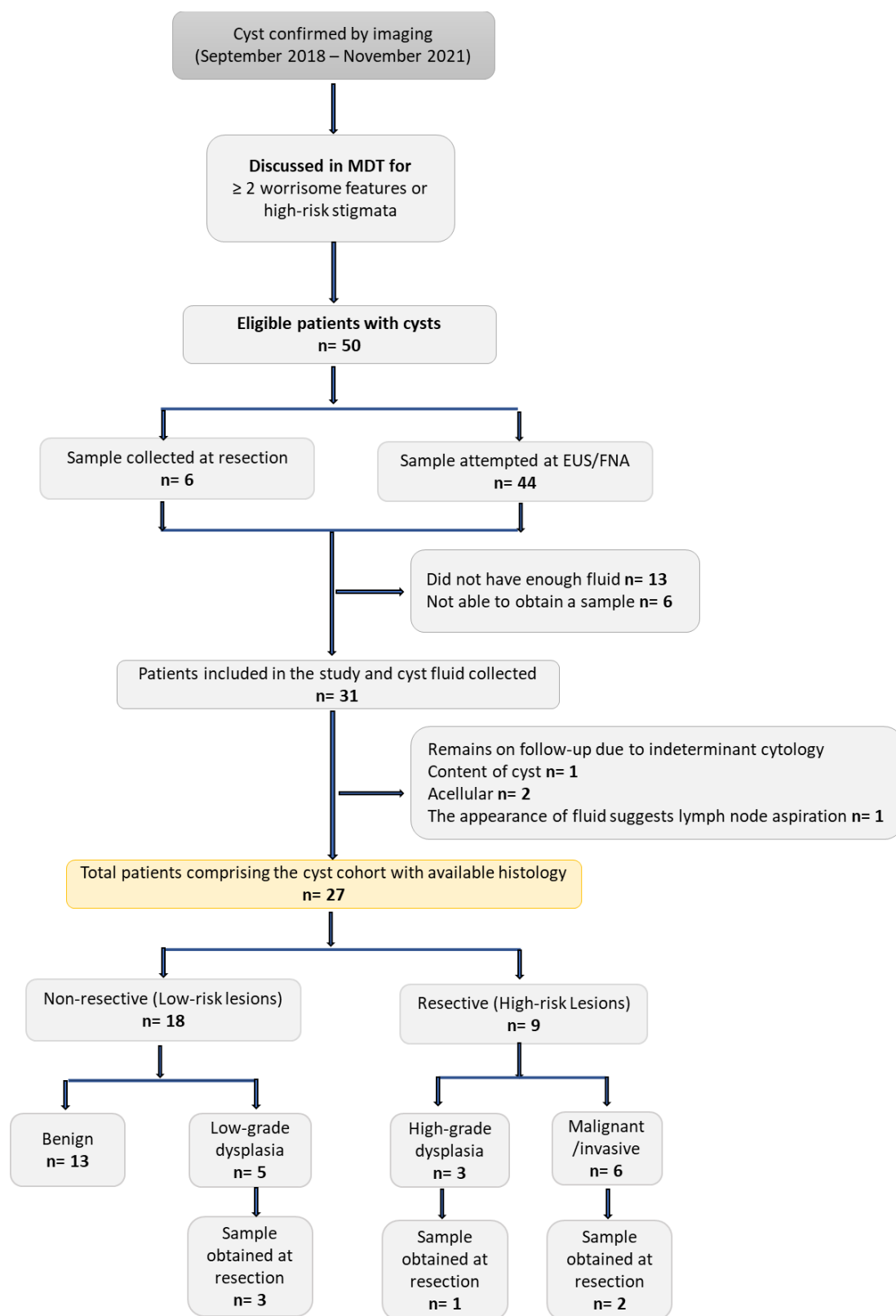
All samples were collected, maintaining patients’ safety and convenience. Cyst fluid obtained for this study was only provided if it was surplus to the sample amount needed for the requirements for routine analyses. Blood samples were collected at the same time as other routine tests. Urine samples were collected for the TEM-PAC study but were not used for the current study (Figure 26).

Figure 26: Study design within the umbrella study ‘TEM-PAC’



The study TEM-PAC aims to collect samples from 50 patients with a pancreatic cyst (Cyst fluid, serum/blood and urine), 50 patients with localised PC (resectable and non-resectable, serum/blood and urine) and 80 patients with benign hepatobiliary conditions and normal controls (serum/blood and urine). For this sub-study, samples collected till November 2021 were released for analysis, 31 for the cyst cohort, 29 for the cancer cohort and 12 for the control cohort. Cyst fluid and serum samples were analysed for indicator of malignant transformation (highlighted in blue dashed line).

Figure 27: Cyst study cohort



It is important to note that the initial protocol specified that blood serum, cystic fluid, and urine samples were required. However, subsequent amendments were made to include plasma and whole blood to accommodate the bioinformatics studies that were planned (Appendix 2). Figure 27 shows the number of patients included and the numbers breakdown between the resective and the non-resective groups.

For this particular sub-study, blood serum was the only human tissue that was consistently available in all of the cases. As a result, it was used for this exploratory investigation.

A unique patient identifier was allocated for all patients in this study to ensure anonymity. This unique number for the individual patient was used as a coding number for sample collection, data collection, and filling out the case report form (CRF). The same number was used for reporting results. A document linking the code numbers and patient's identification is secured in a locked cabinet in the Queen's Centre for Oncology and Haematology Trials Office at Castle Hill Hospital, Hull University Teaching Hospital NHS Trust. Only the authorised study team members had access to the information, and the researchers performing the laboratory analysis were blinded. In my position as an hepatopancreaticobiliary (HPB) fellow with clinical responsibilities (including HPB clinic and Hepatobiliary and Pancreatic Multidisciplinary Team (HPB MDT)), I played a key role in identifying and enlisting most of the participants for the study. Additionally, I oversaw the research nursing team, and my main focus was overseeing the acquisition of cystic fluid samples. However, due to the COVID-19 pandemic, the overall TEM-PAC study had to be put on hold for 9 months (March 2020 - November 2020). During this time, I was redeployed to frontline clinical work within the Hull University Teaching Hospitals (HUTH) NHS trust, as per the guidance provided by Yorkshire & the Humber Health Education England (Y&H HEE) and the medical school. Similarly, the research nursing team was also reassigned to clinical work for a period of 8 months.

The study is conducted in accordance with the International Conference for Harmonisation of Good Clinical Practice (ICH GCP) guidelines and the Research Governance Framework for

Health and Social Care. All samples were registered in the university system (University of Hull) in line with the Human Tissue Act (HTA) regulations.

3.5. Materials and Methods

3.5.1. Subject Selection

Patients were recruited into three groups as part of the TEM-PAC study. This included a cyst cohort, a cancer cohort and a control cohort.

The patients for the cyst cohort were selected from the patients who had a pancreatic cyst with suspected malignancy and were under follow-up for PCL. These patients are investigated further with EUS-FNA or undergo surgical resection, and this group is the main cohort for the sub-study in this thesis.

The PC cohort included patients diagnosed with localised pancreatic cancer. This consisted of patients undergoing successful surgical resection, patients with whom resection was attempted but failed and patients with radiologically inoperable and locally advanced cancers.

A control cohort is planned to be age, and gender-matched to the 50 'cyst' patients with full set of samples. This group can only be completely recruited and mapped once the whole cystic cohort has accrued. The control cohort will include patients undergoing hepatobiliary surgery or endoscopic interventions for benign inflammatory conditions, for example, endoscopic retrograde cholangiopancreatography (ERCP), biliary drainage and stenting, endoscopic cyst gastrostomy for pancreatic pseudocyst. This group has also been delayed in recruitment due to the COVID-19 disruption of elective surgery and endoscopic lists.

For the main protocol, please see appendix 1. Below is a summary of the main points.

3.5.2. Inclusion and Exclusion Criteria

The inclusion and exclusion criteria for the study are outlined in the main TEM-PAC protocol in Appendix. The general criteria for inclusion require participants to be at least 18 years old and capable of providing written informed consent. Exclusion criteria include the inability to provide written informed consent, known communicable diseases such as human

immunodeficiency virus (HIV) and hepatitis C virus (HCV), and a history of other malignant conditions within the last five years.

For the pancreatic cyst cohort, individuals with cystic lesions that require further diagnostic intervention procedures, including EUS-FNA as agreed upon by the MDT, are eligible for inclusion. Alternatively, patients with resectable lesions suspicious of pancreatic malignancy and recommended for surgery by the MDT can also be included.

In the PC cohort, participants with localised PC that can be removed through resection, such as distal pancreatectomy, total pancreatectomy, or Whipple's procedure, are eligible for inclusion. Additionally, patients with inoperable localised PC referred for further management, such as the malignant control subgroup, can be included.

Lastly, the control cohort includes participants referred for endoscopic cystogastrostomy for complicated acute pancreatitis characterised by peripancreatic fluid collections and pseudocysts in development or matured, non-resolving and requiring further intervention. Those referred for cholecystectomy for cholecystitis/cholelithiasis or endoscopy investigation for dyspepsia are also included as part of the normal control subgroup.

3.5.3. Subject recruitment

The potential patients were identified through the pancreatic multidisciplinary meeting or outpatient clinic. Those eligible were approached by the research team member. A patient information leaflet (PIF) specific to each cohort of patients (see appendix) explaining the purpose and structure of the study was provided to all patients at the first contact. This was usually at the consultation with the specialist team after discussing their further treatment or diagnostic plan. In such a way, they had enough time to consider and discuss their participation with their family, friends and general practitioner. We ensured that the patients were fully informed on the conduct of the study and had access and contact to the research team with any questions.

3.5.3.1. Pancreatic cyst cohort

The patients approached for the cyst cohort either had high stigmata features or ≥ 2 worrisome features. High-risk stigmata include main pancreatic duct diameter (MPD) ≥ 10 or enhancing solid component within the cyst. The worrisome features had cyst size ≥ 3 cm, thickening or enhancing cyst wall, non-enhancing mural nodule, MPD 5-9 mm, and abrupt change in calibre of MPD diameter with distal atrophy.

The research team approached the patients during the consultation, in which they were informed that they needed to have the cyst aspirated. After two to four weeks, they were consented when they attended the endoscopy procedure, and the study samples were taken. For cases who went directly to surgery, consent was taken on their scheduled appointment, and cyst fluid samples were taken 'on the table' (Figure 28).

3.5.3.2. Pancreatic cancer cohort

Most of the patients with resectable localised PC patients were inpatients in surgical wards. A research team member approached them in the hospital ward. They were given at least 24 hours to consider participation before the designated research nurse took consent in accordance with Good Clinical Practice (GCP). Blood samples were taken at the same time as phlebotomy for regular investigations. Patients with non-resectable locally advanced PC were approached at their scheduled outpatient clinic appointment in Oncology. Participants who were interested consented at their pre-assessment appointment at the nurse-led chemotherapy clinic 1-2 weeks after the initial consultation. Samples were taken simultaneously with their first blood before commencing chemotherapy (Figure 29).

3.5.3.3. Control Cohort

Control patients due to have cholecystectomy were initially contacted by telephone with information about the study at least one week before they attended their pre-assessment appointment. The designated research nurse took consent at the pre-assessment appointment, and blood samples were taken at the same time as pre-assessment blood.

Figure 28: Cyst patient pathway

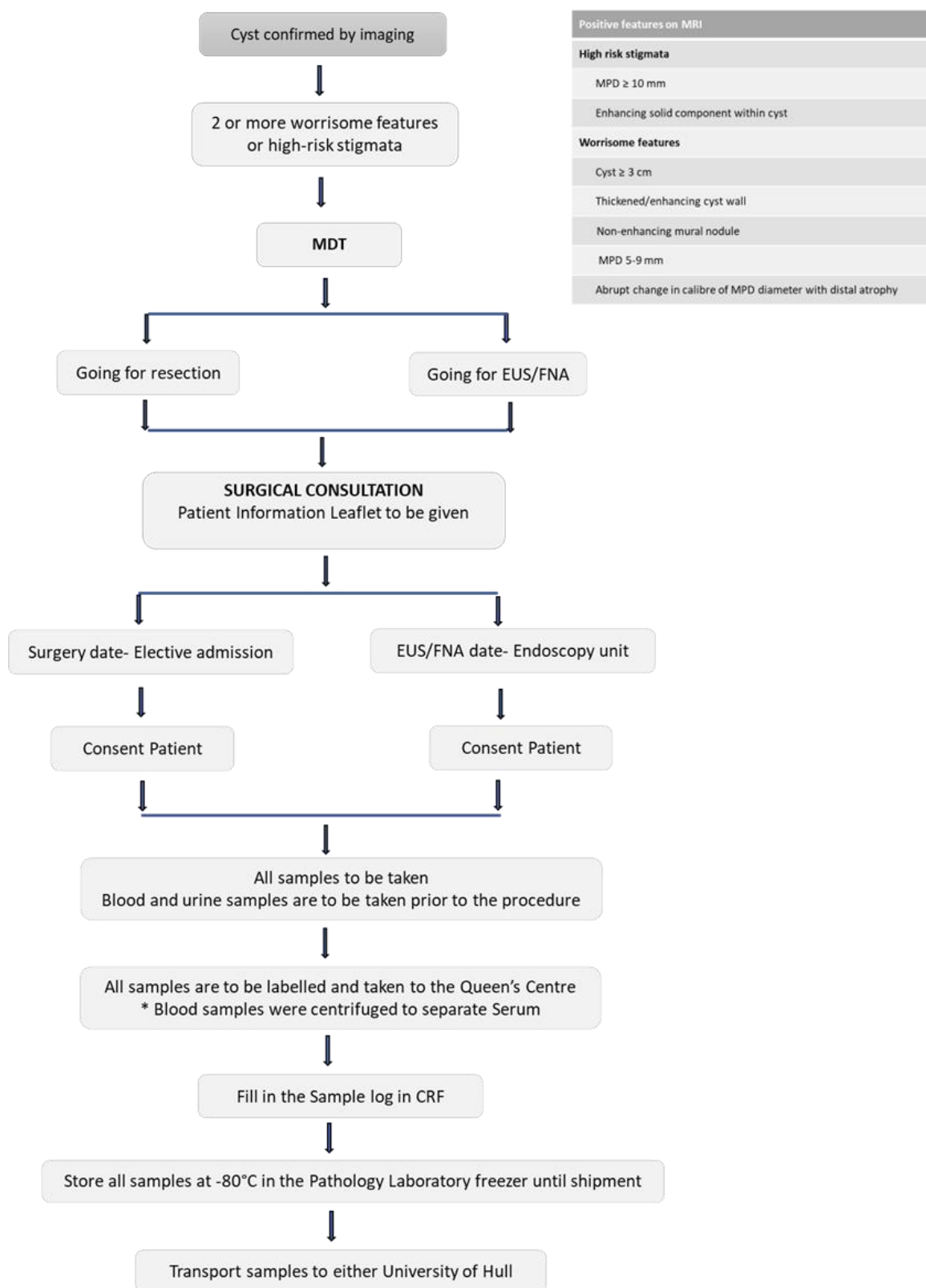
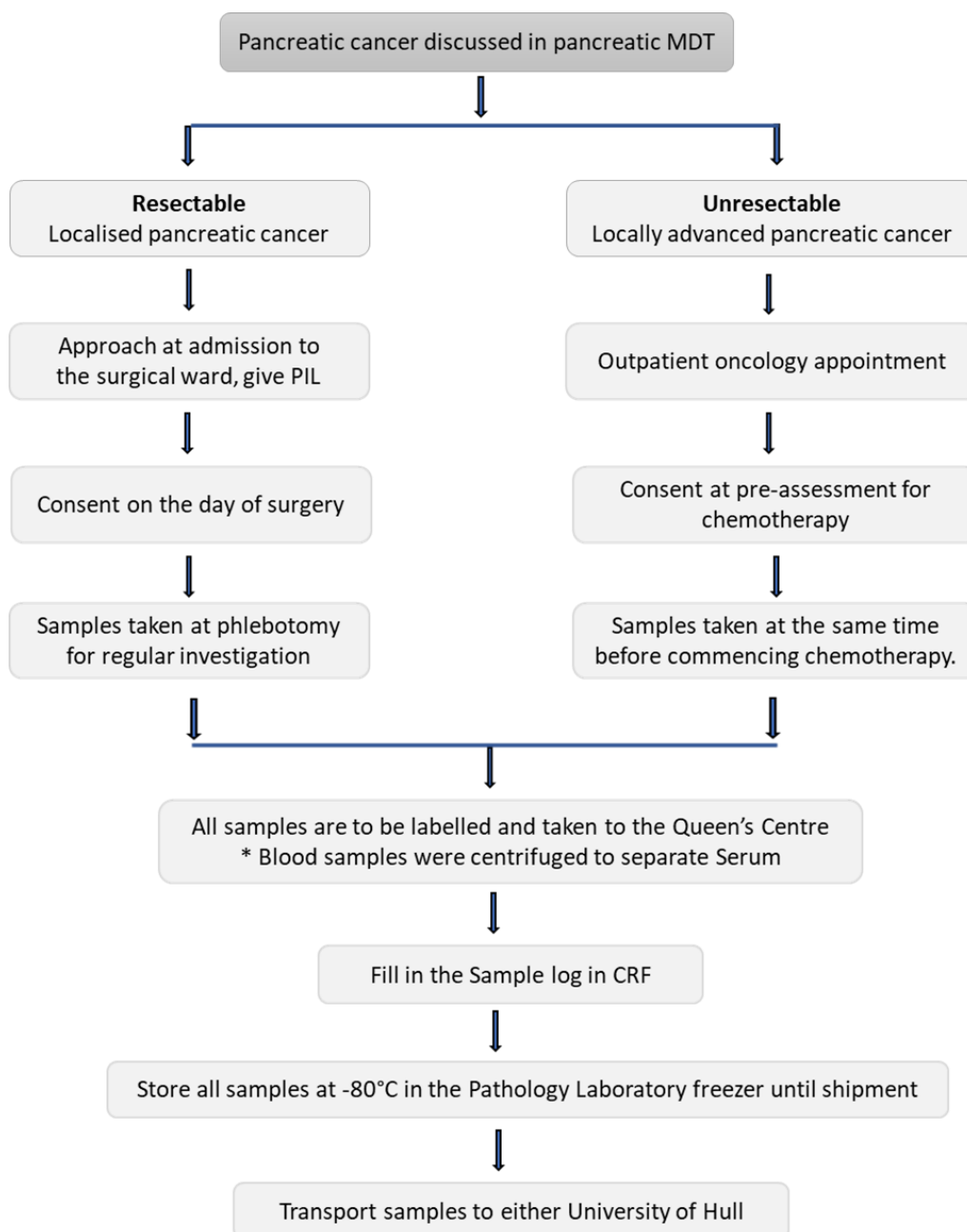


Figure 29: Pancreatic cancer patient pathway



Patients were given a urine sample bottle at this appointment and asked to bring a urine sample when they attended for cholecystectomy.

Patients with complicated acute pancreatitis have a repeat CT scan at 6-8 weeks to determine whether the pseudocyst has resolved/was resolving. Control patients with non-resolving pseudocysts were approached with information about the study at their first clinic appointment after the repeat CT scan. Consent and study samples were taken when they attended the EUS suite for endoscopic cystogastrostomy.

A research team member initially approached control patients with dyspepsia during an appointment at the EUS suite for an endoscopy. Consent was taken by the designated research nurse at the follow-up consultation in the gastric clinic one to two weeks after their endoscopy. Blood samples were taken at the same time as scheduled follow-up blood, and patients were asked to provide a urine sample at this appointment (Figure 30).

3.5.4. Samples collection

3.5.4.1. Cyst fluid Samples

The top third of the drained cystic fluid (3 to 10 ml) was collected in a sterile tube with no preservatives; the amount was less for smaller cysts with a solid component. For a proportion of cases, there was no cystic fluid made available for research purposes. Fluid was stored at -80°C freezer.

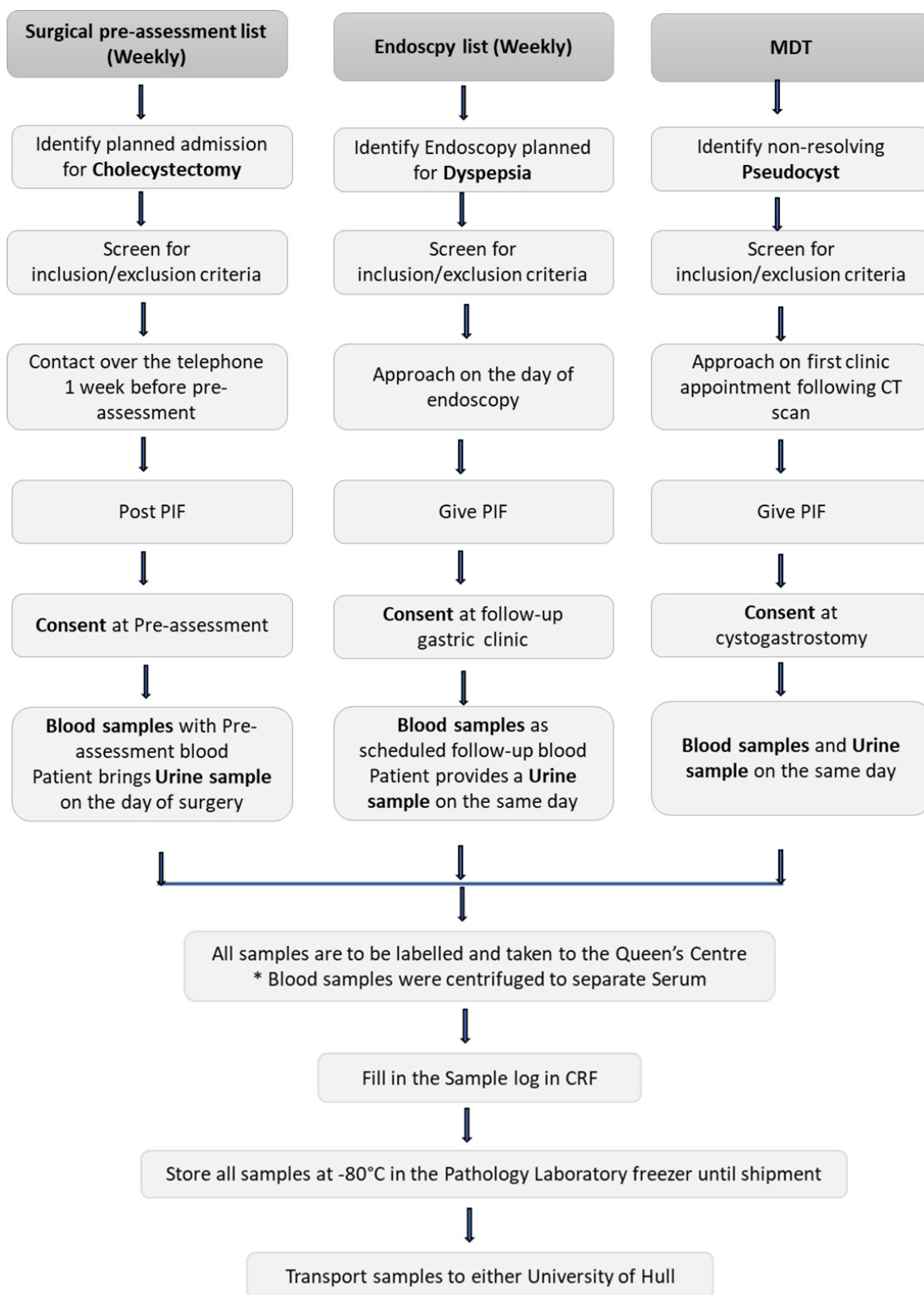
3.5.4.2. Serum samples

10 ml blood (2x yellow-top tubes) was collected per patient. Samples were centrifuged at 1000-2000 x g to separate out serum fractions. The serum fraction was transferred to a fresh sterile container before storage in a -80°C freezer.

3.5.5. Data collection

All samples were coded with a unique identifier before transport to the laboratories. They were numbered consecutively, starting from CHH 001, CHH 002, CHH 003, etc. Laboratory

Figure 30: Control patient pathway



experiments were done in a blinded fashion. All data reported was anonymous and identified by a study number only.

Data were collected on a CRF (see appendix), including the type of cyst, volume removed, final histological diagnosis and stage. Data were collected and retained in accordance with the Data Protection Act 2018 and the General Data Protection Regulation (GDPR).

All data are stored on password-protected NHS computers, with user-restricted access and in adherence to the Trust Information Governance Policy. Data were transferred to the University of Hull encrypted over a secure network. IT Services Department has a backup procedure approved by auditors for disaster recovery. Study documents (paper and electronic) are retained in a safe location.

3.5.6. Enzyme-linked immunosorbent assay (ELISA)

The Bradford assay was used to measure the total protein concentration of cyst fluid samples (Section 2.4.1). Before assessing the protein concentration in cyst fluid samples, a test assay was performed using two cyst fluids at different concentrations. The fluid samples (019 and 075) were diluted in PBS at 75% v/v, 50% v/v and 25% v/v. Without dilution, the protein concentration of one of the cyst fluids was outside the range of the upper end of the standard curve. Following this trial assay, the cyst fluid samples were diluted in PBS at 1:10 (10% v/v, 2 µl cyst fluid in 18 µl of PBS) before running the Bradford assay to ensure the correct measurement of the cyst fluid protein concentration.

The Quantikine® ELISA kit was used to measure the concentration of TF antigen in the patient's cyst fluid and serum samples (Section 2.4.2). This kit is among several TF-ELISA kits that have been used in published reports, and their applications differ by study (421). The Quantikine kit was found to exhibit a significant correlation with TF levels, indicating that it is a suitable tool for detecting TF derived from cancer cells (422-425). This assay applies the quantitative sandwich enzyme immunoassay technique. All samples were 2-fold diluted with Calibrator Diluent RD5-20 (150 µl of sample + 150 µl of Calibrator Diluent RD5-20), and the test was performed in duplicates. Standards and samples are pipetted into the wells of a

monoclonal antibody specific for human Coagulation Factor III pre-coated microplate. The immobilised antibody binds any Coagulation Factor III present in the standards and samples. Any unbound substances are washed, and an enzyme-linked polyclonal antibody specific for human Coagulation Factor III is added to the wells. After a wash, a substrate solution is added to the wells to remove any unbound antibody-enzyme reagent. Colour develops in proportion to the amount of Coagulation Factor III bound in the initial step. The colour development is stopped, and the intensity of the colour is measured.

The AssayPro Human Factor VII ELISA kit was used to determine the concentration of fVIIa antigen in the patient's cyst fluid sample (Section 2.4.3). This assay employs a similar quantitative sandwich enzyme immunoassay technique except for a biotinylated polyclonal antibody specific for human fVII is used, which is recognised by a SP conjugate. 50 µl of each sample was used for this assay.

The ELISA method was chosen as it has several advantages over other techniques. Firstly, it has a simple procedure, which makes it easy to use. Secondly, it is highly specific and sensitive due to the antigen-antibody reaction it employs. Thirdly, it is highly efficient since simultaneous analyses can be conducted without complex sample pre-treatment. Fourthly, it is generally considered safe and eco-friendly because it does not require radioactive substances or large amounts of organic solvents. Finally, the ELISA method is a cost-effective assay as it uses low-cost reagents. Overall, these advantages make ELISA a preferred choice for various research and diagnostic applications.

Prior to conducting the analysis of the entire cyst cohort samples, the Quantikine® ELISA kit was tested on cyst and serum samples from four patients (007, 013, 027, 029) in order to optimise its application. The test was performed in duplicates, with all samples being diluted 2-fold. In addition, Triton-X was added to the samples at a concentration of 1% v/v and again quantified using ELISA. It was necessary to investigate whether the use of Triton-X would result in a more accurate measurement of TF antigen by lysing the lipid bilayer of the MV and potentially releasing encrypted TF antigen.

3.5.7. Statistical analysis methods

Data analyses were performed with SPSS v27, IBM Corp TM, STATA SE17 and PRISM GraphPad. Categorical variables were summarised using frequency and percentage. Comparisons between categorical variables were performed with Fisher's exact test. The level of TF and fVIIa proteins were measured, and the fVIIa:TF ratios were calculated. Data were expressed as mean with a SEM and 95% confidence interval (CI) where applicable, and statistical significance was considered when $p \leq 0.05$. An optimum cut-off value for TF concentration was determined using a receiver operating characteristic (ROC) curve and compared to the conventional assessment parameters, including radiological features, CEA and amylase. The odds ratio was calculated by logistic regression to evaluate the association of TF concentration with high-risk cysts.

3.6. Results

From September 2018 to Nov 2021, patients with pancreatic cysts were screened for eligibility. 50 patients with high-risk stigmata or ≥ 2 worrisome features were approached and consented to participation in the study. 44 patients underwent EUS-FNA, and 6 had cyst fluid aspiration at the surgical resection of the cystic lesions. In 19 patients, it was not possible to acquire cyst fluid samples as no excess samples remained following routine procedures or due to technical difficulties. The remaining 31 patients constituted our study cyst cohort (Figure 27). After the laboratory analysis of the TF and fVIIa cyst cohort, follow-up data for histopathologic cyst type were disclosed. For 4 patients, the histopathological cyst type were indeterminant; these cases remained suspicious but, due to comorbidity or age, have not proceeded to resection and remain on close follow up. In conclusion, 27 patients with clinical data and laboratory parameters (Figure 27, Figure 31) are the subject of the analyses in this study.

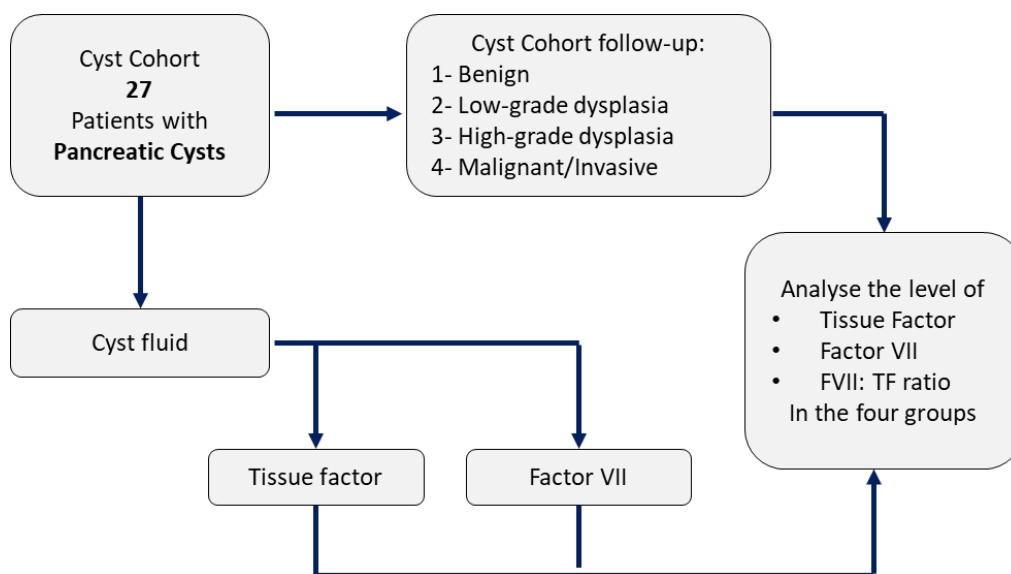
3.6.1. Characteristics of the cyst cohort

The clinical, radiographic and pathologic characteristics of the cyst cohort are summarised in Table 24, Table 25, Table 26 and Figure 32. The median age of the whole cyst cohort was 64 years (interquartile range 53-73). 59.1% (14/27) were male. 25.9% (7/27) were diabetic, and 7.4% (2/27) had pre-diabetes. 18.5% (5/27) had a history of chronic pancreatitis. 25.9% (7/27) had high-risk radiographic stigmata, 14.8% (4/27) ≥ 2 worrisome features, and 66.7% (18/27) had at least one worrisome feature. The pathological cyst type on follow-up revealed that the cyst cohort comprised of patients with IPMN (6/27), MCN (4/27), pseudocyst (7/27), serous cyst (2/27), IPMN with a solid mass (3/27), cyst with a solid mass (3/27) and unspecified benign cyst (2/27). Those with a solid mass (6) were confirmed to be malignant pancreatic cysts on follow-up and consisted of 4 adenocarcinomas, 1 mucinous adenocarcinoma and 1 basaloid squamous cell carcinoma.

3.6.2. The physical appearance of the cyst fluid

The majority (44.4%) of the cyst fluid samples were clear; however, there were variations in the appearance of the cyst fluid (Table 27). 8 (29.6%) cyst fluid samples were bloodstained. 7

Figure 31: Study design



Cyst fluid was collected from 27 patients with PCL and analysed in a blinded fashion. The concentration of TF and fVIIa proteins was quantified using ELISA, and the fVIIa:TF ratios were calculated. The findings were subsequently compared with the histopathological or cytological classification of the cyst type.

Table 24: Clinical characteristics of the cyst cohort (No=27)

Characteristics	Benign (13) n (%)	LGD (5) n (%)	HGD (3) n (%)	Malignant (6) n (%)
Sex				
Female	5 (38.5)	3 (60)	3 (100)	2 (33.3)
Male	8 (61.5)	2 (40)	0 (0)	4 (66.7)
Diabetes				
Pre-diabetes	1 (7.7)	1 (20)	0 (0)	0 (0)
Diabetes	3 (23.1)	0 (0)	2 (66.7)	2 (33.3)
History of chronic pancreatitis	4 (30.8)	1 (20)	0 (0)	(0)

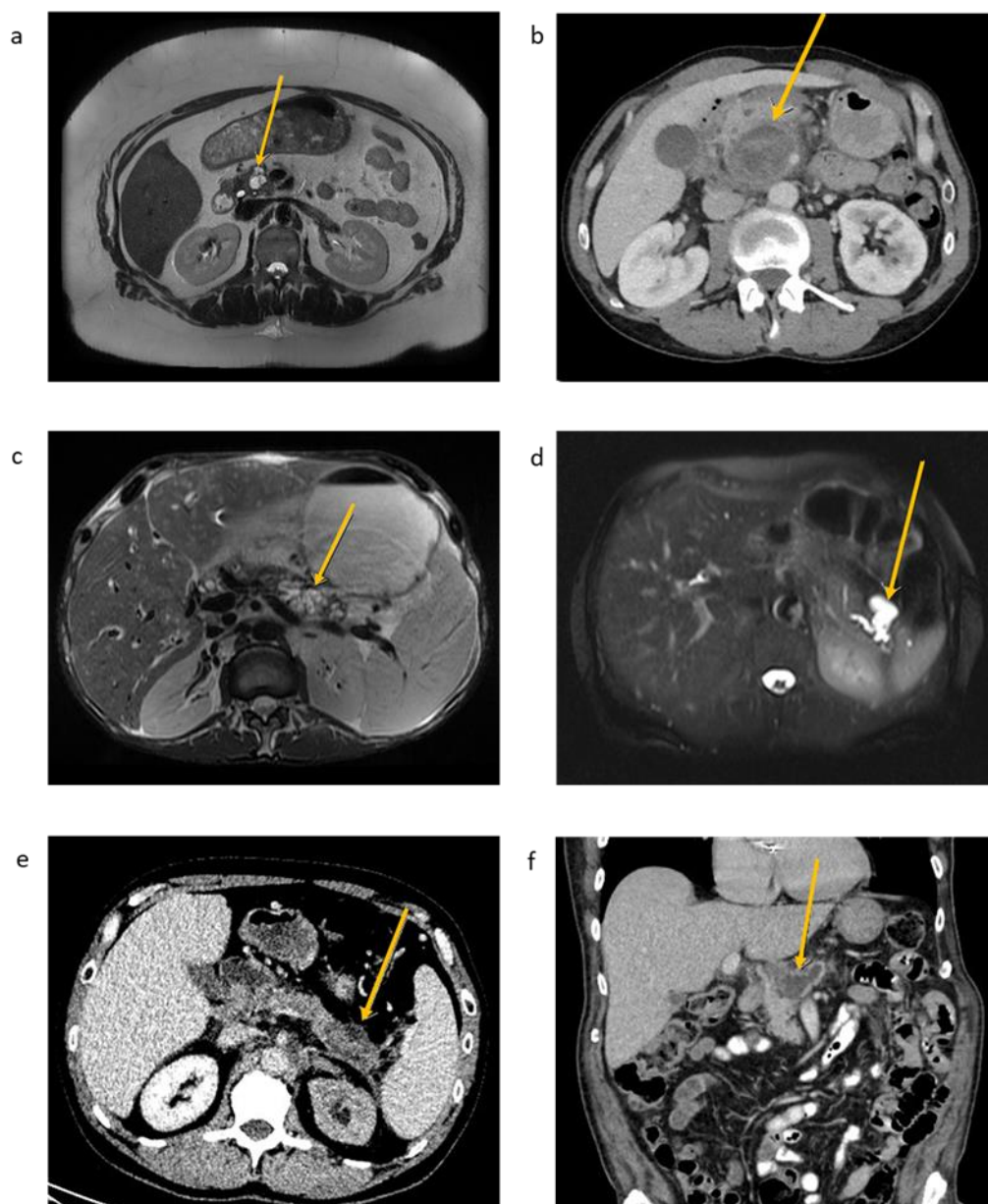
Table 25: Radiographic characteristics of cyst cohort (No=27)

	Benign (13)	LGD (5)	HGD (3)	Malignant (6)
High-risk stigmata				
MPD \geq 10 mm	1		1	2
Enhancing solid components within cyst	1		1	1
Worrisome features				
Cyst \geq 3 cm	8	3		2
Thickened/enhancing cyst wall	4			1
Non-enhancing mural nodule	1	1		
MPD 5-9 mm	1	1		
Abrupt change in calibre of MPD diameter with distal atrophy				

Table 26: Pathological characteristics of cyst cohort (No=27)

Pathological cyst type	Benign (13)	LGD (5)	HGD (3)	Malignant (6)
IPMN (22.2%)	2	3	1	
MCN (14.8%)	2		2	
Pseudocyst (29.5%)	6	1		
Serous cyst (7.4%)	1	1		
Cyst with a solid mass (11.1%)				3
IPMN with a solid mass (11.1%)				3
Cyst (unspecified) (7.4%)	2			

Figure 32: Radiological appearance of PCLs



Example of imaging of PCLs; a- MRI scan showing unilocular cystic lesion arising from the uncinus process of the pancreas- serous cyst; b- CT scan showing pseudocyst; c- MRI showing main duct IPMN; d- MRI showing branch-duct IPMN in the tail of pancreas; e- CT scan showing solid cystic lesion on the tail of pancreas; f- CT scan showing IPMN with a solid mass within the cystic lesion in the head of the pancreas

Table 27: Physical appearance of the cyst fluid

Appearance	n (%)
Clear	12 (44.4)
Bloodstained	8 (29.6)
Light brown	3 (11.1)
Straw colour	1 (3.7)
white	1 (3.7)
yellow	1 (3.7)
Dark brown	1 (3.7)

(25.9%) samples were viscous, and 2 (7.4%) appeared cloudy (Figure 33).

The presence of mucin constitutes a part of the routine investigation following EUS-FNA of cyst fluid. These data were available only for 17 cyst samples. Mucin was detected on 7/17 (41%) cyst fluids and given the missing data, was not included in these analyses.

3.6.3. Pancreatic cyst patients stratification in risk groups

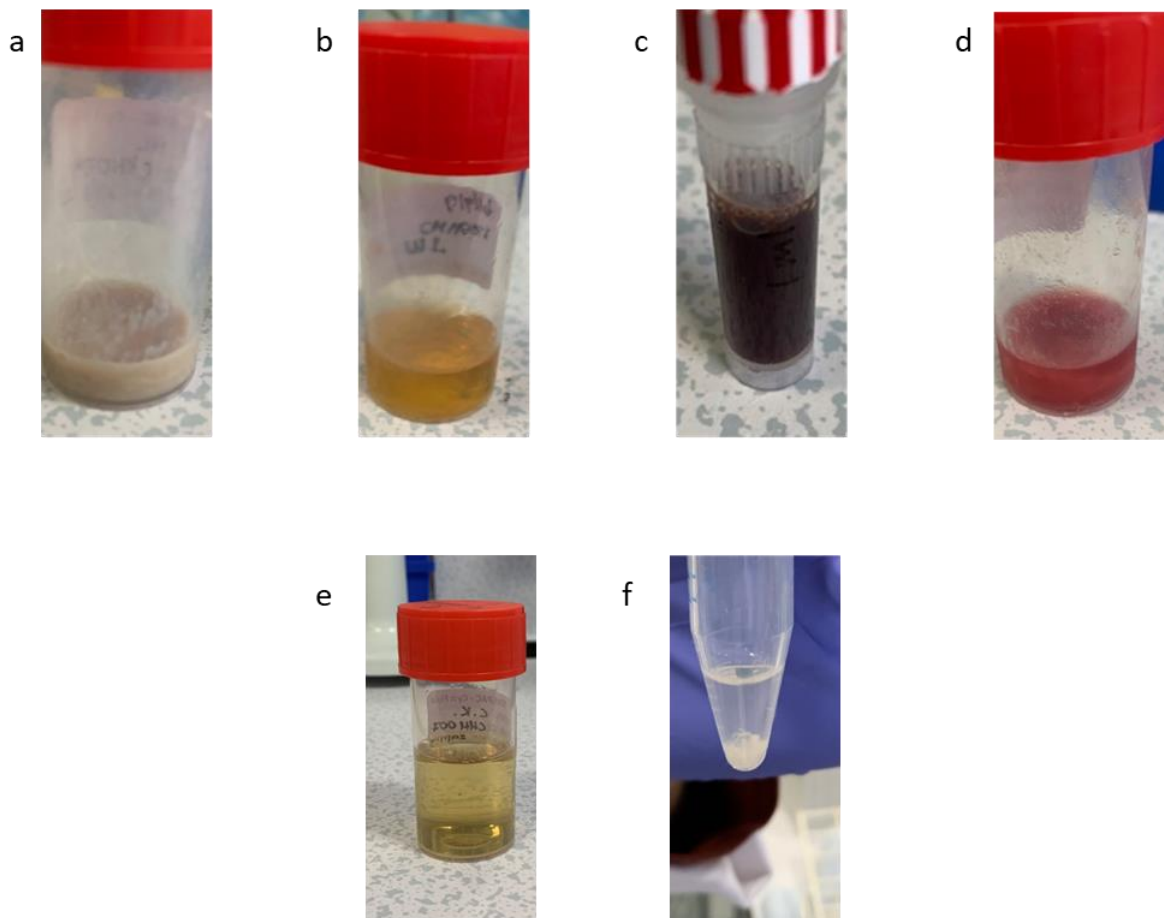
The patients in the cyst cohort were stratified into two risk groups based on the pathological cyst type. The low-risk 'non-resective' group included patients with benign cysts and LGD, and the high-risk 'resective' group included patients with HGD and invasive/malignant cysts. The clinical, radiographic and pathologic characteristics of the cyst cohort stratified by disease risk are summarised in Table 28. The non-resective disease was identified in 18 (66.7%), and 9 (33.3%) had resective disease. The median age at the aspiration of suspected cyst fluid was similar in both groups. Males represented 44.4% of the resective group. There was no gender-specific difference in the disease risk groups. Diabetes was more common in the resective group, 44.4% (n=4), while a history of chronic pancreatitis was present in 27.8% (n=5) of the non-resective group. High-risk stigmata were associated with the resective group, present in 55.6% (n=5). At least one radiographic worrisome feature was more frequent in the non-resective group (n=15, 83.3%).

3.6.4. Optimisation of the measurement of TF antigen with Quantikine® TF ELISA kit

Samples from 4 patients were used to optimise the application of an ELISA kit for the analysis of TF concentration in cyst fluid and serum samples. The samples were diluted 2-fold and tested in duplicates, and Triton-X was added to study whether lysis of the samples would result in a more accurate measurement of TF antigen. The outcome was similar for serum samples when compared between untreated and Triton-X solubilised samples (Figure 34 & Figure 35). For most samples, TF concentration was within the standard curve range (Figure 36).

We used the Bland-Altman plot (426) to compare, evaluate, and visualise the differences in measurements between the two methods of processing cyst fluid and serum samples before

Figure 33: Appearance of the cyst fluids

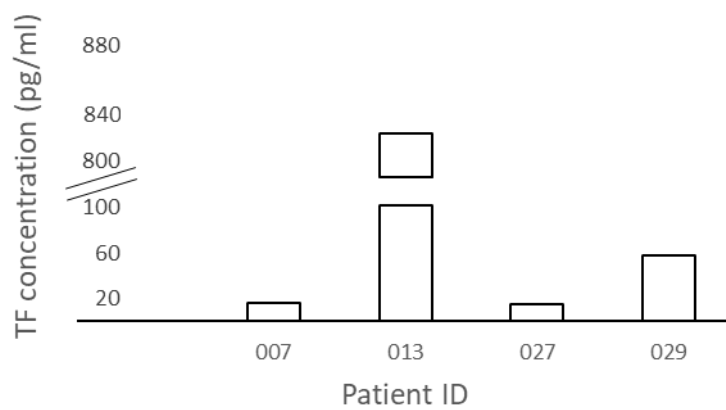


Variations in the appearance of the cyst fluid a- viscous light brown, b- clear yellow, c- clear brown, d- clear blood stained, e- clear straw, f- clear with mucous.

Table 28: Clinical, biologic, radiographic, and pathologic characteristics with univariate analysis, stratified by non-resective and resective groups

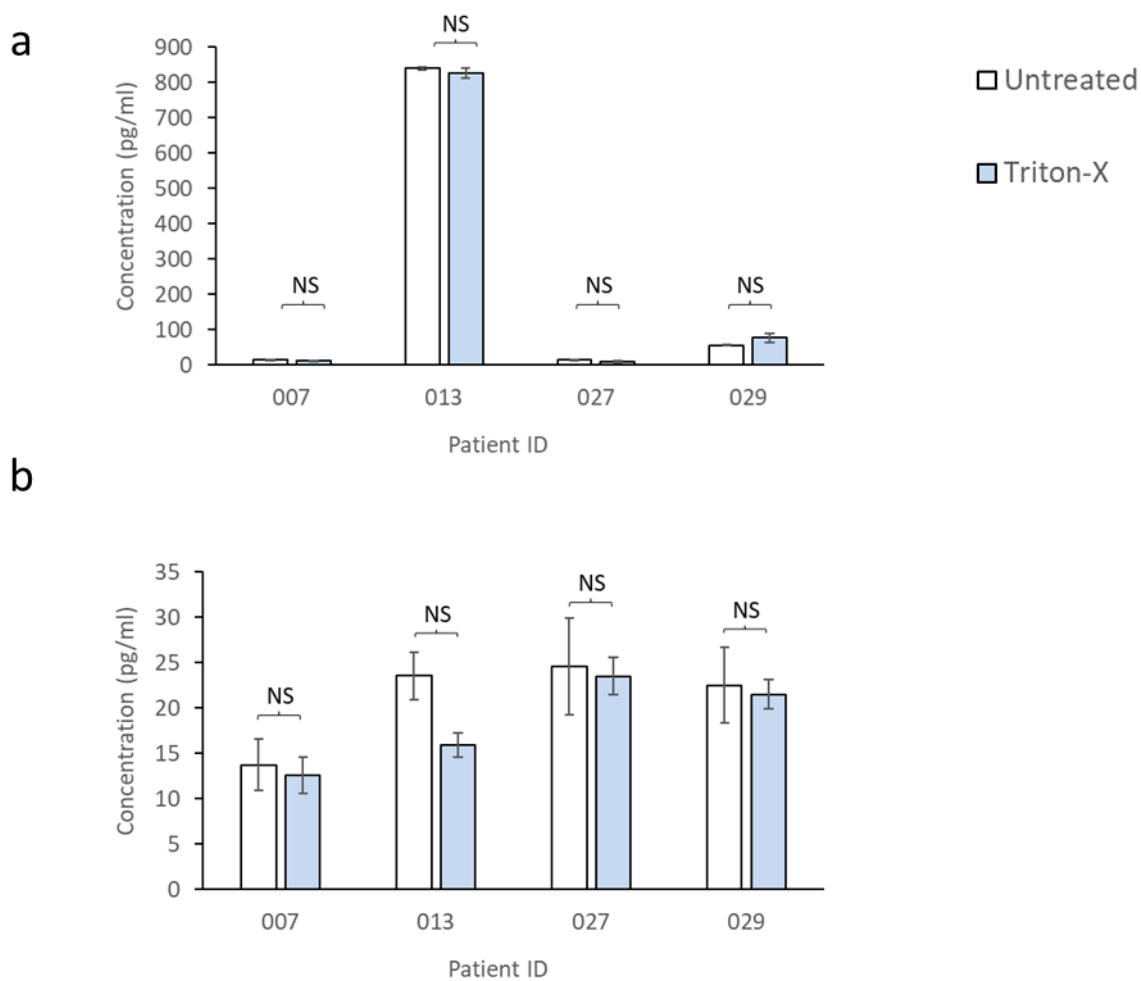
	Total n=27 n (%)	Non- resective n=18 n (%)	Resective n=9 n (%)	p value
Sex (male)	14 (51.9)	10 (55.6)	4 (44.4)	0.603
Median age: years (IQR)	64 (53-73)	66 (53-74)	63 (53-70)	0.726
Co-morbidities				
Diabetes	9 (33.3)	5 (27.8)	4 (44.4)	0.432
Chronic pancreatitis	5 (18.5)	5 (27.8)	0 (0)	0.136
High-risk stigmata	7 (25.9)	2 (11.1)	5 (55.6)	0.023
MPD \geq 10 mm	4 (14.8)	1 (5.6)	3 (33.3)	0.093
Enhancing solid components within cyst	3 (11.1)	1 (5.6)	2 (22.2)	0.250
Worrisome features (\geq2)	4 (14.8)	4 (22.2)	0 (0)	0.268
Cyst \geq 3 cm	13 (48.1)	11 (61.1)	2 (22.2)	0.103
Thickened/enhancing cyst wall	5 (18.5)	4 (22.2)	1 (11.1)	0.636
Non-enhancing mural nodule	2 (7.4)	2 (11.1)	0 (0)	0.538
MPD 5-9 mm	2 (7.4)	2 (11.1)	0 (0)	0.538
Abrupt change in calibre of MPD diameter with distal atrophy	0 (0)	0 (0)	0 (0)	.

Figure 34: Optimisation of TF ELISA in cyst fluid samples



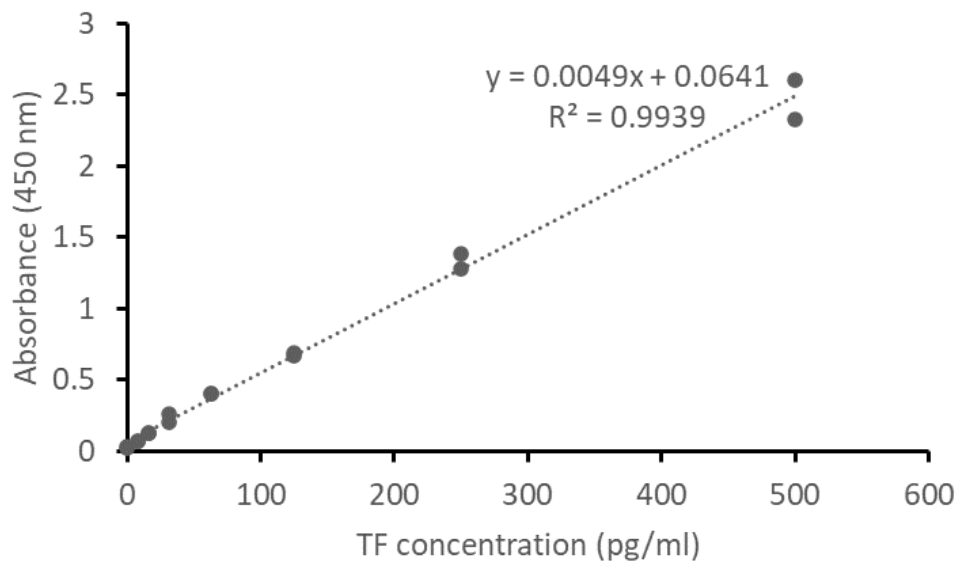
Cyst samples from four patients were assessed by TF-ELISA for TF concentration. (n=2, the data represent one experiment carried out in duplicate).

Figure 35: Assessment of the presence of TF in patient samples



a- Cyst and b- serum samples from four patients were assessed by TF-ELISA for TF concentration. In addition, each sample was incubated with Triton-X (1% v/v) for 5 min before quantification of TF antigen. (n=2, the data represent one experiment carried out in duplicate; data = mean values \pm SD; independent t-test, NS = not significant)

Figure 36: Standard curve for determining TF concentration using TF-ELISA



The standard curve was constructed using a serial dilution (0-500 pg/ml) of recombinant TF provided with the kit. The standards (150 μ l) were placed in 96-well plates and assessed by ELISA. The absorption of the samples was then measured at 450 nm using a plate reader (n=2).

assessing TF levels using ELISA. The plot displays the difference between the two measures against their averages (means).

The Y-axis represents the difference in measurements between the untreated and Triton-X solubilised samples, while the X-axis shows the average of the two methods.

In the case of cyst fluids, a one-sample t-test revealed a non-statistically significant p-value of 0.493, allowing us to proceed with the Bland-Altman plot. Upon investigating proportional bias, we found no points outside the 95% confidence interval. Further regression analysis indicated a beta value for the mean of 0.02, close to '0', and yielded non-statistically significant results ($p = 0.199$), suggesting the absence of proportional bias (Figure 37(a)).

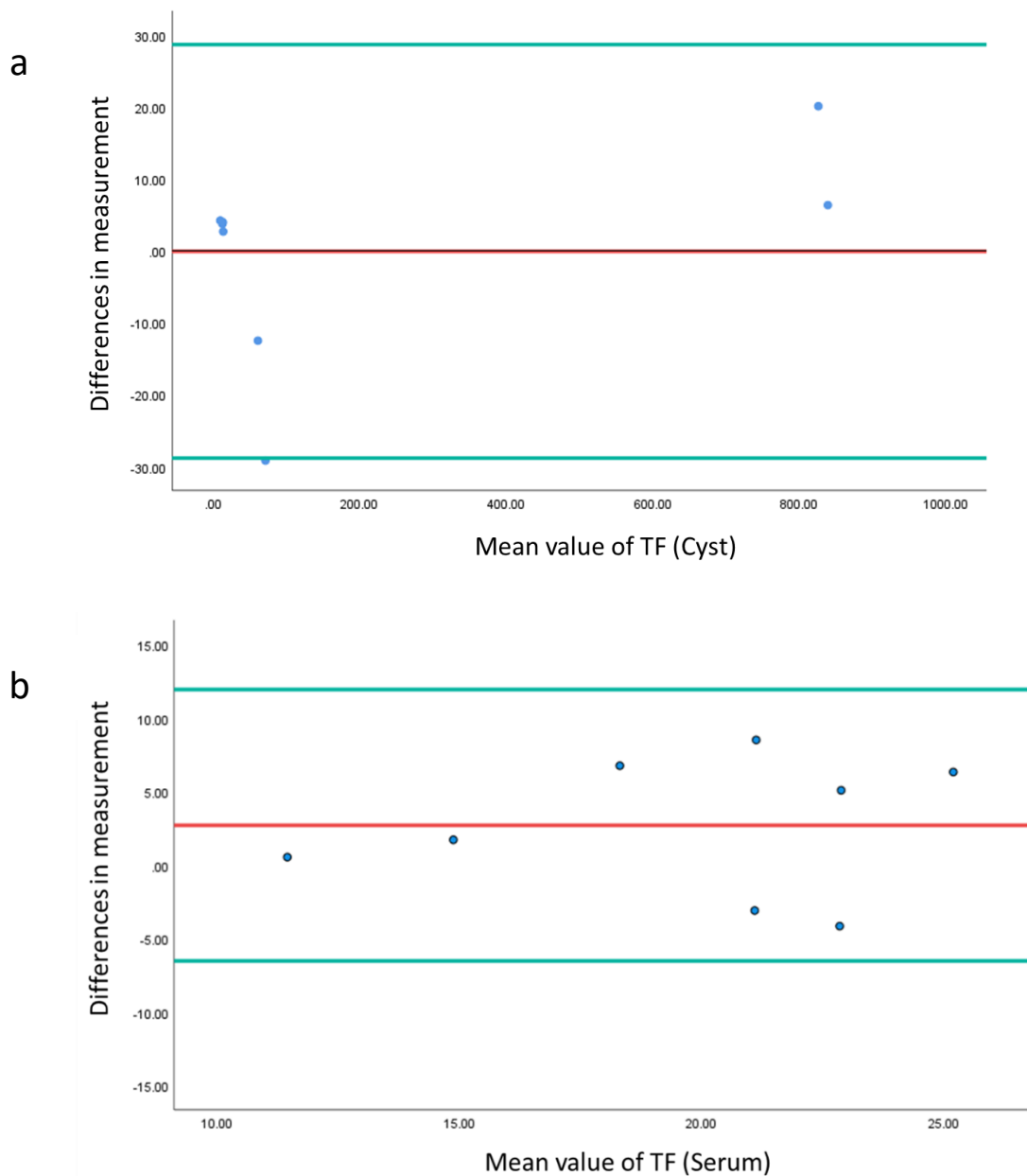
For serum samples, the one-sample t-test showed a non-statistically significant p-value of 0.074, permitting us to use the Bland-Altman plot. Similar to cyst fluid samples, no points fell outside the 95% confidence interval when investigating proportional bias. The regression analysis for serum samples resulted in a beta value for the mean of 0.15, close to '0', and yielded non-statistically significant results ($p=0.718$), indicating the absence of proportional bias (Figure 37(b)).

Overall, the average discrepancy between the two methods is small, regardless of the four histopathological cyst types considered. The narrow limits of agreement suggest minimal bias, consistent variability across the graph, and a near-equivalence between the two methods.

3.6.5. Measurement of protein concentration in the cyst fluid

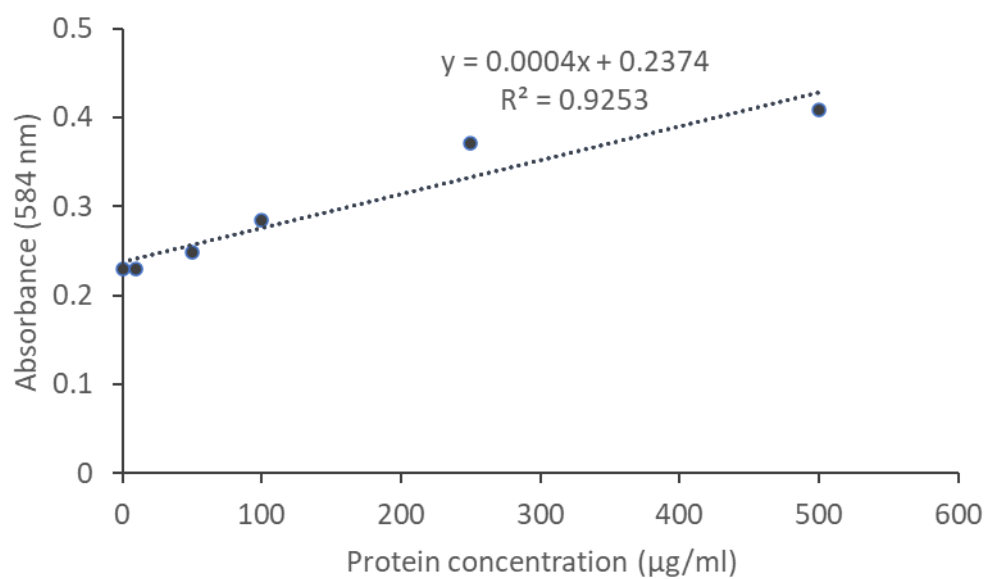
The total protein concentration of cyst fluid samples were measured using the Bradford assay (Figure 38) (Section 2.4.1). The mean protein concentration between the four histopathological groups did not vary significantly ($p=0.804$). The mean concentration was 3222 ± 584 $\mu\text{g/ml}$ in the benign, 3285 ± 1050 $\mu\text{g/ml}$ in LGD, 4671 ± 781 $\mu\text{g/ml}$ in HGD and 3796 ± 532 $\mu\text{g/ml}$ in the malignant group. The median concentration was 4021 $\mu\text{g/ml}$ (IQR 3475) in the benign, 4002 $\mu\text{g/ml}$ (IQR 4619) in the LGD, 4671 $\mu\text{g/ml}$ in HGD and 3933 $\mu\text{g/ml}$ (IQR 2313) in the malignant group (Figure 39). No significant difference in the median value of protein concentration was detected between the groups. These data indicate a

Figure 37: Bland-Altman plots assessing agreement in TF concentration measurements performed with and without Triton-X



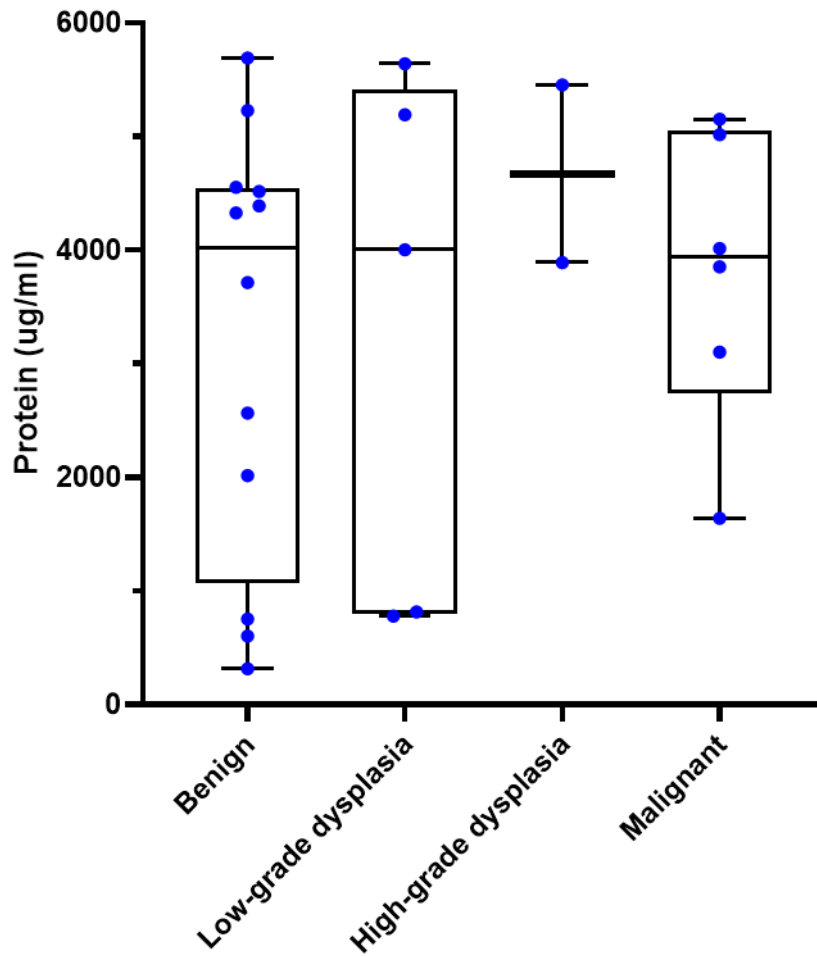
a- Cyst and b- serum samples from four patients were assessed by TF-ELISA for TF concentration. In addition, each sample was incubated with Triton-X (1% v/v) for 5 min before quantification of TF antigen. Bland-Altman plots were used to visualised the differences in measurements of TF concentration with and without Triton-X.

Figure 38: Standard curve for determining protein concentrations using the Bradford assay



The standard curve was constructed using a serial dilution (0-500 µg/ml) of lipid-free BSA stock solution (10 mg/ml). The standards were placed in 96-well plates. The absorption values were measured at 584 nm using a plate reader (n=2).

Figure 39: Assessment of protein concentration in the cyst fluid samples



Protein concentration in the four histological groups. Protein was measured using the Bradford assay (n= 2, the experiment was carried out in duplicate; data = median with interquartile range; the Kruskal-Wallis test, *p* not significant).

considerable variation in protein concentration within each group, with a comparable range of minimum and maximum protein levels between groups.

3.6.6. Measurement of TF in the cyst fluid

The Quantikine® ELISA kit was used to measure the concentration of TF antigen in the cyst fluid samples against a standard curve (Figure 40). There was a significant difference in mean and median TF concentration between the four histopathological groups ($p=0.008$ for the mean and $p=0.019$ for the median, Kruskal-Wallis test (Figure 41 (a)). The mean TF concentration was significantly higher ($p=0.004$, Kolmogorov-Smirnov test) in the resective group (HGD & malignant; 1.17 ± 0.22 ng/ml, 95% CI 0.68, 1.67) vs the non-resective group (benign & LGD; 0.27 ± 0.08 ng/ml, 95% CI 0.1, 0.44) (Figure 41(b)).

3.6.7. Analysis of TF concentration per unit of total protein (TP)

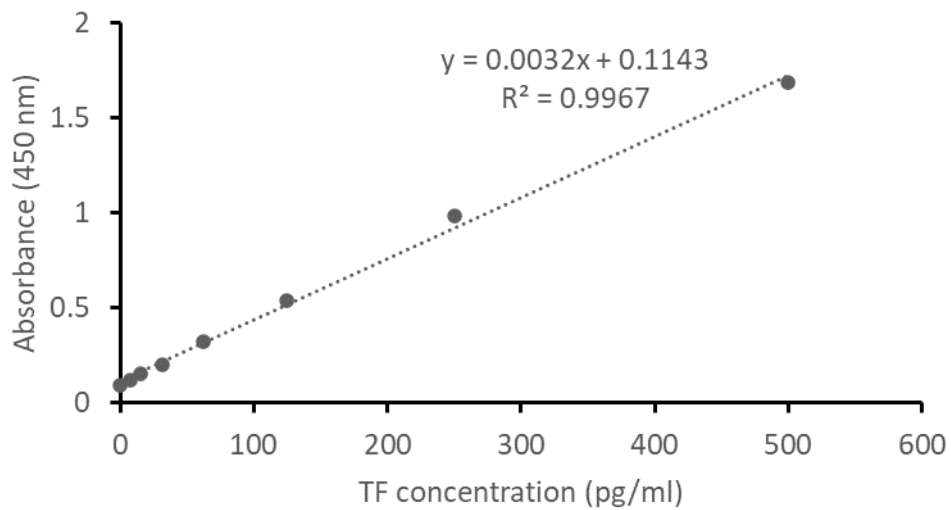
A ratio of TF and total protein concentration was calculated to assess the relative concentration of TF in the cyst fluid per unit of total protein. TF concentration was in pg/ml and TP concentration in $\mu\text{g/ml}$. Hence the proportion of TF in cyst fluid was represented as pg/ μg . There was a significant difference in mean and median TF/TP ratio between the four histopathological groups ($p=0.007$ for the mean and $p=0.006$ for the median, Kruskal-Wallis test, Figure 42 (a)). The mean TF/TP ratio was significantly higher ($p=0.006$, Kolmogorov-Smirnov test) in the resective group (3.37 ± 0.67 pg/ μg , 95% CI 1.18, 4.95) vs the non-resective group (0.8 ± 0.22 pg/ μg , 95% CI 0.33, 1.27) (Figure 42).

3.6.8. Measurement of fVIIa in the cyst fluid

The AssayPro Human Factor VII ELISA kit was used to determine the concentration of fVIIa antigen in the patient's cyst fluid sample against a standard curve (Figure 43).

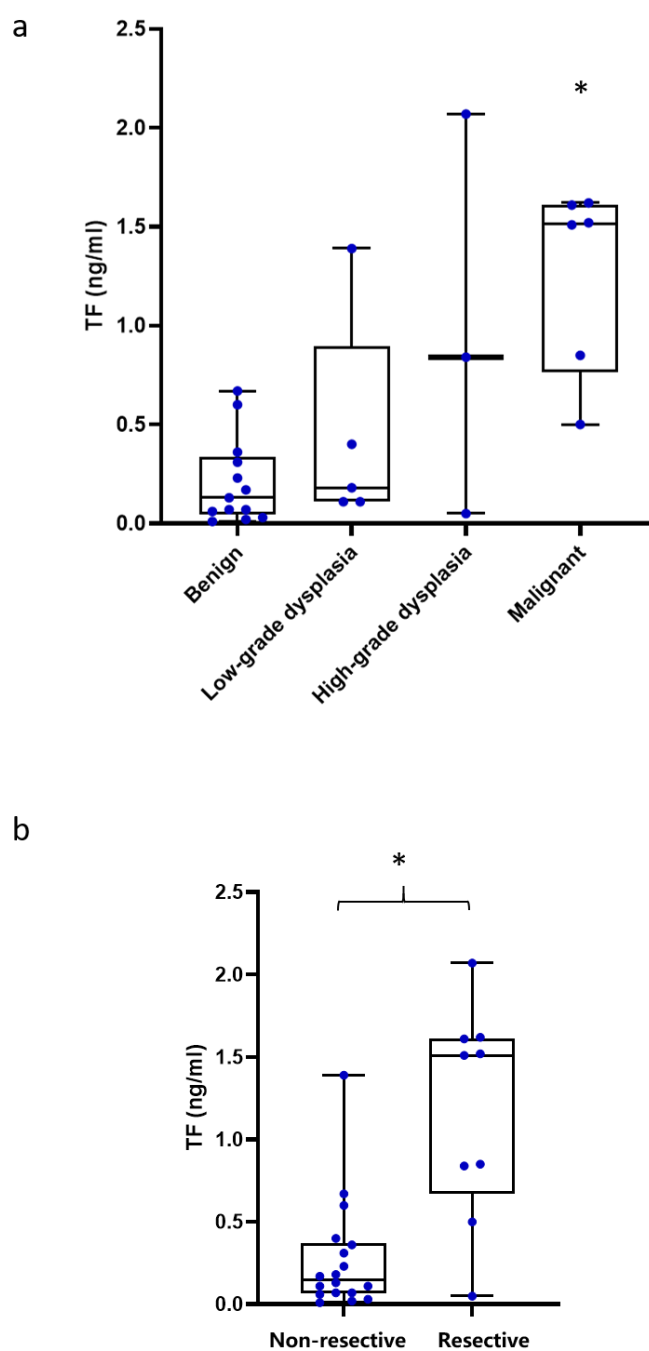
There was a trend of increase in the mean and median concentration of fVIIa with the progression of histological grade of disease in the four histopathological groups ($p=0.251$ for the mean and $p=0.602$ for the median, Kruskal-Wallis test, Figure 44) but the difference was not statistically significant. In addition, the degree of rise in fVIIa concentration was lesser

Figure 40: Standard curve for determining TF concentration in the cyst cohort using TF-ELISA



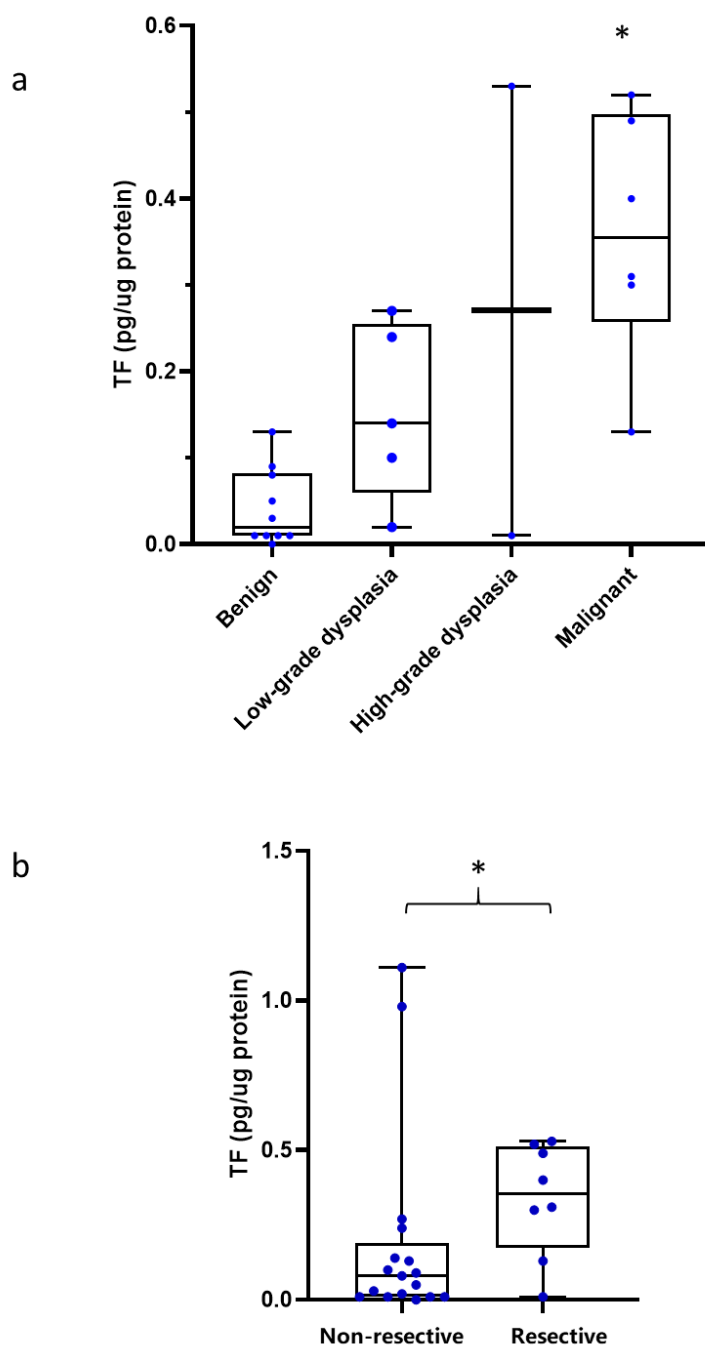
The standard curve was constructed using a serial dilution (0-500 pg/ml) of recombinant TF provided with the kit. The standards (150 μ l) were placed in 96-well plates and assessed by ELISA. The absorption of the samples was then measured at 450 nm using a plate reader (n=2).

Figure 41: Assessment of TF concentration in the cyst fluid samples



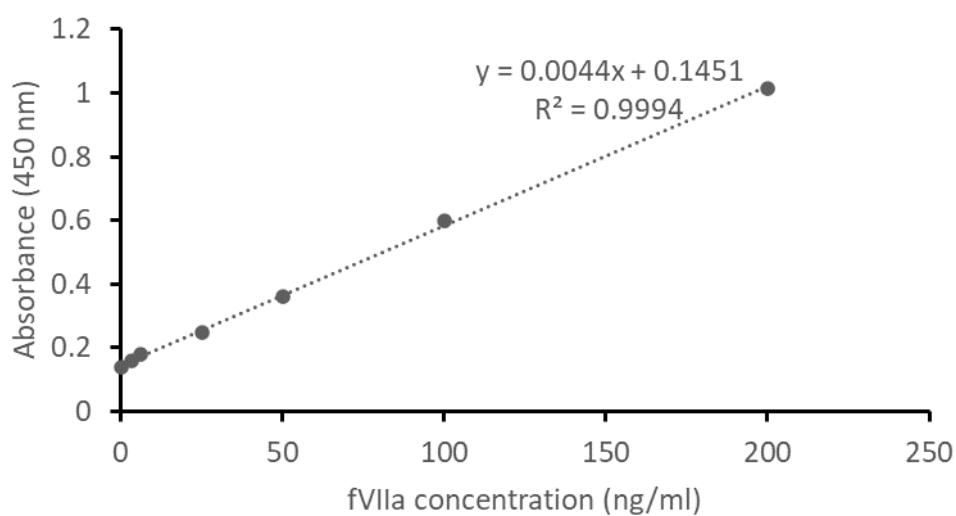
TF concentration was measured using the ELISA test (one experiment was carried out in duplicates); a- in the four histological groups (data = median with interquartile range; the Kruskal-Wallis test, $p = 0.008$); b-in the two risk groups (data = median with interquartile range; Kolmogorov-Smirnov test, $p = 0.004$).

Figure 42: Analysis of cyst fluid TF/total protein ratio



TF/TP analysis; a- in the four histological groups (data = median with interquartile range; the Kruskal-Wallis test, $p = 0.007$); b-in the two risk groups (data = median with interquartile range; Kolmogorov-Smirnov test, $p = 0.006$).

Figure 43: Standard curve for determining fVIIa concentration using fVIIa-ELISA



The standard curve was constructed using a serial dilution (0-200 ng/ml) of recombinant TF provided with the kit. The standards (50 μ l) were placed in 96-well plates and assessed by ELISA. The absorption of the samples was then measured at 450 nm using a plate reader (n=2).

than TF. The mean fVIIa concentration was higher ($p=0.187$, Kolmogorov-Smirnov test) in the resective group (78.97 ± 24.59 ng/ml, 95% CI 22.25, 135.67) vs non-resective group (35 ± 11.77 ng/ml, 95% CI 10.07, 59.72) (Figure 44).

3.6.9. Analysis of the ratio of fVII:TF in the cyst fluid

To investigate the possibility that the relative concentration of fVIIa and TF will differ in the histological groups, the ratio of fVIIa and TF was calculated. There was a gradual decline in the ratio of fVIIa and TF with the progression of histological grade of disease in the four histopathological groups ($p=0.963$ for the mean and $p=0.743$ for the median, Kruskal-Wallis test), but the difference was not statistically significant (Figure 45). The mean fVIIa:TF was marginally lower ($p=0.744$, Kolmogorov-Smirnov test) in the resective group (84.82 ± 43.8 , 95% CI 0, 185.04) vs the non-resective group (437.46 ± 219.72 , 95% CI 0, 901.0295% CI 10.07, 59.72) (Figure 45).

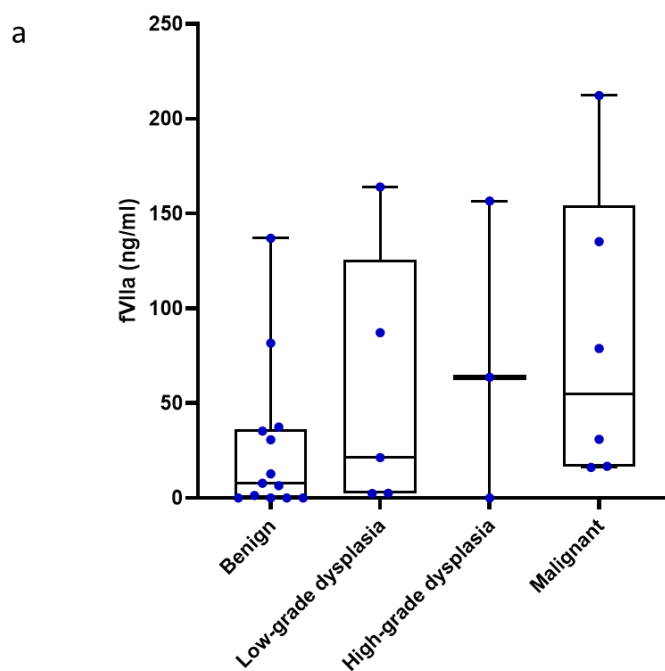
3.6.10. Estimation of a cut-off value of TF as an indicator of malignancy

A receiver operating characteristic curve, or ROC curve, was plotted to establish the diagnostic ability of TF to differentiate between non-resective and resective diseases. An area under the curve (AUC) of 0.5 suggests no discrimination, 0.7 to 0.8 is considered acceptable, 0.8 to 0.9 is considered excellent, and more than 0.9 is considered outstanding. The ROC curve plotted for TF concentration (Figure 46) showed an AUC of 0.877 (95% CI 0.701, 1), $p=0.002$. This suggests that TF has high accuracy in distinguishing between resective and non-resective diseases. A cut-off point of 0.75 ng/ml (Table 29) achieved a 78% sensitivity, 94% specificity, positive predictive value (PPV) of 88%, negative predictive value (NPV) of 89% and an accuracy of 89%.

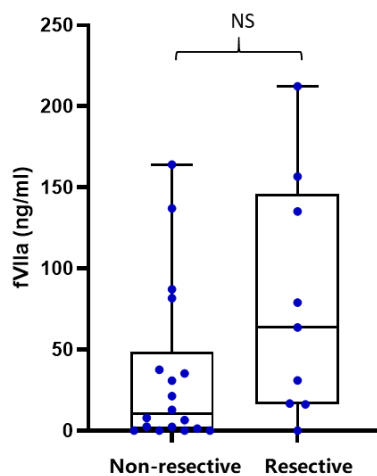
3.6.11. Investigation of the diagnostic ability of fVIIa (ng/ml) concentration and fVIIa:TF

A ROC curve was plotted to investigate the diagnostic ability of fVIIa to differentiate between non-resective and resective diseases. The ROC curve plotted for fVIIa concentration

Figure 44: Assessment of fVIIa concentration in the cyst fluid samples

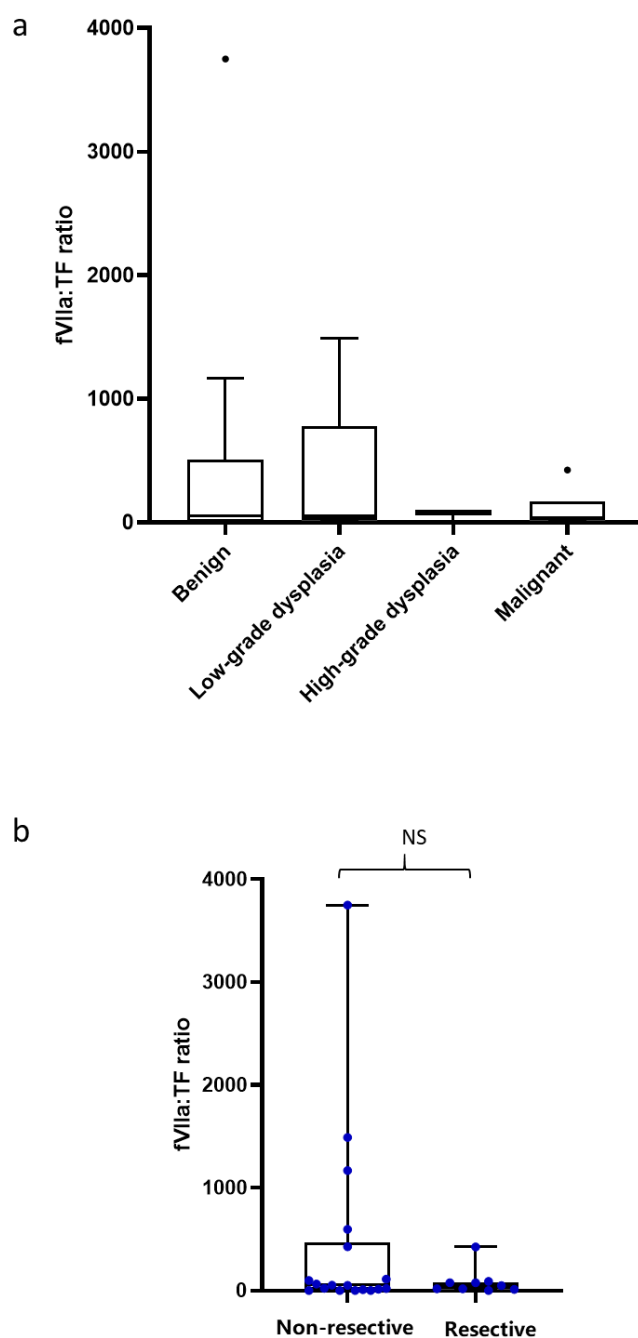


b



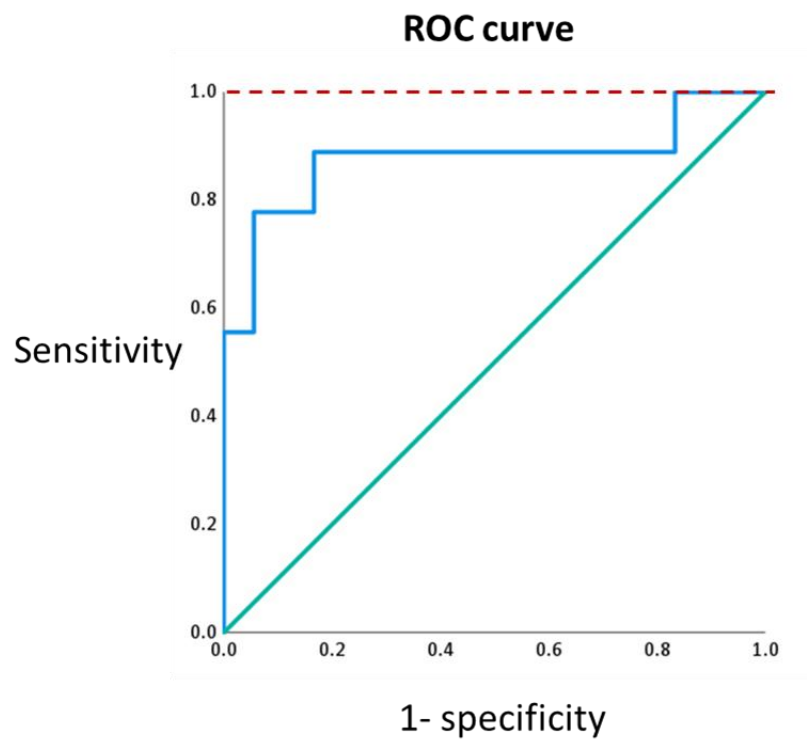
fVIIa concentration was measured using the ELISA test (one experiment was carried out in duplicates); a- in the four histological groups (data = median with interquartile range; the Kruskal-Wallis test, p =not significant (NS)); b-in the two risk groups (data= median with interquartile range; Kolmogorov-Smirnov test, p = NS).

Figure 45: Analysis of fVII:TF ratio



fVIIa:TF ratio was calculated; a- in the four histological groups (data = median with interquartile range; the Kruskal-Wallis test, $p =$ not significant (NS)); b-in the two risk groups (data = median with interquartile range; Kolmogorov-Smirnov test, $p=$ NS).

Figure 46: ROC curve of TF (ng/ml)



The cut-off value for TF concentration was determined by using the ROC curve. AUC of 0.877 (95% CI 0.701, 1), $p=0.002$.

Table 29: Coordinates of the ROC curve for TF

Positive if greater than or equal to	Sensitivity	1 - Specificity
-0.9900	1.000	1.000
0.0150	1.000	0.944
0.0250	1.000	0.889
0.0400	1.000	0.833
0.0550	0.889	0.833
0.0650	0.889	0.778
0.0900	0.889	0.667
0.1200	0.889	0.556
0.1500	0.889	0.500
0.1750	0.889	0.444
0.2050	0.889	0.389
0.2700	0.889	0.333
0.3350	0.889	0.278
0.3800	0.889	0.222
0.4500	0.889	0.167
0.5500	0.778	0.167
0.6350	0.778	0.111
0.7550	0.778	0.056
0.8450	0.667	0.056
1.1200	0.556	0.056
1.4500	0.556	0.000
1.5150	0.444	0.000
1.5650	0.333	0.000
1.6150	0.222	0.000
1.8450	0.111	0.000
3.0700	0.000	0.000

(Figure 47) showed an AUC of 0.698 (95% CI 0.484, 0.911), $p=0.100$. This indicates that the AUC is not significantly different from 0.5, and the fVIIa concentration was not suitable for this purpose.

Similarly, the ROC curve plotted for fVIIa:TF ratio (Figure 47) showed an AUC of 0.451 (95% CI 0.233, 0.668), $p=0.681$, which suggests that the ratio is not applicable as a diagnostic test.

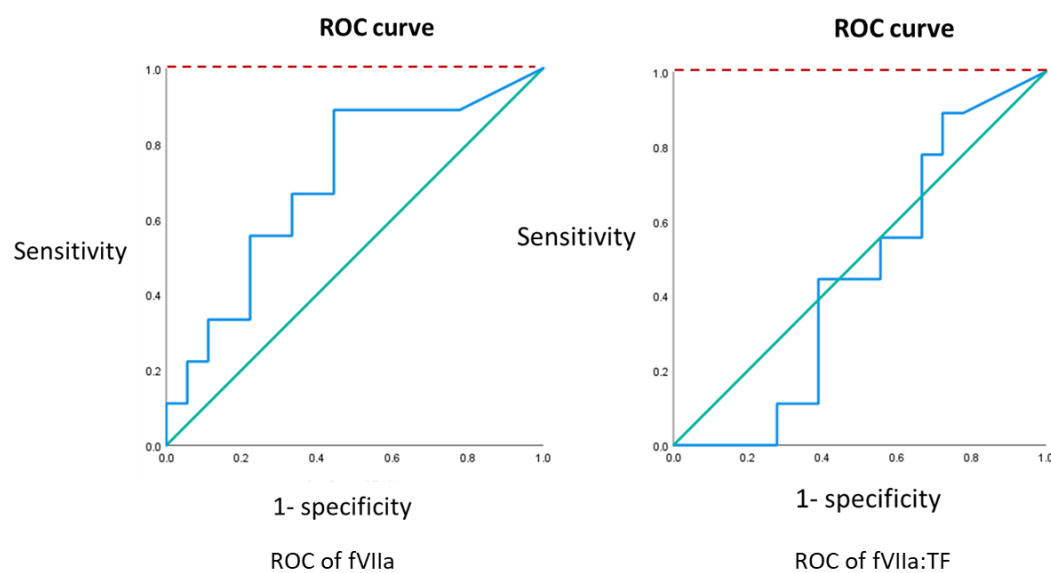
3.6.12. Analysis of the association of high-risk cyst

The association of the resective group with current assessment parameters and exploratory proteins were analysed using nonparametric Spearman's correlations. TF (≥ 0.75 ng/ml) showed a significant strong positive correlation with resective cysts ($p < 0.001$). There was a significant moderate positive correlation of TF with radiographic high-risk stigmata ($p= 0.004$). A significant moderate positive correlation was found between the resective cysts and radiographic high-risk stigmata ($p= 0.012$) and CEA ≥ 192 ng/ml ($p= 0.036$). However, none of the radiographic features individually had a significant correlation. CEA of ≥ 192 ng/ml showed a significant moderate positive correlation with TF. There was no correlation between diabetes and resective cysts, and a moderate negative correlation was observed with chronic pancreatitis (not significant) (Table 30, Table 31). Logistic regression analysis showed the odds ratio for TF was 59.5 (95% CI 4.6, 767.2), which was significantly ($p=0.002$) higher compared to radiographic high-risk stigmata and CEA (≥ 192 ng/ml) (Table 32).

3.6.13. Measurement of TF in the serum samples

From September 2018 to November 2021, 71 patients were recruited in the study TEM-PAC. This included 29 in the cancer cohort (18 advanced and 11 resected), and 12 in the control cohort (cholecystectomies). The Quantikine® ELISA kit was used to measure the concentration of TF antigen in the serum samples from these cases and the 27 samples from the patients with cystic lesions. The mean serum concentration of TF between the four histopathological groups of cysts did not vary significantly ($p=0.484$); a similar outcome was observed for the median value of TF ($p=0.277$) (Figure 48). Furthermore, no significant difference in the mean ($p=0.296$) or median (0.424) value of TF was detected between the cyst, cancer and control

Figure 47: ROC for fVIIa (ng/ml) and fVIIa:TF



AUC of fVIIa ROC 0.698(95% CI 0.484, 0.911), $p=0.100$; AUC of fVIIa:TF 0.451 (95% CI 0.233, 0.668), $p=0.681$.

Table 30: Association of the high-risk cyst with current parameters

Parameters	Correlation Coefficient	p-value
High-risk stigmata	0.478	0.012
MPD \geq 10 mm	0.369	0.059
Enhancing solid components within cyst	0.250	0.209
Worrisome features	-0.295	0.135
Cyst \geq 3 cm	-0.367	0.060
Thickened/enhancing cyst wall	-0.135	0.502
Non-enhancing mural nodule	-0.200	0.317
MPD 5-9 mm	-0.200	0.317
Abrupt change in calibre of MPD diameter with distal atrophy	.	.
Diabetes	0.167	0.406
Chronic pancreatitis	-0.337	0.086
CEA \geq 192 ng/ml	0.471	0.036
Amylase	0.286	0.222

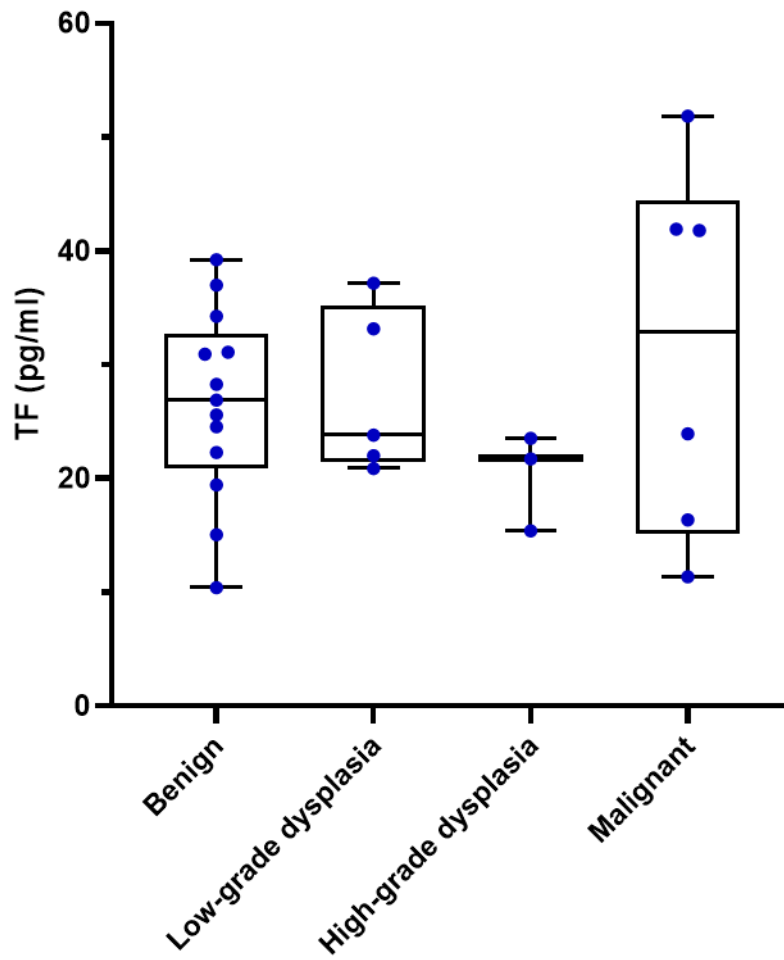
Table 31: Association of TF with resective cysts and current parameters

Parameters	Correlation Coefficient	p-value
TF with resective cysts	0.746	<0.001
TF with radiographic high-risk stigmata	0.542	0.004
TF with CEA \geq 192 ng/ml	0.514	0.020

Table 32: Univariate analysis of factors associated with resective cysts

Predicting resective cyst	OR (95% CI)	<i>p</i>
Radiological high-risk feature	10 (1.4, 71.9)	0.022
MPD \geq 10 mm	8.5 (0.7, 98.2)	0.087
Enhancing solid components within cyst	4.9 (0.3, 62.6)	0.226
CEA (192 ng/ml)	11 (0.9, 130.3)	0.057
TF (cut off 0.75 ng/ml)	59.5 (4.6, 767.2)	0.002

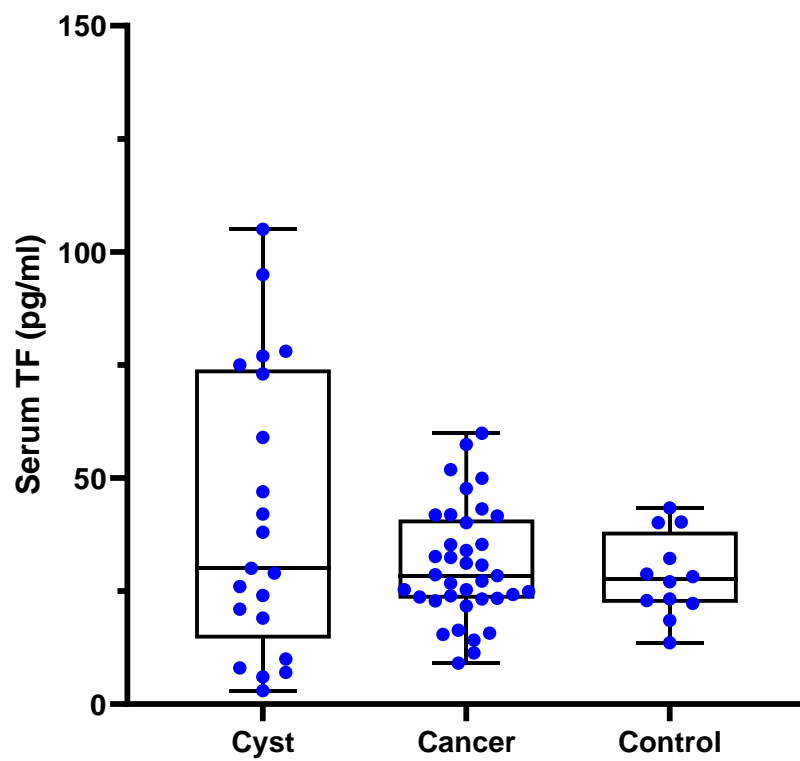
Figure 48: Assessment of TF concentration in the cyst patients' serum samples



TF concentration in the four histological groups (N=27). TF was measured using TF-ELISA (one experiment was carried out in duplicates; data = median with interquartile range; the Kruskal-Wallis test, p not significant)

cohort (Figure 49). These data indicate an absence of considerable variation in TF concentration within the three study cohorts as well as between the groups of the cyst cohort.

Figure 49: Assessment of serum TF concentration in the three cohorts of patients



TF concentration in the three study cohorts. TF was measured using TF-ELISA (one experiment was carried out in duplicates; data = median with interquartile range; the Kruskal-Wallis test, p not significant).

3.7. Discussion

PDAC is a highly aggressive cancer that can only be cured through surgery for early-stage tumours. Precursor lesions, including PanIN, IPMN, and MCN, are associated with PDAC and affect disease biology, therapy efficacy, and prognosis. Physicians categorise precursor lesions and predict invasive disease risk based on international guidelines using symptoms, imaging modalities, and chemical and cytological findings (46, 427). Advanced imaging has led to more benign cases being identified, and the incidence of invasive carcinoma is low (428). Surgical removal of PCLs with 'high-risk stigmata' is the best cure but has significant morbidity and mortality (429). There are no definite criteria for determining surgical intervention for PCL patients. Moreover, a debate exists on managing asymptomatic pancreatic cysts (430). The current challenge is understanding the precursor lesion tumour biology and identifying indicators of invasive tumours that can be used as reliable biomarkers. The current guidelines for managing pancreatic cysts are not cost-effective and could potentially result in early mortality. However, if diagnostic specificity could be increased to above 67%, there could be a significant improvement in both cost-effectiveness and survival rates for pancreatic cyst surveillance management strategies (431).

Pancreatic cancers are often metastatic by the time they are diagnosed, making them difficult to cure. Early detection and treatment offer the best opportunity for reducing pancreatic cancer mortality. For early detection, a curable lesion that gives rise to non-curable pancreatic cancers must be identified and characterised first. There is a significant window of opportunity to detect these curable precursor lesions (IPMN, PCN and PanINs) before they become non-curable. A method that can distinguish lesions that are likely to progress to advanced cancer rapidly (HGD) from those that are not (LGD) would be highly beneficial to identify the precursor cysts that need surgical intervention.

This study of TF/ fVIIa tumour-regulatory signalling molecules was conducted under the TEM-PAC study. TF is consistently upregulated in various human malignancies and plays a central role in the coagulation cascade. Its elevated expression in cancer may involve cancer cells, adjacent stroma and circulating blood. TF expression correlates with histological grade,

aggressiveness, and poor prognosis, and it is a major contributor to phenotypic alterations that induce cancer invasiveness and angiogenesis necessary for tumour growth. The presence of TF in the tumour microenvironment may promote the transition from a dormant or latent state of cancer progression to a tumorigenic state by modifying the phenotypic functional state and molecular evolution of tumour cells; thus making TF a probable marker of transition.

The TF/fVIIa complex is known to affect cell proliferation, leading to cell cycle arrest or apoptosis. TF is released during inflammation, disease or injury, and TF+MV interact with endothelial cells, which can be harmful if not effectively processed. A recent study discovered that the concentration of TF and the ratio of fVIIa:TF in MV determine the outcome of endothelial or malignant cell exposure to the MV. Chronic exposure to TF+MV may exhaust the ability of endothelial cells to counteract the proapoptotic property of TF. As the malignant process progresses, TF levels are expected to increase while the counteractive mechanisms, such as fVIIa, may diminish. As a result, certain inflammatory cysts with elevated levels of TF may be classified as benign if they demonstrate strong counteraction. Overall, TF and fVII play crucial roles in the complex interplay between coagulation, inflammation, and cancer (Figure 25). This is the rationale behind assessing TF and fVII levels and fVIIa:TF ratio in the PCyF as a marker for malignant transformation.

This study analysed the clinical, radiographic, and pathologic characteristics of 27 patients with PCLs who underwent EUS and fine needle aspiration or cyst fluid aspiration at the surgical resection of the cystic lesions. The median age of the patients was 64 years, and 59.1% were male. The cyst cohort comprised of patients with various pathological cyst types, including IPMN, MCN, pseudocyst, serous cyst, IPMN with a solid mass, cyst with a solid mass, and unspecified benign cyst.

The patients were stratified into two risk groups based on the pathological cyst type. The low-risk 'non-resective' group included patients with benign cysts and LGD; the high-risk 'resective' group included patients with HGD and invasive/malignant cysts. The non-resective disease was identified in 66.7% of patients, while 33.3% had resective disease. Diabetes was more

common in the resective group, while a history of chronic pancreatitis was present in the non-resective group.

The TF antigen concentration in PCyF was significantly different between the four histopathological groups, with a significant ($p=0.004$) higher concentration observed in the resective group compared to the non-resective group. The mean TF concentration was 1.17 ± 0.22 ng/ml (95% CI 0.68, 1.67) in the resective group and 0.27 ± 0.08 ng/ml (95% CI 0.1, 0.44) in the non-resective group. Similarly, the TF/TP ratio was significantly higher in the resective group (3.37 ± 0.67 pg/ μ g) compared to the non-resective group (0.8 ± 0.22 pg/ μ g).

The fVIIa concentration in the PCyF was found to increase with the progression of the histological grade of the disease. However, the degree of rise in fVIIa concentration was less than that of TF. The mean fVIIa concentration was higher in the resective group compared to the non-resective group. The ratio of fVIIa and TF decreased with the progression of histological grade. The mean fVIIa:TF ratio was marginally lower in the resective group (84.82 ± 43.8 , 95% CI 0, 185.04) compared to the non-resective group (437.46 ± 219.72 , 95% CI 0, 901.0295% CI 10.07, 59.72) (Figure 45). But, these differences were not statistically significant. Hence there seems to be no added value to fVIIa assessment but remains as important findings considering the small sample size.

TF at a cut-off value of 0.75 ng/ml showed high diagnostic ability in differentiating between resective and non-resective diseases, with an AUC of 0.877. This suggests that TF has a high accuracy in distinguishing between the two disease types, with a high specificity (94%) and high PPV (88%), indicating that TF is a reliable diagnostic test. On the other hand, fVIIa concentration (AUC 0.698) and fVIIa:TF ratio (AUC 0.451) showed low diagnostic accuracy for distinguishing between resective and non-resective diseases.

ICG categorise IPMNs into low-risk, worrisome, and high-risk stigmata groups based on radiological features (45, 46, 430, 432) (Table 12, Table 13 & Table 14). These guidelines have a sensitivity of 50% and a specificity of 89.1% (430). EUS with FNA is recommended for further analysis. Although the guidelines have shown improved sensitivity and accuracy, up to 77% of patients may have noninvasive lesions and undergo pancreatic resection (362, 433-436).

This indicates the need for more objective tests to identify patients at the greatest risk of malignancy.

Cyst fluid analysis can help distinguish between benign and malignant pancreatic lesions, and several tests are available to diagnose premalignant cysts. These tests include cytology, tumour markers (e.g., CEA), biochemical markers (e.g., amylase), and cyst fluid mucin. CEA is the most accurate for discriminating between mucinous and nonmucinous cysts but cannot distinguish between premalignant and malignant cysts (377-380). Amylase in PCyF can be particularly useful in identifying pseudocysts, as the amylase content of pseudocysts is usually high, while neoplastic cysts generally have low levels. However, elevated amylase levels can occur in cystic tumours of all types. Hence, the efficacy of amylase measurements in pancreatic cyst fluids is limited, though low values indicate a neoplastic tumour (378, 380, 437, 438). It is essential to differentiate pseudocysts from malignant cystic tumours when selecting appropriate surgical procedures. Table 33 and Table 34 show the diagnostic performance of current predictors of malignancy in PCLs. A cut-off point of 0.75 ng/ml TF achieved a 78% sensitivity, 94% specificity, positive predictive value (PPV) of 88%, negative predictive value (NPV) of 89% and an accuracy of 89%, indicating that TF is a reliable diagnostic test for any PCLs that is at high risk of transforming into invasive malignancy.

In this study, 'high-risk stigmata' could stratify the resective group, but individually the high-risk features (MPD \geq 10 mm, $p=0.09$; enhancing solid components within the cyst, $p=0.25$) or the 'worrisome features' could not stratify the resective and non-resective group. Though there was a significant moderate positive correlation between resective cysts and radiographic high-risk stigmata ($p=0.012$), none of the radiographic features individually had any significant correlation. Whereas TF (\geq 0.75 ng/ml) had a significant strong positive correlation (correlation coefficient 0.745) with resective cysts ($p < 0.001$) and moderate positive correlation (correlation coefficient 0.514) with radiographic high-risk stigmata ($p=0.004$) and CEA of ≥ 192 ng/ml (correlation coefficient 0.514, $p=0.02$) (see Table 31 and

Table 33: Diagnostic performance of current cyst fluid markers used to identify a malignant cyst

Cyst fluid marker	Sensitivity (%)	Specificity (%)
CEA \geq 192 ng/ml (382)	64	83
Mucin (387)	80	40
Amylase < 250 U/L (385)	62.5	69.4
Cytology (375)	63	88
TF (present study)	78	94

Table 34: Diagnostic performance of predictors of malignancy in BD-IPMNs

	Sensitivity (95% CI)	Specificity (95% CI)	Positive PV (95% CI)	Negative PV (95% CI)
Worrisome features	95	46.3	18.1	98.7
Size of cyst ≥ 30 mm	85	55.6	19.3	96.7
Size of cyst ≥ 5 mm	25	87.5	20	90.3
Presence of MN on EUS	33.3	94.7	33.3	94.7
TF (current study)	78	94	88	89

BD-IPMNs, branch-duct intraductal papillary mucinous neoplasms; CI, confidence interval; PV, predictive value; MPD, main pancreatic duct; MN, mural nodule; EUS, endoscopic ultrasonography. Worrisome features comprised pancreatic duct diameter of 5–9 mm or cyst size ≥ 30 mm.

Table 32). The odds of diagnosing a resective cyst were significantly high with TF (OR 59.5, 95% CI 4.6, 767.2, $p=0.002$) (Table 33).

However, the serum TF levels in the cyst patients did not have any diagnostic value compared to the control cohort or known locally advanced cancers. One possible explanation for the lack of significant variation in TF concentration observed between cohorts and within cyst categories is that serum samples were used, whereas plasma is the preferred sample for assessing TF levels. However, as the TEM-PAC study aimed to investigate multiple tumour regulatory proteins, serum samples were initially collected. To address this issue, a recent protocol amendment was made to collect plasma samples for all cohorts, which will also be investigated for TF.

The current clinical study is a pilot feasibility study. The crude number of samples in the cyst study cohort was calculated based on the expectation of the number of cystic lesions that could be recruited in the four-year study period. Once the whole cohort is recruited, a power calculation for the future definitive study will be performed.

The level of CEA in the cyst fluid was accessed from the hospital record; these were measured as part of the standard protocol. Among the 27 cyst samples, CEA levels were unavailable for 7 patients with viscous samples, and amylase levels were unavailable for 6 patients. Missing data for CEA and amylase could have affected their correlation with resective cysts and high TF levels. A definitive study with a larger sample size ensuring the availability of standard biochemical markers will provide a better comparative interpretation of the results.

Once the recruitment for the TEM-PAC study is finished and the target sample size is met, additional analysis will be conducted encompassing all cohorts, including those with cysts, cancer, and controls. This expanded analysis will serve two main purposes. Firstly, it will enable the confirmation of the findings from the pilot study, providing a validation of the initial results. Secondly, it will allow for the calculation of statistical power for a larger study, ensuring that the sample size is appropriate to establish the validity of the study outcome with a higher degree of confidence.

In addition to validating the previous findings, the study will also continue its investigation into improved methods for classifying cystic lesions. The goal is to develop an approach that not only distinguishes between cysts that require resection and those that do not but also identifies specific molecular signatures associated with the four histopathological categories. By refining the classification methodology, the study aims to enhance diagnostic accuracy and enable more targeted and effective treatment strategies for patients with cystic lesions.

Overall, in this current study, cyst fluid TF concentration correlates with progression to a malignant phenotype and can distinguish precursor PCLs with a high risk of malignancy. Our hypothesis that a reducing fVIIa:TF ratio across the range of transformation could suggest a decrease in the body's ability to control the disease was not supported by the findings. However, there may be differential findings between the actual pre-malignant lesion gradings and the overtly malignant lesions but the limited sample size did not allow for these sub-analyses. This issue will be revisited once the whole cohort has accrued or if larger numbers of cystic lesions can be studied through collaborative projects with other centres.

In conclusion, TF as a stand-alone marker could potentially improve the ability to identify the malignant potential of PCLs before surgery and provide a more robust method for monitoring ambiguous cystic lesions. However, additional research and a more definitive prospective study is required with a larger group of patients to verify these results.

Chapter 4

Examination of the role of exogenous TF on EMT and pancreatic cancer progression

4.1. Introduction

The clinical study found that TF levels significantly increased with the histological stage, indicating a progression from normal ductal epithelium to invasive adenocarcinoma. Cyst-associated TF levels correlated with cytological progression to the malignant phenotype and differentiated between LGD and HGD. Therefore, this study aimed to investigate whether the concentration of TF that initiates EMT in pancreatic cell lines is comparable to the concentrations found in pancreatic cyst fluids.

4.1.1. Epithelial-mesenchymal transition

EMT is a cellular process where epithelial cells lose their epithelial characteristics and acquire mesenchymal properties in response to changes in gene expression and post-translational regulation mechanisms. This is triggered by signals from the microenvironment and leads to increased migratory capacity, fibroblast-like morphology, invasive properties, resistance to apoptosis, and significantly increased production of extracellular matrix components (439).

EMT is a key normal step during embryogenesis and is closely linked to endodermic transformations, gastrulation, and the development of various organs and systems. In embryonic development, epithelial cells have high plasticity and can switch between an epithelial and mesenchymal phenotype. However, once organ development is complete, these cells usually have terminally differentiated and can no longer undergo this transformation (440). In adults, EMT is involved in wound healing, tissue regeneration, organ fibrosis, and the progression of cancer (441). Stable cell-cell junctions, apical-basal polarity, and interactions with the basement membrane characterise the epithelial state of the cells. The changes in gene expression and post-translational regulation mechanisms during EMT lead to the repression of these epithelial characteristics and the acquisition of mesenchymal characteristics.

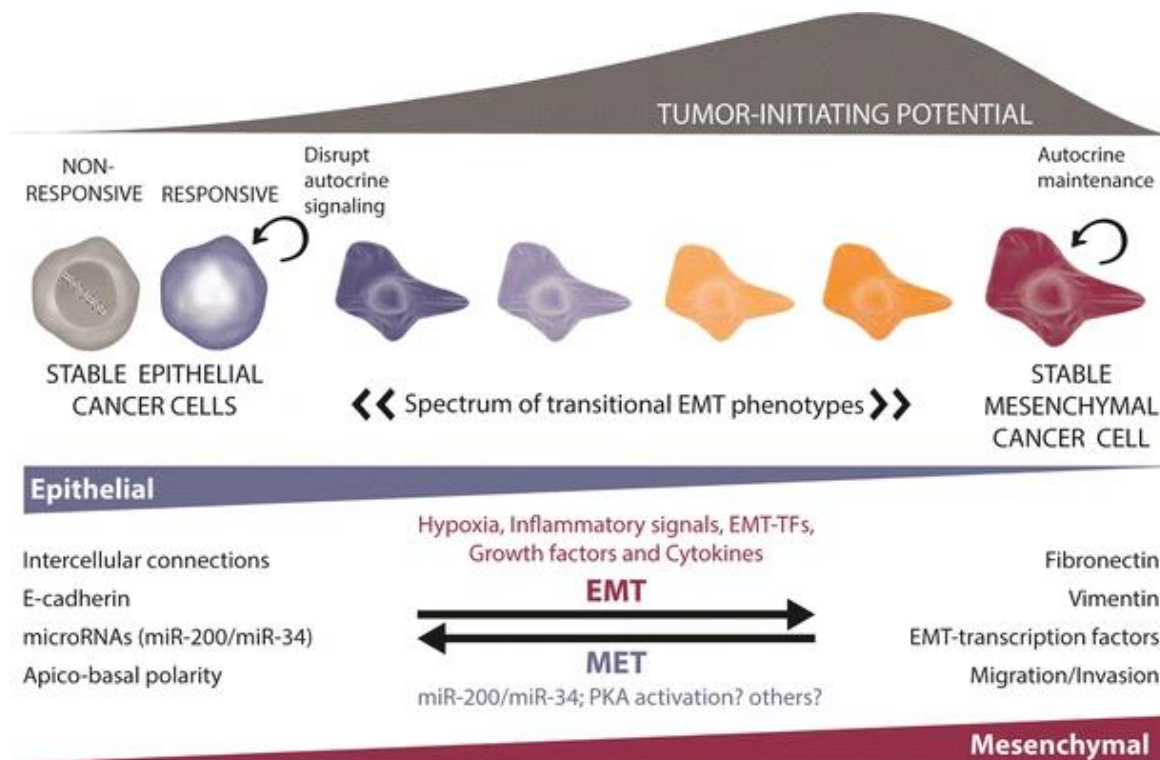
Induction of EMT plays a crucial role in the phenotypic progression towards increased invasiveness during the multistep progression of initially benign carcinomas (442-447). Cancer cells undergo a gradation of phenotypic states characterised by combinations of both

epithelial and mesenchymal markers (442, 447, 448) (Figure 50). Several molecular processes are involved in initiating and completing EMT. These include the activation of transcription factors, the expression of specific cell-surface proteins, the reorganisation and expression of cytoskeletal proteins, the production of enzymes that degrade the extracellular matrix, and changes in the expression of certain microRNAs. In this process, epithelial cells undergo a loss of their epithelial markers (such as E-cadherin, occludin, claudin, and laminin 1) and acquire mesenchymal markers such as N-cadherin, vimentin, and fibronectin (439).

The induction of the EMT program in both normal and neoplastic epithelial cells is governed by a core transcriptional network that involves a small group of master regulators known as EMT-TFs. These factors, including Slug, Snail, Twist, and Zeb1, play a significant role in orchestrating the different aspects of the EMT program (449, 450). The activation of various combinations of EMT-TFs can give carcinoma cells increased migratory and invasive capabilities, which facilitates their movement from primary tumour sites into the bloodstream, ultimately leading to the metastatic potential of EMT-responsive cells (451, 452). All these factors are often used as biomarkers to indicate that a cell has undergone EMT (Table 35).

The TME affects the phenotype of epithelial cancer cells through the mediation of various signalling molecules involved in heterotypic cell-cell interactions. Wnt, TGF β , and Notch ligands are among the central signalling molecules that play a role in this process. As research on the connections between EMT and carcinomas advances, an increasing number of signalling molecules are being implicated in driving the EMT program. Growth factors, such as epidermal growth factor, insulin-like growth factor, hepatocyte growth factor, fibroblast growth factor and platelet-derived growth factor, have been shown to trigger the EMT program. In addition, hypoxia-inducible signals, inflammatory signals, and cytokines, such as hypoxia-inducible factor (HIF)1- α , NF- κ B, IL-1 β and TNF α , have also been implicated in EMT activation within individual carcinoma cells (449, 453, 454). The complex network of signals that determine EMT activation is facilitated by heterotypic interactions between carcinoma cells and cells in the tumour microenvironment.

Figure 50: Spectrum of EMT phenotypes in cancer



Some epithelial cancer cells are not responsive to EMT-inducing signals and are unable to undergo the EMT (non-responsive epithelial cancer cell). Yet other epithelial cancer cells are responsive to EMT-inducing signals (responsive epithelial cancer cell). Following disruption of the autocrine signals that previously maintained their epithelial cell state, the cells transition toward a mesenchymal cancer cell state. Once the cancer cells have undergone a complete EMT, autocrine signalling can maintain the resulting mesenchymal phenotype in the absence of the EMT-inducing signals. As epithelial cancer cells move toward that mesenchymal state, they transition through partial-EMT states, which are suggested to be transient and possibly reversible. Progression through the EMT is associated with the acquisition of tumour-initiating potential, and peaks at some point along the partial-EMT spectrum. However, further progression to a stable, highly mesenchymal cancer cell state diminishes tumour-initiating potential. Below is a list of the main factors that favour residence in either the epithelial or mesenchymal cell states. (EMT, epithelial-to-mesenchymal transition; EMT-TF, EMT-transcription factors; MET, mesenchymal-to-epithelial transition). Taken from (447).

Table 35: Markers of EMT in cancer

	Cell-surface proteins	Cytoskeletal markers	Extracellular proteins	Transcriptional factors	MicroRNAs
Acquired biomarkers	N-cadherin OB-Cadherin $\alpha 5\beta 1$ Integrin $\alpha V\beta 6$ Integrin Syndecan-1	FSP-1 Vimentin α -SMA β -Catenin	Fibronectin $\alpha 1$ (I) Collagen $\alpha 1$ (III) collagen	Snail Snug ZEB1 Twist LEF-1 Ets-1	miR-21
Attenuated biomarkers	E-cadherin ZO-1	Cytokeratin	$\alpha 1$ (IV) Collagen Laminin 1		mir-200 family

Taken from (455)

4.1.2. EMT signalling pathways in PDAC

The activation of EMT during the progression of carcinomas depends on molecular signals produced by the tumour-associated stroma in PDAC, such as TGF β , TNF α , and hepatocyte growth factor, via different signalling pathways. For instance, the EMT requires cooperation between the Ras oncogene and receptor tyrosine kinases, which induce a downstream hyperactive Raf/MAPK signal associated with endogenous TGF β signalling (456). In mouse models, sustained signalling by TGF- β was essential for the maintenance of EMT in epithelial cells and for metastases (457). Snail and dEF1/ZEB1-mediated regulation of E-cadherin is the target of K-Ras in PC cells (458). Wnt/b-catenin, Notch, and Hedgehog signalling pathways also play a central role in the EMT and cancer progression (459, 460). Aberrant activation of the Hedgehog signalling pathway in PC patients is associated with a loss of E-cadherin expression and promotion of EMT (461). Inhibition of the Hedgehog cellular signalling pathway can down-regulate Snail and up-regulate E-cadherin, with subsequent inhibition of the EMT and a significant decrease in cell invasiveness in PC cell lines (462).

4.1.3. Invasive behaviour precedes frank tumourigenesis in PDAC

During the onset of EMT, cellular invasion and dissemination within the bloodstream may occur even before a malignant tumours are detectable. PanIN lesions exhibit invasive traits *in vitro* (463). Studies suggest that pancreatic cells can cross the basement membrane and enter the bloodstream before such invasive behaviour is detected macroscopically, which can lead to distant organ seeding. Circulating pancreatic cells (CPCs) are derived from acinar cells that are undergoing EMT, and these cells acquire stem cell-like characteristics and have tumour-initiating properties. A lineage labelling system used to tag and track pancreatic epithelial cells in a mouse model of PC showed that the tagged cells invaded and entered the bloodstream unexpectedly early before frank malignancy could be detected by rigorous histologic analysis. There seeding of distant organs may occur before and or concurrent with tumour formation at the primary site (463). These findings explain the high mortality rate observed in patients who had surgical resection of small pancreatic neoplasms without metastasis. In addition, metastatic PDAC has been observed in a group of patients who underwent pancreatectomy for chronic pancreatitis, with only PanIN lesions being detected upon examination of the surgically removed pancreas (464).

4.1.4. Inflammation promotes EMT in pre-malignant lesions

Inflammation has a significant impact on tumour development, from initiation to metastasis. Immune cells such as macrophages and lymphocytes are recruited to the primary tumour and play a vital role in establishing the inflammatory TME (111). This inflammation facilitates the invasion and dissemination of CTC via EMT. Tumour-associated macrophages (TAMs) are known to interact significantly with tumour cells during invasion and dissemination, indicating a correlation with EMT (465, 466). There is a strong correlation between chronic pancreatitis and PC (467), and inflammation is considered a significant event during carcinogenesis and premalignant lesion progression (468, 469). Studies in mice have shown that acute pancreatitis induces the formation of acinar-to-ductal metaplasia with inflammation, PanIN, and defects in epithelial characteristics, resulting in an increase in CD24+CD44+ CPCs in the circulation (463).

At the molecular level, TNF α stabilises SNAIL via activation of the NF- κ B pathway. TNF α also activates the NF- κ B pathway, which promotes tumour cell motility, tumour development and metastatic progression (470, 471). The TGF β pathway plays a role in inflammation, and the resulting inflammation regulates EMT. Studies have demonstrated that TGF β signalling collaborates with the Wnt, Notch, and MAPK pathways to facilitate EMT during various morphological processes. The TGF β /Smad pathway has been shown to compounds with Ras activation to promote EMT (472). However, as the inflammatory microenvironment increases the likelihood of mutations crucial in tumorigenesis, TGF β suppresses epithelial cell proliferation and early tumour growth. This causes some tumours to acquire inactivating mutations in TGF β signalling components. Thus, the stability of SNAIL expression and the TGF β signalling pathway is promoted by inflammation, which in turn promotes EMT. Additionally, the effectiveness of anti-inflammatory agents in reducing mortality further supports the proposed association between inflammation and tumour progression (473).

4.1.5. Role of TF on EMT

The relationship between EMT and TF has not been widely explored. The expression of both fITF and asTF is strongly induced by inflammatory cytokines such as TNF α or ILs in endothelial and blood cells. Moreover, both coagulation-dependent and independent functions of TF contribute to the development of cancer and metastases. During EMT, TF expression is upregulated, providing tumour

cells with enhanced coagulant properties that facilitate the early stages of metastatic colonisation. In a study, CTCs expressing both vimentin and TF were identified in 86.3% of metastatic breast cancer (MBC) patients, while CTCs expressing only vimentin without TF were rare. The study also found that the EMT-TFs ZEB1 and Snail modulate TF expression, strengthening the EMT-TF axis (298). Other studies have reported that the enhanced TF expression and release of TF+MV from cancer cells induced EMT through EGFR activation and/or E-cadherin blockade (215, 276, 474). These support the observed correlation between vimentin and TF expression in triple-negative breast cancer (TNBC) biopsies (298). Most importantly, the association between vimentin and TF expression in a subpopulation of CTCs of MBC patients suggested that the local activation of coagulation triggered by increased TF expression could trap EMT+ CTCs in platelet/fibrin-microthrombi, thus enhancing their survival and early colonisation in organs.

4.1.6. Ectopic synthesis of coagulation fVII influences cell migration and invasion

FVII is the natural ligand to TF and partners in haemostatic and non-haemostatic functions. It is synthesised only in the liver and circulates as an inactive zymogen. The exact mechanisms underlying ectopic fVII synthesis in cancer cells are not fully understood. However, it has been suggested that cancer cells may acquire the ability to produce fVII as a result of genetic mutations or epigenetic changes that alter the expression of fVII and its regulatory factors. In addition, factors such as hypoxia and inflammation, which are commonly present in the tumour microenvironment, may also contribute to ectopic fVII synthesis in cancer cells. Various non-hepatic cancer cells are known to ectopically express the fVII gene. Furthermore, inhibition of the TF-fVII complex on these cancer cell surfaces reduces cell motility and invasion (163). In addition, fVII-expressing cells invariably express TF and γ -glutamyl carboxylase, the key enzyme for requisite posttranslational modification of fVIIa. Ectopically expressed functional fVIIa on the surface of cancer cells in turn form a TF-fVIIa complex that triggers fXa generation. In previous studies, fVII was found to be associated with TF-positive tumour cells (257, 475). Moreover, ectopic fVII expression was shown to be regulated by hypoxic conditions through the hypoxia-induced association of HIF2 α with the fVII promoter in ovarian cancer. While hepatocyte nuclear factor (HNF)4 and specificity protein (Sp)1 have been identified as crucial regulators of fVII expression in hepatocytes (476-478), their contribution to ectopic fVII expression is

not clear. A study investigated the epigenetic mechanisms of fVII expression in breast cancer cells and found that, unlike in hepatocytes, HNF4 is not required for fVII expression in cancer cells. Instead, the recruitment of p300 and cyclic AMP–responsive element binding protein (CREB)–binding protein (CBP) to the active fVII promoter is selective in breast cancer cells, and Sp1 binding is necessary for both hepatic and cancer cell expression (479). These findings suggest that the induction of fVII expression in cancer cells depends on cancer type specific mechanisms.

Current evidence indicates that TF plays a role in promoting EMT in cancer by enhancing the coagulant properties of tumour cells during the early stages of metastatic colonisation. Upregulation of TF expression during EMT and correlation with vimentin expression have been described in various cancers. Local activation of coagulation triggered by enhanced TF expression could trap EMT+ CTCs in platelet/fibrin-microthrombi, favouring their survival and early seeding in the colonised organ (Figure 13). Thus, investigating the influence of TF on pancreatic epithelial cells *in vitro* would allow us to correlate the clinical findings of high TF levels in PCyF with HGD.

Precursor lesions like PanIN (LGD) expressing mutant *KRAS* undergo progression to higher grade lesions (HGD) and invasive PDAC after acquiring subsequent inactivating mutations in tumour suppressor genes such as *CDKN2A* and *TP53* (and often *SMAD4*). Deletion of the *CDKN2A* gene responsible for p16^{INKa} (p16) expression is one of the primary steps in advanced cancer formation and a hallmark of aggressive tumour behaviour. P16 is a member of the INK family (including p16^{INKa}, p15^{INKb}, p18^{INKc}, and p19^{INKd}) that is activated in response to various stimuli, blocking the activity of the cyclin D/Cdk 4/6 complex and preventing phosphorylation of the retinoblastoma protein. This, in turn, prevents the expression of genes required for the S-phase of cell cycle progression via the E2F transcription factor. Thus, p16 acts as a gatekeeper at the G1/S checkpoint of the cell cycle. The loss of the p16 function is the final regulatory step that commits cells to DNA synthesis during the cell cycle in response to pro-mitogenic signals. However, while the loss of the *CDK2NA* locus is linked to tumorigenesis, there is no automatic correlation between the loss of p16 function and the development of malignancy. Therefore, it is suggested that additional environmental factors may be required to trigger a malignant phenotype. Since TF was found to be an indicator in the cyst fluid

samples that could differentiate between LGD and HGD, it was relevant to examine whether TF had any impact on p16 expression.

4.2. Aims

- To investigate if TF can cause phenotypic changes in the pancreatic cell lines (normal epithelium and malignant cell lines) and whether the TF level initiating EMT is comparable to the concentrations found in the pancreatic cyst fluids.
- To investigate if TF influences the expression of HNF4 α and subsequent fVII expression.
- To examine the influence of TF on the mediators of cell cycle and apoptosis.
- To establish a spheroid model with a co-culture of pancreatic epithelial cells and CAF that can be used to reproduce *in vivo* characteristics of the PDAC tumour microenvironment.

4.3. Methods

Five cell lines were used during this study which were hTERT-HPNE, hTERT-HPNE E6/E7/K-RasG12D, hTERT-HPNE E6/E7/K-RasG12D/st, AsPC-1 and BxPC-3 (see chapter 2).

4.3.1. Optimisation of markers of EMT

Three cell lines, hTERT-HPNE, hTERT-HPNE E6/E7/K-RasG12D and hTERT-HPNE E6/E7/K-RasG12D/st, were used to identify the appropriate marker of EMT for further experiments in this study. Cells (5×10^4) were cultured in T25 flasks. The expression of markers of EMT, including vimentin, cadherin 11 and fibronectin, was assessed with western blot assay. In addition, the expression of E-cadherin and N-cadherin on the surface of hTERT-HPNE cells was examined by fluorescence microscopy.

4.3.2. Optimisation of TGF β as a positive control to induce EMT

TGF β signalling plays an important role in EMT and is a convenient way to induce EMT in epithelial cells (480). In this study, TGF β was used as a positive control treatment to induce EMT for several experiments in this study. To determine the optimal TGF β concentration and duration of incubation with TGF β , hTERT-HPNE and AsPC-1 cells were used. Cells (1.75×10^5) were incubated with TGF β (3 ng/ml) in 6-well plates and collected on day 2, day 4 and day 6. The cells were then lysed in Laemmli buffer, and the vimentin expression was assessed by western blot analysis (section 2.4.5) to establish the optimum incubation duration with TGF β for future experiments. In addition, in order to optimise the concentration of TGF β , cells (1.75×10^5) were incubated for 2 days with TGF β at 0 - 6 ng/ml, and the expression of vimentin expression was assessed by western blot analysis.

4.3.3. Examination of TF in cell lysate and media

Prior to investigating the influence of TF on EMT, the baseline TF expression in the hTERT-HPNE and hTERT-HPNE E6/E7/K-RasG12D/st cell lines was examined. Cells (1×10^5) were seeded in T25 flasks, and conditioned media were collected at 24 and 72 hours. The cells were collected and lysed with cell lysis buffer at 24 hours. TF concentration was measured in cell lysate and the conditioned media using the Quantikine[®] ELISA kit (section 2.4.2).

4.3.4. Examination of the influence of TF and fVIIa on the expression of vimentin in cell lines

The hTERT-HPNE, hTERT-HPNE E6/E7/K-RasG12D, hTERT-HPNE E6/E7/K-RasG12D/st and AsPC-1 cells (1×10^5) were seeded in 6-well plates and treated with TF (2 U/ml), fVIIa (5 nM), TF (2 U/ml) + fVIIa (5 nM) and PAR2-AP (20 μ M) for 2 days. We incubated cells with TGF β (5 ng/ml) as a positive control. Untreated cells were collected as a negative control. The expression of vimentin in cells was measured by western blot analysis.

In addition, the expression of vimentin mRNA was assessed by RT-qPCR following incubation of hTERT-HPNE, AsPC-1 and BxPC-3 cells with PAR2-AP (20 μ M). Cells (10^5) were treated with TGF β (5 ng/ml) as positive control. The cells were lysed after 2 days, and the mRNA was extracted using Monarch[®] total RNA Miniprep Kit and GoTaq[®] 1-Step RT-qPCR System (section 0). The expression of vimentin and β -actin mRNA were measured, and the relative vimentin expression levels were calculated against β -actin using the 2- $\Delta\Delta$ Ct method.

4.3.5. Examination of the induction of vimentin expression on treatment with TF

The optimal TF concentration for the highest expression of vimentin was examined in hTERT-HPNE and AsPC-1 cells. Cells (5×10^4) were seeded in 24-well plates and incubated with TF at 0 - 4 U/ml or with TGF β (5 ng/ml), along with untreated cells. Cells were collected after 2 days and lysed in Laemmli buffer, and the expression of vimentin was assessed by western blot analysis.

Another set of cells (5×10^4) were seeded in 24-well plates and incubated with TF at 0 - 4 U/ml, or TGF β (5 ng/ml). The cells were lysed after 2 days, and the mRNA was extracted using Monarch[®] total RNA Miniprep Kit and GoTaq[®] 1-Step RT-qPCR System. The expression of vimentin and β -actin mRNA were measured, and the relative vimentin expression levels were calculated against β -actin using the 2- $\Delta\Delta$ Ct method.

4.3.6. Examination of the expression of fVII and HNF4 α in cells

The presence of fVII and HNF4 α were examined in the hTERT-HPNE and AsPC-1 cells. Cells (10^5) were seeded in T25 flasks. Cells were collected after 2 days and lysed in Laemmli buffer, and the expression of full-length fVII, the heavy chain of fVII and HNF4 α were assessed by western blot analysis.

In addition, hTERT-HPNE and AsPC-1 cells (10^5) were seeded in 6-well plates. The cells were lysed after 2 days, and the mRNA was extracted using Monarch® total RNA Miniprep Kit and GoTaq® 1-Step RT-qPCR System (see methods chapter 2). The expression of fVII and β -actin mRNA were measured, and the relative fVII mRNA expression levels were calculated against β -actin using the $2^{-\Delta\Delta C_t}$ method.

4.3.7. Examination of the influence of TF on the expression of HNF4 α in different cell lines

Next, the hTERT-HPNE and AsPC-1 cells (10^5) were seeded in 6-well plates and incubated with TF (2 U/ml) and TGF β (5 ng/ml). The expression of HNF4 α was assessed by western blot analysis. Additionally, hTERT-HPNE cells (5×10^4) were seeded in 24-well plates and incubated with TF at 0.5 U/ml. Cells treated with TF and untreated samples were collected after 2 days. The expression of HNF4 α and β -actin mRNA were measured using RT-qPCR, and the relative HNF4 α mRNA expression levels were calculated against β -actin using the $2^{-\Delta\Delta C_t}$ method.

4.3.8. Examination of the influence of different concentrations of TF on the mediators of cell proliferation and apoptosis

hTERT-HPNE and AsPC-1 cells (5×10^4) were seeded in 21-well plates and incubated with TF at 0 - 4 U/ml or with TGF β (5 ng/ml), along with untreated samples. The cells were then lysed after 2 days. The expression of cyclin D1 mRNA was assessed using primers sequenced F- 3'-GAG ACC ATC CCC CTG ACG GC-5' and R- 3'- TCT TCC TCC TCC TCG GCG GC-5'. Bax mRNA was assessed using primers sequenced F- 3'-TCA CCC AAC CAC CCT GGT CTT-5' and R- 3'- TGG CAG CTG ACA TGT TTT CTG AC-5'. The quantity of each proteins mRNA was normalised against that of β -actin using RT-qPCR, and the relative analysis of cyclin D1 and bax mRNA was calculated using the $2^{-\Delta\Delta C_t}$ method.

4.3.9. Examination of the influence of TF on the expression of p16 protein

The presence of the p16 protein was first assessed in hTERT-HPNE and AsPC-1 cells using western blot analysis to investigate the influence of TF on the cell cycle regulatory proteins. Then cells (10^5) were seeded in 6-well plates and incubated with TF (2 U/ml), TGF β (5 ng/ml), along with untreated cells. Cells were collected after 2 days and lysed in Laemmli buffer, and the expression of the p16 protein was assessed by western blot analysis.

4.3.10. Establish a spheroid model by co-culture of CAF and pancreatic cells

To establish a spheroid model, hTERT-HPNE, hTERT-HPNE E6/E7/K-RasG12D, hTERT-HPNE E6/E7/K-RasG12D/st cell lines were co-cultured with cancer associate fibroblast (CAF) cells. Pancreatic epithelial cells (0.1×10^5) were seeded in a Nunclon Sphera non-adherent 96-well plate at concentrations of 25%, 50%, 75% and 100%, along with the complementary percentage of CAF cells. The plate was incubated at 37°C for 1 day, the spheroids were observed by bright field microscopy at x10 magnification, and the diameter of the spheroids formed was measured using ImageJ.

4.4. Results

4.4.1. Optimisation of detection of markers of EMT

The expression of vimentin, cadherin 11 and fibronectin was assessed using western blot. The proteins were measured in hTERT-HPNE, hTERT-HPNE E6/E7/K-RasG12D and hTERT-HPNE E6/E7/K-RasG12D/st cells and the culture media of the cells. Examination of the collected samples indicated a band corresponding to vimentin (~54 kDa) in all three cell lines and also the respective conditioned media (Figure 51). However, the examination of cadherin 11 and fibronectin did not produce clear bands (Figure 52). Therefore, vimentin was used as the marker of EMT in subsequent experiments.

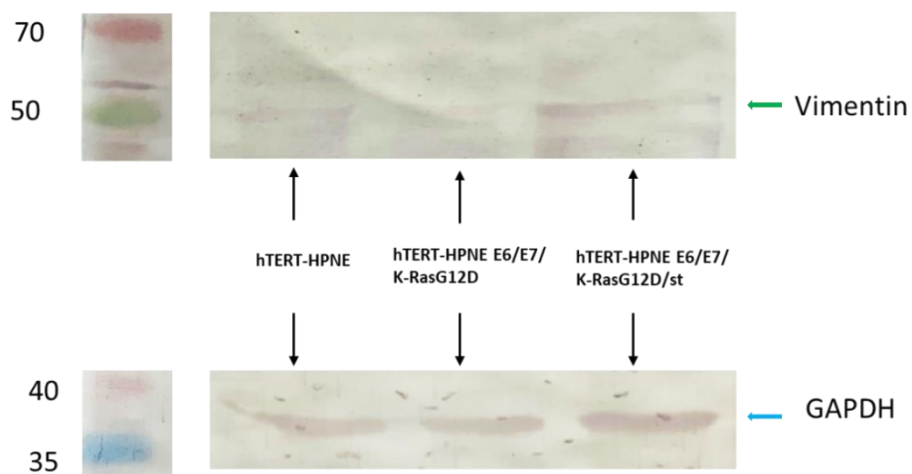
4.4.2. Utilisation of fluorescent microscopy for detection of E-cadherin and N-cadherin

The expression of E-cadherin and N-cadherin on the surface of hTERT-HPNE cells were measured as indicators of EMT. Cells were incubated with TGF β (5 ng/ml) or PAR2-AP (20 μ M). Surface expression of E-cadherin and N-cadherin was assessed using PE-conjugated mouse monoclonal anti-E-cadherin antibody (diluted 1: 200 v/v in antibody diluent) and AF488-conjugated mouse monoclonal anti-N-cadherin antibody (diluted 1: 200 v/v in antibody diluent). The stained cells were then examined by fluorescence microscopy. Examination of cells indicated the expression of N-cadherin in both untreated and in cells incubated with TGF β or PAR2-AP. However, it was not possible to detect E-cadherin in any of the cell samples (Figure 53). Consequently, measurement of E-cadherin and N-cadherin protein with fluorescence microscopy was not adopted as a means of assessing markers of EMT.

4.4.3. Determination of optimal concentration and duration of TGF β for induction of EMT

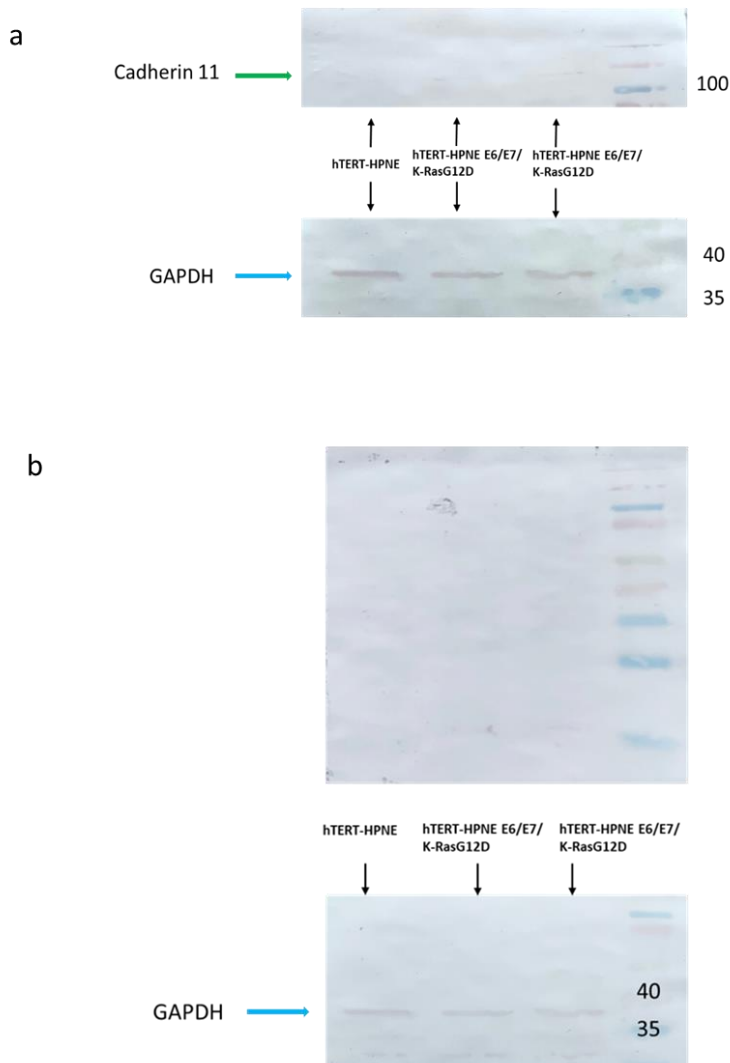
Sets of hTERT-HPNE and AsPC1 cells were incubated with 3 ng/ml TGF β . Treated and untreated cells were collected on day 2, day 4 and day 6 and the expression of vimentin was assessed. Maximal expression of vimentin was observed on day 2 for both hTERT-HPNE (Figure 54) and AsPC-1 cells (Figure 55). In addition, the hTERT-HPNE and AsPC1 cells were incubated with different concentrations of TGF β (0 - 5 ng/ml) and vimentin expression was examined on day 2. Western blot analysis of vimentin expression (normalised to GAPDH) indicated maximal expression with 5 ng/ml,

Figure 51: Detection of vimentin expression in cell line and conditioned media



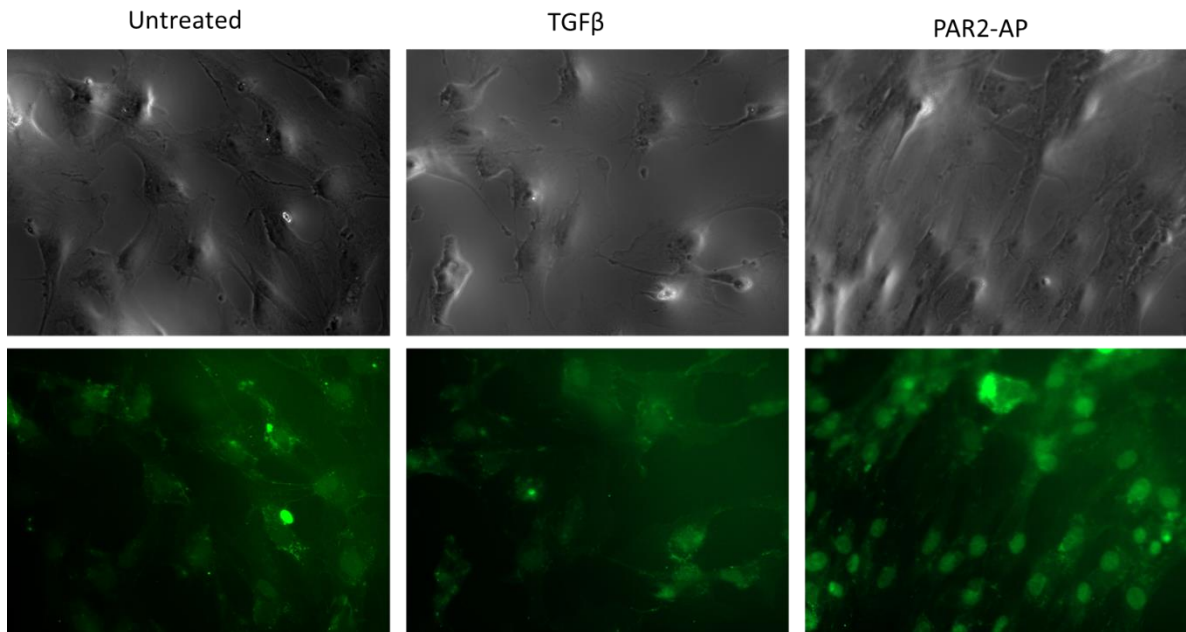
hTERT-HPNE, hTERT-HPNE E6/E7/K-RasG12D and hTERT-HPNE E6/E7/K-RasG12D/st cells (10^5) were collected. The cells were then lysed in Laemmli buffer and the proteins were separated by SDS-PAGE, and the vimentin expression was assessed by western blot using mouse anti-vimentin monoclonal antibody (diluted 1:3000 v/v in TBST). The membranes were incubated with AP-conjugated goat anti-mouse immunoglobulin (Ig) G antibody (diluted 1:3000 v/v in TBST). The membranes were then developed using Western Blue stabilised substrate for AP.

Figure 52: Detection of cadherin 11 and Fibronectin expression in cell lines



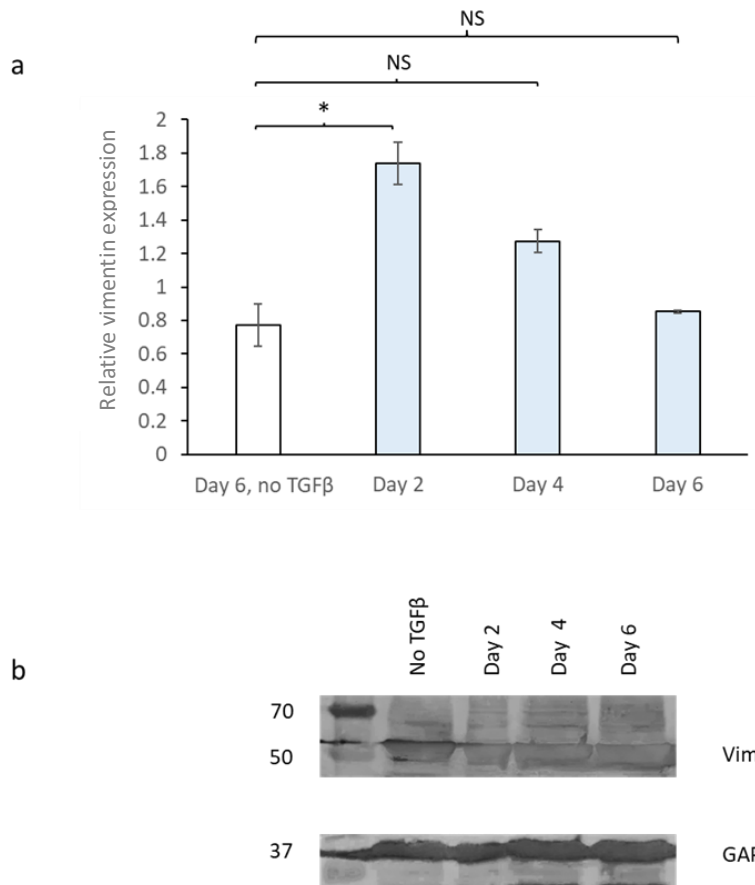
hTERT-HPNE, hTERT-HPNE E6/E7/K-RasG12D and hTERT-HPNE E6/E7/K-RasG12D/st cell (10^5) were collected. The cells were then lysed in Laemmli buffer; proteins were separated by SDS-PAGE, and the a- cadherin-11 and b- Fibronectin expression was assessed by western blot using mouse anti-cadherin-11 monoclonal antibody and mouse anti-fibronectin antibody (diluted 1:3000 v/v in TBST). The membranes were incubated with AP-conjugated goat anti-mouse IgG antibody (diluted 1:3000 v/v in TBST). The membranes were then developed using Western Blue stabilised substrate for AP.

Figure 53: Detection of cell surface N-cadherin by fluorescence microscopy



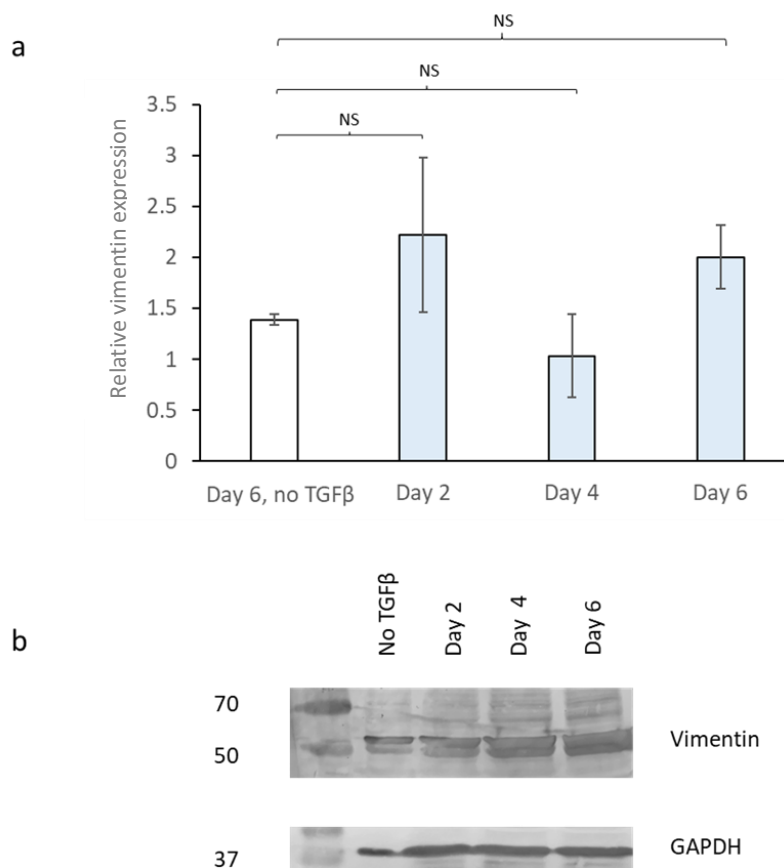
hTERT-HPNE cells (1×10^5) were incubated in glass dishes with TGF β or PAR2-AP along with untreated cells. N-cadherin was detected using an AF488-conjugated mouse monoclonal anti-N-cadherin antibody (diluted 1:200 v/v in antibody diluent). The cells were assessed by fluorescence microscopy at x 40 magnification.

Figure 54: Determination of the duration of incubation with TGFβ as a positive control in hTERT-HPNE cells



hTERT-HPNE cells (1.75×10^5) were incubated with TGFβ (3 ng/ml), and cells were collected on day 2, day 4 and on day 6, untreated cells were also collected. The cells were then lysed in Laemmli buffer; proteins were separated by SDS-PAGE, and the vimentin expression was assessed by western blot using mouse anti-vimentin monoclonal antibody (diluted 1:3000 v/v in TBST). The membranes were incubated with AP-conjugated goat anti-mouse IgG antibody (diluted 1:3000 v/v in TBST). The membranes were then developed using Western Blue stabilised substrate for AP (n=3, Images represent one experiment carried out in triplicates; data = mean values \pm SEM; one-way ANOVA, * = $p < 0.05$ NS = not significant).

Figure 55: Determination of the duration of incubation with TGFβ as a positive control in AsPC-1 cells



AsPC-1 cells (1.75×10^5) were incubated with TGFβ (3 ng/ml), and cells were collected on day 2, day 4 and on day 6, untreated cells were also collected. The cells were then lysed in Laemmli buffer; proteins were separated by SDS-PAGE, and the vimentin expression was assessed by western blot using mouse anti-vimentin monoclonal antibody (diluted 1:3000 v/v in TBST). The membranes were incubated with AP-conjugated goat anti-mouse IgG antibody (diluted 1:3000 v/v in TBST). The membranes were then developed using Western Blue stabilised substrate for AP (n=3, Images represent one experiment carried out in triplicates; data = mean values \pm SEM; one-way ANOVA, NS = not significant).

for both hTERT-HPNE (Figure 56) and AsPC-1 cells (Figure 57). Subsequent studies were carried out with 5 ng/ml of TGF β and incubated for 2 days.

4.4.4. Examination of TF concentration in cell lysate and media

The presence of TF in the hTERT-HPNE and hTERT-HPNE E6/E7/K-RasG12D/st cells and the conditioned media was examined using the Quantikine[®] ELISA kit (Figure 58). The mean concentration of TF did not vary significantly between hTERT-HPNE and hTERT-HPNE E6/E7/K-RasG12D/st cells.

The conditioned media of hTERT-HPNE E6/E7/K-RasG12D/st cells had a higher TF concentration than that of hTERT-HPNE, both at 24 hours and 72 hours, as shown in Figure 59. In addition, the TF concentration in the conditioned media of hTERT-HPNE E6/E7/K-RasG12D/st cells at 72 hours was greater than that at 24 hours.

4.4.5. Examination of the influence of TF and fVIIa on the expression of vimentin in cell lines

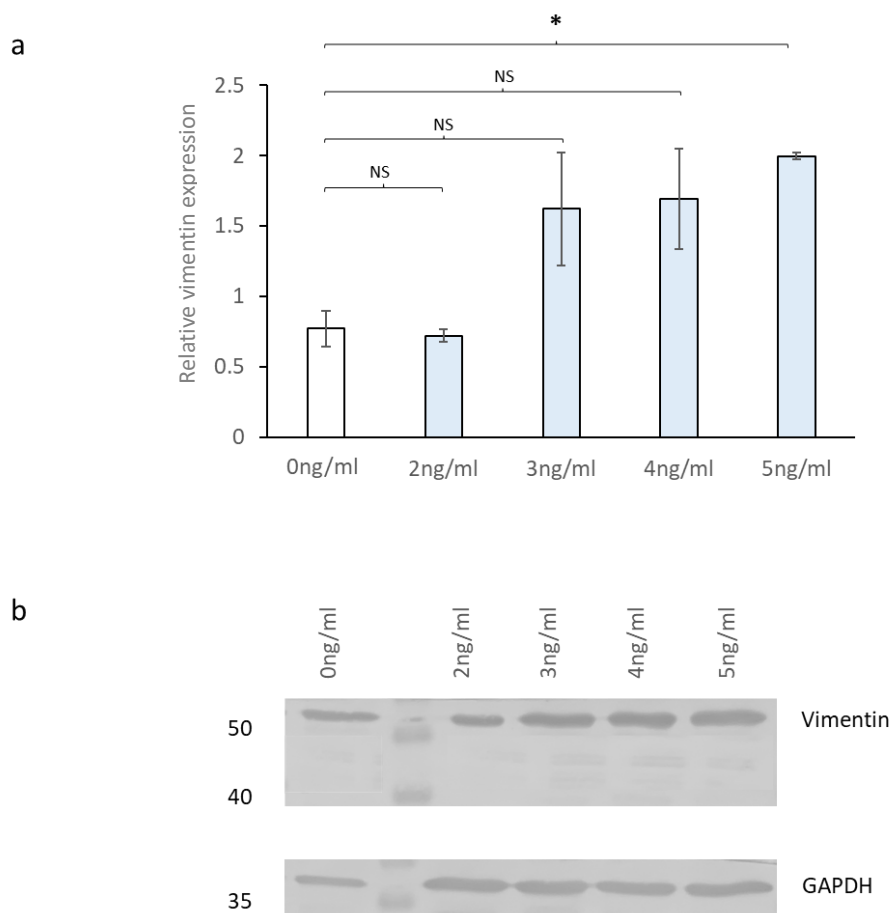
The expression of vimentin in cells following exposure to TF and fVIIa was measured by western blot analysis. The hTERT-HPNE, hTERT-HPNE E6/E7/K-RasG12D, hTERT-HPNE E6/E7/K-RasG12D/st and AsPC-1 cells were incubated with TF (2 U/ml) or fVIIa (5 nM) or TF (2 U/ml) + fVIIa (5 nM) or PAR2-AP (20 μ M) or TGF β (5 ng/ml) for 2 days.

In hTERT-HPNE cells, treatment with TF or PAR2-AP resulted in an increase in vimentin expression, which was comparable to that caused by TGF β . Treatment with fVIIa resulted in a decrease in vimentin expression. When the hTERT-HPNE cells were treated with a combination of TF and fVIIa, the expression of vimentin was moderated with the addition of fVIIa (Figure 60).

In AsPC-1 cells, treatment of cells with TF or PAR2-AP or fVIIa resulted in vimentin expression levels that were similar to those observed in cells treated with TGF β . Additionally, treating cells with the combination of TF and fVIIa did not lead to a decrease in vimentin expression (Figure 63).

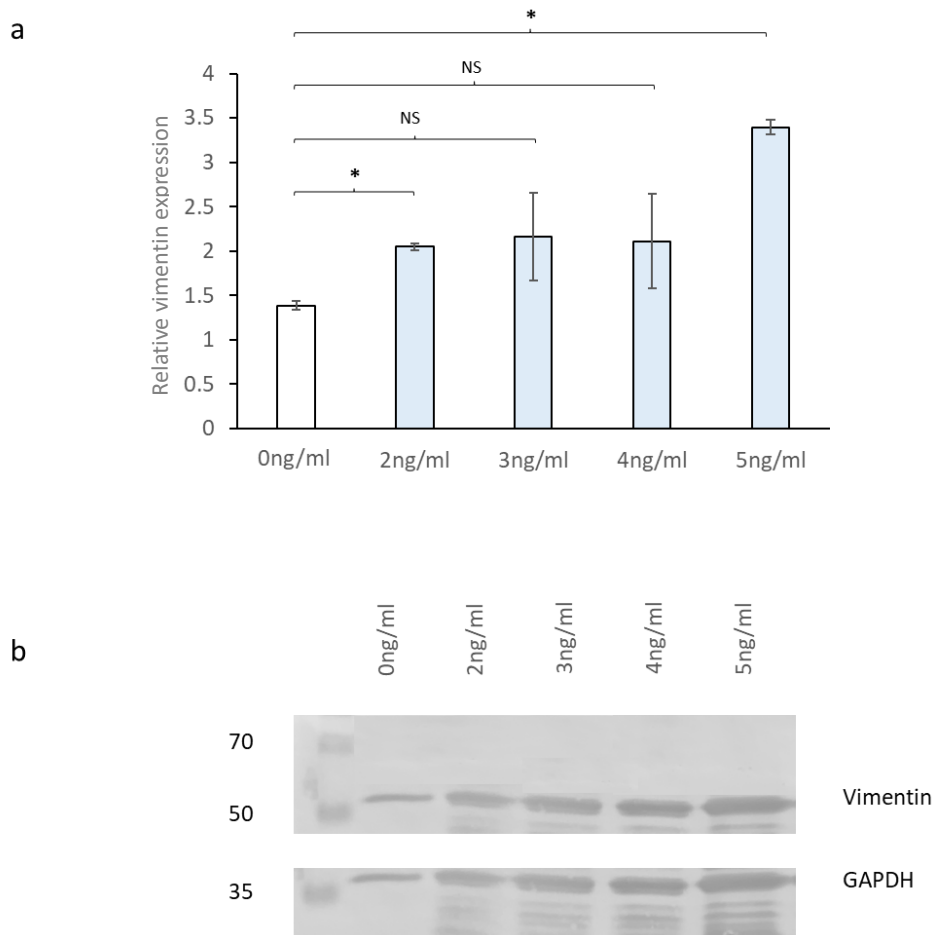
Cell lines with only K-RasG12D mutation did not exhibit any differences in vimentin expression when treated with TF or PAR2-AP or fVIIa compared to TGF β (Figure 61, Figure 62).

Figure 56: Determination of the optimal TGFβ concentration as a positive control in hTERT-HPNE cells



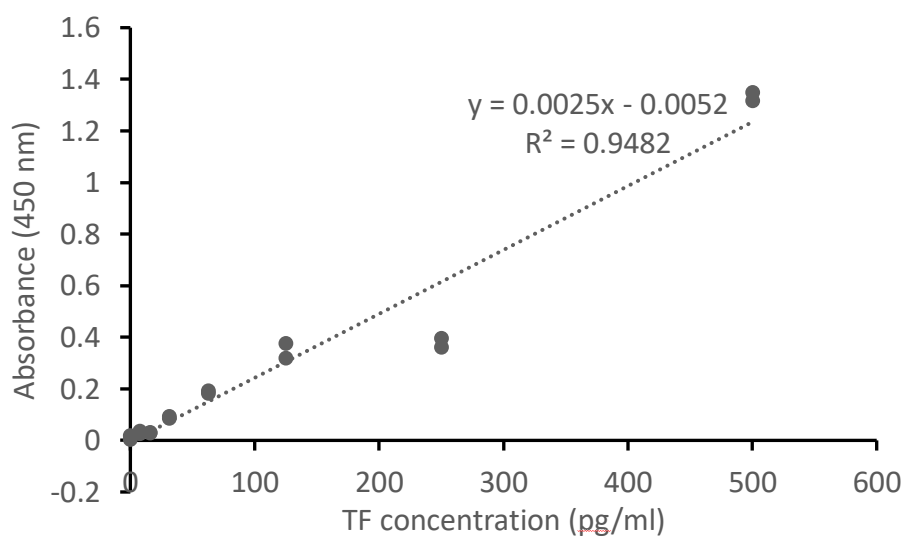
hTERT-HPNE cells (1.75×10^5) were incubated for 2 days with TGFβ at 0 ng/ml to 5 ng/ml. The cells were then lysed in Laemmli buffer; proteins were separated by SDS-PAGE, and the vimentin expression was assessed by western blot using mouse anti-vimentin monoclonal antibody (diluted 1:3000 v/v in TBST). The membranes were incubated with AP-conjugated goat anti-mouse IgG antibody (diluted 1:3000 v/v in TBST). The membranes were then developed using Western Blue stabilised substrate for AP (n=3, Images represent one experiment carried out in triplicates; data = mean values \pm SEM; one-way ANOVA, * = $p < 0.05$, NS = not significant).

Figure 57: Determination of the optimal TGFβ concentration as a positive control in AsPC-1 cells



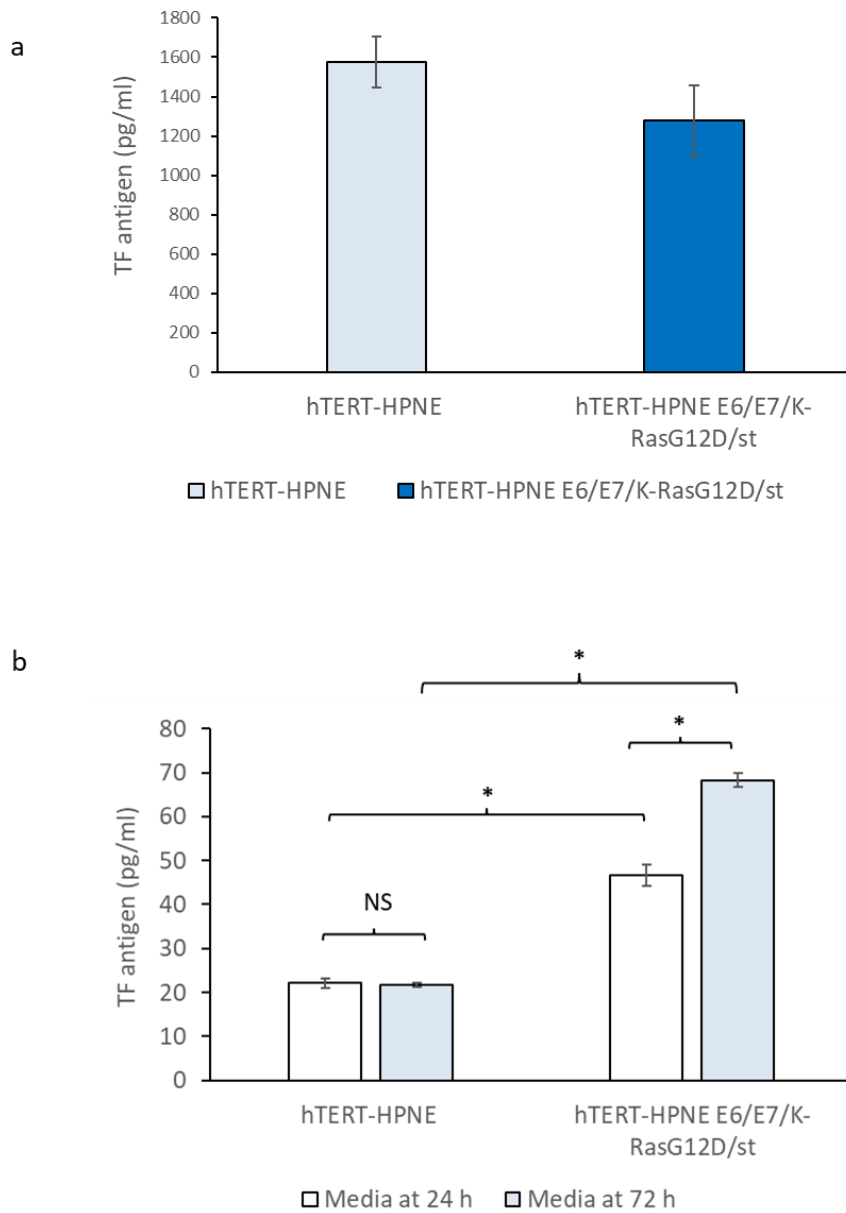
AsPC-1 cells (1.75×10^5) were incubated for 2 days with TGFβ at 0 ng/ml to 5 ng/ml. The cells were then lysed in Laemmli buffer; proteins were separated by SDS-PAGE, and the vimentin expression was assessed by western blot using mouse anti-vimentin monoclonal antibody (diluted 1:3000 v/v in TBST). The membranes were incubated with AP-conjugated goat anti-mouse IgG antibody (diluted 1:3000 v/v in TBST). The membranes were then developed using Western Blue stabilised substrate for AP (n=3, Images represent one experiment carried out in triplicates; data = mean values \pm SEM; one-way ANOVA, * = $p < 0.05$, NS = not significant).

Figure 58: Standard curve for the determination of TF antigen concentration



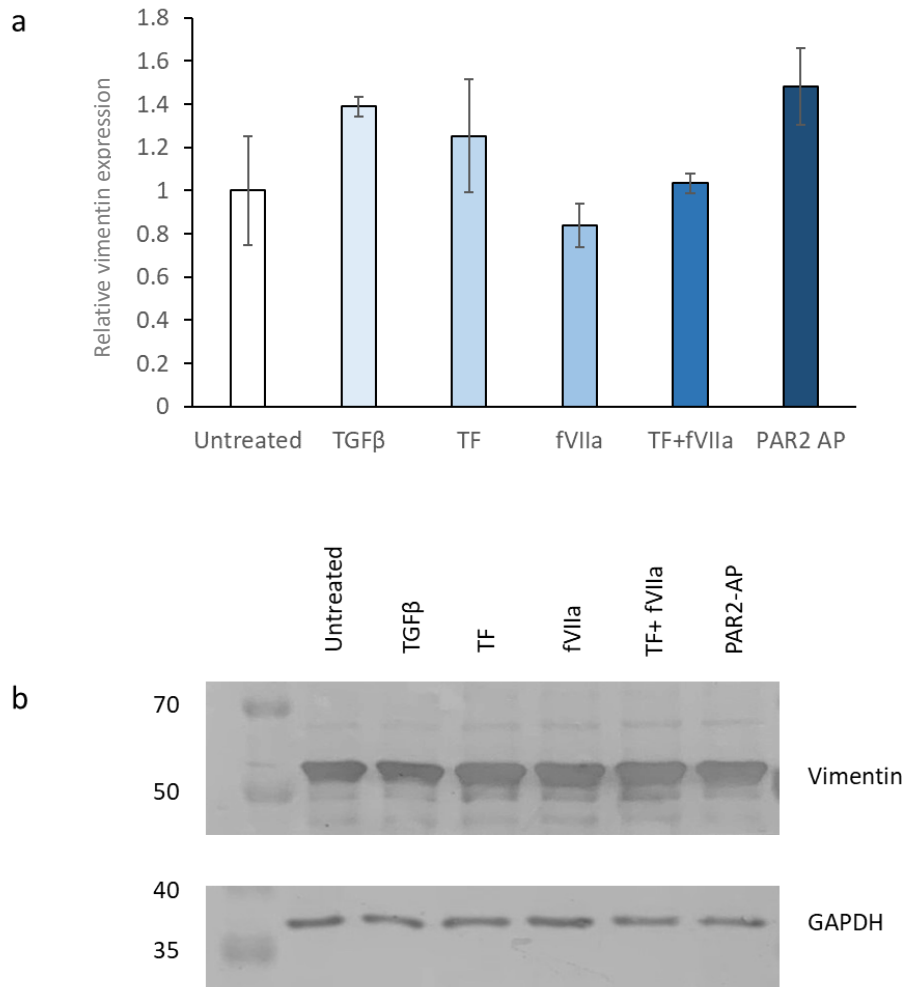
The standard curve was constructed using a serial dilution (0-500 pg/ml) of recombinant TF provided with the kit. The standards (150 μ l) were placed in 96-well plates and assessed by ELISA. The absorption of the samples was then measured at 450 nm using a plate reader (n=2).

Figure 59: Measurement of TF antigen in cells and corresponding media



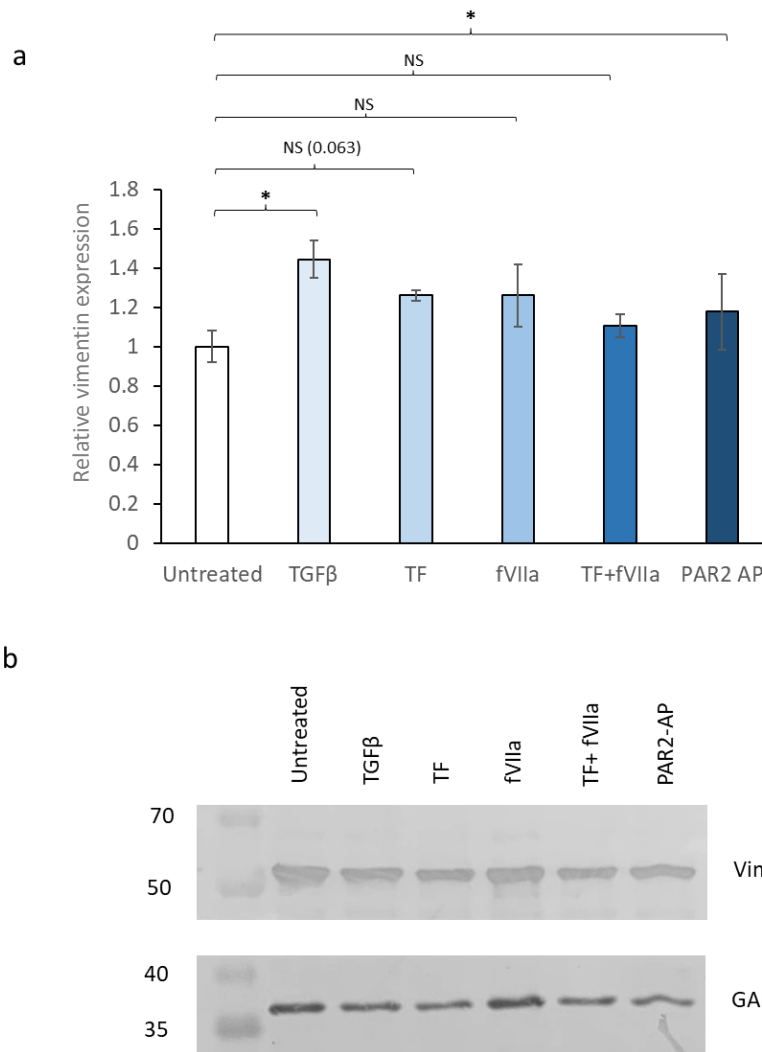
hTERT-HPNE and hTERT-HPNE E6/E7/K-RasG12D/st cells (2×10^5) were lysed with cell culture lysis buffer at 24 hours. The conditioned media from both cell lines were collected at 24 and 72 hours. TF concentration was measured using the ELISA test ($n=2$, the experiment was carried out in duplicates). a- TF concentration in the cell lysate (data = mean \pm SD); b- TF concentration in the conditioned media of the cell lines at 24 hours and 72 hours (data= mean \pm SD; independent samples t-test, * = $p < 0.05$, NS = not significant).

Figure 60: Examination of expression of vimentin in hTERT-HPNE cells



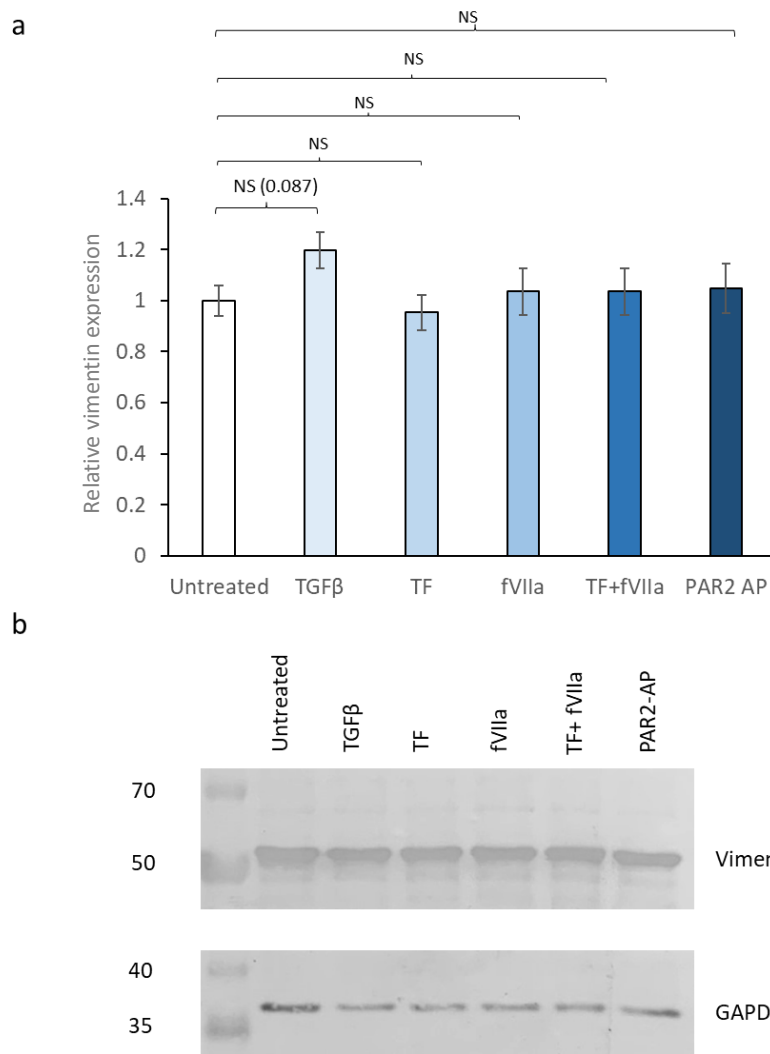
hTERT-HPNE cells (10^5) were seeded in 6-well plates and incubated with TF (2 U/ml) or fVIIa (5 nM) or TF (2 U/ml) + fVIIa (5 nM) or PAR2-AP (20 μ M), for 2 days. Treated and untreated cells were collected and lysed in Laemmli buffer; proteins were separated by SDS-PAGE, and the vimentin expression was assessed by western blot using mouse anti-vimentin monoclonal antibody (diluted 1:3000 v/v in TBST). The membranes were incubated with AP-conjugated goat anti-mouse IgG antibody (diluted 1:3000 v/v in TBST). The membranes were then developed using Western Blue stabilised substrate for AP (n=6, Images represent three experiments carried out in duplicates; data = mean values \pm SEM; one-way ANOVA, * = $p < 0.05$ NS = not significant).

Figure 61: Examination of expression of vimentin in hTERT-HPNE E6/E7/K-RasG12D cells



hTERT-HPNE E6/E7/K-RasG12D cells (10^5) were seeded in 6-well plates and incubated with TF (2 U/ml) or fVIIa (5 nM) or TF (2 U/ml)+ fVIIa (5 nM) or PAR2-AP (20 μ M), for 2 days. Treated and untreated cells were collected and lysed in Laemmli buffer; proteins were separated by SDS-PAGE, and the vimentin expression was assessed by western blot using mouse anti-vimentin monoclonal antibody (diluted 1:3000 v/v in TBST). The membranes were incubated with AP-conjugated goat anti-mouse IgG antibody (diluted 1:3000 v/v in TBST). The membranes were then developed using Western Blue stabilised substrate for AP (n=6, Images represent three experiments carried out in duplicates; data = mean values \pm SEM; one-way ANOVA, * = $p < 0.05$ NS = not significant).

Figure 62: Examination of expression of vimentin in hTERT-HPNE E6/E7/K-RasG12D/st cells



hTERT-HPNE E6/E7/K-RasG12D/st cells (10^5) were seeded in 6-well plates and incubated with TF (2 U/ml) or fVIIa (5 nM) or TF (2 U/ml)+ fVIIa (5 nM) or PAR2-AP (20 μ M), for 2 days. Treated and untreated cells were collected and lysed in Laemmli buffer; proteins were separated by SDS-PAGE, and the vimentin expression was assessed by western blot using mouse anti-vimentin monoclonal antibody (diluted 1:3000 v/v in TBST). The membranes were incubated with AP-conjugated goat anti-mouse IgG antibody (diluted 1:3000 v/v in TBST). The membranes were then developed using Western Blue stabilised substrate for AP (n=6, Images represent three experiments carried out in duplicates; data = mean values \pm SEM; one-way ANOVA, * = $p < 0.05$ NS = not significant).

We examined vimentin mRNA expression in hTERT-HPNE, AsPC-1, and BxPC-3 cells treated with PAR2-AP using RT-qPCR. PAR2-AP exposure led to the upregulation of vimentin expression in the malignant cell lines. In AsPC-1 cells treated with PAR2-AP, vimentin mRNA was upregulated (1.9 ± 0.6) compared to untreated cells (1 ± 0.2) or those treated with TGF β (1.4 ± 0.6). Similarly, vimentin mRNA expression was upregulated in PAR2-AP treated BxPC-3 cells (1.8 ± 0.7) compared to untreated cells (1.1 ± 0.3) and TGF β treated cells (1.1 ± 0.3) (Figure 64).

4.4.6. Examination of the influence of TF concentration on vimentin expression

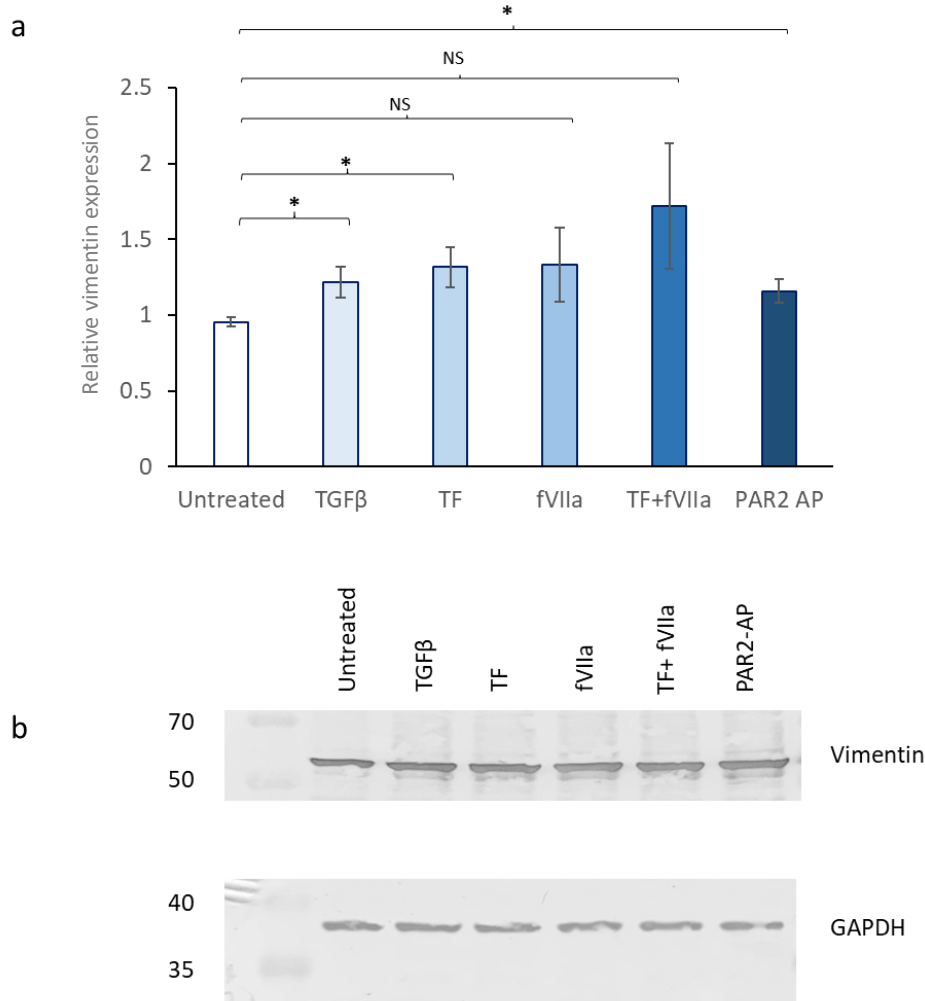
hTERT-HPNE and AsPC-1 cells were incubated with a range of TF concentration (0.1 – 4 U/ml) along with a set treated with TGF β (5 ng/ml) used as a positive control. In hTERT-HPNE cells, western blot analysis of vimentin protein revealed that the expression of vimentin did not differ with exposure to different concentrations of TF when compared to TGF β (Figure 65). Similarly, we observed no significant changes in vimentin expression in AsPC-1 cells treated with different concentrations of TF (Figure 66).

hTERT-HPNE and AsPC-1 cells were incubated with TF at 0.5 U/ml or 2 U/ml or 4 U /ml or TGF β (5 ng/ml). The vimentin mRNA expression was examined using RT-qPCR. In hTERT-HPNE cells, exposure to TF at a concentration of 0.5 U/ml resulted in the upregulation of vimentin mRNA expression compared to TGF β (5 ng/ml) or untreated cells. Treatment with TF at 2 U/ml or 4 U/ml, as well as TGF β (5 ng/ml), did not lead to significant changes in vimentin mRNA expression in hTERT-HPNE cells (Figure 67). In the AsPC-1 cells, expression of vimentin mRNA on exposure to TF 0.5 U/ml, TF 2 U/ml, TF 4 U /ml or TGF β (5 ng/ml) showed a small increase when compared to untreated cells; however, these were not statistically significant (Figure 68).

4.4.7. Examination of the level of expression of fVII

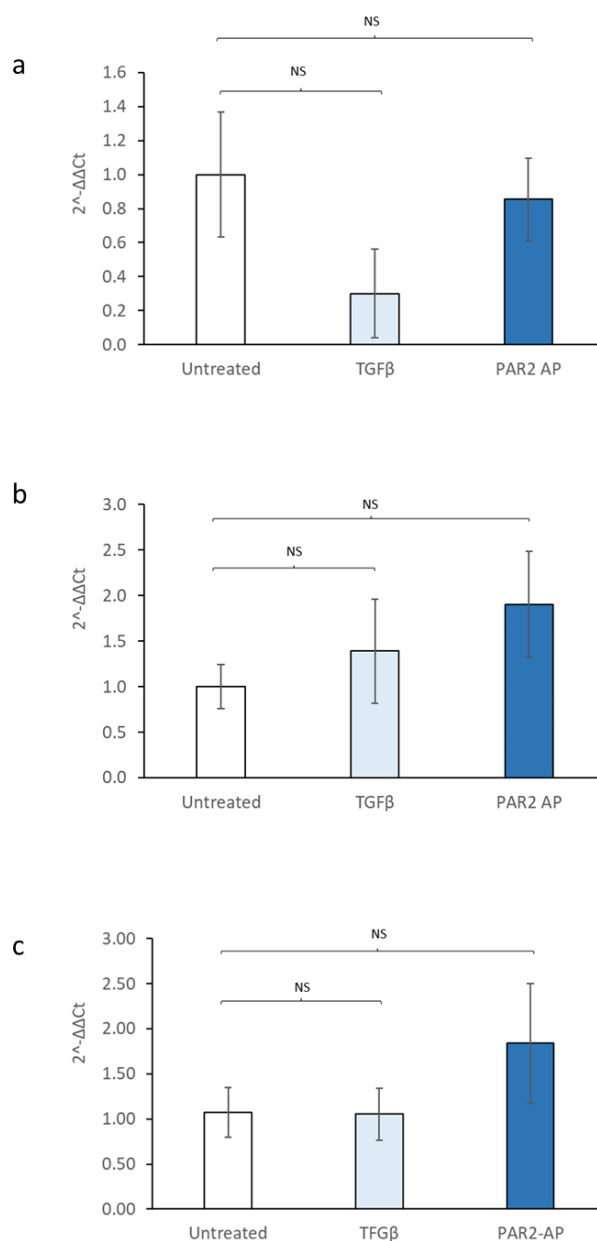
The presence of fVII was assessed using western blot in hTERT-HPNE and AsPC-1 cells. Clear bands indicating the presence of both full-length fVII (~ 50 kDa in molecular weight) and its active form, fVII heavy chain (~ 30 kDa in molecular weight), were detectable in both cell lines. (Figure 69, Figure 70). The expression of activated fVII (fVIIa) was higher in the AsPC-1 cells compared to the hTERT-HPNE cells (Figure 71).

Figure 63: Examination of expression of vimentin in AsPC-1



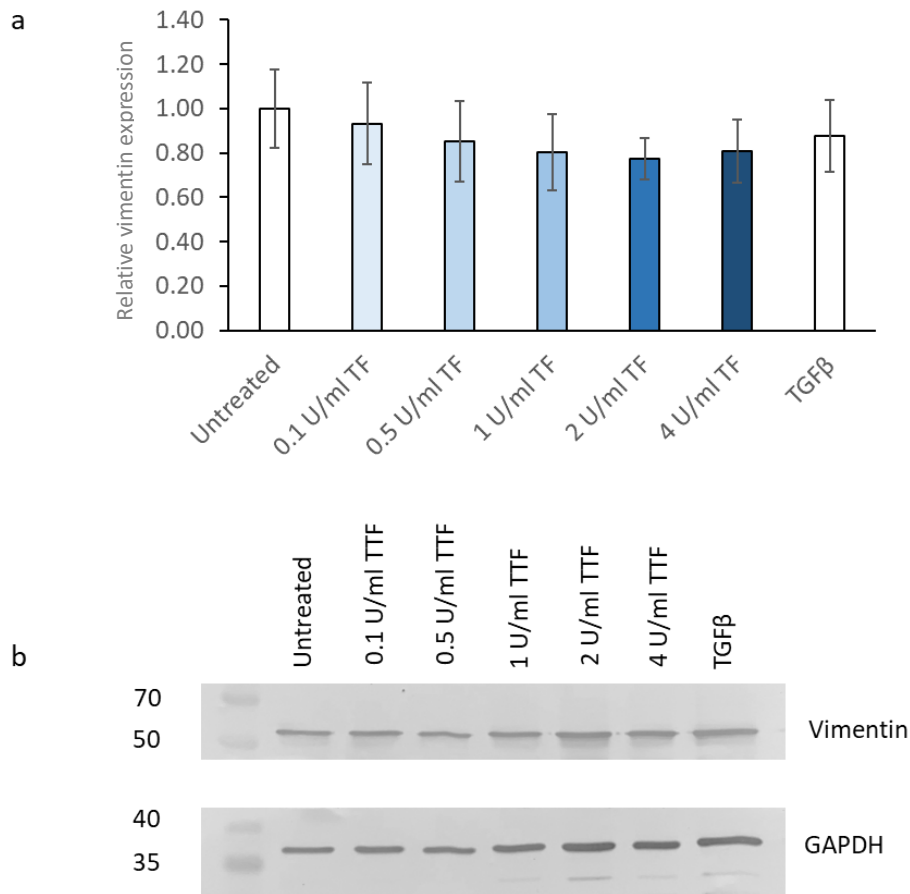
AsPC-1 cells (10^5) were seeded in 6-well plates and incubated with TF (2 U/ml) or fVIIa (5 nM) or TF (2 U/ml) + fVIIa (5 nM) or PAR2-AP (20 μ M), for 2 days. Treated and untreated cells were collected and lysed in Laemmli buffer; proteins were separated by SDS-PAGE, and the vimentin expression was assessed by western blot using mouse anti-vimentin monoclonal antibody (diluted 1:3000 v/v in TBST). The membranes were incubated with AP-conjugated goat anti-mouse IgG antibody (diluted 1:3000 v/v in TBST). The membranes were then developed using Western Blue stabilised substrate for AP (n=6, Images represent three experiments carried out in duplicates; data = mean values \pm SEM; one-way ANOVA, * = $p < 0.05$ NS = not significant).

Figure 64: Examination of expression of vimentin mRNA in cell lines



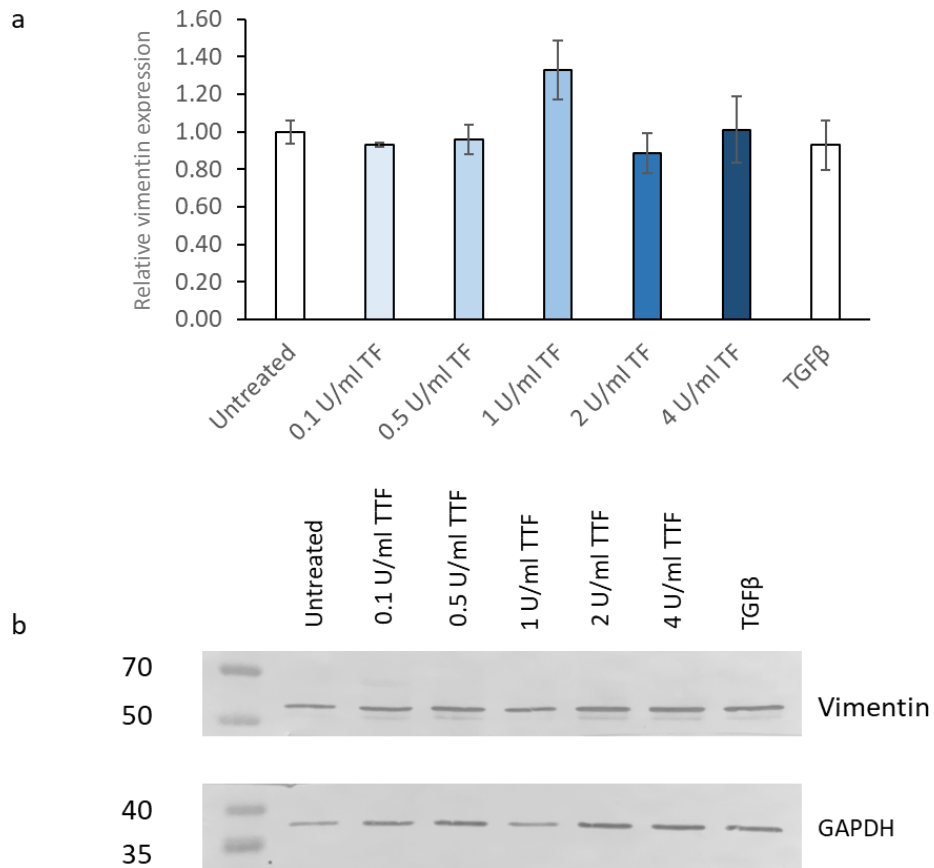
a- hTERT-HPNE (10^5), b- AsPC1 (10^5), and c- BxPC3 (10^5) cells were incubated with PAR2-AP or TGFβ for 2 days. The treated and untreated cells were then lysed, and the mRNA extracted using Monarch® total RNA Miniprep Kit and GoTaq® 1-Step RT-qPCR System was used. The expression of vimentin and β-actin mRNA were measured using RT-qPCR, and the relative vimentin mRNA expression levels were calculated against β-actin using the $2^{-\Delta\Delta Ct}$ method (n=6, three experiments carried out in duplicates; data = mean values ± SEM; independent t-test, NS = not significant).

Figure 65: Expression of vimentin following the incubation of hTERT-HPNE cells with TF



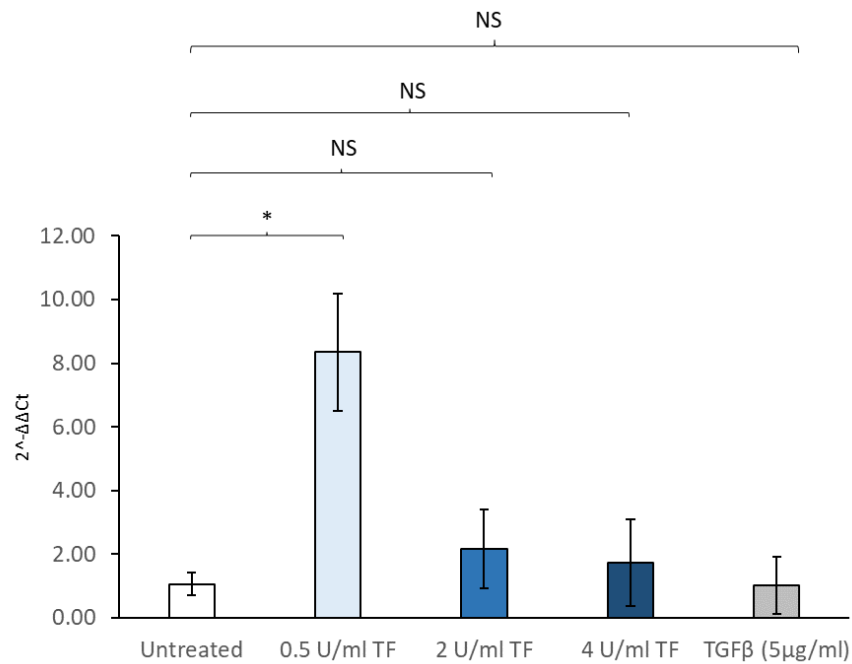
hTERT-HPNE cells (5×10^4) were seeded in 24-well plates and incubated with TF (0 - 4 U/ml) or with TGFβ (5 ng/ml), along with untreated control. Cells were collected after 2 days and lysed in Laemmli buffer and the proteins were separated by SDS-PAGE. The vimentin expression was assessed by western blot using mouse anti-vimentin monoclonal antibody (diluted 1:3000 v/v in TBST). The membranes were incubated with AP-conjugated goat anti-mouse IgG antibody (diluted 1:3000 v/v in TBST). The membranes were then developed using Western Blue stabilised substrate for AP (n=3, Images represent three experiments; data = mean values \pm SEM; Independent samples t-test).

Figure 66: Expression of vimentin following the incubation of AsPC-1 cells with TF



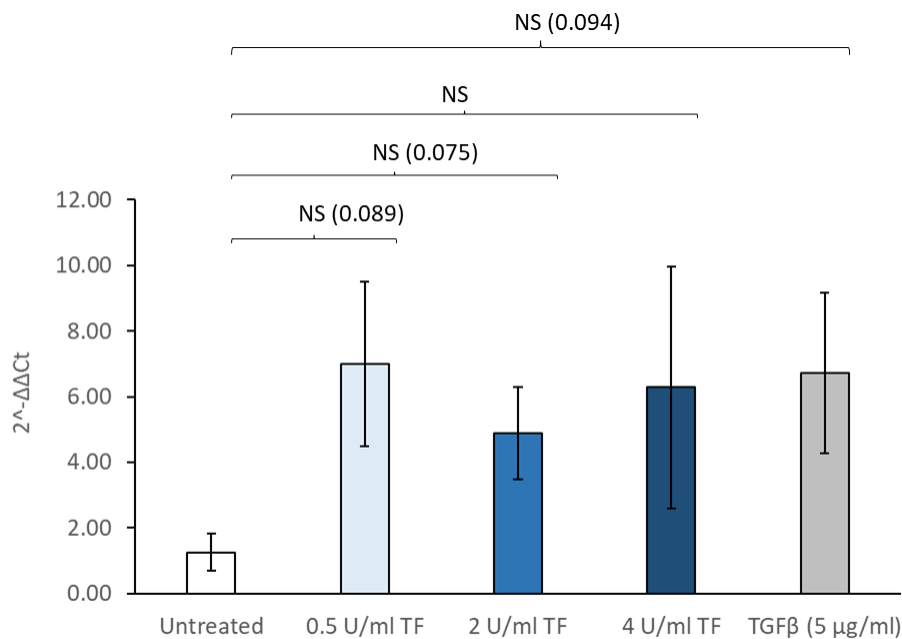
AsPC-1 cells (5×10^4) were seeded in 24-well plates and incubated with TF (0 - 4 U/ml) or with TGFβ (5 ng/ml), along with untreated control. Cells were collected after 2 days and lysed in Laemmli buffer and the proteins were separated by SDS-PAGE. The vimentin expression was assessed by western blot using mouse anti-vimentin monoclonal antibody (diluted 1:3000 v/v in TBST). The membranes were incubated with AP-conjugated goat anti-mouse IgG antibody (diluted 1:3000 v/v in TBST). The membranes were then developed using Western Blue stabilised substrate for AP (n=3, Images represent three experiments; data = mean values \pm SEM; Independent samples t-test).

Figure 67: Expression of vimentin mRNA following the incubation of hTERT-HPNE cells with TF



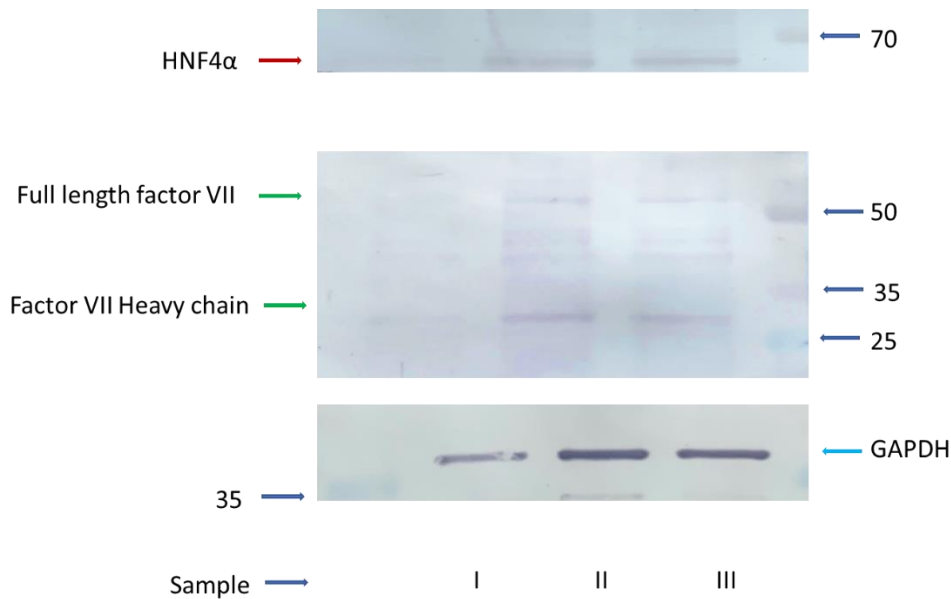
hTERT-HPNE cells (5×10^4) were seeded in 24-well plates and incubated with TF (0 - 4 U/ml) or with TGF β (5 ng/ml), along with untreated control. Cells were collected after 2 days and lysed. The mRNA extracted using Monarch[®] total RNA Miniprep Kit and GoTaq[®] 1-Step RT-qPCR System was used. The expression of vimentin and β -actin mRNA were measured using RT-qPCR, and the relative vimentin mRNA expression levels were calculated against β -actin using the $2^{-\Delta\Delta C_t}$ method (n=3, three experiments carried out; data = mean values \pm SEM; one-way ANOVA, * = $p < 0.05$ NS = not significant).

Figure 68: Expression of vimentin mRNA following the incubation of in AsPC-1 cells with TF



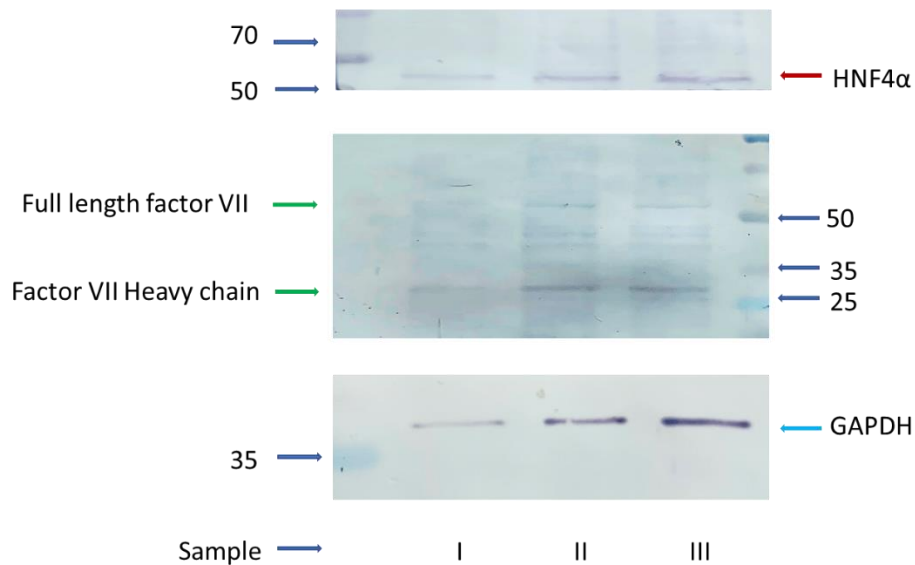
AsPC1 cells (5×10^4) were seeded in 24-well plates and incubated with TF (0 - 4 U/ml) or with TGFβ (5 ng/ml), along with an untreated control. Cells were collected after 2 days and then lysed. The mRNA extracted using Monarch[®] total RNA Miniprep Kit and GoTaq[®] 1-Step RT-qPCR System was used. The expression of vimentin and β-actin mRNA were measured using RT-qPCR, and the relative vimentin mRNA expression levels were calculated against β-actin using the $2^{-\Delta\Delta C_t}$ method (n=3, three experiments carried out; data = mean values ± SEM; one-way ANOVA, * = $p < 0.05$ NS = not significant).

Figure 69: Examination of the presence of fVII and HNF4 α in hTERT-HPNE cells



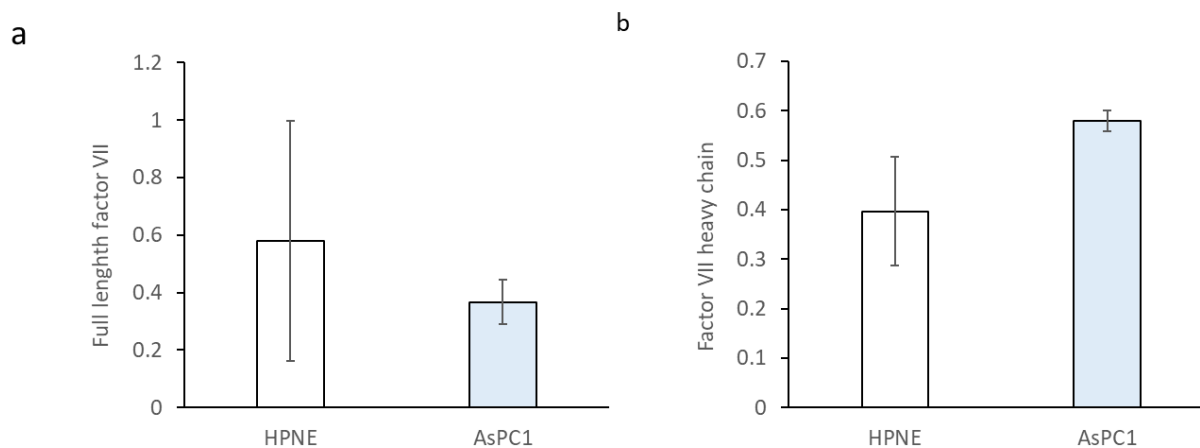
hTERT-HPNE cells (10^5) were seeded in a T25 flask and collected after 2 days. The cells were then lysed in Laemmli buffer and the proteins were separated by SDS-PAGE. Expression of fVII was assessed by western blot using rabbit anti-fVII polyclonal antibody (1:3000 v/v in TBST), the membranes were incubated with AP-conjugated mouse anti-rabbit IgG antibody 1:3000 v/v in TBST). The expression of HNF4 α was assessed by western blot using mouse anti-HNF4 α monoclonal antibody (diluted 1:3000 v/v in TBST), the membranes were incubated with AP-conjugated goat anti-mouse IgG antibody (diluted 1:3000 v/v in TBST). The membranes were then developed using Western Blue stabilised substrate for AP.

Figure 70: Examination of the presence of fVII and HNF4 α in AsPC-1 cells



AsPC-1 cells (10^5) were seeded in a T25 flask and collected after 2 days. The cells were then lysed in Laemmli buffer and the proteins were separated by SDS-PAGE. Expression of fVII was assessed by western blot using rabbit anti-fVII polyclonal antibody (1:3000 v/v in TBST), the membranes were incubated with AP-conjugated mouse anti-rabbit IgG antibody 1:3000 v/v in TBST). The expression of HNF4 α was assessed by western blot using mouse anti-HNF4 α monoclonal antibody (diluted 1:3000 v/v in TBST), the membranes were incubated with AP-conjugated goat anti-mouse IgG antibody (diluted 1:3000 v/v in TBST). The membranes were then developed using Western Blue stabilised substrate for AP.

Figure 71: Assessment of fVII levels in hTERT-HPNE and AsPC-1 cells



hTERT-HPNE and AsPC-1 cells (10^5) were seeded and incubated in T25 flasks. Cells were collected after 2 days and lysed in Laemmli buffer and proteins were separated by SDS-PAGE. The expression of a- full-length fVII and b- heavy chain of fVII were assessed by western blot assay using rabbit anti-fVII polyclonal antibody (diluted 1:3000 v/v in TBST). The membranes were incubated with AP-conjugated mouse anti-rabbit IgG antibody (diluted 1:3000 v/v in TBST). The membranes were then developed using Western Blue stabilised substrate for AP (n=6, Images represent three experiments carried out in duplicates; data = mean values \pm SEM; independent samples t-test).

The level of fVII mRNA expression was examined in both hTERT-HPNE and AsPC-1 cells using RT-qPCR. AsPC-1 cells showed a higher expression of fVII mRNA compared to hTERT-HPNE cells (Figure 72).

4.4.8. Examination of the level of expression of HNF4 α

The presence of HNF4 α was assessed using western blot in hTERT-HPNE and AsPC-1 cells. Clear bands indicating the presence of HNF α (molecular weight \sim 53 kDa) were observed in both cell lines (Figure 69, Figure 70). The expression of HNF4 α was significantly higher in the AsPC-1 cells than in the hTERT-HPNE cells (Figure 73).

4.4.9. Examination of the influence of TF on the expression of HNF4 α in cell lines

Next, to examine the influence of TF on the expression of HNF4 α , hTERT-HPNE and AsPC-1 cells were incubated with TF (2 U/ml) and TGF β (5 ng/ml) along with an untreated control. Cells were collected after 2 days. The level of HNF4 α was assessed using Western blot analysis. Treatment of the cells with TF (2 U/ml) resulted in an increase in HNF4 α expression in the hTERT-HPNE cells, which was comparable to that by TGF β (Figure 74). However, incubation of AsPC-1 cells with TF (2 U/ml) did not result in any alteration in the expression of HNF4 α (Figure 75).

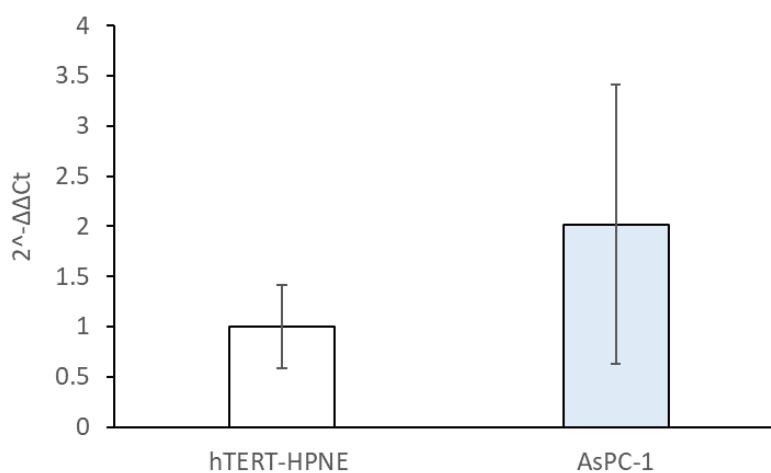
In addition, incubation of hTERT-HPNE cells with a lower concentration of TF (0.5 U/ml) resulted in upregulation in the HNF4 α mRNA expression compared to the untreated sample (Figure 76).

4.4.10. Examination of the influence of various concentrations of TF on cyclin D1

To examine the influence of various concentrations of TF (0.5 - 4 U/ml) on cell proliferation, expression of cyclin D1 mRNA was assessed by RT-qPCR in hTERT-HPNE and AsPC-1 cells. Incubation of hTERT-HPNE with 0.5 U/ml TF resulted in significant upregulation of cyclin D1 (12.1 ± 2.4) compared to the untreated sample (1 ± 0.2) or the TGF β treated sample (1 ± 0.2). Exposure of hTERT-HPNE with higher concentrations of TF (2 U/ml or 4 U/ml) did not lead to an increase in the expression of cyclin D1 mRNA expression (Figure 77).

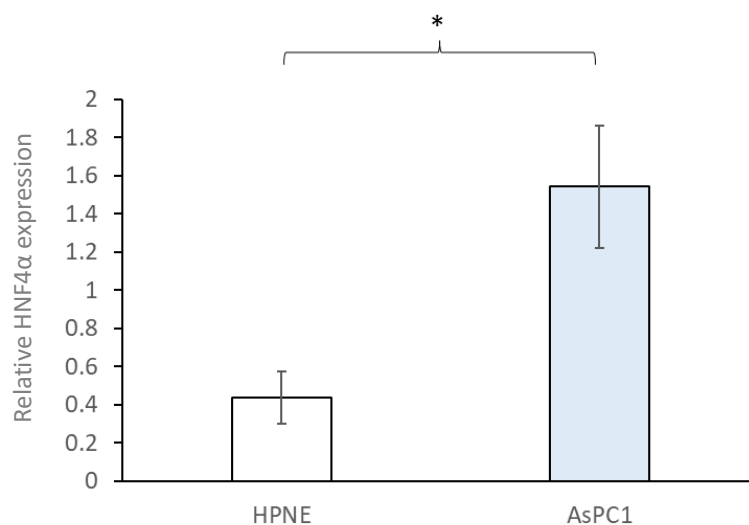
In the same way, treating AsPC-1 with 0.5 U/ml TF resulted in a significant increase in cyclin D1 expression (6.9 ± 1.7) when compared to the untreated sample (1 ± 0.6) or TGF β -treated sample (0.4

Figure 72: Examination of the expression of fVII mRNA in hTERT-HPNE and AsPC-1 cells



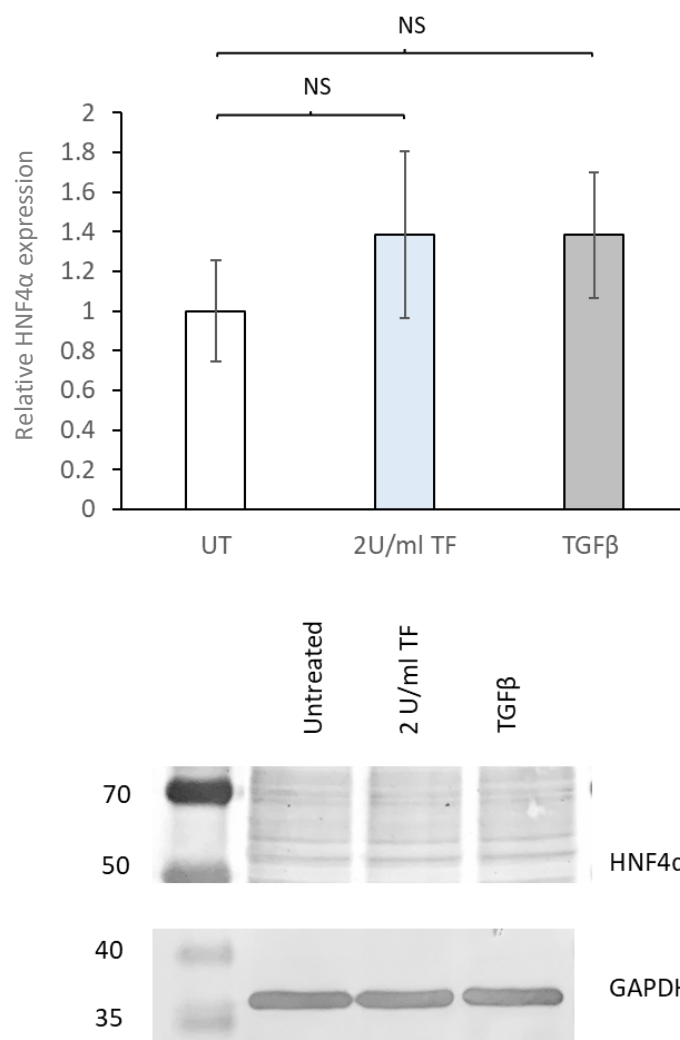
hTERT-HPNE and AsPC-1 cells (10^5) were seeded in 6-well plates. The cells were collected after 2 days and lysed. The mRNA extracted using Monarch[®] total RNA Miniprep Kit and GoTaq[®] 1-Step RT-qPCR System was used. The expression of fVII and β -actin mRNA were measured using RT-qPCR, and the relative fVII mRNA expression levels were calculated against β -actin using the $2^{-\Delta\Delta C_t}$ method (n=3, three experiments carried out; data = mean values \pm SEM; independent samples t-test, NS = not significant).

Figure 73: Assessment HNF4 α levels in hTERT-HPNE and AsPC-1 cells



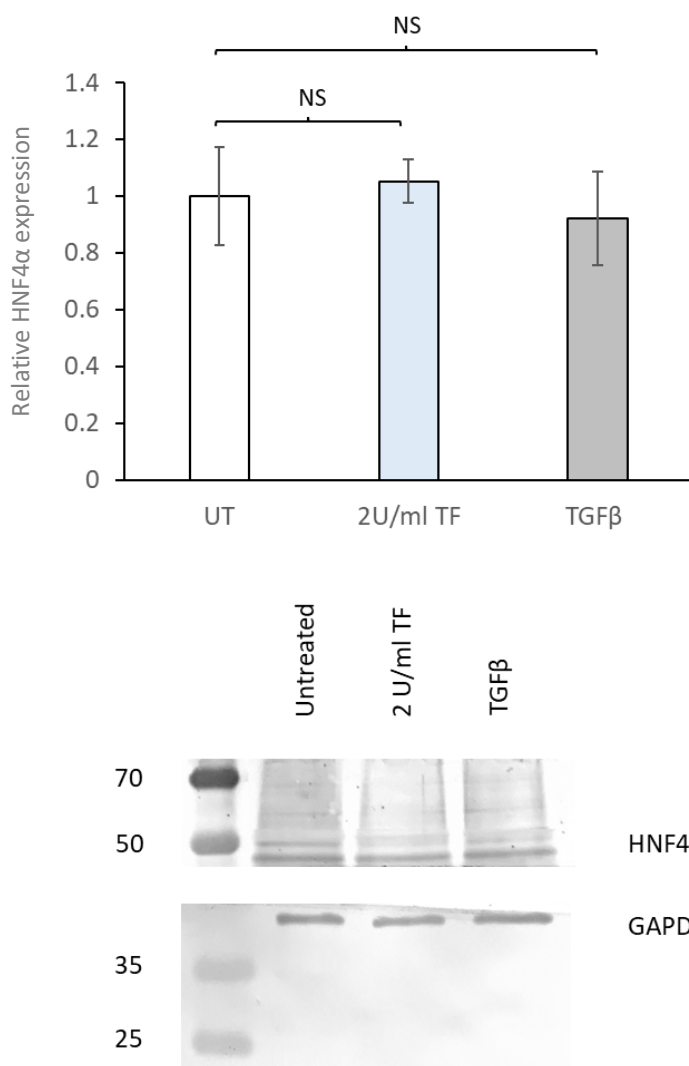
hTERT-HPNE and AsPC-1 cells (10^5) were seeded and incubated in T25 flasks. Cells were collected after 2 days and lysed in Laemmli buffer and proteins were separated by SDS-PAGE. The expression of HNF4 α was assessed by western blot using mouse anti-HNF4 α monoclonal antibody (diluted 1:3000 v/v in TBST). The membranes were incubated with AP-conjugated goat anti-mouse IgG antibody (diluted 1:3000 v/v in TBST). The membranes were then developed using Western Blue stabilised substrate for AP (n=6, Images represent three experiments carried out in duplicates; data = mean values \pm SEM; independent samples t-test, * = p < 0.05).

Figure 74: Examination of the influence of TF on HNF4 α expression in hTERT-HPNE cells



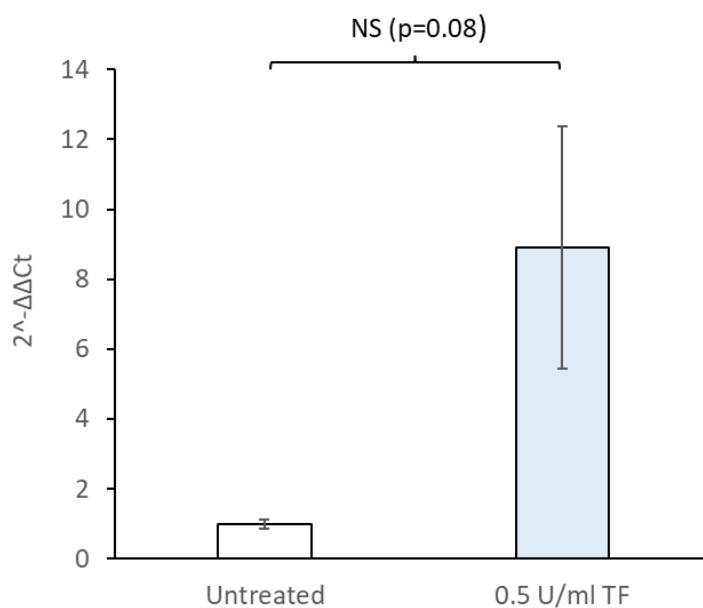
hTERT-HPNE cells (10^5) were seeded in 6-well plates and incubated with TF at 2 U/ml or TGF β (5 ng/ml), along with untreated controls. Cells were collected after 2 days and lysed in Laemmli buffer; proteins were separated by SDS-PAGE. The expression of HNF4 α was assessed by western blot, using a mouse anti-HNF4 α monoclonal antibody (diluted 1:3000 v/v in TBST). The membranes were incubated with AP-conjugated goat anti-mouse IgG antibody (diluted 1:3000 v/v in TBST). The membranes were then developed using Western Blue stabilised substrate for AP (n=6, Images represent three experiments carried out in duplicates; data = mean values \pm SEM; one-way ANOVA, NS = not significant).

Figure 75: Examination of the influence of TF on HNF4 α expression in AsPC-1 cells



AsPC-1 cells (10^5) were seeded in 6-well plates and incubated with TF at 2 U/ml or TGF β (5 ng/ml), along with untreated controls. Cells were collected after 2 days and lysed in Laemmli buffer; proteins were separated by SDS-PAGE. The expression of HNF4 α was assessed by western blot, using a mouse anti-HNF4 α monoclonal antibody (diluted 1:3000 v/v in TBST). The membranes were incubated with AP-conjugated goat anti-mouse IgG antibody (diluted 1:3000 v/v in TBST). The membranes were then developed using Western Blue stabilised substrate for AP (n=6, Images represent three experiments carried out in duplicates; data = mean values \pm SEM; one-way ANOVA, NS = not significant).

Figure 76: Examination of the influence of TF on HNF4 α mRNA expression in hTERT-HPNE cells



hTERT-HPNE cells (5×10^4) were seeded in 24-well plates and incubated with TF at 0.5 U/ml along with untreated samples. The cells were collected after 2 days and then lysed, mRNA was extracted using Monarch[®] total RNA Miniprep Kit and GoTaq[®] 1-Step RT-qPCR System. The expression of HNF4 α and β -actin mRNA were measured using RT-qPCR, and the relative amount of HNF4 α mRNA expression levels were calculated against β -actin using the $2^{-\Delta\Delta Ct}$ method (n=3, three experiments carried out; data = mean values \pm SEM; independent samples t-test, NS = not significant).

± 0.1). However, exposing hTERT-HPNE to higher concentrations of TF (1 U/ml or 2 U/ml) did not induce an increase in cyclin D1 mRNA expression (Figure 77).

4.4.11. Examination of the influence of various concentrations of TF on bax

To examine the influence of various concentrations of TF (0.5 - 4 U/ml) on cell apoptosis, the expression of bax mRNA was assessed by RT-qPCR in hTERT-HPNE and AsPC-1 cells. Incubation of hTERT-HPNE with 4 U/ml TF resulted in upregulation of bax (6.3 ± 4.5) compared to the untreated sample (1 ± 0.6) or the TGF β treated sample (0.6 ± 0.1). Exposure of hTERT-HPNE with a lower concentration of TF (0.5 U/ml) did not increase the expression of bax mRNA (Figure 78).

Treating AsPC-1 with 2 U/ml TF resulted in an increase in bax expression (7.4 ± 5.3) when compared to the untreated sample (1 ± 0.5) or TGF β -treated sample (0.8 ± 0.1). However, exposing AsPC-1 cells to lower concentrations of TF (0.5 U/ml) did not induce an increase in bax mRNA expression (Figure 78).

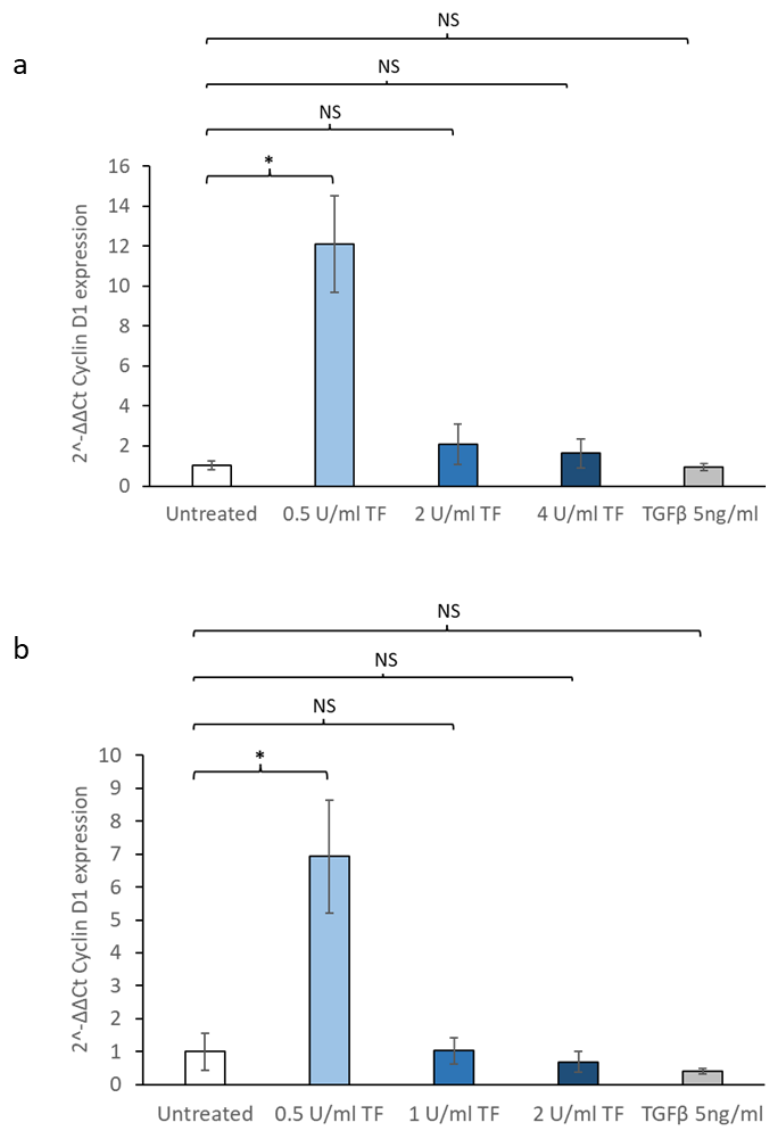
4.4.12. Examination of the influence of TF on the expression of p16 protein

Both hTERT-HPNE and AsPC-1 cells were initially examined for the presence of p16 protein using western blot. Bands indicated the presence of p16 bands was detectable in both cell lines (Figure 79). To examine the influences of TF on the expression of p16, hTERT-HPNE and AsPC-1 cells were incubated with TF (2 U/ml) or TGF β (5 ng/ml) along with a set of untreated samples. Cells were collected after 2 days and the level of p16 protein was assessed using western blot. In hTERT-HPNE cells, treatment with TF (2 U/ml) led to an increase in p16 protein expression compared to that of the untreated cells, which was similar to the effects of TGF β (Figure 80). However, incubation of AsPC-1 cells with TF (2 U/ml) did not result in any alteration in p16 expression (Figure 81).

4.4.13. Establishing a spheroid model by the co-culture of CAF and the pancreatic cells

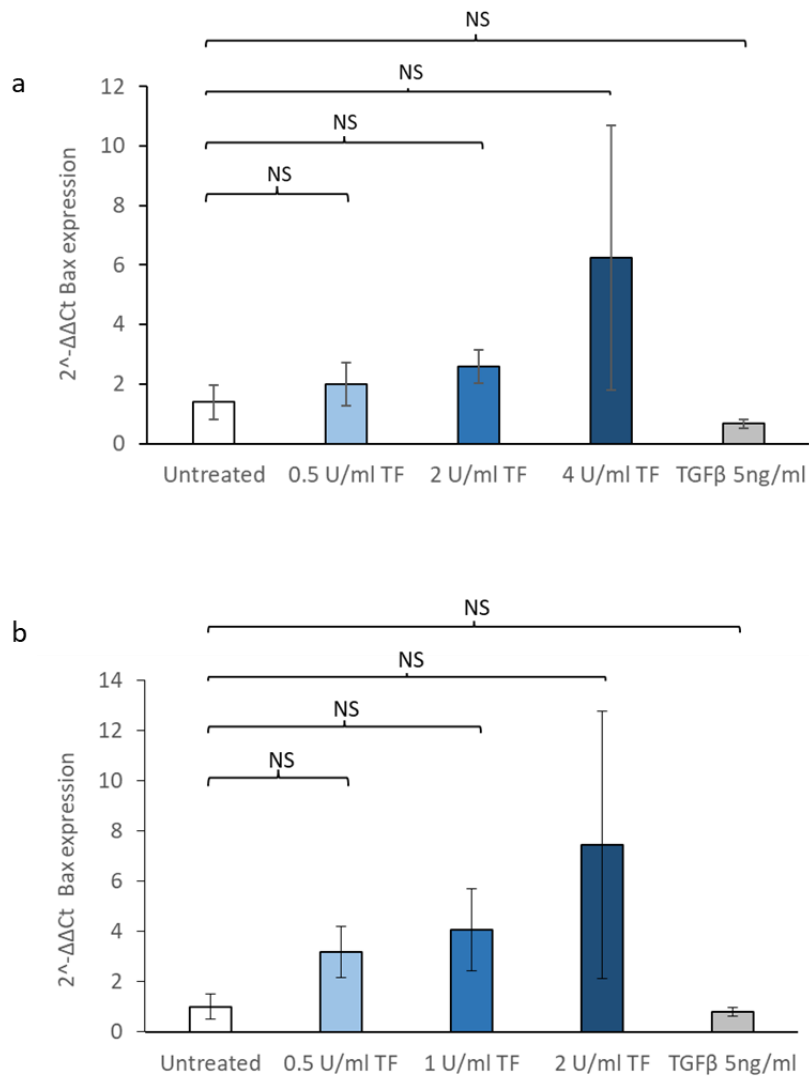
Cancer-associated fibroblast (CAF) cells were co-cultured with hTERT-HPNE, hTERT-HPNE E6/E7/K-RasG12D, hTERT-HPNE E6/E7/K-RasG12D/st cell lines to establish a compact spheroid model that can be used to reproduce *in vivo* characteristics or interaction. We co-cultured pancreatic epithelial cells (Pan) with CAF cells in different ratios (1:3, 1:1, 3:1 Pan:CAF) to capture the spectrum of varying

Figure 77: Examination of the influence of different concentrations of TF on cyclin D1



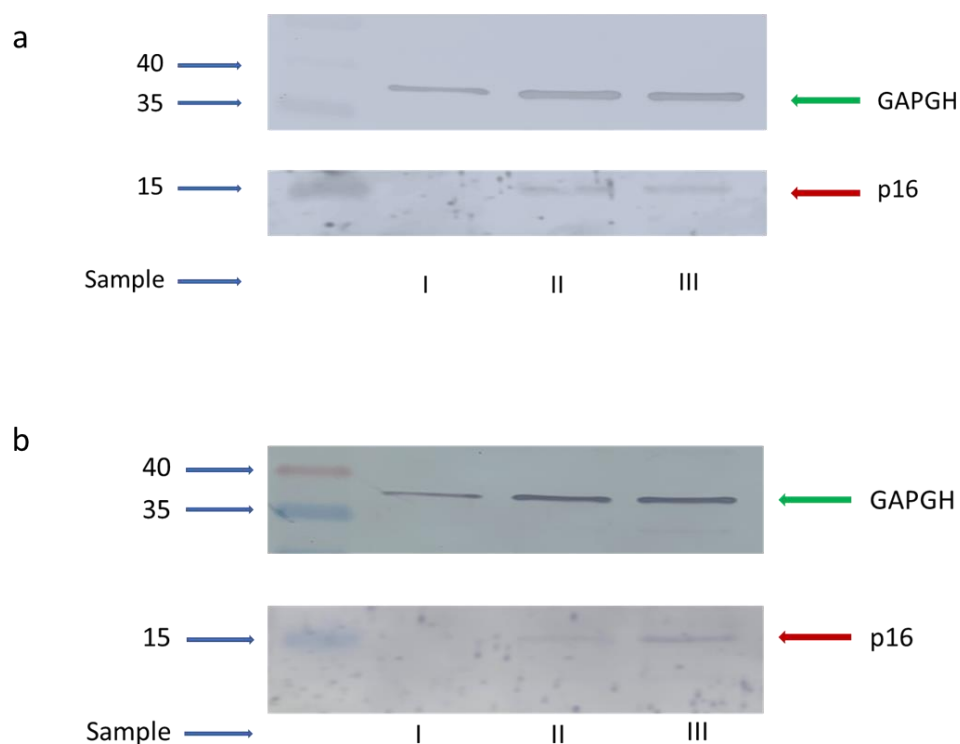
a- hTERT-HPNE and b- AsPC-1 cells (5×10^4) were seeded in 24-well plates and incubated with TF (0 - 4 U/ml) or TGFβ (5 ng/ml), along with untreated samples. The cells were collected after 2 days and then lysed; the mRNA extracted using Monarch® total RNA Miniprep Kit and GoTaq® 1-Step RT-qPCR System was used. The expression of cyclin D1 and β-actin mRNA were measured using RT-qPCR, and the relative amount of cyclin D1 mRNA expression levels were calculated against β-actin using the $2^{-\Delta\Delta C_t}$ method (n=3, three experiments carried out; data = mean values \pm SEM; one-way ANOVA, * = $p < 0.05$ NS = not significant).

Figure 78: Examination of the influence of different concentrations of TF on bax



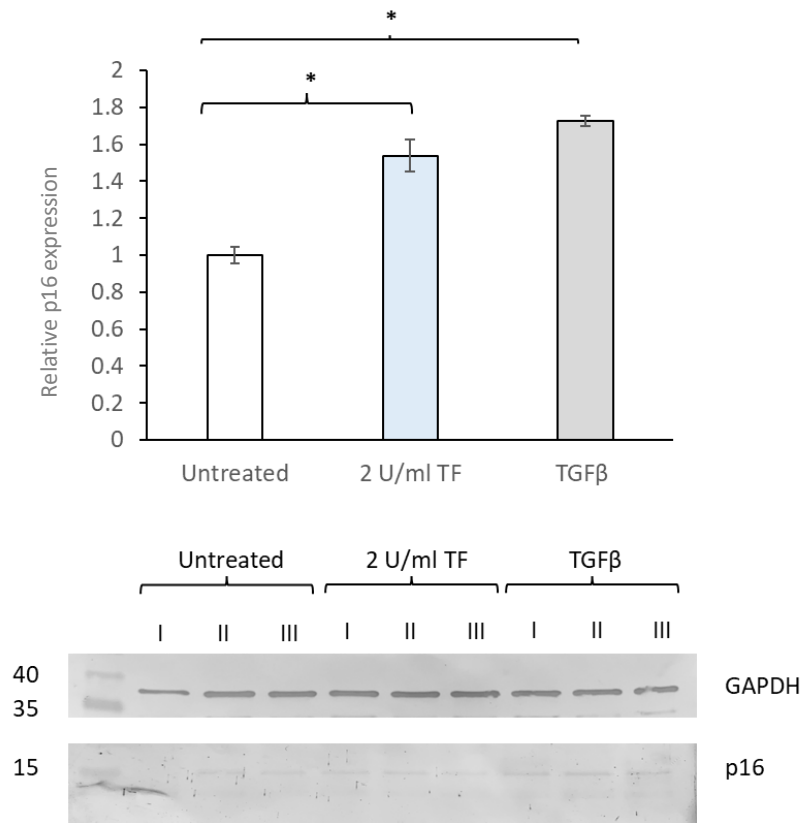
a- hTERT-HPNE and b- AsPC-1 cells (5×10^4) were seeded in 24-well plates and incubated with TF (0 - 4 U/ml) or TGFβ (5 ng/ml), along with untreated samples. The cells were collected after 2 days and then lysed; the mRNA extracted using Monarch® total RNA Miniprep Kit and GoTaq® 1-Step RT-qPCR System was used. The expression of bax and β-actin mRNA were measured using RT-qPCR, and the relative amount of bax mRNA expression levels were calculated against β-actin using the $2^{-\Delta\Delta C_t}$ method (n=3, three experiments carried out; data = mean values ± SEM; one-way ANOVA, * = $p < 0.05$, NS = not significant).

Figure 79: Examination of the presence of p16 protein in hTERT-HPNE and AsPC-1 cells



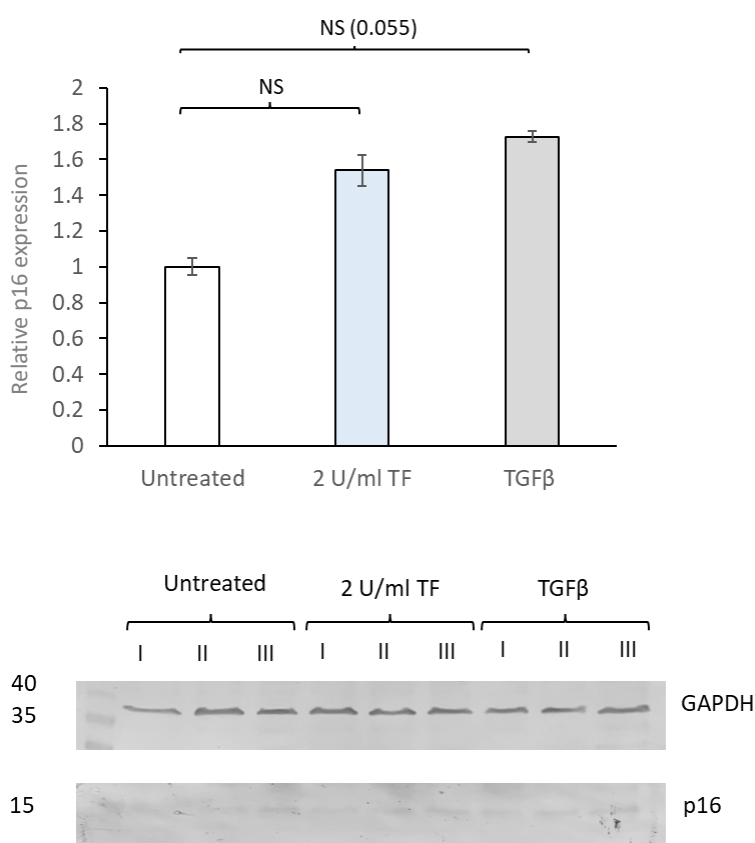
a- hTERT-HPNE and b- AsPC-1 cells (10^5) were seeded in T25 flask. Cells were collected after 2 days and lysed in Laemmli buffer; the proteins were separated by SDS-PAGE. Expression of p16 was assessed by western blot using goat polyclonal anti-p16 antibody (1:3000 v/v in TBST), the membranes were incubated with AP-conjugated mouse anti-goat IgG antibody 1:3000 v/v in TBST). The membranes were then developed using Western Blue stabilised substrate for AP.

Figure 80: Examination of the influence of TF on the expression of p16 protein in hTERT-HPNE cells



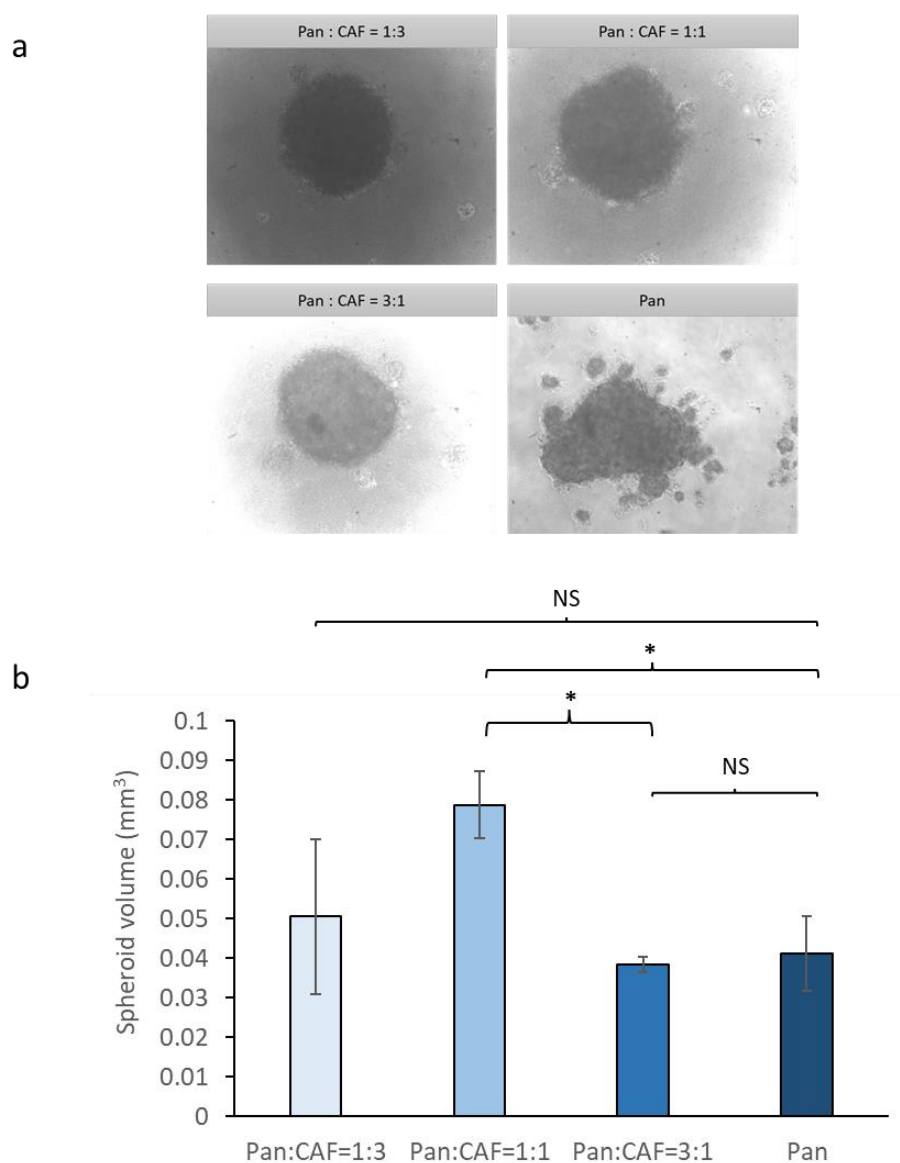
hTERT-HPNE cells (10^5) were seeded in 6-well plates and incubated with TF at 2 U/ml or TGFβ (5 ng/ml), along with an untreated control. Cells were collected after 2 days and lysed in Laemmli buffer; the proteins were separated by SDS-PAGE. The expression of the p16 protein was assessed by western blot using goat polyclonal anti-p16 antibody (diluted 1:3000 v/v in TBST). The membranes were incubated with AP-conjugated mouse anti-goat IgG antibody (diluted 1:3000 v/v in TBST). The membranes were then developed using Western Blue stabilised substrate for AP (n=6, Images represent three experiments carried out in duplicates; data = mean values \pm SEM; one-way ANOVA, * = $p < 0.05$).

Figure 81: Examination of the influence of TF on the expression of p16 protein in AsPC-1 cells



AsPC-1 cells (10^5) were seeded in 6-well plates and incubated with TF at 2 U/ml or TGFβ (5 ng/ml), along with an untreated control. Cells were collected after 2 days and lysed in Laemmli buffer, the proteins were separated by SDS-PAGE. The expression of the p16 protein was assessed by western blot using goat polyclonal anti-p16 antibody (diluted 1:3000 v/v in TBST). The membranes were incubated with AP-conjugated mouse anti-goat IgG antibody (diluted 1:3000 v/v in TBST). The membranes were then developed using Western Blue stabilised substrate for AP (n=6, Images represent three experiments carried out in duplicates; data = mean values \pm SEM; one-way ANOVA, * = $p < 0.05$).

Figure 82: hTERT-HPNE and CAF cells for spheroid formation

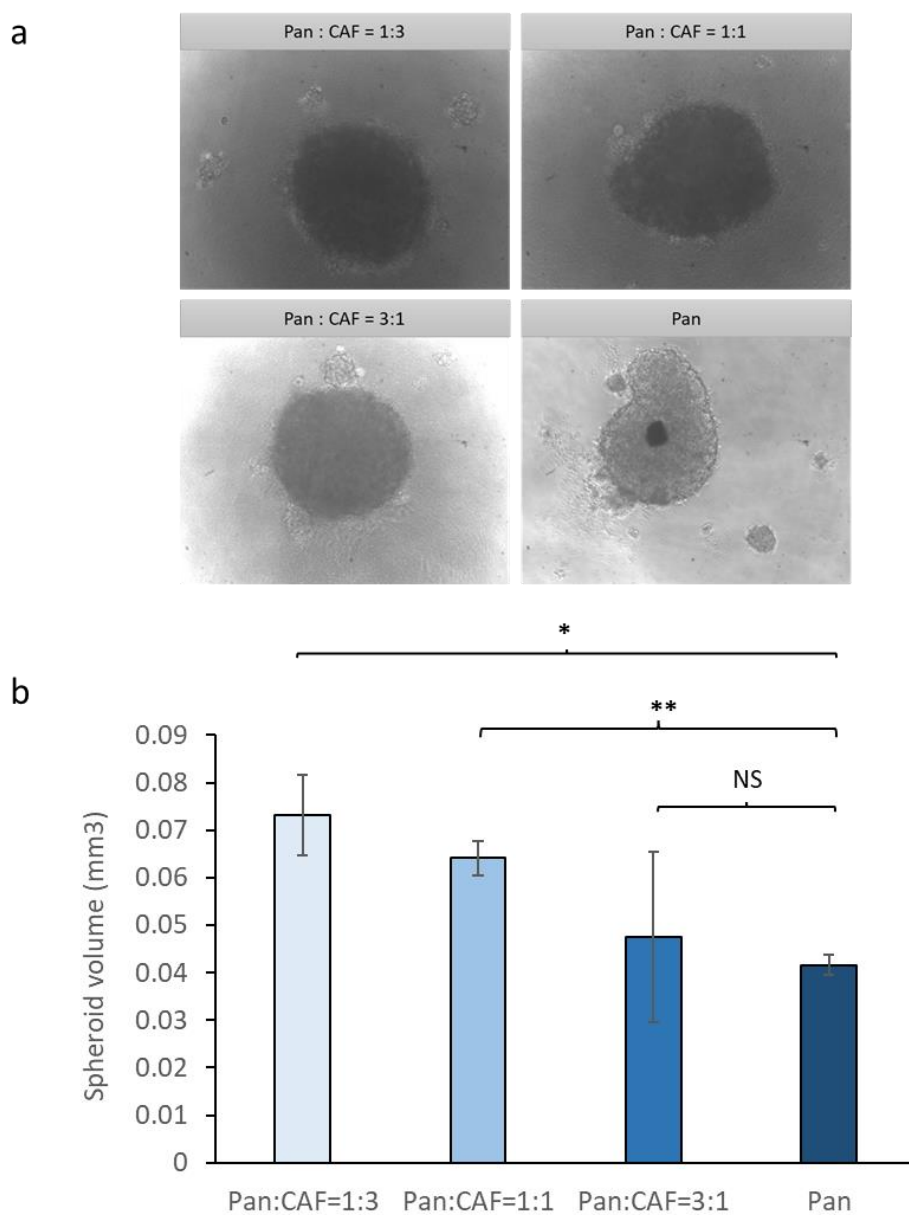


hTERT-HPNE and CAF cells (10^5) were seeded in a non-adherent 96-well plate at ratios of 1:3, 1:1, and 3:1 (Pan:CAF). The hTERT-HPNE cells were also monocultured. The plate was incubated at 37°C for 1 day. a- the spheroids were analysed by bright field microscopy at x10 magnification, b- the diameter of the spheroids formed was measured using ImageJ (n=3, three experiments carried; data = mean values \pm SEM; independent t-test, NS = not significant * = $p < 0.05$).

stromal content in human primary PDACs. All three cell lines were also monocultured to compare with the co-culture model. The size and shape of the spheroids were analysed using bright field microscopy after 1 day. The diameters of the spheroids formed were measured using imageJ and volume of the spheroids were calculated ($\text{Volume} = \frac{4}{3} \pi r^3$, r is the radius).

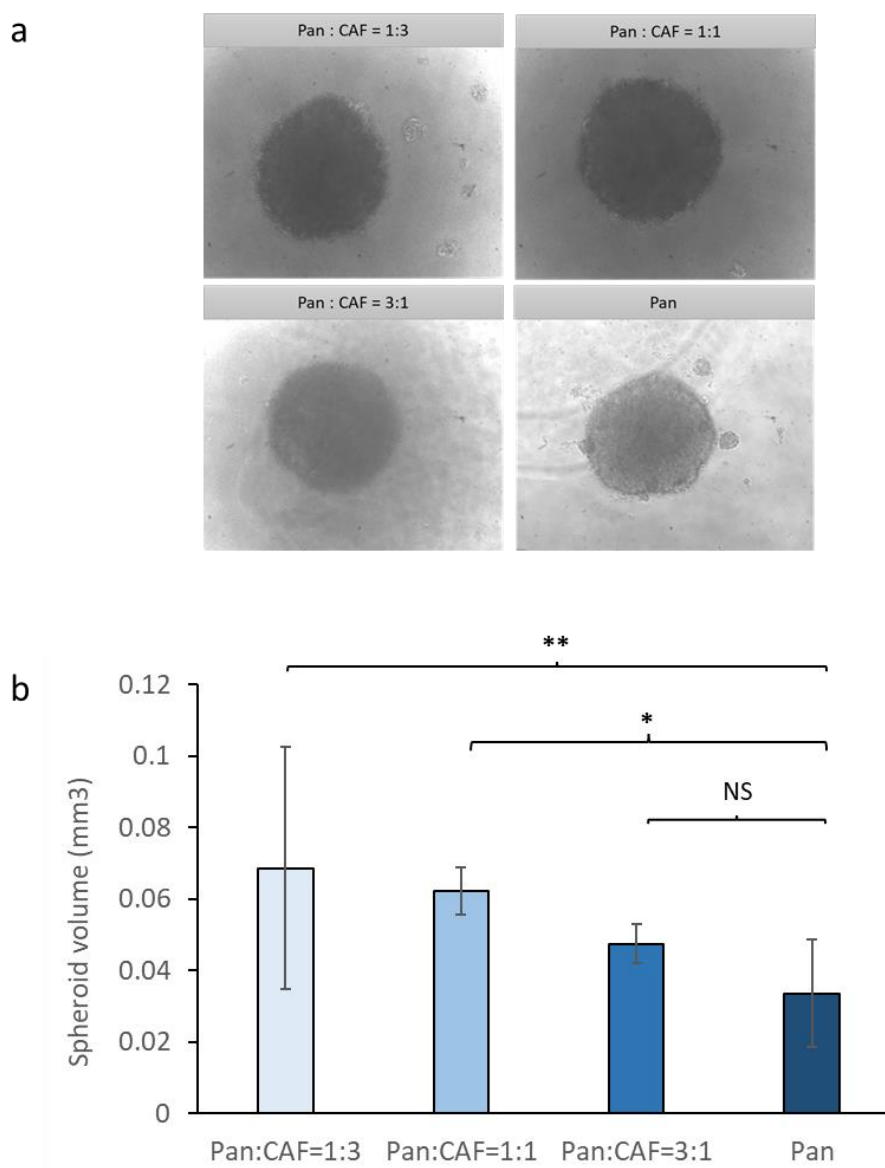
The hTERT-HPNE cells formed spheroids when co-cultured with CAF cells at 1:3, 1:1, and 3:1 ratios, while they did not form spheroids in monoculture. The spheroid of hTERT-HPNE cells with CAFs at a ratio of 1:1 was less compact compared to when co-cultured at 3:1 ratio Figure 82. The hTERT-HPNE E6/E7/K-RasG12D cells formed spheroids both when co-cultured with CAF cells at ratios of 1:3, 1:1, 3:1 and when monocultured. However, the spheroids were less intact when they were monocultured (Figure 83). The hTERT-HPNE E6/E7/K-RasG12D/st cells also formed spheroids both in co-culture with CAF cells at all ratios and in monoculture, and the intactness of spheroids was maintained in both conditions (Figure 84). However, for hTERT-HPNE E6/E7/K-RasG12D and hTERT-HPNE E6/E7/K-RasG12D/st cells, spheroids were less compact at 1:3 and 1:1 ratios with CAFs when compared to monoculture (Figure 83, Figure 84).

Figure 83: hTERT-HPNE E6/E7/K-RasG12D and CAF cells for spheroid formation



hTERT-HPNE E6/E7/K-RasG12D and CAF cells (10^5) were seeded in a non-adherent 96-well plate at ratios of 1:3, 1:1 and, 3:1 (Pan:CAF). The hTERT-HPNE E6/E7/K-RasG12D cells were also monocultured. The plate was incubated at 37°C for 1 day. a- the spheroids were analysed by bright field microscopy at x10 magnification, b- the diameter of the spheroids formed was measured using ImageJ (n=3, three experiments carried; data = mean values \pm SEM; independent t-test, NS = not significant, * = $p < 0.05$).

Figure 84: hTERT-HPNE E6/E7/K-RasG12D/st and CAF cells for spheroid formation



hTERT-HPNE E6/E7/K-RasG12D/st and CAF cells (10^5) were seeded in a non-adherent 96-well plate at ratios of 1:3, 1:1 and, 3:1 (Pan:CAF). The hTERT-HPNE E6/E7/K-RasG12D/st cells were also monocultured. The plate was incubated at 37°C for 1 day. a- the spheroids were analysed by bright field microscopy at x10 magnification, b- the diameter of the spheroids formed was measured using ImageJ (n=3, three experiments carried; data = mean values \pm SEM; independent t-test, NS = not significant, * = $p < 0.05$).

4.5. Discussion

Metastasis occurs early during tumour development, as evidenced by the appearance of metastatic lesions years after the resection of small tumours with no evidence of metastasis at diagnosis (481). This concept is particularly relevant to pancreatic cancer, where most patients are diagnosed with metastatic disease. Even patients who undergo surgical resection of small pancreatic tumours with clear margins and no evidence of metastasis have a high mortality rate due to metastatic disease within five years (482). Studies in breast and lung cancers (483, 484) suggest that metastatic seeding may be mediated by cells that do not meet the agreed definition of cancer. A lineage-labelling system used to identify cells of pancreatic epithelial origin during stochastic tumour progression also revealed EMT in premalignant lesions, primarily in PanIN 2 and 3 lesions (2.7% and 6.8%, respectively), but not in PanIN 1 lesion (463). Additionally, EMT was prevalent in ADM areas, especially in lesions surrounded by abundant inflammatory cells. These findings suggest that cellular dissemination leading to metastasis may occur before an identifiable primary tumour forms, which has significant clinical and biological implications.

Inflammation can promote changes in the microenvironment of the primary site of neoplasia and enhance invasion and dissemination through EMT. TF expression is known to be induced by inflammatory cytokines, and it can also trigger a variety of cellular responses that promote inflammation. TF promotes the recruitment of inflammatory cells to the site of injury or infection, facilitating their migration through the extracellular matrix. Therefore, TF contributes to the development and maintenance of an inflammatory microenvironment, which in turn may promote cancer progression. TF has also been shown to participate in EMT, for example, TF-induced activation of the Wnt/ β -catenin signalling pathway in retinal pigment epithelium ARPE-19 cells (485). Additionally, TF increases β -catenin expression through the AKT/glycogen synthase kinase (GSK)3 β signalling in breast cancer (486) and inactivates E-cadherin expression and upregulation of vimentin expression through EGFR in human epidermal squamous cell carcinoma (215). Finally, TF regulated human coronary artery smooth muscle cell migration via Wnt signalling (487). In this context, the capability of the inflammatory actions of TF to modulate EMT was investigated. In order to achieve this, a marker for the progression of cells through EMT was required. The increased expression of

vimentin was selected as the marker of EMT in this current study. Various other methods can also be used for detecting epithelial to mesenchymal transition (EMT) in cellular models. Some commonly used techniques include immunofluorescence staining, which involves using fluorescently labelled antibodies to detect and visualise the expression and localisation of EMT markers. It allows for assessing changes in protein expression and cellular morphology associated with EMT. Common EMT markers include E-cadherin, claudins, occludins, catenins, desmoglein and desmocollin (epithelial marker) and N-cadherin, vimentin, fibronectin, smooth muscle actin (SMA) (mesenchymal markers). Immunofluorescence staining can provide spatial information on EMT marker expression within cells and tissues. Quantitative PCR (qPCR): This method allows for measuring changes in mRNA expression levels of EMT-related genes. It provides quantitative information on gene expression changes associated with EMT. Commonly studied genes include Slug, Snail, Twist, and Zeb1, mir-200. Flow cytometry technique allows for the quantification of cell surface marker expression, including EMT markers, at the single-cell level; for e.g.- surface markers expressed in cells in an epithelial state (EpCAM and CD24/CD104), protein markers expressed in cells in a mesenchymal state (CD44). It enables the identification and characterisation of distinct cell populations within a heterogeneous cell population based on their surface marker expression profiles.

Vimentin is an intermediate filament protein commonly used as a marker for mesenchymal cells. It is a frequent marker for identifying cancer cells that undergo EMT (488, 489). Vimentin expression positively correlates with enhanced cell invasiveness and metastasis (490). While optimising the detection of EMT markers in this study, vimentin was found to be expressed in all cell lines. However, E-cadherin, cadherin 11 and fibronectin were not. This finding suggests that vimentin may be a more reliable marker of EMT and was used as a marker of EMT in subsequent experiments. The maximal expression of vimentin was observed on day 2 with 5 ng/ml of TGF β in both hTERT-HPNE and AsPC-1 cells. This was consistent with the concentration and incubation period of EMT induction with TGF β reported in the literature (491, 492). Therefore, subsequent studies were carried out with 5 ng/ml TGF β and incubated for 2 days as a positive control.

Once the increased expression of vimentin as the marker of EMT was verified, the effect of TF and fVIIa on vimentin expression was examined in different cell lines, which showed that TF and fVIIa

could modulate vimentin expression. TF and fVIIa had differential effects on the expression of vimentin. In hTERT-HPNE cells, treatment with TF or PAR2-AP led to an increase in vimentin expression, while treatment with fVIIa led to a decrease in vimentin expression. Interestingly, when hTERT-HPNE cells were treated with a combination of TF and fVIIa, the expression of vimentin was moderated with the addition of fVIIa resulting in a decrease in vimentin expression. However, treating AsPC-1 cells with the TF and fVIIa did not alter vimentin expression, which suggests a differential behaviour of already transformed cells. This supports the notion that induction of EMT by TF might be an early event at the pre-invasive stage. In addition, PAR2-AP exposure led to the upregulation of vimentin mRNA expression in malignant cell lines. These findings suggest that PAR2, which is activated by a variety of serine proteases, may play a role in regulating EMT in PC cells, as also evident in other cancer cells (493).

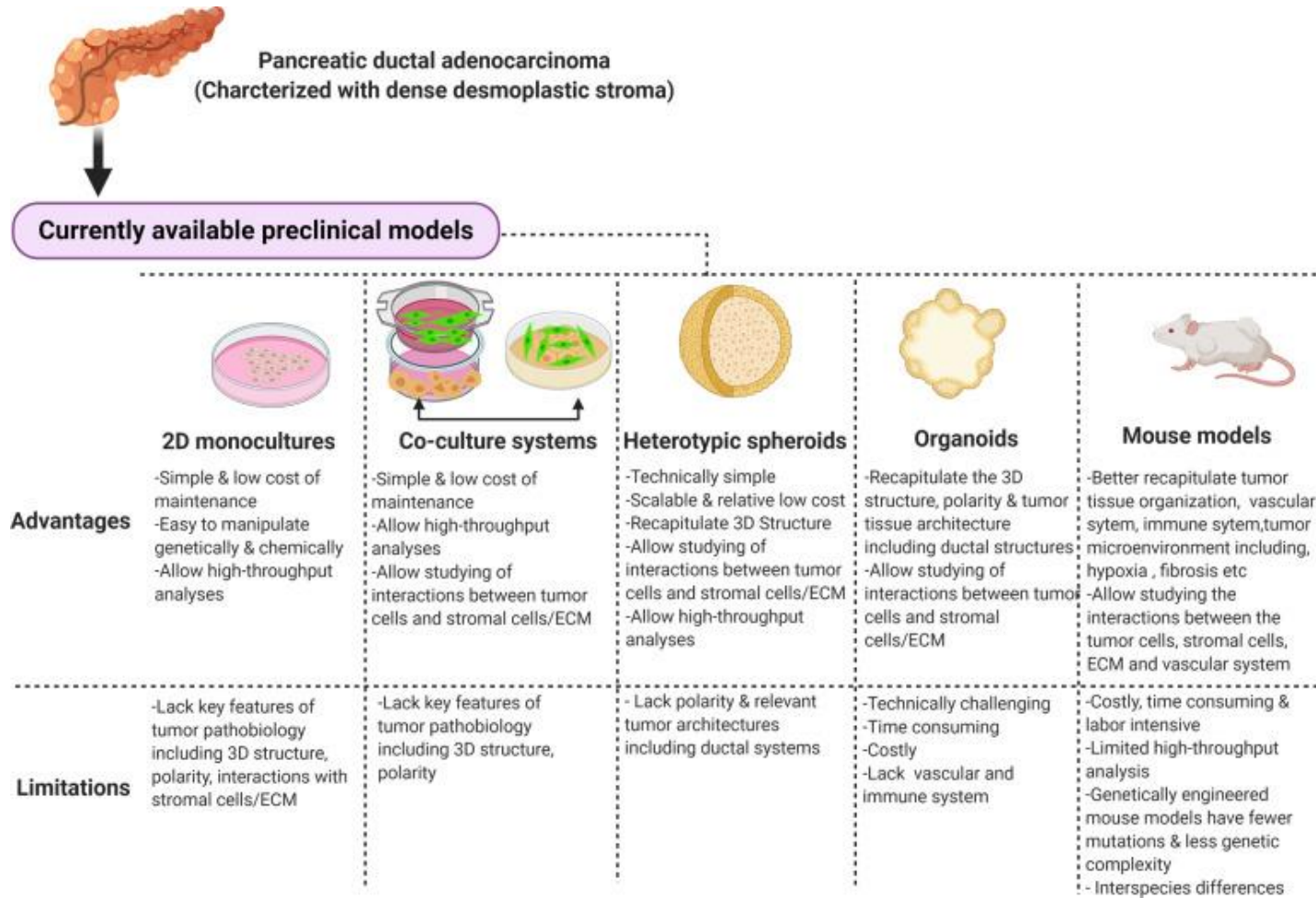
This *in vitro* study has shown that the effects of TF on vimentin expression may be concentration-dependent in benign cells. In hTERT-HPNE cells, exposure to TF at a concentration of 0.65 ng/ml resulted in the upregulation of vimentin mRNA expression, indicating induction of EMT. This TF concentration is comparable to that identified in the clinical samples as a cut-off value (TF = 0.75 ng/ml) distinguishing between non-resective (benign and LGD) and resective (HGD and invasive cancer) disease. However, in AsPC-1 cells, vimentin expression was not dependent on TF concentrations. This indicates that the influence of TF on EMT occurs early during the formation of precursor lesions. Further assessment is needed to establish this concept. Several pre-clinical models of PDAC are currently available for EMT-studies (494). We should shift the focus from primarily monitoring changes in a few easily observable molecular markers and instead describe EMT and MET as functional alterations in the biological properties of cells. By adopting this perspective, the true role of EMT in animal development and pathological processes can be better understood. Therefore, whenever possible in experiments, the assessment of EMT should involve the consideration of both cellular properties and the use of multiple molecular markers. This comprehensive approach will provide a more accurate and faithful representation of the function of EMT in various biological contexts.

Both hTERT-HPNE and AsPC-1 cells expressed full-length fVII and its active form, fVIIa. However, the expression of fVIIa was higher in AsPC-1 cells compared to hTERT-HPNE cells. This supports the suggestion that cancer cells may acquire the ability to produce fVII as a result of genetic mutations or epigenetic changes that alter the expression of fVII and its regulatory factors. Furthermore, the expression of HNF4 α was higher in AsPC-1 cells compared to hTERT-HPNE cells, suggesting that HNF4 α is one of the transcription factors responsible for promoting the expression of fVII in these cell types. This adds to previous studies that found that ectopic expression of fVII in PC can also be induced by the recruitment of p300/CBP and Sp1 (479). Incubation of hTERT-HPNE cells with TF resulted in an increase in HNF4 α expression, however, had no influence on the AsPC-1 cells. These findings indicate that TF increases the expression of HNF4 α in pancreatic epithelial cells before they become invasive.

Finally, the current study demonstrated that the expression of cyclin D1 (a protein involved in cell cycle regulation), bax (a pro-apoptotic protein), and p16 (a tumour suppressor protein) can be influenced by TF in hTERT-HPNE and AsPC-1 cells. However, the outcomes vary based on the concentration of TF. Incubating hTERT-HPNE or AsPC-1 cells with low TF concentration (0.65 ng/ml) significantly increased cyclin D1 mRNA expression, while higher concentrations (5.2 ng/ml) increased bax mRNA expression. TF exposure increased p16 protein expression in hTERT-HPNE cells but not in malignant cells. These results suggest that TF can modulate the expression of genes/proteins related to cell proliferation and apoptosis in a concentration-dependent manner, with varying effects on benign and malignant cells. Further investigation is needed to explore the effect on cell cycle regulators on long-term exposure to TF.

Co-cultures of cancer cells with CAFs are often used as *in vitro* models of EMT (Figure 85) (495). The spheroid assay, also known as the 3D cell culture assay or tumour spheroid assay, is a widely used technique in cell culture experiments to study cell behaviour and interactions in a more physiologically relevant environment than traditional 2D cell cultures. While the spheroid assay has several advantages, it also has some limitations (496). For example, spheroids are complex structures with cells in different layers and gradients of nutrients and oxygen. The variability in size, shape, and cellular composition among different spheroids can make it challenging to obtain consistent and

Figure 85: Summary of advantages and limitation of currently available pre-clinical models of PDAC (494)



reproducible results. As spheroids grow larger, nutrient and oxygen diffusion becomes limited, leading to gradients of these essential factors within the spheroid. This limitation can affect the viability and functionality of cells in the core of the spheroid, making it difficult to study their behaviour accurately. The outer layer of cells in a spheroid may differ from the inner cells due to differences in nutrient and oxygen availability (497). This can pose challenges when studying drug penetration or evaluating the response of all cells to experimental treatments. Spheroid cultures require specialised techniques, such as hanging-drop cultures, low-adherent plates, or specialised scaffolds, which may involve additional equipment, expertise, and resources compared to traditional 2D cell cultures. Imaging and analysing spheroids can be more challenging than 2D cultures due to the three-dimensional nature of the structures. It may require specialised microscopy techniques or image analysis algorithms to accurately assess spheroid characteristics. Despite these limitations, the spheroid assay remains a valuable tool in cell culture experiments, offering more physiological relevance than 2D cultures and providing insights into cell behaviour, drug efficacy, and tissue development.

A spheroid model was established by co-culturing pancreatic epithelial cells with CAF cells. A 1:3 to 3:1 ratio of cancer cells to CAF cells was used as it was in the range reported to have *in vivo* relevancy, where the ratios of 1:1 to 1:3 have commonly been used (495, 498, 499). The findings in this study suggest that co-culture with CAF cells can enhance the formation of spheroids in pancreatic epithelial cells at a ratio of 1:1. On the other hand, the degree of compactness and intactness was highest at a ratio of 1:3 in malignant cell lines (hTERT-HPNE E6/E7/K-RasG12D/st). Our model of co-culturing cancer cells and CAFs in the form of spheroids could provide a more physiologically relevant model to study the EMT. EMT can be induced in the co-culture spheroids using various approaches. This can include adding specific growth factors, cytokines, or other factors known to induce EMT. Optimise the treatment conditions, such as concentration and duration, based on previous 2D studies or preliminary experiments. EMT-related changes can be monitored or assessed in the co-culture spheroids by analysing the expression of EMT markers, such as epithelial markers (e.g., E-cadherin) and mesenchymal markers (e.g., N-cadherin, vimentin), through techniques like immunofluorescence staining, Western blotting, quantitative PCR or flow cytometry. Additionally, changes in cell morphology, cell migration, invasion, and metastatic potential can be assessed.

Transwell migration and invasion assays can be used to evaluate the migratory and invasive potential of cells within the spheroids by assessing the ability of these cells to migrate or invade through a porous membrane towards chemoattractants or extracellular matrix components. Advanced microscopy techniques like 3D imaging and confocal microscopy can be utilised to visualise the spheroids in three dimensions and assess changes in morphology, cell-cell interactions, and cellular distribution of EMT markers. Confocal microscopy can provide high-resolution images of spheroids, enabling detailed analysis of cellular behaviour and EMT-associated changes. Additionally, it is essential to validate the observed EMT changes using multiple techniques and controls to ensure the robustness of the findings.

Several studies demonstrate the use of spheroid co-culture models involving pancreatic cancer cells and stromal components, such as CAFs, to investigate EMT and its role in pancreatic cancer progression (500-502). Using the spheroid model developed as part of our study, we will further investigate the role of TF on EMT and explore the effect of TF inhibition on EMT.

This study described the influence of TF on EMT and cell cycle regulators. Exogenous TF induced EMT at a concentration of 0.65 ng/ml, which is comparable to the concentration found in the resective precursor lesions (> 0.75 ng/ml). Understanding the mechanisms by which TF influence EMT or regulates the G1/S checkpoint may provide essential knowledge for future investigations of TF-targeted diagnostic tool and therapy.

Chapter 5

General discussion

Pancreatic cancer is the seventh leading cause of cancer death globally in both sexes (503). It accounts for almost as many deaths (466,000) as cases (496,000) because of its poor prognosis. Incidence is highest in Europe, Northern America, and Australia/New Zealand. Due to the increasing prevalence of obesity, diabetes, and alcohol consumption, both incidence and mortality rates have either been stable or have slightly increased. However, improvements in diagnostic and cancer registration practices may also be in play in some countries. It has been projected in a study of 28 European countries that pancreatic cancer will surpass breast cancer as the third leading cause of cancer death by 2025. PDAC is highly aggressive, and surgical intervention is currently the only curative option for early-stage tumours. PDAC is associated with distinct precursor lesions (41), including PanIN, IPMN, and MCN, which may impact disease biology, prognosis, and therapy efficacy. Physicians rely on symptom assessment, imaging techniques, and cytological findings to categorise precursor lesions and predict the risk of progression to invasive disease based on the International Association of Pancreatology (IAP) and the European Study Group on Cystic Tumours of the Pancreas guidelines (46, 427). Despite the increasing identification of incidental cystic radiopathology with advanced imaging, the incidence of lesions associated with invasive carcinoma remains low (~10%). Among histologically confirmed IPMN cases, approximately 30% of resected cases are found to have invasive tumours. Patients with "high-risk stigmata", as defined by the IAP guidelines, have a 5-year risk of PDAC development of approximately 50% (428). Another notable feature of PDAC is its multifocal nature and the appearance of recurrences distant from the resection margin (504, 505).

While surgical removal of precursor lesions is currently the best option for a cure, it can be associated with significant morbidity and mortality (429), and disease recurrence rates range from 1.3% - 8% and 46% - 67% for noninvasive IPMNs and invasive carcinomas associated with IPMN, respectively (506-508). At present, there are no definite criteria besides those of broad morphological features to guide surgical intervention for PCLs or IPMN patients (46, 509). Moreover, there is still uncertainty about the appropriate guidelines for the management of asymptomatic pancreatic cysts (430). Therefore, major unmet needs in the field include a better understanding of the biology of precursor lesions, as well as identifying a reliable indicator for the development of invasive tumours.

In 2006, the initial guidelines for managing IPMN were published as Sendai guidelines (432), which were later updated to the Fukuoka guidelines in 2012 (45) and later again in 2017 (46). These guidelines, also called ICG, categorise IPMNs as MD-IPMN, BD-IPMN, and mixed-type IPMNs based on imaging and histology. The guidelines classify all IPMNs into three categories: low-risk, those with "worrisome features," and those with "high-risk stigmata." Additionally, the American Gastroenterological Association (AGA) guidelines (430) for pancreatic cysts define high-risk lesion characteristics as a size of ≥ 3 cm, a dilated MPD, and mural nodules. The AGA guidelines recommend EUS with a FNA of cyst fluid for further analysis of high-risk lesions, which helps decide whether to observe or resect the lesion. The AGA guidelines have shown improved sensitivity (50%) and accuracy (73.7%) compared to the Fukuoka guidelines but are less specific for managing pancreatic cysts (430). However, despite improved criteria, a significant percentage of patients still undergo pancreatic resection for noninvasive lesions, which may be either benign or have LGD on postoperative pathological examination (up to 77%) (362, 433-436).

The increase in the detection of pancreatic cysts has exerted a significant strain on the healthcare system due to the complexity of pancreatic surgery and the capacity consumption of radiological surveillance. Over the past decade, there has been a sharp rise in the surgical treatment of pancreatic cysts, partly due to incidental detection. During 2014 in the US, about 31% of pancreatic resections were performed to remove cysts, up from just over 10% in 2001 (510). However, this increase has not resulted in a decrease in the number of invasive cancers detected, indicating overdiagnosis and/or overtreatment. The current diagnostic procedures do not accurately distinguish LGD from HGD or invasive cancers, which leads to clinical uncertainty and further contribution to overdiagnosis and overtreatment.

Despite the low probability of benign cysts becoming malignant and the risks associated with pancreatic resection, surgeons and patients often choose to surgically remove cysts even more frequently than suggested by guidelines. Consequently, the overtreatment leads to associated morbidity, mortality, and healthcare costs (431). Therefore, the question arises whether the benefits of treating pancreatic cysts outweigh the harms to the patient.

A recent study reported that both surveillance and surgery for a newly diagnosed incidental pancreatic cyst are costly, with surveillance based on consensus guidelines being the least cost-effective strategy (431). This study suggests that improved specificity would prevent the resection of low-grade cysts and avoid overtreatment and should be a key focus in managing pancreatic cysts. Importantly, the study reported that at 89% specificity, the benefits of avoiding overtreatment outweigh the low risk of missing potential cancers. Therefore, improvements in specificity level should be the target for new diagnostic tests to ameliorate current practice.

A recent systematic review indicates that high-risk individuals attain positive psychological outcomes from participating in PC screening programs (511). However, a later study addressed several potential harms of surveillance, including false positive test results, complications and side effects of diagnostic investigations and overtreatment. Cancer worries appear to be significantly higher during intensified surveillance. This is a further health facet that would benefit from more objective tests to guide clear decision making by identifying and intervening where the risk of malignancy is greatest (512).

In this study, TF/ fVIIa tumour-regulatory signalling molecules were examined under the TEM-PAC study. TF plays a central role in the coagulation cascade and is consistently upregulated in various human malignancies. TF activates several PARs that initiate a diverse array of functions and also influence pathological processes via coagulation-dependent and -independent mechanisms together with other coagulation factors. This study also explored if TF promotes a more invasive phenotype, including EMT, through in vitro experiments with various cell lines. The impact of TF on the regulation of fVII expression and cell proliferation was also examined.

The involvement of the coagulation system in cancer progression was reported has been identified from early to late stages, affecting tumour initiation, growth, and angiogenesis. In addition, different ratios of fVIIa to TF within MV could lead to varying outcomes in cultured primary endothelial cells. Both the concentration of TF with which the cells came into contact and the fVIIa:TF ratio appear to be critical in determining the fate of endothelial cells (section 1.7.5). The presence of TF in the tumour microenvironment may promote the transition from a dormant or latent state of carcinogenesis to a tumorigenic state by modifying the phenotypic functional state and molecular evolution of tumour cells.

Evidence suggests that EMT may be prevalent in pancreatic lesions even before the formation of an identifiable primary tumour (section 4.1.3). Inflammation can promote cancer progression by inducing changes in the microenvironment of the primary site and enhancing cellular invasiveness and dissemination through EMT. TF plays a crucial role in this process by promoting cancer progression through activating signalling pathways and regulating EMT-related gene expression. Studies in breast and lung cancers suggest that metastatic seeding may be mediated by cells that do not meet the standard definition of cancer (483, 484).

In the clinical study of this thesis, the potential of measuring TF and fVIIa levels in the pancreatic cyst fluids as an indicator of the malignant transformation of precursor cystic lesions was explored. The data was compared to the current parameters used during the diagnostic work-up of PCL. PCyF samples were examined from 27 patients with PCLs who underwent EUS and FNA or cyst fluid aspiration during surgical resection. The cohort included patients with various pathological cyst types, such as IPMN, MCN, pseudocyst, serous cyst, IPMN with a solid mass, cyst with a solid mass, and unspecified benign cyst. Patients were divided into two risk groups based on cyst type. The low-risk group had benign cysts and LGD, while the high-risk group had HGD and invasive/malignant cysts. Two-thirds of patients had the non-resective disease, and one-third had resective disease.

The concentration of the TF antigen in PCyF increased with the progression of the four histopathological stages, with a significantly higher concentration found in the resective group than in the non-resective group ($p=0.004$). The mean TF concentration was 1.17 ± 0.22 ng/ml (95% CI 0.68, 1.67) in the resective group and 0.27 ± 0.08 ng/ml (95% CI 0.1, 0.44) in the non-resective group. The TF/TP ratio was also higher in the resective group (3.37 ± 0.67 pg/ μ g) than in the non-resective group (0.8 ± 0.22 pg/ μ g). The fVIIa concentration in the PCyF increased with the progression of histological grade, but the rise was less than that of TF. The fVIIa and TF ratio decreased with histological grade progression. The mean fVIIa:TF ratio was marginally lower in the resective group (84.82 ± 43.8 , 95% CI 0, 185.04) than in the non-resective group (437.46 ± 219.72 , 95% CI 0, 901.02), but this difference was not statistically significant (Figure 45).

The diagnostic ability of TF at a cut-off value of 0.75 ng/ml was significantly high in differentiating between resective and non-resective diseases. The AUC at this cut-off value was 0.877, indicating

high accuracy in distinguishing between the two disease types. On the other hand, the fVIIa concentration (AUC 0.698) and fVIIa:TF ratio (AUC 0.451) had low diagnostic accuracy. TF at a cut-off point of 0.75 ng/ml achieved a 78% sensitivity, 94% specificity, PPV of 88%, negative NPV of 89%, and an accuracy of 89%, indicating that TF is a reliable diagnostic test for any PCL that is at high risk of transforming into invasive malignancy and could meet the criteria set for minimum accuracy.

'High-risk stigmata', if combined (MPD \geq 10 mm and enhancing solid components within cyst), could stratify the resective group, but individually the high-risk features or the 'worrisome features' could not stratify the resective and non-resective group. Although a significant moderate positive correlation was found between resective cysts and radiographic high-risk stigmata, none of the radiographic features on their own had any significant correlation. On the other hand, a TF concentration of \geq 0.75 ng/ml had a significantly strong positive correlation (correlation coefficient 0.745) with resective cysts ($p < 0.001$) and a moderate positive correlation (correlation coefficient 0.514) with radiographic high-risk stigmata ($p = 0.004$) and CEA of ≥ 192 ng/ml (correlation coefficient 0.514, $p = 0.02$) (see Table 31 and Table 32). The odds of diagnosing a resective cyst were significantly high with TF (OR 59.5, 95% CI 4.6, 767.2, $p = 0.002$) (Table 33).

The in vitro work of this thesis investigated how TF and fVIIa alter vimentin expression, a mesenchymal marker of EMT, in various cell lines. The results showed that TF and fVIIa have differential effects on vimentin expression. In hTERT-HPNE (benign) cells, treatment with TF led to an increase in vimentin expression, while treatment with fVIIa led to a decrease in vimentin expression. The addition of fVIIa to TF moderated vimentin expression. In benign cells, the effects of TF on vimentin expression appear to be concentration-dependent, with a concentration of 0.65 ng/ml inducing EMT. In contrast, not unexpectedly, as they are already transformed, vimentin expression was not dependent on TF concentration in malignant cells. TF may also regulate the expression of HNF4 α , a transcription factor involved in the expression of fVII, in pancreatic epithelial cells. Additionally, cancer cells may acquire the ability to produce fVIIa through increased expression of HNF4 α . Prior work from our lab laboratory had shown that there is a shift from pro-apoptotic to proliferative properties in endothelial cells when the molar ratio of fVIIa to TF reaches approximately 15:1. It is plausible that frequent exposure to high levels of TF, coupled with depleted reserves of fVII

(resulting in a low fVIIa:TF ratio), may prompt cellular apoptosis. This, in turn, could trigger the signals necessary to induce EMT in pre-malignant cells, thereby facilitating their ability to leave the hostile tumour microenvironment and metastasise to a more favourable environment. Furthermore, it was found that TF can influence the expression of genes related to cell proliferation and apoptosis in a concentration-dependent way. Low concentrations (0.65 ng/ml) of TF increased cyclin D1 mRNA expression, while high concentrations (5.2 ng/ml) increased bax mRNA expression in hTERT-HPNE or AsPC-1 cells. The finding in the in-vitro study suggests that a concentration of 0.65 ng/ml of exogenous TF could induce EMT. This is comparable to the cut-off value of TF concentration found in the clinical study, which identified resective precursor lesions. Further investigations are needed to explore the long-term effects of TF exposure on EMT and cell cycle regulators.

Pancreatic cancer is challenging as it has usually metastasised by the time it is diagnosed. Therefore, early diagnosis and treatment are critical for reducing pancreatic cancer-related deaths. To achieve early detection and treatment of pancreatic neoplasms, several challenges need to be addressed. First, it is essential to identify curable lesions such as HGD that can lead to advanced and incurable pancreatic cancers. Second, the progression from localised curable lesions to advanced cancers must be at a phase where reasonable opportunity exists to detect potentially curable localised lesions that have not metastasised or advanced to a point where surgical removal fails to produce a curative outcome due to early involvement of other tissues despite macroscopic (including PET CT) evidence. Thirdly, a method must be established to differentiate localised lesions with a reasonable risk of progressing to advanced cancer from those with little or no risk of progression, i.e. HGD and LGD. Given the complexities of treating pancreatic lesions, it is crucial to distinguish between the two types of lesions to avoid unnecessary treatments.

As the cyst-associated TF levels appear to correlate with cytological progression to the malignant phenotype and may allow better discrimination of the 'resective' cystic lesion, TF should be considered for further research in larger prospective studies to confirm its potential as a diagnostic marker for pancreatic cancer. In addition, incorporating TF into the standard PCyF markers of malignancy or creating a prediction model with multiple PCyF markers and radiographic high-risk stigmata could potentially enhance the diagnostic precision of current malignancy predictors. Further

research is required to understand the mechanism behind how TF triggers EMT. To investigate this, multiple EMT markers and the co-culture model could be used to examine the effects of TF on cells. Understanding how TF promotes EMT could also provide a basis for developing new therapeutic interventions to inhibit its activity, potentially slowing or halting pancreatic cancer progression. It is also important to explore the potential role of HNF4 α dysregulation in the development of EMT and whether it could be a target for intervention. By pursuing these lines of research, we may better understand the underlying mechanisms of pancreatic cancer and develop more effective treatments for this aggressive disease.

The next steps following the current study are to verify the role of TF in the biological process of EMT, as discussed in the previous chapters. This confirmation will provide a deeper understanding of TF's involvement in cellular transformations and its potential implications in various biological contexts and pathological events. Furthermore, the study has expanded its scope to employ a multi-omics approach in examining cystic lesions. This broader approach incorporates multiple omics disciplines, such as genomics, proteomics, and metabolomics, to gain a comprehensive understanding of the molecular mechanisms underlying cystic lesions. By utilising a multi-omics approach, researchers can explore various molecular aspects simultaneously, providing a more comprehensive and integrated view of the complex nature of cystic lesions. This expansion allows for a deeper exploration of the underlying molecular pathways and potential biomarkers associated with these lesions, paving the way for more targeted and personalised diagnostic and therapeutic strategies in the future.

In conclusion, TF has a pivotal role in the inflammatory microenvironment of PDAC, and our work suggests a driver of the phenotypic malignant state through EMT transformation. Clinically as a stand-alone marker in PCyF, it demonstrated in this study the kind of high specificity (94%) that would meet the criteria to potentially improve the ability to identify the malignant potential of PCLs before surgery and provide a more reliable method for classifying ambiguous cystic lesions, leading to substantial improvements in healthcare costs. The work in this thesis suggests that this is a reasonable marker to be included in further research within the context of a larger prospective study to confirm this potential.

References

1. Blackford AL, Canto MI, Klein AP, Hruban RH, Goggins M. Recent Trends in the Incidence and Survival of Stage 1A Pancreatic Cancer: A Surveillance, Epidemiology, and End Results Analysis. *JNCI: Journal of the National Cancer Institute*. 2020;112(11):1162-9.
2. Hur C, Tramontano AC, Dowling EC, Brooks GA, Jeon A, Brugge WR, et al. Early Pancreatic Ductal Adenocarcinoma Survival Is Dependent on Size: Positive Implications for Future Targeted Screening. *Pancreas*. 2016;45(7):1062-6.
3. Greten FR, Grivennikov SI. Inflammation and Cancer: Triggers, Mechanisms, and Consequences. *Immunity*. 2019;51(1):27-41.
4. van den Berg YW, Osanto S, Reitsma PH, Versteeg HH. The relationship between tissue factor and cancer progression: insights from bench and bedside. *Blood*. 2012;119(4):924-32.
5. Khorana AA, Ahrendt SA, Ryan CK, Francis CW, Hruban RH, Hu YC, et al. Tissue factor expression, angiogenesis, and thrombosis in pancreatic cancer. *Clin Cancer Res*. 2007;13(10):2870-5.
6. Nitori N, Ino Y, Nakanishi Y, Yamada T, Honda K, Yanagihara K, et al. Prognostic Significance of Tissue Factor in Pancreatic Ductal Adenocarcinoma. *Clinical Cancer Research*. 2005;11(7):2531.
7. Kobayashi S, Koizume S, Takahashi T, Ueno M, Oishi R, Nagashima S, et al. Tissue factor and its procoagulant activity on cancer-associated thromboembolism in pancreatic cancer. *Cancer Science*. 2021;112(11):4679-91.
8. Saghazadeh A, Hafizi S, Rezaei N. Inflammation in venous thromboembolism: Cause or consequence? *International Immunopharmacology*. 2015;28(1):655-65.
9. Meissner MH, Wakefield TW, Ascher E, Caprini JA, Comerota AJ, Eklof B, et al. Acute venous disease: venous thrombosis and venous trauma. *Journal of vascular surgery*. 2007;46(6):S25-S53.
10. Kroegel C, Reissig A. Principle mechanisms underlying venous thromboembolism: Epidemiology, risk factors, pathophysiology and pathogenesis. *Respiration*. 2003;70(1):7-30.
11. Cheng KB, Wang LM, Gao HJ, Hu Y. An study on screening the gene clusters associated with pulmonary embolism-deep venous thrombosis by oligo microarray. *National Medical Journal of China*. 2007;87(34):2420-2.
12. Bernard J, Yi ES. Pulmonary thromboendarterectomy: a clinicopathologic study of 200 consecutive pulmonary thromboendarterectomy cases in one institution. *Human Pathology*. 2007;38(6):871-7.
13. Unruh D, Horbinski C. Beyond thrombosis: the impact of tissue factor signaling in cancer. *Journal of Hematology & Oncology*. 2020;13(1):93.
14. Ünlü B, Versteeg HH. Effects of tumor-expressed coagulation factors on cancer progression and venous thrombosis: is there a key factor? *Thrombosis Research*. 2014;133:S76-S84.
15. Pancreatic cancer some key facts: Pancreatic cancer UK; [Available from: <https://www.pancreaticcancer.org.uk/wp-content/uploads/2020/10/mp-pancreatic-cancer-briefing-notes.pdf>].
16. Cancer research UK. Pancreatic cancer incidence statistics 2017, July 27 [Available from: https://www.cancerresearchuk.org/health-professional/cancer-statistics/statistics-by-cancer-type/pancreatic-cancer/incidence?_gl=1*_wMrdq*_gcl_dc*RONMLjE1Nzk5NTY00TAuQ0t1OV84bmtudWNRIVXa0]

[d3b2QybDBDclE.& ga=2.256426251.1201499333.1579956491-1042581081.1579956491#heading-Seven](https://www.cancerresearchuk.org/health-professional/cancer-statistics/statistics-by-cancer-type/pancreatic-cancer/survival? gl=1*1fpryqp* gcl dc*R0NMLjE1Nzk5NTY00TAuQ0t1OV84bmtudWNDRIVXa0d3b2QybDBDclE.& ga=2.256426251.1201499333.1579956491-1042581081.1579956491#heading-Seven).

17. UK CR. Pancreatic cancer survival statistics 2020, Apr 2 [Available from: https://www.cancerresearchuk.org/health-professional/cancer-statistics/statistics-by-cancer-type/pancreatic-cancer/survival? gl=1*1fpryqp* gcl dc*R0NMLjE1Nzk5NTY00TAuQ0t1OV84bmtudWNDRIVXa0d3b2QybDBDclE.& ga=2.101410049.1201499333.1579956491-1042581081.1579956491#heading-Zero].
18. Allen PJ, Kuk D, Castillo CF-D, Basturk O, Wolfgang CL, Cameron JL, et al. Multi-institutional Validation Study of the American Joint Commission on Cancer (8th Edition) Changes for T and N Staging in Patients With Pancreatic Adenocarcinoma. *Annals of surgery*. 2017;265(1):185-91.
19. Lynch SM, Vrieling A, Lubin JH, Kraft P, Mendelsohn JB, Hartge P, et al. Cigarette Smoking and Pancreatic Cancer: A Pooled Analysis From the Pancreatic Cancer Cohort Consortium. *American Journal of Epidemiology*. 2009;170(4):403-13.
20. Farrow DC, Davis S. Risk of pancreatic cancer in relation to medical history and the use of tobacco, alcohol and coffee. *International Journal of Cancer*. 1990;45(5):816-20.
21. Michaud DS, Giovannucci E, Willett WC, Colditz GA, Stampfer MJ, Fuchs CS. Physical Activity, Obesity, Height, and the Risk of Pancreatic Cancer. *JAMA*. 2001;286(8):921-9.
22. Maisonneuve P, Lowenfels AB. Risk factors for pancreatic cancer: a summary review of meta-analytical studies. *International Journal of Epidemiology*. 2014;44(1):186-98.
23. Meng C, Bai C, Brown TD, Hood LE, Tian Q. Human Gut Microbiota and Gastrointestinal Cancer. *Genomics, Proteomics & Bioinformatics*. 2018;16(1):33-49.
24. Batabyal P, Vander Hoorn S, Christophi C, Nikfarjam M. Association of Diabetes Mellitus and Pancreatic Adenocarcinoma: A Meta-Analysis of 88 Studies. *Annals of Surgical Oncology*. 2014;21(7):2453-62.
25. Olson SH, Kurtz RC. Epidemiology of pancreatic cancer and the role of family history. *Journal of Surgical Oncology*. 2013;107(1):1-7.
26. Wolpin BM, Chan AT, Hartge P, Chanock SJ, Kraft P, Hunter DJ, et al. ABO Blood Group and the Risk of Pancreatic Cancer. *JNCI: Journal of the National Cancer Institute*. 2009;101(6):424-31.
27. Yamada A, Komaki Y, Komaki F, Micic D, Zullo S, Sakuraba A. Risk of gastrointestinal cancers in patients with cystic fibrosis: a systematic review and meta-analysis. *The Lancet Oncology*. 2018;19(6):758-67.
28. Lowenfels AB, Maisonneuve P, Cavallini G, Ammann RW, Lankisch PG, Andersen JR, et al. Pancreatitis and the Risk of Pancreatic Cancer. *New England Journal of Medicine*. 1993;328(20):1433-7.
29. Duell EJ, Lucenteforte E, Olson SH, Bracci PM, Li D, Risch HA, et al. Pancreatitis and pancreatic cancer risk: a pooled analysis in the International Pancreatic Cancer Case-Control Consortium (PanC4). *Annals of Oncology*. 2012;23(11):2964-70.
30. Pergolini I, Sahara K, Ferrone CR, Morales-Oyarvide V, Wolpin BM, Mucci LA, et al. Long-term Risk of Pancreatic Malignancy in Patients With Branch Duct Intraductal Papillary Mucinous Neoplasm in a Referral Center. *Gastroenterology*. 2017;153(5):1284-94.e1.
31. Klimstra DS. Noductal neoplasms of the pancreas. *Modern Pathology*. 2007;20(1):S94-S112.

32. Allen PJ, Kuk D, Castillo CF-d, Basturk O, Wolfgang CL, Cameron JL, et al. Multi-institutional Validation Study of the American Joint Commission on Cancer (8th Edition) Changes for T and N Staging in Patients With Pancreatic Adenocarcinoma. *Annals of Surgery*. 2017;265(1).
33. Basturk O EI, Fukushima N, et al. WHO Classification of Tumours, Digestive System Tumours. 5th ed: International Agency for Research on Cancer, Lyon; 2019.
34. Hruban RH PM, Klimstra DS. Atlas of tumor pathology. 6th ed. Washington, DC 2007: Armed Forces Institute of Pathology; 2007.
35. Kamarajah SK, Burns WR, Frankel TL, Cho CS, Nathan H. Validation of the American Joint Commission on Cancer (AJCC) 8th Edition Staging System for Patients with Pancreatic Adenocarcinoma: A Surveillance, Epidemiology and End Results (SEER) Analysis. *Annals of Surgical Oncology*. 2017;24(7):2023-30.
36. Haeberle L, Esposito I. Pathology of pancreatic cancer. *Transl Gastroenterol Hepatol*. 2019;4:50.
37. Cystic-carcinoma-pancreas: Wikimedia commons; 2007 [Available from: https://commons.wikimedia.org/wiki/File:MBq_cystic-carcinoma-pancreas.jpg].
38. Longnecker DS. Histology of pancreatic ductal adenocarcinoma: UpToDate; [Available from: https://www.uptodate.com/contents/pathology-of-exocrine-pancreatic-neoplasms?search=pancreatic%20cancer&topicRef=2501&source=see_link#H17].
39. Maitra A, Adsay NV, Argani P, Iacobuzio-Donahue C, De Marzo A, Cameron JL, et al. Multicomponent Analysis of the Pancreatic Adenocarcinoma Progression Model Using a Pancreatic Intraepithelial Neoplasia Tissue Microarray. *Modern Pathology*. 2003;16(9):902-12.
40. Overbeek KA, Cahen DL, Canto MI, Bruno MJ. Surveillance for neoplasia in the pancreas. *Best Pract Res Clin Gastroenterol*. 2016;30(6):971-86.
41. Matthaei H, Schulick RD, Hruban RH, Maitra A. Cystic precursors to invasive pancreatic cancer. *Nat Rev Gastroenterol Hepatol*. 2011;8(3):141-50.
42. Singhi AD, Koay EJ, Chari ST, Maitra A. Early Detection of Pancreatic Cancer: Opportunities and Challenges. *Gastroenterology*. 2019;156(7):2024-40.
43. Shi C, Hruban RH. Intraductal papillary mucinous neoplasm. *Hum Pathol*. 2012;43(1):1-16.
44. Tanaka M. Intraductal Papillary Mucinous Neoplasm of the Pancreas as the Main Focus for Early Detection of Pancreatic Adenocarcinoma. *Pancreas*. 2018;47(5):544-50.
45. Tanaka M, Fernández-del Castillo C, Adsay V, Chari S, Falconi M, Jang JY, et al. International consensus guidelines 2012 for the management of IPMN and MCN of the pancreas. *Pancreatology*. 2012;12(3):183-97.
46. Tanaka M, Fernández-del Castillo C, Kamisawa T, Jang JY, Levy P, Ohtsuka T, et al. Revisions of international consensus Fukuoka guidelines for the management of IPMN of the pancreas. *Pancreatology*. 2017;17(5):738-53.
47. Kimura W, Moriya T, Hirai I, Hanada K, Abe H, Yanagisawa A, et al. Multicenter study of serous cystic neoplasm of the Japan pancreas society. *Pancreas*. 2012;41(3):380-7.
48. Raval JS, Zeh HJ, Moser AJ, Lee KK, Sanders MK, Navina S, et al. Pancreatic lymphoepithelial cysts express CEA and can contain mucous cells: potential pitfalls in the preoperative diagnosis. *Mod Pathol*. 2010;23(11):1467-76.

49. Berman JJ, Albores-Saavedra J, Bostwick D, DeLellis R, Eble J, Hamilton SR, et al. Precancer: A conceptual working definition: Results of a Consensus Conference. *Cancer Detection and Prevention*. 2006;30(5):387-94.
50. Tada M, Kawabe T, Arizumi M, Togawa O, Matsubara S, Yamamoto N, et al. Pancreatic Cancer in Patients With Pancreatic Cystic Lesions: A Prospective Study in 197 Patients. *Clinical Gastroenterology and Hepatology*. 2006;4(10):1265-70.
51. Hustinx SR, Leoni LM, Yeo CJ, Brown PN, Goggins M, Kern SE, et al. Concordant loss of MTAP and p16/CDKN2A expression in pancreatic intraepithelial neoplasia: evidence of homozygous deletion in a noninvasive precursor lesion. *Modern Pathology*. 2005;18(7):959-63.
52. Moskaluk CA, Hruban RH, Kern SE. p16 and K-ras Gene Mutations in the Intraductal Precursors of Human Pancreatic Adenocarcinoma. *Cancer Research*. 1997;57(11):2140-3.
53. Hruban RH, Maitra A, Kern SE, Goggins M. Precursors to Pancreatic Cancer. *Gastroenterology Clinics of North America*. 2007;36(4):831-49.
54. Belyaev O, Seelig MH, Muller CA, Tannapfel A, Schmidt WE, Uhl W. Intraductal papillary mucinous neoplasms of the pancreas. *J Clin Gastroenterol*. 2008;42(3):284-94.
55. Bassi C, Sarr MG, Lillemoe KD, Reber HA. Natural history of intraductal papillary mucinous neoplasms (IPMN): current evidence and implications for management. *J Gastrointest Surg*. 2008;12(4):645-50.
56. Tanaka M, Kobayashi K, Mizumoto K, Yamaguchi K. Clinical aspects of intraductal papillary mucinous neoplasm of the pancreas. *J Gastroenterol*. 2005;40(7):669-75.
57. Schmidt CM, White PB, Waters JA, Yiannoutsos CT, Cummings OW, Baker M, et al. Intraductal papillary mucinous neoplasms: predictors of malignant and invasive pathology. *Ann Surg*. 2007;246(4):644-51; discussion 51-4.
58. Furukawa T, Klöppel G, Volkan Adsay N, Albores-Saavedra J, Fukushima N, Horii A, et al. Classification of types of intraductal papillary-mucinous neoplasm of the pancreas: a consensus study. *Virchows Arch*. 2005;447(5):794-9.
59. Yonezawa S, Nakamura A, Horinouchi M, Sato E. The expression of several types of mucin is related to the biological behavior of pancreatic neoplasms. *J Hepatobiliary Pancreat Surg*. 2002;9(3):328-41.
60. Moriya T, Kimura W, Semba S, Sakurai F, Hirai I, Ma J, et al. Biological similarities and differences between pancreatic intraepithelial neoplasias and intraductal papillary mucinous neoplasms. *Int J Gastrointest Cancer*. 2005;35(2):111-9.
61. Adsay NV, Merati K, Nassar H, Shia J, Sarkar F, Pierson CR, et al. Pathogenesis of colloid (pure mucinous) carcinoma of exocrine organs: Coupling of gel-forming mucin (MUC2) production with altered cell polarity and abnormal cell-stroma interaction may be the key factor in the morphogenesis and indolent behavior of colloid carcinoma in the breast and pancreas. *Am J Surg Pathol*. 2003;27(5):571-8.
62. Adsay NV, Merati K, Basturk O, Iacobuzio-Donahue C, Levi E, Cheng JD, et al. Pathologically and biologically distinct types of epithelium in intraductal papillary mucinous neoplasms: delineation of an "intestinal" pathway of carcinogenesis in the pancreas. *Am J Surg Pathol*. 2004;28(7):839-48.
63. Biankin AV, Kench JG, Biankin SA, Lee C-S, Morey AL, Dijkman FP, et al. Pancreatic Intraepithelial Neoplasia in Association With Intraductal Papillary Mucinous Neoplasms of the

Pancreas: Implications for Disease Progression and Recurrence. *Am J Surg Pathol*. 2004;28(9):1184-92.

64. McGrath K, Khalid A. Classification of pancreatic cysts, Graphics: UpToDate, Inc. and/or its affiliates; [updated 2023. Available from: https://www.uptodate.com/contents/classification-of-pancreatic-cysts?search=pancreatic%20cyst&source=search_result&selectedTitle=1~100&usage_type=default&display_rank=1.

65. Bernard P, Scoazec J-Y, Joubert M, Kahn X, Le Borgne J, Berger F, et al. Intraductal Papillary-Mucinous Tumors of the Pancreas: Predictive Criteria of Malignancy According to Pathological Examination of 53 Cases. *Archives of Surgery*. 2002;137(11):1274-8.

66. Adsay NV, Pierson C, Sarkar F, Abrams J, Weaver D, Conlon KC, et al. Colloid (mucinous noncystic) carcinoma of the pancreas. *Am J Surg Pathol*. 2001;25(1):26-42.

67. Crippa S, Fernández-Del Castillo C, Salvia R, Finkelstein D, Bassi C, Domínguez I, et al. Mucin-producing neoplasms of the pancreas: an analysis of distinguishing clinical and epidemiologic characteristics. *Clin Gastroenterol Hepatol*. 2010;8(2):213-9.

68. Cubilla AL, Fitzgerald PJ. Morphological lesions associated with human primary invasive nonendocrine pancreas cancer. *Cancer Res*. 1976;36(7 pt 2):2690-8.

69. Fernández-del Castillo C. Mucinous cystic neoplasms. *J Gastrointest Surg*. 2008;12(3):411-3.

70. Wilentz RE, Albores-Saavedra J, Hruban RH. Mucinous cystic neoplasms of the pancreas. *Semin Diagn Pathol*. 2000;17(1):31-42.

71. Wilentz RE, Albores-Saavedra J, Zahurak M, Talamini MA, Yeo CJ, Cameron JL, et al. Pathologic examination accurately predicts prognosis in mucinous cystic neoplasms of the pancreas. *Am J Surg Pathol*. 1999;23(11):1320-7.

72. Crippa S, Salvia R, Warshaw AL, Domínguez I, Bassi C, Falconi M, et al. Mucinous cystic neoplasm of the pancreas is not an aggressive entity: lessons from 163 resected patients. *Ann Surg*. 2008;247(4):571-9.

73. Basturk O, Hong SM, Wood LD, Adsay NV, Albores-Saavedra J, Biankin AV, et al. A Revised Classification System and Recommendations From the Baltimore Consensus Meeting for Neoplastic Precursor Lesions in the Pancreas. *Am J Surg Pathol*. 2015;39(12):1730-41.

74. McDonald OG. The biology of pancreatic cancer morphology. *Pathology*. 2022;54(2):236-47.

75. Connor AA, Gallinger S. Pancreatic cancer evolution and heterogeneity: integrating omics and clinical data. *Nature Reviews Cancer*. 2021.

76. Reiter JG, Iacobuzio-Donahue CA. Pancreatic carcinogenesis — several small steps or one giant leap? *Nature Reviews Gastroenterology & Hepatology*. 2017;14(1):7-8.

77. Notta F, Chan-Seng-Yue M, Lemire M, Li Y, Wilson GW, Connor AA, et al. A renewed model of pancreatic cancer evolution based on genomic rearrangement patterns. *Nature*. 2016;538(7625):378-82.

78. Bhalla S, Melnekoff DT, Aleman A, Leshchenko V, Restrepo P, Keats J, et al. Patient similarity network of newly diagnosed multiple myeloma identifies patient subgroups with distinct genetic features and clinical implications. *Science Advances*. 2021;7(47):eabg9551.

79. Izeradjene K, Combs C, Best M, Gopinathan A, Wagner A, Grady WM, et al.

Kras^{G12D} and *Smad4/Dpc4* Haploinsufficiency Cooperate to

Induce Mucinous Cystic Neoplasms and Invasive Adenocarcinoma of the Pancreas. *Cancer Cell*. 2007;11(3):229-43.

80. Hingorani SR, Wang L, Multani AS, Combs C, Deramaudt TB, Hruban RH, et al. *Trp53^{R172H}* and *Kras^{G12D}* cooperate to promote chromosomal instability and widely metastatic pancreatic ductal adenocarcinoma in mice. *Cancer Cell*. 2005;7(5):469-83.
81. Jones Sn, Zhang X, Parsons DW, Lin JC-H, Leary RJ, Angenendt P, et al. Core Signaling Pathways in Human Pancreatic Cancers Revealed by Global Genomic Analyses. *Science*. 2008;321(5897):1801-6.
82. Biankin AV, Waddell N, Kassahn KS, Gingras M-C, Muthuswamy LB, Johns AL, et al. Pancreatic cancer genomes reveal aberrations in axon guidance pathway genes. *Nature*. 2012;491(7424):399-405.
83. Haeno H, Gonen M, Davis Meghan B, Herman Joseph M, Iacobuzio-Donahue Christine A, Michor F. Computational Modeling of Pancreatic Cancer Reveals Kinetics of Metastasis Suggesting Optimum Treatment Strategies. *Cell*. 2012;148(1):362-75.
84. Yachida S, Jones S, Bozic I, Antal T, Leary R, Fu B, et al. Distant metastasis occurs late during the genetic evolution of pancreatic cancer. *Nature*. 2010;467(7319):1114-7.
85. Hruban RH, van Mansfeld AD, Offerhaus GJ, van Weering DH, Allison DC, Goodman SN, et al. K-ras oncogene activation in adenocarcinoma of the human pancreas. A study of 82 carcinomas using a combination of mutant-enriched polymerase chain reaction analysis and allele-specific oligonucleotide hybridization. *Am J Pathol*. 1993;143(2):545-54.
86. Hruban RH, Goggins M, Parsons J, Kern SE. Progression Model for Pancreatic Cancer. *Clinical Cancer Research*. 2000;6(8):2969.
87. Ying H, Dey P, Yao W, Kimmelman AC, Draetta GF, Maitra A, et al. Genetics and biology of pancreatic ductal adenocarcinoma. *Genes Dev*. 2016;30(4):355-85.
88. Ideno N, Yamaguchi H, Ghosh B, Gupta S, Okumura T, Steffen DJ, et al. GNAS(R201C) Induces Pancreatic Cystic Neoplasms in Mice That Express Activated KRAS by Inhibiting YAP1 Signaling. *Gastroenterology*. 2018;155(5):1593-607.e12.
89. Noë M, Niknafs N, Fischer CG, Hackeng WM, Beleva Guthrie V, Hosoda W, et al. Genomic characterization of malignant progression in neoplastic pancreatic cysts. *Nat Commun*. 2020;11(1):4085.
90. Patra KC, Bardeesy N, Mizukami Y. Diversity of Precursor Lesions For Pancreatic Cancer: The Genetics and Biology of Intraductal Papillary Mucinous Neoplasm. *Clin Transl Gastroenterol*. 2017;8(4):e86.
91. Alonso-Curbelo D, Ho YJ, Burdziak C, Maag JLV, Morris JPt, Chandwani R, et al. A gene-environment-induced epigenetic program initiates tumorigenesis. *Nature*. 2021;590(7847):642-8.
92. Schutte M, Hruban RH, Geradts J, Maynard R, Hilgers W, Rabindran SK, et al. Abrogation of the Rb/p16 tumor-suppressive pathway in virtually all pancreatic carcinomas. *Cancer Res*. 1997;57(15):3126-30.
93. Caldas C, Hahn SA, da Costa LT, Redston MS, Schutte M, Seymour AB, et al. Frequent somatic mutations and homozygous deletions of the p16 (MTS1) gene in pancreatic adenocarcinoma. *Nat Genet*. 1994;8(1):27-32.

94. Redston MS, Caldas C, Seymour AB, Hruban RH, da Costa L, Yeo CJ, et al. p53 mutations in pancreatic carcinoma and evidence of common involvement of homocopolymer tracts in DNA microdeletions. *Cancer Res.* 1994;54(11):3025-33.
95. Hahn SA, Schutte M, Hoque AT, Moskaluk CA, da Costa LT, Rozenblum E, et al. DPC4, a candidate tumor suppressor gene at human chromosome 18q21.1. *Science.* 1996;271(5247):350-3.
96. David CJ, Huang YH, Chen M, Su J, Zou Y, Bardeesy N, et al. TGF- β Tumor Suppression through a Lethal EMT. *Cell.* 2016;164(5):1015-30.
97. Huang YH, Hu J, Chen F, Lecomte N, Basnet H, David CJ, et al. ID1 Mediates Escape from TGF β Tumor Suppression in Pancreatic Cancer. *Cancer Discov.* 2020;10(1):142-57.
98. Omary MB, Lugea A, Lowe AW, Pandol SJ. The pancreatic stellate cell: a star on the rise in pancreatic diseases. *J Clin Invest.* 2007;117(1):50-9.
99. Biffi G, Oni TE, Spielman B, Hao Y, Elyada E, Park Y, et al. IL1-Induced JAK/STAT Signaling Is Antagonized by TGF β to Shape CAF Heterogeneity in Pancreatic Ductal Adenocarcinoma. *Cancer Discov.* 2019;9(2):282-301.
100. Mathew E, Collins MA, Fernandez-Barrena MG, Holtz AM, Yan W, Hogan JO, et al. The transcription factor GLI1 modulates the inflammatory response during pancreatic tissue remodeling. *J Biol Chem.* 2014;289(40):27727-43.
101. Bayne LJ, Beatty GL, Jhala N, Clark CE, Rhim AD, Stanger BZ, et al. Tumor-derived granulocyte-macrophage colony-stimulating factor regulates myeloid inflammation and T cell immunity in pancreatic cancer. *Cancer Cell.* 2012;21(6):822-35.
102. Ischenko I, D'Amico S, Rao M, Li J, Hayman MJ, Powers S, et al. KRAS drives immune evasion in a genetic model of pancreatic cancer. *Nature Communications.* 2021;12(1):1482.
103. Pylayeva-Gupta Y, Lee KE, Hajdu CH, Miller G, Bar-Sagi D. Oncogenic Kras-induced GM-CSF production promotes the development of pancreatic neoplasia. *Cancer Cell.* 2012;21(6):836-47.
104. Laklai H, Miroshnikova YA, Pickup MW, Collisson EA, Kim GE, Barrett AS, et al. Genotype tunes pancreatic ductal adenocarcinoma tissue tension to induce matricellular fibrosis and tumor progression. *Nat Med.* 2016;22(5):497-505.
105. Yamamoto K, Venida A, Yano J, Biancur DE, Kakiuchi M, Gupta S, et al. Autophagy promotes immune evasion of pancreatic cancer by degrading MHC-I. *Nature.* 2020;581(7806):100-5.
106. Freed-Pastor WA, Lambert LJ, Ely ZA, Pattada NB, Bhutkar A, Eng G, et al. The CD155/TIGIT axis promotes and maintains immune evasion in neoantigen-expressing pancreatic cancer. *Cancer Cell.* 2021;39(10):1342-60.e14.
107. Medzhitov R. Origin and physiological roles of inflammation. *Nature.* 2008;454(7203):428-35.
108. Koebel CM, Vermi W, Swann JB, Zerafa N, Rodig SJ, Old LJ, et al. Adaptive immunity maintains occult cancer in an equilibrium state. *Nature.* 2007;450(7171):903-7.
109. Rosenthal R, Cadieux EL, Salgado R, Bakir MA, Moore DA, Hiley CT, et al. Neoantigen-directed immune escape in lung cancer evolution. *Nature.* 2019;567(7749):479-85.
110. McGranahan N, Swanton C. Cancer Evolution Constrained by the Immune Microenvironment. *Cell.* 2017;170(5):825-7.
111. Grivennikov SI, Greten FR, Karin M. Immunity, inflammation, and cancer. *Cell.* 2010;140(6):883-99.

112. Grivennikov SI, Wang K, Mucida D, Stewart CA, Schnabl B, Jauch D, et al. Adenoma-linked barrier defects and microbial products drive IL-23/IL-17-mediated tumour growth. *Nature*. 2012;491(7423):254-8.
113. Komarova EA, Krivokrysenko V, Wang K, Neznanov N, Chernov MV, Komarov PG, et al. p53 is a suppressor of inflammatory response in mice. *Faseb j*. 2005;19(8):1030-2.
114. Andriani GA, Almeida VP, Faggioli F, Mauro M, Tsai WL, Santambrogio L, et al. Whole Chromosome Instability induces senescence and promotes SASP. *Sci Rep*. 2016;6:35218.
115. Davalos AR, Coppe JP, Campisi J, Desprez PY. Senescent cells as a source of inflammatory factors for tumor progression. *Cancer Metastasis Rev*. 2010;29(2):273-83.
116. Woo SR, Corrales L, Gajewski TF. Innate immune recognition of cancer. *Annu Rev Immunol*. 2015;33:445-74.
117. McAllister F, Bailey JM, Alsina J, Nirschl CJ, Sharma R, Fan H, et al. Oncogenic Kras activates a hematopoietic-to-epithelial IL-17 signaling axis in preinvasive pancreatic neoplasia. *Cancer Cell*. 2014;25(5):621-37.
118. Kuraishy A, Karin M, Grivennikov SI. Tumor promotion via injury- and death-induced inflammation. *Immunity*. 2011;35(4):467-77.
119. Canli Ö, Nicolas AM, Gupta J, Finkelmeier F, Goncharova O, Pesic M, et al. Myeloid Cell-Derived Reactive Oxygen Species Induce Epithelial Mutagenesis. *Cancer Cell*. 2017;32(6):869-83.e5.
120. Gronke K, Hernández PP, Zimmermann J, Klose CSN, Kofoed-Branzk M, Guendel F, et al. Interleukin-22 protects intestinal stem cells against genotoxic stress. *Nature*. 2019;566(7743):249-53.
121. Dmitrieva-Posocco O, Dzutsev A, Posocco DF, Hou V, Yuan W, Thovarai V, et al. Cell-Type-Specific Responses to Interleukin-1 Control Microbial Invasion and Tumor-Elicited Inflammation in Colorectal Cancer. *Immunity*. 2019;50(1):166-80.e7.
122. Grivennikov S, Karin E, Terzic J, Mucida D, Yu GY, Vallabhapurapu S, et al. IL-6 and Stat3 are required for survival of intestinal epithelial cells and development of colitis-associated cancer. *Cancer Cell*. 2009;15(2):103-13.
123. Ziegler PK, Bollrath J, Pallangyo CK, Matsutani T, Canli Ö, De Oliveira T, et al. Mitophagy in Intestinal Epithelial Cells Triggers Adaptive Immunity during Tumorigenesis. *Cell*. 2018;174(1):88-101.e16.
124. Greten FR, Eckmann L, Greten TF, Park JM, Li ZW, Egan LJ, et al. IKKbeta links inflammation and tumorigenesis in a mouse model of colitis-associated cancer. *Cell*. 2004;118(3):285-96.
125. Panigrahy D, Gartung A, Yang J, Yang H, Gilligan MM, Sulciner ML, et al. Preoperative stimulation of resolution and inflammation blockade eradicates micrometastases. *J Clin Invest*. 2019;129(7):2964-79.
126. Varga J, Greten FR. Cell plasticity in epithelial homeostasis and tumorigenesis. *Nat Cell Biol*. 2017;19(10):1133-41.
127. de Sousa e Melo F, Kurtova AV, Harnoss JM, Kljavin N, Hoeck JD, Hung J, et al. A distinct role for Lgr5(+) stem cells in primary and metastatic colon cancer. *Nature*. 2017;543(7647):676-80.
128. Francart ME, Lambert J, Vanwynsberghe AM, Thompson EW, Bourcy M, Polette M, et al. Epithelial-mesenchymal plasticity and circulating tumor cells: Travel companions to metastases. *Dev Dyn*. 2018;247(3):432-50.

129. Suarez-Carmona M, Lesage J, Cataldo D, Gilles C. EMT and inflammation: inseparable actors of cancer progression. *Mol Oncol.* 2017;11(7):805-23.
130. Mlecnik B, Bindea G, Angell HK, Maby P, Angelova M, Tougeron D, et al. Integrative Analyses of Colorectal Cancer Show Immunoscore Is a Stronger Predictor of Patient Survival Than Microsatellite Instability. *Immunity.* 2016;44(3):698-711.
131. Kryczek I, Lin Y, Nagarsheth N, Peng D, Zhao L, Zhao E, et al. IL-22(+)CD4(+) T cells promote colorectal cancer stemness via STAT3 transcription factor activation and induction of the methyltransferase DOT1L. *Immunity.* 2014;40(5):772-84.
132. Albregues J, Shields MA, Ng D, Park CG, Ambrico A, Poindexter ME, et al. Neutrophil extracellular traps produced during inflammation awaken dormant cancer cells in mice. *Science.* 2018;361(6409).
133. Koliaraki V, Pallangyo CK, Greten FR, Kollias G. Mesenchymal Cells in Colon Cancer. *Gastroenterology.* 2017;152(5):964-79.
134. Calon A, Espinet E, Palomo-Ponce S, Tauriello DV, Iglesias M, Céspedes MV, et al. Dependency of colorectal cancer on a TGF- β -driven program in stromal cells for metastasis initiation. *Cancer Cell.* 2012;22(5):571-84.
135. Del Pozo Martin Y, Park D, Ramachandran A, Ombrato L, Calvo F, Chakravarty P, et al. Mesenchymal Cancer Cell-Stroma Crosstalk Promotes Niche Activation, Epithelial Reversion, and Metastatic Colonization. *Cell Rep.* 2015;13(11):2456-69.
136. Marusyk A, Tabassum DP, Janiszewska M, Place AE, Trinh A, Rozhok AI, et al. Spatial Proximity to Fibroblasts Impacts Molecular Features and Therapeutic Sensitivity of Breast Cancer Cells Influencing Clinical Outcomes. *Cancer Research.* 2016;76(22):6495-506.
137. Calon A, Lonardo E, Berenguer-Llargo A, Espinet E, Hernando-Momblona X, Iglesias M, et al. Stromal gene expression defines poor-prognosis subtypes in colorectal cancer. *Nat Genet.* 2015;47(4):320-9.
138. Ruhland MK, Loza AJ, Capietto AH, Luo X, Knolhoff BL, Flanagan KC, et al. Stromal senescence establishes an immunosuppressive microenvironment that drives tumorigenesis. *Nat Commun.* 2016;7:11762.
139. Andón FT, Digifico E, Maeda A, Erreni M, Mantovani A, Alonso MJ, et al. Targeting tumor associated macrophages: The new challenge for nanomedicine. *Semin Immunol.* 2017;34:103-13.
140. Cassetta L, Fragkogianni S, Sims AH, Swierczak A, Forrester LM, Zhang H, et al. Human Tumor-Associated Macrophage and Monocyte Transcriptional Landscapes Reveal Cancer-Specific Reprogramming, Biomarkers, and Therapeutic Targets. *Cancer Cell.* 2019;35(4):588-602.e10.
141. Kirkegård J, Mortensen FV, Cronin-Fenton D. Chronic Pancreatitis and Pancreatic Cancer Risk: A Systematic Review and Meta-analysis. *Am J Gastroenterol.* 2017;112(9):1366-72.
142. Batabyal P, Vander Hoorn S, Christophi C, Nikfarjam M. Association of diabetes mellitus and pancreatic adenocarcinoma: a meta-analysis of 88 studies. *Ann Surg Oncol.* 2014;21(7):2453-62.
143. Pannala R, Leirness JB, Bamlet WR, Basu A, Petersen GM, Chari ST. Prevalence and clinical profile of pancreatic cancer-associated diabetes mellitus. *Gastroenterology.* 2008;134(4):981-7.
144. Hotamisligil GS. Inflammation, metaflammation and immunometabolic disorders. *Nature.* 2017;542(7640):177-85.
145. Porta C, Marino A, Consonni FM, Bleve A, Mola S, Storto M, et al. Metabolic influence on the differentiation of suppressive myeloid cells in cancer. *Carcinogenesis.* 2018;39(9):1095-104.

146. Balachandran VP, Łuksza M, Zhao JN, Makarov V, Moral JA, Remark R, et al. Identification of unique neoantigen qualities in long-term survivors of pancreatic cancer. *Nature*. 2017;551(7681):512-6.
147. Evans A, Costello E. The role of inflammatory cells in fostering pancreatic cancer cell growth and invasion. *Front Physiol*. 2012;3:270.
148. Sheikh AA, Vimalachandran D, Thompson CC, Jenkins RE, Nedjadi T, Shekouh A, et al. The expression of S100A8 in pancreatic cancer-associated monocytes is associated with the Smad4 status of pancreatic cancer cells. *Proteomics*. 2007;7(11):1929-40.
149. Ang CW, Nedjadi T, Sheikh AA, Tweedle EM, Tonack S, Honap S, et al. Smad4 loss is associated with fewer S100A8-positive monocytes in colorectal tumors and attenuated response to S100A8 in colorectal and pancreatic cancer cells. *Carcinogenesis*. 2010;31(9):1541-51.
150. Lim SY, Yuzhalin AE, Gordon-Weeks AN, Muschel RJ. Tumor-infiltrating monocytes/macrophages promote tumor invasion and migration by upregulating S100A8 and S100A9 expression in cancer cells. *Oncogene*. 2016;35(44):5735-45.
151. Eisenblaetter M, Flores-Borja F, Lee JJ, Wefers C, Smith H, Hueting R, et al. Visualization of Tumor-Immune Interaction - Target-Specific Imaging of S100A8/A9 Reveals Pre-Metastatic Niche Establishment. *Theranostics*. 2017;7(9):2392-401.
152. Yako YY, Kruger D, Smith M, Brand M. Cytokines as Biomarkers of Pancreatic Ductal Adenocarcinoma: A Systematic Review. *PLoS One*. 2016;11(5):e0154016.
153. Öhlund D, Handly-Santana A, Biffi G, Elyada E, Almeida AS, Ponz-Sarvise M, et al. Distinct populations of inflammatory fibroblasts and myofibroblasts in pancreatic cancer. *J Exp Med*. 2017;214(3):579-96.
154. Ishii N, Araki K, Yokobori T, Hagiwara K, Gantumur D, Yamanaka T, et al. Conophylline suppresses pancreatic cancer desmoplasia and cancer-promoting cytokines produced by cancer-associated fibroblasts. *Cancer Sci*. 2019;110(1):334-44.
155. Stein PD, Beemath A, Meyers FA, Skaf E, Sanchez J, Olson RE. Incidence of venous thromboembolism in patients hospitalized with cancer. *Am J Med*. 2006;119(1):60-8.
156. Ay C, Pabinger I, Cohen AT. Cancer-associated venous thromboembolism: Burden, mechanisms, and management. *Thromb Haemost*. 2017;117(2):219-30.
157. Khorana AA, Francis CW, Culakova E, Kuderer NM, Lyman GH. Thromboembolism is a leading cause of death in cancer patients receiving outpatient chemotherapy. *J Thromb Haemost*. 2007;5(3):632-4.
158. Sørensen HT, Mellekjær L, Olsen JH, Baron JA. Prognosis of cancers associated with venous thromboembolism. *N Engl J Med*. 2000;343(25):1846-50.
159. Khorana AA, Francis CW, Culakova E, Kuderer NM, Lyman GH. Frequency, risk factors, and trends for venous thromboembolism among hospitalized cancer patients. *Cancer*. 2007;110(10):2339-46.
160. Varki A. Trousseau's syndrome: multiple definitions and multiple mechanisms. *Blood*. 2007;110(6):1723-9.
161. Timp JF, Braekkan SK, Versteeg HH, Cannegieter SC. Epidemiology of cancer-associated venous thrombosis. *Blood*. 2013;122(10):1712-23.
162. Ay C, Ünal UK. Epidemiology and risk factors for venous thromboembolism in lung cancer. *Curr Opin Oncol*. 2016;28(2):145-9.

163. Koizume S, Jin MS, Miyagi E, Hirahara F, Nakamura Y, Piao JH, et al. Activation of cancer cell migration and invasion by ectopic synthesis of coagulation factor VII. *Cancer Res.* 2006;66(19):9453-60.
164. Callander NS, Varki N, Rao LV. Immunohistochemical identification of tissue factor in solid tumors. *Cancer.* 1992;70(5):1194-201.
165. Falanga A, Marchetti M, Russo L. The mechanisms of cancer-associated thrombosis. *Thromb Res.* 2015;135 Suppl 1:S8-s11.
166. Khalil J, Bensaid B, Elkacemi H, Afif M, Bensaid Y, Kebdani T, et al. Venous thromboembolism in cancer patients: an underestimated major health problem. *World J Surg Oncol.* 2015;13:204.
167. Ruf W. Tissue factor and PAR signaling in tumor progression. *Thromb Res.* 2007;120 Suppl 2:S7-12.
168. Mousa SA, Linhardt R, Francis JL, Amirkhosravi A. Anti-metastatic effect of a non-anticoagulant low-molecular-weight heparin versus the standard low-molecular-weight heparin, enoxaparin. *Thromb Haemost.* 2006;96(6):816-21.
169. Hisada Y, Mackman N. Tissue Factor and Cancer: Regulation, Tumor Growth, and Metastasis. *Semin Thromb Hemost.* 2019;45(4):385-95.
170. Rao B, Gao Y, Huang J, Gao X, Fu X, Huang M, et al. Mutations of p53 and K-ras correlate TF expression in human colorectal carcinomas: TF downregulation as a marker of poor prognosis. *Int J Colorectal Dis.* 2011;26(5):593-601.
171. Rong Y, Belozarov VE, Tucker-Burden C, Chen G, Durden DL, Olson JJ, et al. Epidermal growth factor receptor and PTEN modulate tissue factor expression in glioblastoma through JunD/activator protein-1 transcriptional activity. *Cancer Res.* 2009;69(6):2540-9.
172. Rong Y, Hu F, Huang R, Mackman N, Horowitz JM, Jensen RL, et al. Early growth response gene-1 regulates hypoxia-induced expression of tissue factor in glioblastoma multiforme through hypoxia-inducible factor-1-independent mechanisms. *Cancer Res.* 2006;66(14):7067-74.
173. Yu JL, May L, Lhotak V, Shahrzad S, Shirasawa S, Weitz JI, et al. Oncogenic events regulate tissue factor expression in colorectal cancer cells: implications for tumor progression and angiogenesis. *Blood.* 2005;105(4):1734-41.
174. Rondon AMR, Kroone C, Kapteijn MY, Versteeg HH, Buijs JT. Role of Tissue Factor in Tumor Progression and Cancer-Associated Thrombosis. *Semin Thromb Hemost.* 2019;45(4):396-412.
175. Yokota N, Koizume S, Miyagi E, Hirahara F, Nakamura Y, Kikuchi K, et al. Self-production of tissue factor-coagulation factor VII complex by ovarian cancer cells. *Br J Cancer.* 2009;101(12):2023-9.
176. Koizume S, Ito S, Miyagi E, Hirahara F, Nakamura Y, Sakuma Y, et al. HIF2 α -Sp1 interaction mediates a deacetylation-dependent FVII-gene activation under hypoxic conditions in ovarian cancer cells. *Nucleic Acids Res.* 2012;40(12):5389-401.
177. Gong J, Jaiswal R, Dalla P, Luk F, Bebawy M. Microparticles in cancer: A review of recent developments and the potential for clinical application. *Semin Cell Dev Biol.* 2015;40:35-40.
178. Rousseau A, Van Dreden P, Khaterchi A, Larsen AK, Elalamy I, Gerotziafas GT. Procoagulant microparticles derived from cancer cells have determinant role in the hypercoagulable state associated with cancer. *Int J Oncol.* 2017;51(6):1793-800.
179. Ender F, Freund A, Quecke T, Steidel C, Zamzow P, von Bubnoff N, et al. Tissue factor activity on microvesicles from cancer patients. *J Cancer Res Clin Oncol.* 2020;146(2):467-75.

180. Bromberg ME, Bailly MA, Konigsberg WH. Role of protease-activated receptor 1 in tumor metastasis promoted by tissue factor. *Thromb Haemost.* 2001;86(5):1210-4.
181. Han N, Jin K, He K, Cao J, Teng L. Protease-activated receptors in cancer: A systematic review. *Oncol Lett.* 2011;2(4):599-608.
182. Graf C, Ruf W. Tissue factor as a mediator of coagulation and signaling in cancer and chronic inflammation. *Thromb Res.* 2018;164 Suppl 1:S143-s7.
183. Jurasz P, Alonso-Escolano D, Radomski MW. Platelet--cancer interactions: mechanisms and pharmacology of tumour cell-induced platelet aggregation. *Br J Pharmacol.* 2004;143(7):819-26.
184. Schlesinger M. Role of platelets and platelet receptors in cancer metastasis. *J Hematol Oncol.* 2018;11(1):125.
185. Falanga A, Russo L, Milesi V, Vignoli A. Mechanisms and risk factors of thrombosis in cancer. *Crit Rev Oncol Hematol.* 2017;118:79-83.
186. Liu Y, Mueller BM. Protease-activated receptor-2 regulates vascular endothelial growth factor expression in MDA-MB-231 cells via MAPK pathways. *Biochem Biophys Res Commun.* 2006;344(4):1263-70.
187. Mousa SA, Petersen LJ. Anti-cancer properties of low-molecular-weight heparin: preclinical evidence. *Thromb Haemost.* 2009;102(2):258-67.
188. Wagner DD, Frenette PS. The vessel wall and its interactions. *Blood.* 2008;111(11):5271-81.
189. Bauer AT, Suckau J, Frank K, Desch A, Goertz L, Wagner AH, et al. von Willebrand factor fibers promote cancer-associated platelet aggregation in malignant melanoma of mice and humans. *Blood.* 2015;125(20):3153-63.
190. Schneider SW, Nuschele S, Wixforth A, Gorzelanny C, Alexander-Katz A, Netz RR, et al. Shear-induced unfolding triggers adhesion of von Willebrand factor fibers. *Proceedings of the National Academy of Sciences.* 2007;104(19):7899-903.
191. Butenas S. Tissue factor structure and function. *Scientifica (Cairo).* 2012;2012:964862.
192. Morrissey JH, Fakhrai H, Edgington TS. Molecular cloning of the cDNA for tissue factor, the cellular receptor for the initiation of the coagulation protease cascade. *Cell.* 1987;50(1):129-35.
193. Spicer EK, Horton R, Bloem L, Bach R, Williams KR, Guha A, et al. Isolation of cDNA clones coding for human tissue factor: primary structure of the protein and cDNA. *Proc Natl Acad Sci U S A.* 1987;84(15):5148-52.
194. Teplyakov A, Obmolova G, Malia TJ, Wu B, Zhao Y, Taudte S, et al. Crystal structure of tissue factor in complex with antibody 10H10 reveals the signaling epitope. *Cell Signal.* 2017;36:139-44.
195. Harlos K, Martin DM, O'Brien DP, Jones EY, Stuart DI, Polikarpov I, et al. Crystal structure of the extracellular region of human tissue factor. *Nature.* 1994;370(6491):662-6.
196. Palta S, Saroa R, Palta A. Overview of the coagulation system. *Indian J Anaesth.* 2014;58(5):515-23.
197. Krudysz-Amblo J, Jennings ME, 2nd, Matthews DE, Mann KG, Butenas S. Differences in the fractional abundances of carbohydrates of natural and recombinant human tissue factor. *Biochim Biophys Acta.* 2011;1810(4):398-405.
198. Ahamed J, Versteeg HH, Kerver M, Chen VM, Mueller BM, Hogg PJ, et al. Disulfide isomerization switches tissue factor from coagulation to cell signaling. *Proc Natl Acad Sci U S A.* 2006;103(38):13932-7.

199. Paborsky LR, Harris RJ. Post-translational modifications of recombinant human tissue factor. *Thromb Res.* 1990;60(5):367-76.
200. Åberg M, Siegbahn A. Tissue factor non-coagulant signaling - molecular mechanisms and biological consequences with a focus on cell migration and apoptosis. *J Thromb Haemost.* 2013;11(5):817-25.
201. Schaffner F, Ruf W. Tissue factor and protease-activated receptor signaling in cancer. *Semin Thromb Hemost.* 2008;34(2):147-53.
202. Kocatürk B, Versteeg HH. Tissue factor-integrin interactions in cancer and thrombosis: every Jack has his Jill. *J Thromb Haemost.* 2013;11 Suppl 1:285-93.
203. Ruf W, Mueller BM. Tissue factor signaling. *Thromb Haemost.* 1999;82(2):175-82.
204. Zioncheck TF, Roy S, Vehar GA. The cytoplasmic domain of tissue factor is phosphorylated by a protein kinase C-dependent mechanism. *J Biol Chem.* 1992;267(6):3561-4.
205. Dorfleutner A, Ruf W. Regulation of tissue factor cytoplasmic domain phosphorylation by palmitoylation. *Blood.* 2003;102(12):3998-4005.
206. van den Berg YW, van den Hengel LG, Myers HR, Ayachi O, Jordanova E, Ruf W, et al. Alternatively spliced tissue factor induces angiogenesis through integrin ligation. *Proc Natl Acad Sci U S A.* 2009;106(46):19497-502.
207. Kocatürk B, Van den Berg YW, Tieken C, Mieog JSD, de Kruijf EM, Engels CC, et al. Alternatively spliced tissue factor promotes breast cancer growth in a β 1 integrin-dependent manner. *Proceedings of the National Academy of Sciences.* 2013;110(28):11517-22.
208. Kocatürk B, Tieken C, Vreeken D, Ünlü B, Engels CC, de Kruijf EM, et al. Alternatively spliced tissue factor synergizes with the estrogen receptor pathway in promoting breast cancer progression. *J Thromb Haemost.* 2015;13(9):1683-93.
209. Rickles FR. Mechanisms of cancer-induced thrombosis in cancer. *Pathophysiol Haemost Thromb.* 2006;35(1-2):103-10.
210. TESSELAAR MET, ROMIJN FPHTM, VAN DER LINDEN IK, PRINS FA, BERTINA RM, OSANTO S. Microparticle-associated tissue factor activity: a link between cancer and thrombosis? *Journal of Thrombosis and Haemostasis.* 2007;5(3):520-7.
211. Contrino J, Hair G, Kreutzer DL, Rickles FR. In situ detection of tissue factor in vascular endothelial cells: correlation with the malignant phenotype of human breast disease. *Nat Med.* 1996;2(2):209-15.
212. Yu JL, May L, Lhotak V, Shahrzad S, Shirasawa S, Weitz JI, et al. Oncogenic events regulate tissue factor expression in colorectal cancer cells: implications for tumor progression and angiogenesis. *Blood.* 2005;105(4):1734-41.
213. Rak J, Milsom C, Magnus N, Yu J. Tissue factor in tumour progression. *Best Pract Res Clin Haematol.* 2009;22(1):71-83.
214. Magnus N, Garnier D, Rak J. Oncogenic epidermal growth factor receptor up-regulates multiple elements of the tissue factor signaling pathway in human glioma cells. *Blood.* 2010;116(5):815-8.
215. Milsom CC, Yu JL, Mackman N, Micallef J, Anderson GM, Guha A, et al. Tissue factor regulation by epidermal growth factor receptor and epithelial-to-mesenchymal transitions: effect on tumor initiation and angiogenesis. *Cancer Res.* 2008;68(24):10068-76.

216. Rong Y, Post DE, Pieper RO, Durden DL, Van Meir EG, Brat DJ. PTEN and Hypoxia Regulate Tissue Factor Expression and Plasma Coagulation by Glioblastoma. *Cancer Research*. 2005;65(4):1406-13.
217. Regina S, Valentin J-B, Lachot Sb, Lemarié E, Rollin Jrm, Gruel Y. Increased Tissue Factor Expression Is Associated with Reduced Survival in Non-Small Cell Lung Cancer and with Mutations of TP53 and PTEN. *Clinical Chemistry*. 2009;55(10):1834-42.
218. Sherief LM, Hassan TH, Zakaria M, Fathy M, Eshak EA, Bebars MA, et al. Tissue factor expression predicts outcome in children with neuroblastoma: A retrospective study. *Oncol Lett*. 2019;18(6):6347-54.
219. Sun L, Liu Y, Lin S, Shang J, Liu J, Li J, et al. Early growth response gene-1 and hypoxia-inducible factor-1 α affect tumor metastasis via regulation of tissue factor. *Acta Oncologica*. 2013;52(4):842-51.
220. Eisenreich A, Zakrzewicz A, Huber K, Thierbach H, Pepke W, Goldin-Lang P, et al. Regulation of pro-angiogenic tissue factor expression in hypoxia-induced human lung cancer cells. *Oncol Rep*. 2013;30(1):462-70.
221. Leppert U, Eisenreich A. The role of tissue factor isoforms in cancer biology. *International Journal of Cancer*. 2015;137(3):497-503.
222. Wang JG, Geddings JE, Aleman MM, Cardenas JC, Chantrathammachart P, Williams JC, et al. Tumor-derived tissue factor activates coagulation and enhances thrombosis in a mouse xenograft model of human pancreatic cancer. *Blood*. 2012;119(23):5543-52.
223. Hu L, Xia L, Zhou H, Wu B, Mu Y, Wu Y, et al. TF/FVIIa/PAR2 promotes cell proliferation and migration via PKC α and ERK-dependent c-Jun/AP-1 pathway in colon cancer cell line SW620. *Tumour Biol*. 2013;34(5):2573-81.
224. Wu B, Zhou H, Hu L, Mu Y, Wu Y. Involvement of PKC α activation in TF/VIIa/PAR2-induced proliferation, migration, and survival of colon cancer cell SW620. *Tumour Biol*. 2013;34(2):837-46.
225. Lwaleed BA, Francis JL, Chisholm M. Urinary tissue factor levels in patients with bladder and prostate cancer. *European Journal of Surgical Oncology (EJSO)*. 2000;26(1):44-9.
226. Förster Y, Meye A, Albrecht S, Kotsch M, Füssel S, Wirth MP, et al. Tissue specific expression and serum levels of human tissue factor in patients with urological cancer. *Cancer Letters*. 2003;193(1):65-73.
227. Patry G, Hovington H, Larue H, Harel F, Fradet Y, Lacombe L. Tissue factor expression correlates with disease-specific survival in patients with node-negative muscle-invasive bladder cancer. *Int J Cancer*. 2008;122(7):1592-7.
228. Takano S, Tsuboi K, Tomono Y, Mitsui Y, Nose T. Tissue factor, osteopontin, α 3 β 1 integrin expression in microvasculature of gliomas associated with vascular endothelial growth factor expression. *Br J Cancer*. 2000;82(12):1967-73.
229. Takeshima H, Nishi T, Kuratsu J, Kamikubo Y, Kochi M, Ushio Y. Suppression of the tissue factor-dependent coagulation cascade: a contributing factor for the development of intratumoral hemorrhage in glioblastoma. *Int J Mol Med*. 2000;6(3):271-6.
230. Hamada K, Kuratsu J, Saitoh Y, Takeshima H, Nishi T, Ushio Y. Expression of tissue factor correlates with grade of malignancy in human glioma. *Cancer*. 1996;77(9):1877-83.
231. Guan M, Jin J, Su B, Liu WW, Lu Y. Tissue factor expression and angiogenesis in human glioma. *Clin Biochem*. 2002;35(4):321-5.

232. Brat DJ, Van Meir EG. Vaso-occlusive and prothrombotic mechanisms associated with tumor hypoxia, necrosis, and accelerated growth in glioblastoma. *Lab Invest.* 2004;84(4):397-405.
233. Hron G, Kollars M, Weber H, Sagaster V, Quehenberger P, Eichinger S, et al. Tissue factor-positive microparticles: cellular origin and association with coagulation activation in patients with colorectal cancer. *Thromb Haemost.* 2007;97(1):119-23.
234. Altomare DF, Rotelli MT, Memeo V, Martinelli E, Guglielmi A, DeFazio M, et al. [Expression of tissue factor and vascular endothelial growth factor in colorectal carcinoma]. *Tumori.* 2003;89(4 Suppl):5-6.
235. Nakasaki T, Wada H, Shigemori C, Miki C, Gabazza EC, Nobori T, et al. Expression of tissue factor and vascular endothelial growth factor is associated with angiogenesis in colorectal cancer. *Am J Hematol.* 2002;69(4):247-54.
236. Seto S, Onodera H, Kaido T, Yoshikawa A, Ishigami S, Arie S, et al. Tissue factor expression in human colorectal carcinoma: correlation with hepatic metastasis and impact on prognosis. *Cancer.* 2000;88(2):295-301.
237. Shigemori C, Wada H, Matsumoto K, Shiku H, Nakamura S, Suzuki H. Tissue factor expression and metastatic potential of colorectal cancer. *Thromb Haemost.* 1998;80(6):894-8.
238. Kataoka H, Uchino H, Asada Y, Hatakeyama K, Nabeshima K, Sumiyoshi A, et al. Analysis of tissue factor and tissue factor pathway inhibitor expression in human colorectal carcinoma cell lines and metastatic sublines to the liver. *Int J Cancer.* 1997;72(5):878-84.
239. Szczepański M, Bardadin K, Zawadzki J, Pypno W. Procoagulant activity of gastric, colorectal, and renal cancer is factor VII-dependent. *J Cancer Res Clin Oncol.* 1988;114(5):519-22.
240. Yamashita H, Kitayama J, Ishikawa M, Nagawa H. Tissue factor expression is a clinical indicator of lymphatic metastasis and poor prognosis in gastric cancer with intestinal phenotype. *J Surg Oncol.* 2007;95(4):324-31.
241. Nadir Y, Katz T, Sarig G, Hoffman R, Oliven A, Rowe JM, et al. Hemostatic balance on the surface of leukemic cells: the role of tissue factor and urokinase plasminogen activator receptor. *Haematologica.* 2005;90(11):1549-56.
242. Nakasaki T, Wada H, Watanabe R, Mori Y, Gabazza EC, Kageyama S, et al. Elevated tissue factor levels in leukemic cell homogenate. *Clin Appl Thromb Hemost.* 2000;6(1):14-7.
243. López-Pedrerá C, Jardí M, del Mar Malagón M, Inglés-Esteve J, Dorado G, Torres A, et al. Tissue factor (TF) and urokinase plasminogen activator receptor (uPAR) and bleeding complications in leukemic patients. *Thromb Haemost.* 1997;77(1):62-70.
244. Tanaka M, Yamanishi H. The expression of tissue factor antigen and activity on the surface of leukemic cells. *Leuk Res.* 1993;17(2):103-11.
245. Bauer KA, Conway EM, Bach R, Konigsberg WH, Griffin JD, Demetri G. Tissue factor gene expression in acute myeloblastic leukemia. *Thromb Res.* 1989;56(3):425-30.
246. Negaard HF, Iversen PO, Østenstad B, Iversen N, Holme PA, Sandset PM. Hypercoagulability in patients with haematological neoplasia: no apparent initiation by tissue factor. *Thromb Haemost.* 2008;99(6):1040-8.
247. Semeraro N, Montemurro P, Giordano P, Santoro N, De Mattia D, Colucci M. Increased mononuclear cell tissue factor and type-2 plasminogen activator inhibitor and reduced plasma fibrinolytic capacity in children with lymphoma. *Thromb Haemost.* 1994;72(1):54-7.

248. Goldin-Lang P, Tran QV, Fichtner I, Eisenreich A, Antoniak S, Schulze K, et al. Tissue factor expression pattern in human non-small cell lung cancer tissues indicate increased blood thrombogenicity and tumor metastasis. *Oncol Rep.* 2008;20(1):123-8.
249. Rauch U, Antoniak S, Boots M, Schulze K, Goldin-Lang P, Stein H, et al. Association of tissue-factor upregulation in squamous-cell carcinoma of the lung with increased tissue factor in circulating blood. *Lancet Oncol.* 2005;6(4):254.
250. Del Conde I, Bharwani LD, Dietzen DJ, Pendurthi U, Thiagarajan P, López JA. Microvesicle-associated tissue factor and Trousseau's syndrome. *J Thromb Haemost.* 2007;5(1):70-4.
251. Langer F, Spath B, Haubold K, Holstein K, Marx G, Wierecky J, et al. Tissue factor procoagulant activity of plasma microparticles in patients with cancer-associated disseminated intravascular coagulation. *Ann Hematol.* 2008;87(6):451-7.
252. Sawada M, Miyake S, Ohdama S, Matsubara O, Masuda S, Yakumaru K, et al. Expression of tissue factor in non-small-cell lung cancers and its relationship to metastasis. *Br J Cancer.* 1999;79(3-4):472-7.
253. Koomägi R, Volm M. Tissue-factor expression in human non-small-cell lung carcinoma measured by immunohistochemistry: correlation between tissue factor and angiogenesis. *Int J Cancer.* 1998;79(1):19-22.
254. Kageshita T, Funasaka Y, Ichihashi M, Ishihara T, Tokuo H, Ono T. Differential expression of tissue factor and tissue factor pathway inhibitor in metastatic melanoma lesions. *Pigment Cell Res.* 2002;15(3):212-6.
255. Uno K, Homma S, Satoh T, Nakanishi K, Abe D, Matsumoto K, et al. Tissue factor expression as a possible determinant of thromboembolism in ovarian cancer. *Br J Cancer.* 2007;96(2):290-5.
256. Han LY, Landen CN, Jr., Kamat AA, Lopez A, Bender DP, Mueller P, et al. Preoperative serum tissue factor levels are an independent prognostic factor in patients with ovarian carcinoma. *J Clin Oncol.* 2006;24(5):755-61.
257. Zacharski LR, Memoli VA, Ornstein DL, Rousseau SM, Kisiel W, Kudryk BJ. Tumor cell procoagulant and urokinase expression in carcinoma of the ovary. *J Natl Cancer Inst.* 1993;85(15):1225-30.
258. Haas SL, Jesnowski R, Steiner M, Hummel F, Ringel J, Burstein C, et al. Expression of tissue factor in pancreatic adenocarcinoma is associated with activation of coagulation. *World J Gastroenterol.* 2006;12(30):4843-9.
259. Kakkar AK, Lemoine NR, Scully MF, Tebbutt S, Williamson RCN. Tissue factor expression correlates with histological grade in human pancreatic cancer. *BJS (British Journal of Surgery).* 1995;82(8):1101-4.
260. Poon RT, Lau CP, Ho JW, Yu WC, Fan ST, Wong J. Tissue factor expression correlates with tumor angiogenesis and invasiveness in human hepatocellular carcinoma. *Clin Cancer Res.* 2003;9(14):5339-45.
261. Kaushal V, Mukunyadzi P, Siegel ER, Dennis RA, Johnson DE, Kohli M. Expression of tissue factor in prostate cancer correlates with malignant phenotype. *Appl Immunohistochem Mol Morphol.* 2008;16(1):1-6.
262. Babiker AA, Ekdahl KN, Nilsson B, Ronquist G. Prothrombotic effects of prostasomes isolated from prostatic cancer cell lines and seminal plasma. *Semin Thromb Hemost.* 2007;33(1):80-6.

263. Langer F, Chun FK, Amirkhosravi A, Friedrich M, Leuenroth S, Eifrig B, et al. Plasma tissue factor antigen in localized prostate cancer: distribution, clinical significance and correlation with haemostatic activation markers. *Thromb Haemost.* 2007;97(3):464-70.
264. Akashi T, Furuya Y, Ohta S, Fuse H. Tissue factor expression and prognosis in patients with metastatic prostate cancer. *Urology.* 2003;62(6):1078-82.
265. Ohta S, Wada H, Nakazaki T, Maeda Y, Nobori T, Shiku H, et al. Expression of tissue factor is associated with clinical features and angiogenesis in prostate cancer. *Anticancer Res.* 2002;22(5):2991-6.
266. Abdulkadir SA, Carvalhal GF, Kaleem Z, Kisiel W, Humphrey PA, Catalona WJ, et al. Tissue factor expression and angiogenesis in human prostate carcinoma. *Hum Pathol.* 2000;31(4):443-7.
267. Kocatürk B, Van den Berg YW, Tieken C, Mieog JS, de Kruijf EM, Engels CC, et al. Alternatively spliced tissue factor promotes breast cancer growth in a β 1 integrin-dependent manner. *Proc Natl Acad Sci U S A.* 2013;110(28):11517-22.
268. Versteeg HH, Spek CA, Slofstra SH, Diks SH, Richel DJ, Peppelenbosch MP. FVIIa:TF Induces Cell Survival via G_{12} / G_{13} -Dependent Jak/STAT Activation and Bcl_{XL} Production. *Circulation Research.* 2004;94(8):1032-40.
269. Sorensen BB, Rao LV, Tornehave D, Gammeltoft S, Petersen LC. Antiapoptotic effect of coagulation factor VIIa. *Blood.* 2003;102(5):1708-15.
270. Versteeg HH, Spek CA, Richel DJ, Peppelenbosch MP. Coagulation factors VIIa and Xa inhibit apoptosis and anoikis. *Oncogene.* 2004;23(2):410-7.
271. Aberg M, Wickström M, Siegbahn A. Simvastatin induces apoptosis in human breast cancer cells in a NF κ B-dependent manner and abolishes the anti-apoptotic signaling of TF/FVIIa and TF/FVIIa/FXa. *Thromb Res.* 2008;122(2):191-202.
272. Aberg M, Johnell M, Wickström M, Siegbahn A. Tissue Factor/ FVIIa prevents the extrinsic pathway of apoptosis by regulation of the tumor suppressor Death-Associated Protein Kinase 1 (DAPK1). *Thromb Res.* 2011;127(2):141-8.
273. Horbinski C, Mojesky C, Kyprianou N. Live free or die: tales of homeless (cells) in cancer. *Am J Pathol.* 2010;177(3):1044-52.
274. Yu Z, Pestell TG, Lisanti MP, Pestell RG. Cancer stem cells. *Int J Biochem Cell Biol.* 2012;44(12):2144-51.
275. Milsom C, Magnus N, Meehan B, Al-Nedawi K, Garnier D, Rak J. Tissue factor and cancer stem cells: is there a linkage? *Arterioscler Thromb Vasc Biol.* 2009;29(12):2005-14.
276. Garnier D, Milsom C, Magnus N, Meehan B, Weitz J, Yu J, et al. Role of the tissue factor pathway in the biology of tumor initiating cells. *Thromb Res.* 2010;125 Suppl 2:S44-50.
277. Milsom C, Anderson GM, Weitz JI, Rak J. Elevated tissue factor procoagulant activity in CD133-positive cancer cells. *J Thromb Haemost.* 2007;5(12):2550-2.
278. Long H, Xie R, Xiang T, Zhao Z, Lin S, Liang Z, et al. Autocrine CCL5 signaling promotes invasion and migration of CD133+ ovarian cancer stem-like cells via NF- κ B-mediated MMP-9 upregulation. *Stem Cells.* 2012;30(10):2309-19.
279. Hu Z, Xu J, Cheng J, McMichael E, Yu L, Carson WE, 3rd. Targeting tissue factor as a novel therapeutic oncotarget for eradication of cancer stem cells isolated from tumor cell lines, tumor xenografts and patients of breast, lung and ovarian cancer. *Oncotarget.* 2017;8(1):1481-94.

280. Shaker H, Harrison H, Clarke R, Landberg G, Bundred NJ, Versteeg HH, et al. Tissue Factor promotes breast cancer stem cell activity in vitro. *Oncotarget*. 2017;8(16):25915-27.
281. Magnus N, Garnier D, Meehan B, McGraw S, Lee TH, Caron M, et al. Tissue factor expression provokes escape from tumor dormancy and leads to genomic alterations. *Proc Natl Acad Sci U S A*. 2014;111(9):3544-9.
282. Clouston HW, Rees PA, Lamb R, Duff SE, Kirwan CC. Effect of Tissue Factor on Colorectal Cancer Stem Cells. *Anticancer Res*. 2018;38(5):2635-42.
283. Vrana JA, Stang MT, Grande JP, Getz MJ. Expression of tissue factor in tumor stroma correlates with progression to invasive human breast cancer: paracrine regulation by carcinoma cell-derived members of the transforming growth factor beta family. *Cancer Res*. 1996;56(21):5063-70.
284. Mueller BM, Reisfeld RA, Edgington TS, Ruf W. Expression of tissue factor by melanoma cells promotes efficient hematogenous metastasis. *Proc Natl Acad Sci U S A*. 1992;89(24):11832-6.
285. Unruh D, Turner K, Srinivasan R, Kocatürk B, Qi X, Chu Z, et al. Alternatively spliced tissue factor contributes to tumor spread and activation of coagulation in pancreatic ductal adenocarcinoma. *Int J Cancer*. 2014;134(1):9-20.
286. Ott I, Weigand B, Michl R, Seitz I, Sabbari-Erfani N, Neumann FJ, et al. Tissue factor cytoplasmic domain stimulates migration by activation of the GTPase Rac1 and the mitogen-activated protein kinase p38. *Circulation*. 2005;111(3):349-55.
287. Ott I, Fischer EG, Miyagi Y, Mueller BM, Ruf W. A role for tissue factor in cell adhesion and migration mediated by interaction with actin-binding protein 280. *J Cell Biol*. 1998;140(5):1241-53.
288. Müller M, Albrecht S, Gölfert F, Hofer A, Funk RH, Magdolen V, et al. Localization of tissue factor in actin-filament-rich membrane areas of epithelial cells. *Exp Cell Res*. 1999;248(1):136-47.
289. Ge L, Ly Y, Hollenberg M, DeFea K. A beta-arrestin-dependent scaffold is associated with prolonged MAPK activation in pseudopodia during protease-activated receptor-2-induced chemotaxis. *J Biol Chem*. 2003;278(36):34418-26.
290. Dorfleutner A, Hintermann E, Tarui T, Takada Y, Ruf W. Cross-talk of integrin alpha3beta1 and tissue factor in cell migration. *Mol Biol Cell*. 2004;15(10):4416-25.
291. Unruh D, Ünlü B, Lewis CS, Qi X, Chu Z, Sturm R, et al. Antibody-based targeting of alternatively spliced tissue factor: a new approach to impede the primary growth and spread of pancreatic ductal adenocarcinoma. *Oncotarget*. 2016;7(18):25264-75.
292. Das K, Prasad R, Roy S, Mukherjee A, Sen P. The Protease Activated Receptor2 Promotes Rab5a Mediated Generation of Pro-metastatic Microvesicles. *Sci Rep*. 2018;8(1):7357.
293. Che SPY, Park JY, Stokol T. Tissue Factor-Expressing Tumor-Derived Extracellular Vesicles Activate Quiescent Endothelial Cells via Protease-Activated Receptor-1. *Front Oncol*. 2017;7:261.
294. Benelhaj NE, Maraveyas A, Featherby S, Collier MEW, Johnson MJ, Ettelaie C. Alteration in endothelial permeability occurs in response to the activation of PAR2 by factor Xa but not directly by the TF-factor VIIa complex. *Thromb Res*. 2019;175:13-20.
295. Gil-Bernabé AM, Ferjancic S, Tlalka M, Zhao L, Allen PD, Im JH, et al. Recruitment of monocytes/macrophages by tissue factor-mediated coagulation is essential for metastatic cell survival and premetastatic niche establishment in mice. *Blood*. 2012;119(13):3164-75.

296. Thomas GM, Brill A, Mezouar S, Crescence L, Gallant M, Dubois C, et al. Tissue factor expressed by circulating cancer cell-derived microparticles drastically increases the incidence of deep vein thrombosis in mice. *J Thromb Haemost.* 2015;13(7):1310-9.
297. Mitra A, Mishra L, Li S. EMT, CTCs and CSCs in tumor relapse and drug-resistance. *Oncotarget.* 2015;6(13):10697-711.
298. Bourcy M, Suarez-Carmona M, Lambert J, Francart M-E, Schroeder H, Delierneux C, et al. Tissue Factor Induced by Epithelial–Mesenchymal Transition Triggers a Procoagulant State That Drives Metastasis of Circulating Tumor Cells. *Cancer Research.* 2016;76(14):4270-82.
299. Palumbo JS, Talmage KE, Massari JV, La Jeunesse CM, Flick MJ, Kombrinck KW, et al. Tumor cell-associated tissue factor and circulating hemostatic factors cooperate to increase metastatic potential through natural killer cell-dependent and-independent mechanisms. *Blood.* 2007;110(1):133-41.
300. Palumbo JS, Kombrinck KW, Drew AF, Grimes TS, Kiser JH, Degen JL, et al. Fibrinogen is an important determinant of the metastatic potential of circulating tumor cells. *Blood.* 2000;96(10):3302-9.
301. Jiang X, Guo YL, Bromberg ME. Formation of tissue factor-factor VIIa-factor Xa complex prevents apoptosis in human breast cancer cells. *Thromb Haemost.* 2006;96(2):196-201.
302. Lopez-Vilchez I, Diaz-Ricart M, White JG, Escolar G, Galan AM. Serotonin enhances platelet procoagulant properties and their activation induced during platelet tissue factor uptake. *Cardiovasc Res.* 2009;84(2):309-16.
303. Geddings JE, Hisada Y, Boulaftali Y, Getz TM, Whelihan M, Fuentes R, et al. Tissue factor-positive tumor microvesicles activate platelets and enhance thrombosis in mice. *J Thromb Haemost.* 2016;14(1):153-66.
304. Hisada Y, Ay C, Auriemma AC, Cooley BC, Mackman N. Human pancreatic tumors grown in mice release tissue factor-positive microvesicles that increase venous clot size. *J Thromb Haemost.* 2017;15(11):2208-17.
305. Abou-Saleh H, Théorêt JF, Yacoub D, Merhi Y. Neutrophil P-selectin-glycoprotein-ligand-1 binding to platelet P-selectin enhances metalloproteinase 2 secretion and platelet-neutrophil aggregation. *Thromb Haemost.* 2005;94(6):1230-5.
306. Wolach O, Martinod K. Casting a NET on cancer: the multiple roles for neutrophil extracellular traps in cancer. *Curr Opin Hematol.* 2022;29(1):53-62.
307. Li H, Yu Y, Gao L, Zheng P, Liu X, Chen H. Tissue factor: a neglected role in cancer biology. *J Thromb Thrombolysis.* 2022;54(1):97-108.
308. Huang H, Zhang H, Onuma AE, Tsung A. Neutrophil Elastase and Neutrophil Extracellular Traps in the Tumor Microenvironment. *Adv Exp Med Biol.* 2020;1263:13-23.
309. Martinod K, Witsch T, Farley K, Gallant M, Remold-O'Donnell E, Wagner DD. Neutrophil elastase-deficient mice form neutrophil extracellular traps in an experimental model of deep vein thrombosis. *J Thromb Haemost.* 2016;14(3):551-8.
310. Liu Y, Zhang Y, Ding Y, Zhuang R. Platelet-mediated tumor metastasis mechanism and the role of cell adhesion molecules. *Crit Rev Oncol Hematol.* 2021;167:103502.
311. Leblanc R, Peyruchaud O. Metastasis: new functional implications of platelets and megakaryocytes. *Blood.* 2016;128(1):24-31.

312. Ward MP, L EK, L AN, Mohamed BM, Kelly T, Bates M, et al. Platelets, immune cells and the coagulation cascade; friend or foe of the circulating tumour cell? *Mol Cancer*. 2021;20(1):59.
313. Eisenreich A, Bogdanov VY, Zakrzewicz A, Pries A, Antoniak S, Poller W, et al. Cdc2-like kinases and DNA topoisomerase I regulate alternative splicing of tissue factor in human endothelial cells. *Circ Res*. 2009;104(5):589-99.
314. Napoleone E, Di Santo A, Lorenzet R. Monocytes upregulate endothelial cell expression of tissue factor: a role for cell-cell contact and cross-talk. *Blood*. 1997;89(2):541-9.
315. Cermak J, Key NS, Bach RR, Balla J, Jacob HS, Vercellotti GM. C-reactive protein induces human peripheral blood monocytes to synthesize tissue factor. *Blood*. 1993;82(2):513-20.
316. Chen Y, Wang J, Yao Y, Yuan W, Kong M, Lin Y, et al. CRP regulates the expression and activity of tissue factor as well as tissue factor pathway inhibitor via NF-kappaB and ERK 1/2 MAPK pathway. *FEBS Lett*. 2009;583(17):2811-8.
317. Perzborn E, Heitmeier S, Buetehorn U, Laux V. Direct thrombin inhibitors, but not the direct factor Xa inhibitor rivaroxaban, increase tissue factor-induced hypercoagulability in vitro and in vivo. *J Thromb Haemost*. 2014;12(7):1054-65.
318. Steffel J, Akhmedov A, Greutert H, Lüscher TF, Tanner FC. Histamine induces tissue factor expression: implications for acute coronary syndromes. *Circulation*. 2005;112(3):341-9.
319. Kawano H, Tsuji H, Nishimura H, Kimura S, Yano S, Ukimura N, et al. Serotonin induces the expression of tissue factor and plasminogen activator inhibitor-1 in cultured rat aortic endothelial cells. *Blood*. 2001;97(6):1697-702.
320. Camera M, Giesen PL, Fallon J, Aufiero BM, Taubman M, Tremoli E, et al. Cooperation between VEGF and TNF-alpha is necessary for exposure of active tissue factor on the surface of human endothelial cells. *Arterioscler Thromb Vasc Biol*. 1999;19(3):531-7.
321. Drake TA, Hannani K, Fei HH, Lavi S, Berliner JA. Minimally oxidized low-density lipoprotein induces tissue factor expression in cultured human endothelial cells. *Am J Pathol*. 1991;138(3):601-7.
322. Guha M, Mackman N. The phosphatidylinositol 3-kinase-Akt pathway limits lipopolysaccharide activation of signaling pathways and expression of inflammatory mediators in human monocytic cells. *J Biol Chem*. 2002;277(35):32124-32.
323. Mach F, Schönbeck U, Bonnefoy JY, Pober JS, Libby P. Activation of monocyte/macrophage functions related to acute atheroma complication by ligation of CD40: induction of collagenase, stromelysin, and tissue factor. *Circulation*. 1997;96(2):396-9.
324. He M, He X, Xie Q, Chen F, He S. Angiotensin II induces the expression of tissue factor and its mechanism in human monocytes. *Thromb Res*. 2006;117(5):579-90.
325. Goldin-Lang P, Niebergall F, Antoniak S, Szotowski B, Rosenthal P, Pels K, et al. Ionizing radiation induces upregulation of cellular procoagulability and tissue factor expression in human peripheral blood mononuclear cells. *Thromb Res*. 2007;120(6):857-64.
326. Yan SF, Mackman N, Kisiel W, Stern DM, Pinsky DJ. Hypoxia/Hypoxemia-Induced activation of the procoagulant pathways and the pathogenesis of ischemia-associated thrombosis. *Arterioscler Thromb Vasc Biol*. 1999;19(9):2029-35.
327. Bao MH, Feng X, Zhang YW, Lou XY, Cheng Y, Zhou HH. Let-7 in cardiovascular diseases, heart development and cardiovascular differentiation from stem cells. *Int J Mol Sci*. 2013;14(11):23086-102.

328. Steffel J, Hermann M, Greutert H, Gay S, Lüscher TF, Ruschitzka F, et al. Celecoxib decreases endothelial tissue factor expression through inhibition of c-Jun terminal NH2 kinase phosphorylation. *Circulation*. 2005;111(13):1685-9.
329. Eto M, Kozai T, Cosentino F, Joch H, Lüscher TF. Statin prevents tissue factor expression in human endothelial cells: role of Rho/Rho-kinase and Akt pathways. *Circulation*. 2002;105(15):1756-9.
330. Mechtcheriakova D, Schabbauer G, Lucerna M, Clauss M, De Martin R, Binder BR, et al. Specificity, diversity, and convergence in VEGF and TNF-alpha signaling events leading to tissue factor up-regulation via EGR-1 in endothelial cells. *Faseb j*. 2001;15(1):230-42.
331. Mackman N. Regulation of the tissue factor gene. *Thromb Haemost*. 1997;78(1):747-54.
332. Krisinger MJ, Goebeler V, Lu Z, Meixner SC, Myles T, Pryzdial EL, et al. Thrombin generates previously unidentified C5 products that support the terminal complement activation pathway. *Blood*. 2012;120(8):1717-25.
333. Markiewski MM, DeAngelis RA, Benencia F, Ricklin-Lichtsteiner SK, Koutoulaki A, Gerard C, et al. Modulation of the antitumor immune response by complement. *Nat Immunol*. 2008;9(11):1225-35.
334. Ferjančič Š, Gil-Bernabé AM, Hill SA, Allen PD, Richardson P, Sparey T, et al. VCAM-1 and VAP-1 recruit myeloid cells that promote pulmonary metastasis in mice. *Blood*. 2013;121(16):3289-97.
335. Broze GJ, Majerus PW. Purification and properties of human coagulation factor VII. *Journal of Biological Chemistry*. 1980;255(4):1242-7.
336. Perera L, Darden TA, Pedersen LG. Probing the structural changes in the light chain of human coagulation factor VIIa due to tissue factor association. *Biophys J*. 1999;77(1):99-113.
337. Vadivel K, Bajaj SP. Structural biology of factor VIIa/tissue factor initiated coagulation. *Front Biosci (Landmark Ed)*. 2012;17(7):2476-94.
338. Thiec F, Cherel G, Christophe OD. Role of the Gla and First Epidermal Growth Factor-like Domains of Factor X in the Prothrombinase and Tissue Factor-Factor VIIa Complexes*. *Journal of Biological Chemistry*. 2003;278(12):10393-9.
339. Stenflo J. Contributions of Gla and EGF-like domains to the function of vitamin K-dependent coagulation factors. *Crit Rev Eukaryot Gene Expr*. 1999;9(1):59-88.
340. Shahbazi S, Mahdian R. Factor VII Gene Defects: Review of Functional Studies and Their Clinical Implications. *Iran Biomed J*. 2019;23(3):165-74.
341. Pike AC, Brzozowski AM, Roberts SM, Olsen OH, Persson E. Structure of human factor VIIa and its implications for the triggering of blood coagulation. *Proc Natl Acad Sci U S A*. 1999;96(16):8925-30.
342. Kemball-Cook G, Johnson DJ, Tuddenham EG, Harlos K. Crystal structure of active site-inhibited human coagulation factor VIIa (des-Gla). *J Struct Biol*. 1999;127(3):213-23.
343. Hollestelle MJ, Geertzen HG, Straatsburg IH, van Gulik TM, van Mourik JA. Factor VIII expression in liver disease. *Thromb Haemost*. 2004;91(2):267-75.
344. Suzuki T, Yamauchi K, Matsushita T, Furumichi T, Furui H, Tsuzuki J, et al. Elevation of factor VII activity and mass in coronary artery disease of varying severity. *Clin Cardiol*. 1991;14(9):731-6.
345. Wilcox JN, Noguchi S, Casanova J. Extrahepatic Synthesis of Factor VII in Human Atherosclerotic Vessels. *Arteriosclerosis, Thrombosis, and Vascular Biology*. 2003;23(1):136-41.

346. Tsao BP, Fair DS, Curtiss LK, Edgington TS. Monocytes can be induced by lipopolysaccharide-triggered T lymphocytes to express functional factor VII/VIIa protease activity. *J Exp Med*. 1984;159(4):1042-57.
347. Wilcox JN, Noguchi S, Casanova J. Extrahepatic synthesis of factor VII in human atherosclerotic vessels. *Arterioscler Thromb Vasc Biol*. 2003;23(1):136-41.
348. Koizume S, Miyagi Y. Tissue Factor–Factor VII Complex as a Key Regulator of Ovarian Cancer Phenotypes. *Biomarkers in Cancer*. 2015;7s2:BIC.S29318.
349. Åberg M, Edén D, Siegbahn A. Activation of β 1 integrins and caveolin-1 by TF/FVIIa promotes IGF-1R signaling and cell survival. *Apoptosis*. 2020;25(7-8):519-34.
350. Cirillo P, Cali G, Golino P, Calabrò P, Forte L, De Rosa S, et al. Tissue factor binding of activated factor VII triggers smooth muscle cell proliferation via extracellular signal-regulated kinase activation. *Circulation*. 2004;109(23):2911-6.
351. Moris M, Bridges MD, Pooley RA, Raimondo M, Woodward TA, Stauffer JA, et al. Association Between Advances in High-Resolution Cross-Section Imaging Technologies and Increase in Prevalence of Pancreatic Cysts From 2005 to 2014. *Clin Gastroenterol Hepatol*. 2016;14(4):585-93.e3.
352. Kromrey ML, Bülow R, Hübner J, Paperlein C, Lerch MM, Ittermann T, et al. Prospective study on the incidence, prevalence and 5-year pancreatic-related mortality of pancreatic cysts in a population-based study. *Gut*. 2018;67(1):138-45.
353. Laffan TA, Horton KM, Klein AP, Berlanstein B, Siegelman SS, Kawamoto S, et al. Prevalence of unsuspected pancreatic cysts on MDCT. *AJR Am J Roentgenol*. 2008;191(3):802-7.
354. Zhang XM, Mitchell DG, Dohke M, Holland GA, Parker L. Pancreatic cysts: depiction on single-shot fast spin-echo MR images. *Radiology*. 2002;223(2):547-53.
355. Girometti R, Intini SG, Cereser L, Bazzocchi M, Como G, Del Pin M, et al. Incidental pancreatic cysts: a frequent finding in liver-transplanted patients as assessed by 3D T2-weighted turbo spin echo magnetic resonance cholangiopancreatography. *Jop*. 2009;10(5):507-14.
356. Fernández-del Castillo C, Targarona J, Thayer SP, Rattner DW, Brugge WR, Warshaw AL. Incidental pancreatic cysts: clinicopathologic characteristics and comparison with symptomatic patients. *Archives of surgery (Chicago, Ill : 1960)*. 2003;138(4):427-34.
357. Babiker HM, Hoilat GJ, Mukkamalla SKR. *Mucinous Cystic Pancreatic Neoplasms*. StatPearls. Treasure Island (FL): StatPearls Publishing

Copyright © 2022, StatPearls Publishing LLC.; 2022.

358. Warshaw AL, Compton CC, Lewandrowski K, Cardenosa G, Mueller PR. Cystic tumors of the pancreas. New clinical, radiologic, and pathologic observations in 67 patients. *Ann Surg*. 1990;212(4):432-43; discussion 44-5.
359. Aronsson L, Marinko S, Ansari D, Andersson R. Adjuvant therapy in invasive intraductal papillary mucinous neoplasm (IPMN) of the pancreas: a systematic review. *Ann Transl Med*. 2019;7(22):689.
360. Assarzagagan N, Babaniamansour S, Shi J. Updates in the Diagnosis of Intraductal Neoplasms of the Pancreas. *Frontiers in Physiology*. 2022;13.
361. Oyama H, Tada M, Takagi K, Tateishi K, Hamada T, Nakai Y, et al. Long-term Risk of Malignancy in Branch-Duct Intraductal Papillary Mucinous Neoplasms. *Gastroenterology*. 2020;158(1):226-37.e5.

362. Valsangkar NP, Morales-Oyarvide V, Thayer SP, Ferrone CR, Wargo JA, Warshaw AL, et al. 851 resected cystic tumors of the pancreas: a 33-year experience at the Massachusetts General Hospital. *Surgery*. 2012;152(3 Suppl 1):S4-S12.
363. Das A, Wells CD, Nguyen CC. Incidental cystic neoplasms of pancreas: what is the optimal interval of imaging surveillance? *Am J Gastroenterol*. 2008;103(7):1657-62.
364. Miller FH, Lopes Vendrami C, Recht HS, Wood CG, Mittal P, Keswani RN, et al. Pancreatic Cystic Lesions and Malignancy: Assessment, Guidelines, and the Field Defect. *Radiographics*. 2022;42(1):87-105.
365. Buerlein RCD, Shami VM. Management of pancreatic cysts and guidelines: what the gastroenterologist needs to know. *Ther Adv Gastrointest Endosc*. 2021;14:26317745211045769.
366. Berland LL, Silverman SG, Gore RM, Mayo-Smith WW, Megibow AJ, Yee J, et al. Managing incidental findings on abdominal CT: white paper of the ACR incidental findings committee. *J Am Coll Radiol*. 2010;7(10):754-73.
367. Bassi C, Crippa S, Salvia R. Intraductal papillary mucinous neoplasms (IPMNs): is it time to (sometimes) spare the knife? *Gut*. 2008;57(3):287-9.
368. Brounts LR, Lehmann RK, Causey MW, Sebesta JA, Brown TA. Natural course and outcome of cystic lesions in the pancreas. *Am J Surg*. 2009;197(5):619-22; discussion 22-3.
369. Salvia R, Crippa S, Falconi M, Bassi C, Guarise A, Scarpa A, et al. Branch-duct intraductal papillary mucinous neoplasms of the pancreas: to operate or not to operate? *Gut*. 2007;56(8):1086-90.
370. Rautou PE, Lévy P, Vullierme MP, O'Toole D, Couvelard A, Cazals-Hatem D, et al. Morphologic changes in branch duct intraductal papillary mucinous neoplasms of the pancreas: a midterm follow-up study. *Clin Gastroenterol Hepatol*. 2008;6(7):807-14.
371. Kang MJ, Jang JY, Kim SJ, Lee KB, Ryu JK, Kim YT, et al. Cyst growth rate predicts malignancy in patients with branch duct intraductal papillary mucinous neoplasms. *Clin Gastroenterol Hepatol*. 2011;9(1):87-93.
372. Kwong WT, Lawson RD, Hunt G, Fehmi SM, Proudfoot JA, Xu R, et al. Rapid Growth Rates of Suspected Pancreatic Cyst Branch Duct Intraductal Papillary Mucinous Neoplasms Predict Malignancy. *Dig Dis Sci*. 2015;60(9):2800-6.
373. Kim TH, Song TJ, Hwang JH, Yoo KS, Lee WJ, Lee KH, et al. Predictors of malignancy in pure branch duct type intraductal papillary mucinous neoplasm of the pancreas: A nationwide multicenter study. *Pancreatol*. 2015;15(4):405-10.
374. van der Waaij LA, van Dullemen HM, Porte RJ. Cyst fluid analysis in the differential diagnosis of pancreatic cystic lesions: a pooled analysis. *Gastrointest Endosc*. 2005;62(3):383-9.
375. Thosani N, Thosani S, Qiao W, Fleming JB, Bhutani MS, Guha S. Role of EUS-FNA-based cytology in the diagnosis of mucinous pancreatic cystic lesions: a systematic review and meta-analysis. *Dig Dis Sci*. 2010;55(10):2756-66.
376. Pitman MB, Centeno BA, Genevay M, Fonseca R, Mino-Kenudson M. Grading epithelial atypia in endoscopic ultrasound-guided fine-needle aspiration of intraductal papillary mucinous neoplasms: an international interobserver concordance study. *Cancer Cytopathol*. 2013;121(12):729-36.
377. Bhutani MS, Gupta V, Guha S, Gheonea DI, Saftoiu A. Pancreatic cyst fluid analysis--a review. *J Gastrointest Liver Dis*. 2011;20(2):175-80.

378. Park WG, Mascarenhas R, Palaez-Luna M, Smyrk TC, O'Kane D, Clain JE, et al. Diagnostic performance of cyst fluid carcinoembryonic antigen and amylase in histologically confirmed pancreatic cysts. *Pancreas*. 2011;40(1):42-5.
379. Sawhney MS, Devarajan S, O'Farrel P, Cury MS, Kundu R, Vollmer CM, et al. Comparison of carcinoembryonic antigen and molecular analysis in pancreatic cyst fluid. *Gastrointest Endosc*. 2009;69(6):1106-10.
380. Attasaranya S, Pais S, LeBlanc J, McHenry L, Sherman S, DeWitt JM. Endoscopic ultrasound-guided fine needle aspiration and cyst fluid analysis for pancreatic cysts. *Jop*. 2007;8(5):553-63.
381. Shen J, Brugge WR, Dimaio CJ, Pitman MB. Molecular analysis of pancreatic cyst fluid: a comparative analysis with current practice of diagnosis. *Cancer*. 2009;117(3):217-27.
382. Khalid A, Zahid M, Finkelstein SD, LeBlanc JK, Kaushik N, Ahmad N, et al. Pancreatic cyst fluid DNA analysis in evaluating pancreatic cysts: a report of the PANDA study. *Gastrointest Endosc*. 2009;69(6):1095-102.
383. Brugge WR, Lauwers GY, Sahani D, Fernandez-del Castillo C, Warshaw AL. Cystic neoplasms of the pancreas. *N Engl J Med*. 2004;351(12):1218-26.
384. Scourtas A, Dudley JC, Brugge WR, Kadayifci A, Mino-Kenudson M, Pitman MB. Preoperative characteristics and cytological features of 136 histologically confirmed pancreatic mucinous cystic neoplasms. *Cancer Cytopathol*. 2017;125(3):169-77.
385. Talar-Wojnarowska R, Pazurek M, Durko L, Degowska M, Rydzewska G, Smigielski J, et al. Pancreatic cyst fluid analysis for differential diagnosis between benign and malignant lesions. *Oncol Lett*. 2013;5(2):613-6.
386. Walsh RM, Henderson JM, Vogt DP, Baker ME, O'Malley C M, Jr., Herts B, et al. Prospective preoperative determination of mucinous pancreatic cystic neoplasms. *Surgery*. 2002;132(4):628-33; discussion 33-4.
387. Morris-Stiff G, Lentz G, Chalikonda S, Johnson M, Biscotti C, Stevens T, et al. Pancreatic cyst aspiration analysis for cystic neoplasms: mucin or carcinoembryonic antigen--which is better? *Surgery*. 2010;148(4):638-44; discussion 44-5.
388. Maker AV, Katabi N, Gonen M, DeMatteo RP, D'Angelica MI, Fong Y, et al. Pancreatic cyst fluid and serum mucin levels predict dysplasia in intraductal papillary mucinous neoplasms of the pancreas. *Ann Surg Oncol*. 2011;18(1):199-206.
389. Sinha J, Cao Z, Dai J, Tang H, Partyka K, Hostetter G, et al. A Gastric Glycoform of MUC5AC Is a Biomarker of Mucinous Cysts of the Pancreas. *PLoS One*. 2016;11(12):e0167070.
390. Kadayifci A, Atar M, Wang JL, Forcione DG, Casey BW, Pitman MB, et al. Value of adding GNAS testing to pancreatic cyst fluid KRAS and carcinoembryonic antigen analysis for the diagnosis of intraductal papillary mucinous neoplasms. *Dig Endosc*. 2017;29(1):111-7.
391. Singhi AD, McGrath K, Brand RE, Khalid A, Zeh HJ, Chennat JS, et al. Preoperative next-generation sequencing of pancreatic cyst fluid is highly accurate in cyst classification and detection of advanced neoplasia. *Gut*. 2018;67(12):2131-41.
392. Ren R, Krishna SG, Chen W, Frankel WL, Shen R, Zhao W, et al. Activation of the RAS pathway through uncommon BRAF mutations in mucinous pancreatic cysts without KRAS mutation. *Mod Pathol*. 2021;34(2):438-44.

393. Turner RC, Melnychuk JT, Chen W, Jones D, Krishna SG. Molecular Analysis of Pancreatic Cyst Fluid for the Management of Intraductal Papillary Mucinous Neoplasms. *Diagnostics (Basel)*. 2022;12(11).
394. Lee KM, Nguyen C, Ulrich AB, Pour PM, Ouellette MM. Immortalization with telomerase of the Nestin-positive cells of the human pancreas. *Biochemical and Biophysical Research Communications*. 2003;301(4):1038-44.
395. Campbell PM, Groehler AL, Lee KM, Ouellette MM, Khazak V, Der CJ. K-Ras Promotes Growth Transformation and Invasion of Immortalized Human Pancreatic Cells by Raf and Phosphatidylinositol 3-Kinase Signaling. *Cancer Research*. 2007;67(5):2098-106.
396. Human Coagulation Factor III/Tissue Factor Quantikine ELISA: R&D Systems®, Inc; [2017:[Available from: https://resources.rndsystems.com/pdfs/datasheets/dcf300.pdf?v=20220822&_ga=2.138222131.201812935.1661165396-921892190.1660048912.
397. Human Factor VII (Factor 7) AssayMax™ ELISA Kit: Universal Biologicals; [Available from: https://assaypro.com/Resources/pdf/EF1007_1.pdf.
398. Monarch® Total RNA Miniprep Kit: New England Biolabs; [updated 2020. Available from: <https://www.neb.com/-/media/nebus/files/manuals/manualt2010.pdf>.
399. Livak KJ, Schmittgen TD. Analysis of relative gene expression data using real-time quantitative PCR and the 2(-Delta Delta C) method. *Methods*. 2001;25(4):402-8.
400. Bustin SA, Benes V, Garson JA, Hellemans J, Huggett J, Kubista M, et al. The MIQE guidelines: minimum information for publication of quantitative real-time PCR experiments. *Clin Chem*. 2009;55(4):611-22.
401. Milsom C, Yu J, May L, Magnus N, Rak J. Diverse Roles of Tissue Factor-Expressing Cell Subsets in Tumor Progression. *Semin Thromb Hemost*. 2008;34(02):170-81.
402. Thaler J, Ay C, Mackman N, Metz-Schimmerl S, Stift J, Kaider A, et al. Microparticle-associated tissue factor activity in patients with pancreatic cancer: correlation with clinicopathological features. *Eur J Clin Invest*. 2013;43(3):277-85.
403. Date K, Ettelaie C, Maraveyas A. Tissue factor-bearing microparticles and inflammation: a potential mechanism for the development of venous thromboembolism in cancer. *J Thromb Haemost*. 2017;15(12):2289-99.
404. Echrish HH, Xiao Y, Madden LA, Allgar V, Cooke J, Wedgwood K, et al. Effect of resection of localized pancreaticobiliary adenocarcinoma on angiogenic markers and tissue factor related pro-thrombotic and pro-angiogenic activity. *Thrombosis Research*. 2014;134(2):479-87.
405. Zwicker JI, Liebman HA, Neuberg D, Lacroix R, Bauer KA, Furie BC, et al. Tumor-Derived Tissue Factor Bearing Microparticles Are Associated With Venous Thromboembolic Events in Malignancy. *Clinical Cancer Research*. 2009;15(22):6830-40.
406. Contrino J, Hair G, Kreutzer DL, Rickles FR. In situ detection of tissue factor in vascular endothelial cells: Correlation with the malignant phenotype of human breast disease. *Nature Medicine*. 1996;2(2):209-15.
407. Rao B, Gao Y, Huang J, Gao X, Fu X, Huang M, et al. Mutations of p53 and K-ras correlate TF expression in human colorectal carcinomas: TF downregulation as a marker of poor prognosis. *International Journal of Colorectal Disease*. 2011;26(5):593-601.

408. Rong Y, Belozarov VE, Tucker-Burden C, Chen G, Durden DL, Olson JJ, et al. Epidermal Growth Factor Receptor and PTEN Modulate Tissue Factor Expression in Glioblastoma through JunD/Activator Protein-1 Transcriptional Activity. *Cancer Research*. 2009;69(6):2540-9.
409. Bromberg ME, Sundaram R, Homer RJ, Garen A, Konigsberg WH. Role of tissue factor in metastasis: functions of the cytoplasmic and extracellular domains of the molecule. *Thromb Haemost*. 1999;82(1):88-92.
410. Koomägi R, Volm M. Tissue-factor expression in human non-small-cell lung carcinoma measured by immunohistochemistry: Correlation between tissue factor and angiogenesis. *International Journal of Cancer*. 1998;79(1):19-22.
411. Milsom CC, Yu JL, Mackman N, Micallef J, Anderson GM, Guha A, et al. Tissue Factor Regulation by Epidermal Growth Factor Receptor and Epithelial-to-Mesenchymal Transitions: Effect on Tumor Initiation and Angiogenesis. *Cancer Research*. 2008;68(24):10068-76.
412. Versteeg HH, Schaffner F, Kerver M, Petersen HH, Ahamed J, Felding-Habermann B, et al. Inhibition of tissue factor signaling suppresses tumor growth. *Blood*. 2008;111(1):190-9.
413. Garnier D, Magnus N, D'Asti E, Hashemi M, Meehan B, Milsom C, et al. Genetic pathways linking hemostasis and cancer. *Thromb Res*. 2012;129 Suppl 1:S22-9.
414. Pradier A, Ettelaie C. The influence of exogenous tissue factor on the regulators of proliferation and apoptosis in endothelial cells. *J Vasc Res*. 2008;45(1):19-32.
415. Alkistis Frentzou G, Collier ME, Seymour AM, Ettelaie C. Differential induction of cellular proliferation, hypertrophy and apoptosis in H9c2 cardiomyocytes by exogenous tissue factor. *Mol Cell Biochem*. 2010;345(1-2):119-30.
416. ElKeab AM, Collier ME, Maraveyas A, Ettelaie C. Accumulation of tissue factor in endothelial cells induces cell apoptosis, mediated through p38 and p53 activation. *Thromb Haemost*. 2015;114(2):364-78.
417. Aharon A, Tamari T, Brenner B. Monocyte-derived microparticles and exosomes induce procoagulant and apoptotic effects on endothelial cells. *Thromb Haemost*. 2008;100(5):878-85.
418. Shinagawa K, Ploplis VA, Castellino FJ. A severe deficiency of coagulation factor VIIa results in attenuation of the asthmatic response in mice. *Am J Physiol Lung Cell Mol Physiol*. 2009;296(5):L763-70.
419. ElKeab AM, Collier MEW, Maraveyas A, Ettelaie C. Accumulation of tissue factor in endothelial cells induces cell apoptosis, mediated through p38 and p53 activation. *Thromb Haemost*. 2015;114(08):364-78.
420. Madkhali Y, Featherby S, Collier ME, Maraveyas A, Greenman J, Ettelaie C. The Ratio of Factor VIIa:Tissue Factor Content within Microvesicles Determines the Differential Influence on Endothelial Cells. *TH Open*. 2019;3(2):e132-e45.
421. Koizume S, Miyagi Y. Tissue factor in cancer-associated thromboembolism: possible mechanisms and clinical applications. *Br J Cancer*. 2022.
422. Claussen C, Rausch AV, Lezius S, Amirkhosravi A, Davila M, Francis JL, et al. Microvesicle-associated tissue factor procoagulant activity for the preoperative diagnosis of ovarian cancer. *Thromb Res*. 2016;141:39-48.
423. Khorana AA, Kamphuisen PW, Meyer G, Bauersachs R, Janas MS, Jarner MF, et al. Tissue Factor As a Predictor of Recurrent Venous Thromboembolism in Malignancy: Biomarker Analyses of the CATCH Trial. *J Clin Oncol*. 2017;35(10):1078-85.

424. Collier MEW, Ettelaie C, Goult BT, Maraveyas A, Goodall AH. Investigation of the Filamin A-Dependent Mechanisms of Tissue Factor Incorporation into Microvesicles. *Thromb Haemost.* 2017;117(11):2034-44.
425. Lee RD, Barcel DA, Williams JC, Wang JG, Boles JC, Manly DA, et al. Pre-analytical and analytical variables affecting the measurement of plasma-derived microparticle tissue factor activity. *Thromb Res.* 2012;129(1):80-5.
426. Bland JM, Altman DG. Statistical methods for assessing agreement between two methods of clinical measurement. *Lancet.* 1986;1(8476):307-10.
427. Del Chiaro M, Verbeke C, Salvia R, Klöppel G, Werner J, McKay C, et al. European experts consensus statement on cystic tumours of the pancreas. *Dig Liver Dis.* 2013;45(9):703-11.
428. Mukewar S, de Pretis N, Aryal-Khanal A, Ahmed N, Sah R, Enders F, et al. Fukuoka criteria accurately predict risk for adverse outcomes during follow-up of pancreatic cysts presumed to be intraductal papillary mucinous neoplasms. *Gut.* 2017;66(10):1811-7.
429. Fernández-del Castillo C, Adsay NV. Intraductal papillary mucinous neoplasms of the pancreas. *Gastroenterology.* 2010;139(3):708-13, 13.e1-2.
430. Vege SS, Ziring B, Jain R, Moayyedi P. American gastroenterological association institute guideline on the diagnosis and management of asymptomatic neoplastic pancreatic cysts. *Gastroenterology.* 2015;148(4):819-22; quiz12-3.
431. Sharib J, Esserman L, Koay EJ, Maitra A, Shen Y, Kirkwood KS, et al. Cost-effectiveness of consensus guideline based management of pancreatic cysts: The sensitivity and specificity required for guidelines to be cost-effective. *Surgery.* 2020;168(4):601-9.
432. Tanaka M, Chari S, Adsay V, Fernandez-del Castillo C, Falconi M, Shimizu M, et al. International consensus guidelines for management of intraductal papillary mucinous neoplasms and mucinous cystic neoplasms of the pancreas. *Pancreatology.* 2006;6(1-2):17-32.
433. Gaujoux S, Brennan MF, Gonen M, D'Angelica MI, DeMatteo R, Fong Y, et al. Cystic lesions of the pancreas: changes in the presentation and management of 1,424 patients at a single institution over a 15-year time period. *J Am Coll Surg.* 2011;212(4):590-600; discussion -3.
434. Ånonsen K, Sahakyan MA, Kleive D, Waage A, Verbeke C, Hauge T, et al. Trends in management and outcome of cystic pancreatic lesions - analysis of 322 cases undergoing surgical resection. *Scand J Gastroenterol.* 2019;54(8):1051-7.
435. Vaalavuo Y, Antila A, Ahola R, Siiki A, Vornanen M, Ukkonen M, et al. Characteristics and long-term survival of resected pancreatic cystic neoplasms in Finland. The first nationwide retrospective cohort analysis. *Pancreatology.* 2019;19(3):456-61.
436. Kang JS, Park T, Han Y, Lee S, Lim H, Kim H, et al. Clinical validation of the 2017 international consensus guidelines on intraductal papillary mucinous neoplasm of the pancreas. *Ann Surg Treat Res.* 2019;97(2):58-64.
437. Snozek CL, Mascarenhas RC, O'Kane DJ. Use of cyst fluid CEA, CA19-9, and amylase for evaluation of pancreatic lesions. *Clin Biochem.* 2009;42(15):1585-8.
438. Gonzalez Obeso E, Murphy E, Brugge W, Deshpande V. Pseudocyst of the pancreas: the role of cytology and special stains for mucin. *Cancer.* 2009;117(2):101-7.
439. Kalluri R, Weinberg RA. The basics of epithelial-mesenchymal transition. *J Clin Invest.* 2009;119(6):1420-8.

440. Kalluri R, Neilson EG. Epithelial-mesenchymal transition and its implications for fibrosis. *J Clin Invest.* 2003;112(12):1776-84.
441. Kalluri R. EMT: when epithelial cells decide to become mesenchymal-like cells. *J Clin Invest.* 2009;119(6):1417-9.
442. Nieto MA, Huang RY, Jackson RA, Thiery JP. EMT: 2016. *Cell.* 2016;166(1):21-45.
443. Ocaña OH, Córcoles R, Fabra A, Moreno-Bueno G, Acloque H, Vega S, et al. Metastatic colonization requires the repression of the epithelial-mesenchymal transition inducer Prrx1. *Cancer Cell.* 2012;22(6):709-24.
444. Tsai JH, Donaher JL, Murphy DA, Chau S, Yang J. Spatiotemporal regulation of epithelial-mesenchymal transition is essential for squamous cell carcinoma metastasis. *Cancer Cell.* 2012;22(6):725-36.
445. Tsai JH, Yang J. Epithelial-mesenchymal plasticity in carcinoma metastasis. *Genes Dev.* 2013;27(20):2192-206.
446. Brabletz T. To differentiate or not--routes towards metastasis. *Nat Rev Cancer.* 2012;12(6):425-36.
447. Chaffer CL, San Juan BP, Lim E, Weinberg RA. EMT, cell plasticity and metastasis. *Cancer Metastasis Rev.* 2016;35(4):645-54.
448. Lambert AW, Pattabiraman DR, Weinberg RA. Emerging Biological Principles of Metastasis. *Cell.* 2017;168(4):670-91.
449. Lamouille S, Xu J, Derynck R. Molecular mechanisms of epithelial-mesenchymal transition. *Nat Rev Mol Cell Biol.* 2014;15(3):178-96.
450. Peinado H, Olmeda D, Cano A. Snail, Zeb and bHLH factors in tumour progression: an alliance against the epithelial phenotype? *Nat Rev Cancer.* 2007;7(6):415-28.
451. Thiery JP, Acloque H, Huang RY, Nieto MA. Epithelial-mesenchymal transitions in development and disease. *Cell.* 2009;139(5):871-90.
452. Chaffer CL, Weinberg RA. A perspective on cancer cell metastasis. *Science.* 2011;331(6024):1559-64.
453. Smith BN, Bhowmick NA. Role of EMT in Metastasis and Therapy Resistance. *J Clin Med.* 2016;5(2).
454. Guo W. Concise review: breast cancer stem cells: regulatory networks, stem cell niches, and disease relevance. *Stem Cells Transl Med.* 2014;3(8):942-8.
455. Zeisberg M, Neilson EG. Biomarkers for epithelial-mesenchymal transitions. *J Clin Invest.* 2009;119(6):1429-37.
456. Huber MA, Kraut N, Beug H. Molecular requirements for epithelial-mesenchymal transition during tumor progression. *Curr Opin Cell Biol.* 2005;17(5):548-58.
457. Yingling JM, Blanchard KL, Sawyer JS. Development of TGF-beta signalling inhibitors for cancer therapy. *Nat Rev Drug Discov.* 2004;3(12):1011-22.
458. Rachagani S, Senapati S, Chakraborty S, Ponnusamy MP, Kumar S, Smith LM, et al. Activated Kras^{G12D} is associated with invasion and metastasis of pancreatic cancer cells through inhibition of E-cadherin. *Br J Cancer.* 2011;104(6):1038-48.
459. Thiery JP. Epithelial-mesenchymal transitions in development and pathologies. *Curr Opin Cell Biol.* 2003;15(6):740-6.

460. Espinoza I, Pochampally R, Xing F, Watabe K, Miele L. Notch signaling: targeting cancer stem cells and epithelial-to-mesenchymal transition. *Onco Targets Ther.* 2013;6:1249-59.
461. Zhou BP, Hung MC. Wnt, hedgehog and snail: sister pathways that control by GSK-3beta and beta-Trcp in the regulation of metastasis. *Cell Cycle.* 2005;4(6):772-6.
462. Feldmann G, Dhara S, Fendrich V, Bedja D, Beaty R, Mullendore M, et al. Blockade of hedgehog signaling inhibits pancreatic cancer invasion and metastases: a new paradigm for combination therapy in solid cancers. *Cancer Res.* 2007;67(5):2187-96.
463. Rhim Andrew D, Mirek Emily T, Aiello Nicole M, Maitra A, Bailey Jennifer M, McAllister F, et al. EMT and Dissemination Precede Pancreatic Tumor Formation. *Cell.* 2012;148(1):349-61.
464. Sakorafas GH, Sarr MG. Pancreatic cancer after surgery for chronic pancreatitis. *Dig Liver Dis.* 2003;35(7):482-5.
465. Condeelis J, Pollard JW. Macrophages: Obligate Partners for Tumor Cell Migration, Invasion, and Metastasis. *Cell.* 2006;124(2):263-6.
466. Wyckoff JB, Wang Y, Lin EY, Li J-f, Goswami S, Stanley ER, et al. Direct Visualization of Macrophage-Assisted Tumor Cell Intravasation in Mammary Tumors. *Cancer Research.* 2007;67(6):2649-56.
467. Grover S, Syngal S. Hereditary Pancreatic Cancer. *Gastroenterology.* 2010;139(4):1076-80.e2.
468. Guerra C, Schuhmacher AJ, Canamero M, Grippo PJ, Verdaguer L, Perez-Gallego L, et al. Chronic pancreatitis is essential for induction of pancreatic ductal adenocarcinoma by K-Ras oncogenes in adult mice. *Cancer Cell.* 2007;11(3):291-302.
469. Guerra C, Collado M, Navas C, Schuhmacher AJ, Hernandez-Porras I, Canamero M, et al. Pancreatitis-induced inflammation contributes to pancreatic cancer by inhibiting oncogene-induced senescence. *Cancer Cell.* 2011;19(6):728-39.
470. Wu Y, Deng J, Rychahou PG, Qiu S, Evers BM, Zhou BP. Stabilization of snail by NF-kappaB is required for inflammation-induced cell migration and invasion. *Cancer cell.* 2009;15(5):416-28.
471. Karin M. Nuclear factor-kappaB in cancer development and progression. *Nature.* 2006;441(7092):431-6.
472. Grünert S, Jechlinger M, Beug H. Diverse cellular and molecular mechanisms contribute to epithelial plasticity and metastasis. *Nature Reviews Molecular Cell Biology.* 2003;4(8):657-65.
473. Rothwell PM, Fowkes FGR, Belch JFF, Ogawa H, Warlow CP, Meade TW. Effect of daily aspirin on long-term risk of death due to cancer: analysis of individual patient data from randomised trials. *The Lancet.* 2011;377(9759):31-41.
474. Garnier D, Magnus N, Lee TH, Bentley V, Meehan B, Milsom C, et al. Cancer cells induced to express mesenchymal phenotype release exosome-like extracellular vesicles carrying tissue factor. *J Biol Chem.* 2012;287(52):43565-72.
475. Fischer EG, Riewald M, Huang HY, Miyagi Y, Kubota Y, Mueller BM, et al. Tumor cell adhesion and migration supported by interaction of a receptor-protease complex with its inhibitor. *J Clin Invest.* 1999;104(9):1213-21.
476. Pollak ES, Hung HL, Godin W, Overton GC, High KA. Functional characterization of the human factor VII 5'-flanking region. *J Biol Chem.* 1996;271(3):1738-47.
477. Erdmann D, Heim J. Orphan nuclear receptor HNF-4 binds to the human coagulation factor VII promoter. *J Biol Chem.* 1995;270(39):22988-96.

478. Greenberg D, Miao CH, Ho WT, Chung DW, Davie EW. Liver-specific expression of the human factor VII gene. *Proc Natl Acad Sci U S A*. 1995;92(26):12347-51.
479. Koizume S, Yokota N, Miyagi E, Hirahara F, Nakamura Y, Sakuma Y, et al. Hepatocyte nuclear factor-4-independent synthesis of coagulation factor VII in breast cancer cells and its inhibition by targeting selective histone acetyltransferases. *Mol Cancer Res*. 2009;7(12):1928-36.
480. Xu J, Lamouille S, Derynck R. TGF- β -induced epithelial to mesenchymal transition. *Cell Research*. 2009;19(2):156-72.
481. Pantel K, Brakenhoff RH, Brandt B. Detection, clinical relevance and specific biological properties of disseminating tumour cells. *Nat Rev Cancer*. 2008;8(5):329-40.
482. Neoptolemos JP, Stocken DD, Friess H, Bassi C, Dunn JA, Hickey H, et al. A randomized trial of chemoradiotherapy and chemotherapy after resection of pancreatic cancer. *N Engl J Med*. 2004;350(12):1200-10.
483. Hüsemann Y, Geigl JB, Schubert F, Musiani P, Meyer M, Burghart E, et al. Systemic spread is an early step in breast cancer. *Cancer Cell*. 2008;13(1):58-68.
484. Podsypanina K, Du YC, Jechlinger M, Beverly LJ, Hambardzumyan D, Varmus H. Seeding and propagation of untransformed mouse mammary cells in the lung. *Science*. 2008;321(5897):1841-4.
485. Wang Y, Sang A, Zhu M, Zhang G, Guan H, Ji M, et al. Tissue factor induces VEGF expression via activation of the Wnt/ β -catenin signaling pathway in ARPE-19 cells. *Mol Vis*. 2016;22:886-97.
486. Roy A, Ansari SA, Das K, Prasad R, Bhattacharya A, Mallik S, et al. Coagulation factor VIIa-mediated protease-activated receptor 2 activation leads to β -catenin accumulation via the AKT/GSK3 β pathway and contributes to breast cancer progression. *J Biol Chem*. 2017;292(33):13688-701.
487. Peña E, Arderiu G, Badimon L. Tissue factor induces human coronary artery smooth muscle cell motility through Wnt-signalling. *J Thromb Haemost*. 2013;11(10):1880-91.
488. Boyer B, Tucker GC, Vallés AM, Gavrilovic J, Thiery JP. Reversible transition towards a fibroblastic phenotype in a rat carcinoma cell line. *Int J Cancer Suppl*. 1989;4:69-75.
489. Yang J, Mani SA, Donaher JL, Ramaswamy S, Itzykson RA, Come C, et al. Twist, a master regulator of morphogenesis, plays an essential role in tumor metastasis. *Cell*. 2004;117(7):927-39.
490. Raymond WA, Leong AS. Vimentin--a new prognostic parameter in breast carcinoma? *J Pathol*. 1989;158(2):107-14.
491. Brown KA, Aakre ME, Gorska AE, Price JO, Eltom SE, Pietenpol JA, et al. Induction by transforming growth factor- β 1 of epithelial to mesenchymal transition is a rare event in vitro. *Breast Cancer Research*. 2004;6(3):R215.
492. Kasai H, Allen JT, Mason RM, Kamimura T, Zhang Z. TGF-beta1 induces human alveolar epithelial to mesenchymal cell transition (EMT). *Respir Res*. 2005;6(1):56.
493. Tsai C-C, Chou Y-T, Fu H-W. Protease-activated receptor 2 induces migration and promotes Slug-mediated epithelial-mesenchymal transition in lung adenocarcinoma cells. *Biochimica et Biophysica Acta (BBA) - Molecular Cell Research*. 2019;1866(3):486-503.
494. Bulle A, Lim K-H. Beyond just a tight fortress: contribution of stroma to epithelial-mesenchymal transition in pancreatic cancer. *Signal Transduction and Targeted Therapy*. 2020;5(1):249.
495. Kim SA, Lee EK, Kuh HJ. Co-culture of 3D tumor spheroids with fibroblasts as a model for epithelial-mesenchymal transition in vitro. *Exp Cell Res*. 2015;335(2):187-96.

496. Fröhlich E. Issues with Cancer Spheroid Models in Therapeutic Drug Screening. *Curr Pharm Des.* 2020;26(18):2137-48.
497. Ryu NE, Lee SH, Park H. Spheroid Culture System Methods and Applications for Mesenchymal Stem Cells. *Cells.* 2019;8(12).
498. Jeong SY, Lee JH, Shin Y, Chung S, Kuh HJ. Co-Culture of Tumor Spheroids and Fibroblasts in a Collagen Matrix-Incorporated Microfluidic Chip Mimics Reciprocal Activation in Solid Tumor Microenvironment. *PLoS One.* 2016;11(7):e0159013.
499. Fujiwara M, Kanayama K, Hirokawa YS, Shiraishi T. ASF-4-1 fibroblast-rich culture increases chemoresistance and mTOR expression of pancreatic cancer BxPC-3 cells at the invasive front in vitro, and promotes tumor growth and invasion in vivo. *Oncol Lett.* 2016;11(4):2773-9.
500. Hwang RF, Moore T, Arumugam T, Ramachandran V, Amos KD, Rivera A, et al. Cancer-associated stromal fibroblasts promote pancreatic tumor progression. *Cancer Res.* 2008;68(3):918-26.
501. Rhim AD, Oberstein PE, Thomas DH, Mirek ET, Palermo CF, Sastra SA, et al. Stromal elements act to restrain, rather than support, pancreatic ductal adenocarcinoma. *Cancer Cell.* 2014;25(6):735-47.
502. Seino T, Kawasaki S, Shimokawa M, Tamagawa H, Toshimitsu K, Fujii M, et al. Human Pancreatic Tumor Organoids Reveal Loss of Stem Cell Niche Factor Dependence during Disease Progression. *Cell Stem Cell.* 2018;22(3):454-67.e6.
503. Sung H, Ferlay J, Siegel RL, Laversanne M, Soerjomataram I, Jemal A, et al. Global Cancer Statistics 2020: GLOBOCAN Estimates of Incidence and Mortality Worldwide for 36 Cancers in 185 Countries. *CA: A Cancer Journal for Clinicians.* 2021;71(3):209-49.
504. Izawa T, Obara T, Tanno S, Mizukami Y, Yanagawa N, Kohgo Y. Clonality and field cancerization in intraductal papillary-mucinous tumors of the pancreas. *Cancer.* 2001;92(7):1807-17.
505. Frankel TL, LaFemina J, Bamboat ZM, D'Angelica MI, DeMatteo RP, Fong Y, et al. Dysplasia at the surgical margin is associated with recurrence after resection of non-invasive intraductal papillary mucinous neoplasms. *HPB (Oxford).* 2013;15(10):814-21.
506. Wada K, Kozarek RA, Traverso LW. Outcomes following resection of invasive and noninvasive intraductal papillary mucinous neoplasms of the pancreas. *Am J Surg.* 2005;189(5):632-6; discussion 7.
507. Raut CP, Cleary KR, Staerckel GA, Abbruzzese JL, Wolff RA, Lee JH, et al. Intraductal papillary mucinous neoplasms of the pancreas: effect of invasion and pancreatic margin status on recurrence and survival. *Ann Surg Oncol.* 2006;13(4):582-94.
508. Chari ST, Yadav D, Smyrk TC, DiMagno EP, Miller LJ, Raimondo M, et al. Study of recurrence after surgical resection of intraductal papillary mucinous neoplasm of the pancreas. *Gastroenterology.* 2002;123(5):1500-7.
509. Maguchi H, Tanno S, Mizuno N, Hanada K, Kobayashi G, Hatori T, et al. Natural history of branch duct intraductal papillary mucinous neoplasms of the pancreas: a multicenter study in Japan. *Pancreas.* 2011;40(3):364-70.
510. Rockville M. HCUPnet Healthcare Cost and Project Utilization: Agency for Healthcare Research and Quality,

; [Available from: <https://hcupnet.ahrq.gov/>].

511. Cazacu IM, Luzuriaga Chavez AA, Saftoiu A, Bhutani MS. Psychological impact of pancreatic cancer screening by EUS or magnetic resonance imaging in high-risk individuals: A systematic review. *Endosc Ultrasound*. 2019;8(1):17-24.
512. Overbeek KA, Cahen DL, Kamps A, Konings ICAW, Harinck F, Kuenen MA, et al. Patient-reported burden of intensified surveillance and surgery in high-risk individuals under pancreatic cancer surveillance. *Familial Cancer*. 2020;19(3):247-58.

List of symbols and abbreviations

%	Percentage
°C	Degree celsius
ACG	American College of Gastroenterology
ADP	Adenosine diphosphate
AF	Alexa Fluor
AFIP	Armed Forces Institute of Pathology
AGA	American Gastroenterology Association
Ang2	Angiopoietin-2
ANOVA	Analysis of Variance
AP	Activating peptide
AP	Alkaline phosphatase
AP-1	Activator protein-1
Arg	Arginine
ASGE	American Society of Gastrointestinal Endoscopy
Asp	Aspartic acid
asTF	Alternatively-spliced TF
ATCC	American Type Culture Collection
bFGF	Basic fibroblast growth factor
BSA	Bovine serum albumin
CA19-9	carbohydrate antigen 19-9
Ca ⁺²	Calcium ion
CAF	Cancer-associated fibroblasts
CAT	Cancer-associated thrombosis
CBP	CREB-binding protein
CCL2	Chemokines C-C motif chemokine ligand 2 (CCL2)
CD	Cluster of differentiation
cDNA	Complementary deoxyribonucleic acid
CEA	Carcinoembryonic antigen
CI	Confidence interval
CO ₂	Carbon dioxide
CPCs	Circulating pancreatic cells
CREB	Cyclic AMP-responsive element binding protein
CRF	Case report form
CSC	Cancer stem-like cell
CT	Computed tomography
CTCs	Circulating tumour cells
CXCL12	C-X-C motif chemokine ligand 12

Cys	Cysteine
Da	Dalton
DAPI	4',6-diamidino-2-phenylindole
DC	DC-dendritic cells
DDR	DNA damage response
DMEM	Dulbeco's modified essential medium
DMSO	Dimethyl sulphoxide
DNA	Deoxyribonucleic acid
EDTA	Ethylenediaminetetraacetic acid
EGFR	Epidermal growth factor receptor
ELISA	Enzyme-linked immunosorbent assay
EMT	Epithelial-to-mesenchymal transition
EMT-TFs	EMT-inducing transcription factors
ERCP	Endoscopic retrograde cholangiopancreatography
ERG-1	Early growth-response gene product-1
ERK	Extracellular signal-regulated kinase
Escherichia coli	E.coli
EUROPAC	European Registry of Hereditary Pancreatitis & Familial Pancreatic Cancer
EUS	Endoscopic ultrasonography
f	Factor
FCS	Foetal calf serum
FNA	Fine needle aspiration
GAPDH	Glyceraldehyde-3-phosphate dehydrogenase
gDNA	Genomic DNA
GDPR	General Data Protection Regulation
GNAS	Guanine nucleotide binding protein
GTP	Guanosine triphosphate
H ₂ SO ₄	Sulfuric acid
HCl	Hydrochloric acid
HCV	Hepatitis C virus
HGD	High-grade dysplasia
HIF	Hypoxia inducible factor
HIV	Human immunodeficiency virus
HPB	Hepatopancreaticobiliary
HPB MDT	Hepatobiliary and Pancreatic Multidisciplinary Team
HPNE	Human pancreatic nestin-expressing ductal cells
HPV	Human papillomavirus
HRA	Health Research Authority
HRD	Homologous recombination deficiency
HTA	Human Tissue Act

hTERT	Human telomerase reverse transcriptase
HUTH	Hull University Teaching Hospitals
IAP	International Association of Pancreatology
iCAFs	Inflammatory-type fibroblasts
ICAM-1	Intercellular adhesion molecule-1
ICG	International Consensus Guidelines
ICH GCP	International Conference for Harmonisation of Good Clinical Practice
IFN- γ	Interferon γ
IgG	Immunoglobulin G
IL	Interleukin
Ile	Isoleucine
IPMN	Intraductal Papillary Mucinous Neoplasm
JAK	Janus kinase
JNK	JUN amino-terminal kinase
KRAS	Kirsten rat sarcoma virus
LGD	Low-grade dysplasia
LPS	Lipopolysaccharide
Lys	Lysine
MBC	Metastatic breast cancer
MCN	Mucinous Cystic Neoplasm
MDSC	Myeloid derived suppressor cells
MET	Mesenchymal-to-epithelial transition
min	Minute
MMRD	Mismatch repair deficiency
MPD	Main pancreatic duct diameter
MRCP	Magnetic resonance cholangiopancreatography
MRI	Magnetic resonance imaging
mRNA	Messenger Ribonucleic acid
myCAFs	Myofibroblast-type fibroblasts
n	Nano
N	Normality
NET	Neutrophil extracellular trap
NF-kB	Nuclear factor-kappa B
NICE	National Institute of Health and Care Excellence
NPV	Negative predictive value
NS	Not significant
p16	p16 ^{INKa}
PanIN	Pancreatic intraepithelial neoplasia
PAR	Protease-activated receptor
PBS	Phosphate buffer saline
PBST	PBS containing Tween-20

PC	Pancreatic cancer
PCL	Pancreatic cystic lesions
PCN	Pancreatic cystic neoplasm
PDAC	Pancreatic ductal adenocarcinoma
PD-L1	Programmed death ligand 1
PE	R-phycoerythrin
PI3K	Phosphoinositide 3-kinases
PIF	Patient information leaflet
PIK3CA	Phosphatidylinositol-4,5-bisphosphate 3-kinase catalytic subunit alpha
PKC	Protein Kinase C
PPV	Positive predictive value
PSC	Pancreatic stellate cells
PTEN	Phosphatase and Tensin Homolog deleted on Chromosome 10
RAS	Rat sarcoma
REC	Research Ethics Committee
RNA	Ribonucleic acid
ROC	Receiver operating characteristic
ROS	Reactive oxygen species
RT-qPCR	Reverse transcription-quantitative polymerase chain reaction
SCT	Serous cystic tumour
SDS	Sodium dodecyl sulphate
SDS-PAGE	Sodium dodecyl sulphate - polyacrylamide gel electrophoresis
SEM	Standard error of mean
Ser	Serine
SP	Streptavidin-peroxidase
SPN	Solid pseudopapillary neoplasm
STAT	Signal transducer and activator of transcription
TAM	Tumour-associated macrophages.
TBS	Tris-HCl buffered saline
TBST	TBS containing Tween-20
TEMED	N,N,N',N'-tetramethylethylenediamine
TF	Tissue factor
TF+MV	TF-bearing microvesicles
TGF β	Transforming growth factor β
TME	Tumour microenvironment
TNBC	Triple-negative breast cancer
TNF α	Tumour necrosis factor α
Treg	Regulatory T-lymphocytes
Tris	Tris(hydroxymethyl)aminomethane
TNM stage	Tumour, Node, Metastasis stage
UK	United Kingdom

v/v	Volume to volume
VCAM-1	Vascular cell adhesion molecule-1
VEGF	Vascular endothelial growth factor
VTE	Venous thromboembolism
vWF	von Willebrand factor
w/v	Weight to volume
WHO	World Health Organisation
α	Alpha
β	Beta
μ	Micro

Appendix 1



Queen's Centre for Oncology and Haematology
Castle Hill Hospital
Castle Road
Cottingham
HU16 5JQ

Study of Tumour Regulatory Molecules as Markers of Malignancy in Pancreatic Cystic Lesions (TEM-PAC)

Protocol

Version 1.9

REC Reference Number: 18/LO/0736

R&D Reference Number: R2224

Chief Investigator: Professor Anthony Maraveyas
Department of Academic Oncology
Queen's Centre for Oncology and Haematology
Castle Hill Hospital
Castle Road, Cottingham
Hull, HU16 5JQ

Tel: 01482 461245

Email: anthony.maraveyas@nhs.net

This trial will be conducted in compliance with the protocol, GCP and the applicable regulatory requirements.

SignatureDate

The study Sponsor is Hull University Teaching Hospitals NHS Trust

Sponsor: Hull University Teaching Hospitals NHS Trust
 R&D Department
 Office 13, 2nd Floor Daisy Building
 Castle Hill Hospital
 Castle Road, Cottingham
 Hull, HU16 5JQ

SignatureDate

Contact details:

Chief Investigator	Professor Anthony Maraveyas, Professor and Honorary Consultant in Oncology Queen’s Centre for Oncology & Haematology Castle Hill Hospital Castle Road, Cottingham Hull, HU16 5JQ, UK	Tel: 01482 461245 Email: anthony.maraveyas@nhs.net
Co-Investigators	Dr Camille Ettelaie Lecturer in Biomedical Sciences Faculty of Health Science University of Hull Cottingham Road Hull, HU6 7RX, UK	Tel: 01482 465528 Email: C.Ettelaie@hull.ac.uk
	Dr Leonid Nikitenko Faculty of Health Sciences University of Hull Cottingham Road Hull, HU6 7RX, UK	Tel: Email: L.Nikitenko@hull.ac.uk
	Dr Abdul Razack	Tel:

	<p>Consultant Gastro-intestinal and Abdominal Radiologist Department of Radiology Castle Hill Hospital Castle Road, Cottingham Hull, HU16 5JQ, UK</p>	<p>Email: abdul.razack@nhs.net</p>
	<p>Mr Pavlos Lykoudis Consultant HPB Surgeon Department of Upper Gastrointestinal Surgery Castle Hill Hospital Castle Road, Cottingham Hull, HU16 5JQ, UK</p>	<p>Tel: Email: pavlos.lykoudis@nhs.net</p>
	<p>Dr Alexander Buchanan Specialist Registrar in General Surgery Castle Hill Hospital Castle Road, Cottingham Hull, HU16 5JQ, UK</p>	<p>Tel: Email: alex.buchanan1@nhs.net</p>
<i>Study Statistician</i>	<p>Dr Chao Huang Senior Lecturer in Statistics Allam Medical Building University of Hull, Cottingham Road Hull, HU6 7RX, UK</p>	<p>Tel: 01482 463281 Email: Chao.Huang@hyms.ac.uk</p>

Study Summary

The effective diagnosis of pancreatic cancer is often quite challenging, due to a lack of disease-specific symptoms, resulting in the majority of patients presenting with advanced disease, with an associated dismal prognosis. Earlier detection of pancreatic cancer, at a stage where surgery is feasible, would greatly increase the 5-year survival rate. Detecting pancreatic cancer early is therefore vital to improve the prognosis for these patients.

Pre-cancerous pancreatic cysts are an early indicator of malignant transformation. The ideal screening test would be capable of detecting pancreatic cancer at these initial stages. Current procedures for pancreatic cancer diagnosis are invasive, uncomfortable and costly, and can be considered unnecessary in those cysts found to be benign.

We propose to study a number of tumour regulatory molecules that have been the subject of research in laboratories at the University of Hull (e.g., tissue factor (TF), adrenomedullin (AM) using enzyme-linked immunosorbent assays (ELISA) tests) that have been studied in the context of carcinogenic transformation in more common malignancies but have yet to be fully tested in pancreatic malignant transformation. The recent introduction of platform technologies at the University of Hull has broadened this area of investigation by giving us access to next generation genomic sequencing and proteomic analyses of small amounts of tissue samples. We intend to analyse pancreatic cystic fluid samples using these technologies to discover new regulatory molecules.

Altogether, this study will measure the levels of novel regulatory molecules and genetic changes involved with pancreatic cancer carcinogenesis using a combination of conventional techniques (e.g. ELISA) and state-of-the-art platform technologies in pancreatic cysts from those patients in whom cancer may be suspected, to determine the potential of these molecules to serve as markers to detect early changes towards pancreatic cancer.

Lay Summary

Pancreatic cancer is difficult to diagnose early as it does not usually cause any signs or symptoms in these early stages. Once it reaches a more advanced stage, it is very difficult to treat and survival is poor. Diagnosing pancreatic cancer often requires a number of different tests, some of which can be invasive and uncomfortable. A non-invasive test capable of detecting pancreatic cancer in its earliest stages would therefore increase chances of survival and improve patient quality of life. Cysts found in the pancreas are often not cancerous, but on occasions are found to develop into pancreatic cancer. Detecting changes in these cysts before a cancer develops may provide a good way to detect cancer early.

We intend to use new laboratory tests that measure the levels of different proteins and also the changes in genes in blood, urine and cystic fluid samples. Initial studies in common cancers such as in breast, prostate and colon have shown promise for these protein-based or gene-based techniques to detect changes in cells that indicate early stages of development of a cancer. So we now intend to see if these tests are also effective in early detection of pancreatic cancer. In this study, these proteins will be measured in urine, blood and, where available, cystic fluid samples from patients diagnosed with cancer, or having investigations for pancreatic cysts, to determine whether they can serve as markers for early pancreatic cancer.

Background Information

Pancreatic cancer (PaC) is relatively rare, with a reported crude incidence rate in the UK for 2016-2018 of 15.8 per 100,000 population [1]. Despite this, it currently stands as the fifth leading cause of cancer death in

the UK. While a marked improvement in survival over time has been observed with other cancer types, the 5-year survival rate for PaC remains fairly dismal at 5%, with only moderate improvement in over 40 years. Of particular note, progress is hampered by its remarkably high incidence-to-mortality rate. Figures from 2016-2018 acknowledged an incidence of 10,500 newly diagnosed cases each year, which was almost matched by 9,600 deaths each year, for the same period [1].

The dismal prognosis associated with PaC can be largely attributed to the fact that disease-specific symptoms are rarely clinically apparent until the advanced stages of the disease [2] and consequently, of those patients with known stage at diagnosis, the majority (79%) present with stage III or IV disease [3]. At this point tumours have progressed beyond a stage where surgery is feasible, with almost half (46%) in England diagnosed after presenting as an emergency [4]. The most common type, pancreatic ductal adenocarcinoma (PDAC) is deemed resectable at the time of diagnosis in only 15-20% patients [2], and a margin-negative (R0) resection is achieved in only a small minority (less than 10%) [5].

For unresectable cancers, realistic therapy options are very limited, and can offer palliation only [6]. Systemic chemotherapy in this setting can only achieve a modest survival gain of 4-6 months. The best prospect for long-term survival is surgical resection followed by adjuvant chemotherapy, which extends median survival to 14-22 months, but still rarely offers a cure [5]. There has been some progress from the current standard of care of single-agent gemcitabine, with the introduction of new combination chemotherapy regimens, such as GEM-CAP [7], FOLFIRINOX [8] and nab-paclitaxel plus gemcitabine [9]. Although these have improved overall and progression-free survival, they also had a tendency to increase toxicity, and ultimately brought little long-term survival advantage.

The key point is that patients diagnosed in time for surgery have a much more favourable prognosis and have a much improved chance of surviving beyond 5 years after diagnosis. Within a population of resectable PaC, 5-year survival has been reported to exceed 75% in a subset with well-differentiated stage I cancers of <1 cm [10]. It is therefore vital to develop an effective screening method that is capable of accurately detecting PaC in its early stages (preinvasive or early invasive), as this could potentially dramatically improve prognosis for PaC patients. For successful adoption, the ideal screening test should, with appropriately high sensitivity and specificity, detect tumours which are small (preferably T1N0M0 margin-negative PaC) and confined to the pancreas, as well as high-grade dysplastic precursor lesions (pancreatic intraepithelial neoplasias [PanINs], intraductal papillary mucinous neoplasms [IPMNs] and mucinous cystic neoplasms [MCNs] [11, 12], collectively recognised as cystic lesions of the pancreas with malignant potential.

Recent advancements in imaging technology have led to the more frequent, often incidental detection of these cystic pancreatic lesions [13]. Indeed incidental pancreatic cysts are identified in approximately 1% of all patients undergoing cross-sectional imaging of the abdomen for unrelated indications [14]. However, while some lesions may indeed represent significant precursors of invasive adenocarcinoma, many of the small, asymptomatic lesions detected may in fact be completely benign or inconsequential.

The vast majority of potentially malignant lesions are of the IPMN type, and exhibit varying degrees of dysplasia. They are typically seen to form in either the main pancreatic duct ("main duct type"; MD-IPMN) or in one of its side branches ("branch duct type"; BD-IPMN). The associated risk of malignancy is high for MD-IPMNs (60-70%) and therefore the mainstay of treatment is surgical resection [15]. However the risk is generally much lower in BD-IPMNs (15-20%) [15, 16], and management of these lesions is more complicated; a large majority are found to be indolent at long-term follow-up, while the mean time interval for significant growth of these lesions is longer than two years [17]. Indeed one study found 77% of resected BD-IPMNs were benign, and another indicated only 4% of patients with BD-IPMN developed cancer after a 4-year surveillance period [16]. As such, observation alone may be adequate for a large proportion of these lesions

[16]. The surveillance approach carries costs, and also impacts on the psychological wellbeing of patients, who may be undergoing regular scans for what may ultimately prove to be a benign condition.

In the context of curative surgery being a serious procedure with high levels of morbidity and complications (30-50%), and mortality between 2-4% [16, 18], one recognises the challenges of surgery for patients with benign lesions. Therefore the risks associated with surgery must be carefully weighed against the potential benefits of resecting these lesions.

The key is to target all IPMNs displaying high-grade dysplasia or invasive cancer for surgical resection, but at the same time avoiding any unnecessary surgery and “overtreatment” of benign pancreatic cysts [16]. Despite the high sensitivity in detecting cystic lesions, the specificity unfortunately remains low, and current imaging modalities are unable to accurately differentiate between malignant, premalignant and benign cysts [18, 19], with insufficient predictive value to affirm resectability [20]. Current guidelines recommend larger lesions (>3 cm) that raise suspicion of malignancy should undergo diagnostic workup, often consisting of more invasive diagnostic procedures, which can impact on patient morbidity, as well as incur significant healthcare costs. Smaller lesions (<3 cm), which may be more difficult to characterise, often require continuous radiological follow-up at regular intervals; this prolonged uncertainty can result in considerable anxiety.

For pancreatic cysts, the amount of fluid removed for diagnostic tests varies from 10 to 50 ml and is sent for various tests (amylase, carcinoembryonic antigen [CEA] and mucin). Even when these investigations are implemented, their diagnostic accuracy is suboptimal, leaving a number of patients with equivocal findings that then need close costly follow-up and repeat investigations upon suspicion of changing characteristics of the cystic lesion.

Detecting PaC in its early stages will involve screening asymptomatic individuals. However, conventional population-based screening methods, as have been established, for example, for breast, cervical and bowel cancers, are not viable for PaC due to its comparatively low prevalence. Confirmative diagnosis of PaC is currently reliant upon costly and invasive procedures, such as endoscopic ultrasound (EUS) with fine needle aspiration (FNA), which would be impractical to implement as a general population screening method and itself carries a 2-6% risk of adverse events including pancreatitis and infection [21, 22]. Therefore, identifying early changes in easy to access tissue samples (such as urine and blood) would be a major breakthrough.

Tissue Factor (TF)

It has been established that localised pancreatic tumours are often characterised by high levels of tissue factor (TF) expression, which have been further correlated with histologic grade and poor prognosis [23-25], and are also predicted to contribute to the hypercoagulable state found in malignancy. This increased TF expression is also detectable in pancreatic precursor lesions (PanINs and IPMNs) [25], yet is absent from normal pancreas [23-25], confirming its appearance in early pancreatic neoplastic transformation.

Furthermore, our own data indicates that positive TF expression in tumours of PaC patients can be significantly correlated with elevated circulating levels of TF-bearing microparticles (TF+MPs) [26], which are further associated with risk of mortality [27, 28]. Our own study [26], and an earlier study by Zwicker et al. [29] further showed that the levels of TF+MP in PaC patients are reduced following pancreatectomy.

The presence of tissue factor (TF) in urine has been reported as a potential diagnostic marker for several cancers, including bladder, prostate, breast and colorectal cancers [30-32]. TF is synthesised initially as an unphosphorylated protein, but can subsequently undergo phosphorylation at two serine positions (Ser253 and Ser258) [33, 34]. Phosphorylation of TF is critically involved in intracellular signal transduction pathways,

regulates TF procoagulant activity in vivo and has been implicated in cell migration, signalling and tumour metastasis [35]. We have been at the forefront of understanding the serine switches involved in the signal transduction of TF and how it is released in TF-bearing MP into the circulation [33, 34, 36, 37] and then into the urine.

Adrenomedullin (AM)

We and others have established the role of a multifunctional secreted peptide adrenomedullin (AM), encoded by ADM gene, in carcinogenesis through its contribution to tumour angiogenesis and metastatic spread [38-40]. The expression of ADM mRNA and AM protein is upregulated in PDAC tissues in comparison to normal pancreatic tissues [39, 41, 42]. In other studies, the 5 candidate gene (including ADM) list demonstrated significant power to predict patient survival in two distinct patient cohorts and was independent of AJCC TNM staging [43]. AM mediates its activities through binding to G-protein-coupled receptor (GPCR) calcitonin receptor like-receptor (CLR, encoded by the CALCRL gene) [44]. Our recent work suggests that CLR is up-regulated in invasive front in pancreatic cancer tissues (Nikitenko LL, unpublished). These findings warrant the need for exploring the potential for AM as a marker for detection of PaC at early stages of malignant transformation, including the analysis of its levels in pancreatic cysts.

We recognise that this field is changing and there will be opportunity to study new promising protein markers on these rare and valuable samples; some of these targets may be generated by the platform based analyses.

Genomic Analysis

Next generation sequencing (NGS) is a state-of-the-art technology that has been successfully applied for the detection of different types of cancer using liquid biopsies [45]. NGS has been used on PaC cystic fluid, although the progress with early detection of this type of cancer has been limited by detection of alteration in known oncogenes and tumour suppressors [46-48]. NGS approaches include whole genome sequencing (WGS), a comprehensive method for analysing entire genomes. WGS has been successfully used for analysis of many cancer types, including PaC [49, 50]. However, to date WGS has not yet been applied for testing the feasibility of its use for cystic fluid to detect changes that would indicate early stages of development of PaC. This warrants the need for exploring WGS in our study for analysing entire genome using DNA obtained from pancreatic cystic fluid and comparing it to DNA derived from peripheral blood mononuclear cells (PBMCs) from the same patient, with a potential for identifying changes associated early stages of malignant transformation.

Proteomic Analysis

To our knowledge, the proteomic analysis of PaC samples has been extremely limited to date. In particular, research efforts have been focussed on identification of global protease activity, glycomic and proteomic profiling of a limited number of MCN and IPMN cystic fluid samples [51, 52]. Only one study was conducted to analyse proteome and phosphorylome in PaC on a limited number of tissue samples [53]. To our knowledge, the global scale proteomic analysis (including post-translational modifications, such as phosphorylation, oxidation, acetylation etc.) of pancreatic cystic fluid from suspected PaC patients has not yet been conducted. This warrants the need for exploring this (liquid chromatography-tandem mass spectrometry (LC-MS/MS) - based proteomic approach) platform technology for analysing entire proteome (unmodified and modified proteins) obtained from pancreatic cysts, with a potential for identifying changes associated early stages of malignant transformation.

In summary, a non-invasive diagnostic biomarker test (or tests) that can detect the presence of early stage PaC would be invaluable and could allow targeting of patients when the disease is in its earliest and most treatable stages, but could also spare morbid surgery for patients that do not need it, thereby reducing the number, cost and associated morbidity of subsequent work-up procedures and surgery.

The study is intended to test the accuracy of promising biomarkers, existing and those that may arise from platform technologies, in early PaC detection, gathering preliminary data to inform the design of a larger trial. Additionally, demonstration of the use of these assays in PaC will complement the already tested cancer types and may have relevance to other cancer types with indeterminate lesions.

Pancreatic Stellate Cells

The tumour stroma consists of extracellular matrix and also particularly, pancreatic stellate cells which exist as fibroblast-like cells [54]. The break-up of the tumour and release of cells into the bloodstream begins at the early stages of metastasis [55]. Consequently, the presence of the stellate cells in the bloodstream has been proposed as an early warning for metastatic processes, leading to poor prognosis. We propose that measuring the number of stellate cells in blood samples, could be an indicator of the disease spreading. Moreover, characterising the properties of the tumour-associated stellate cells by NGS, could produce an insight into the tumour environment and the state of the cancer cell functions.

PancRISK Score for Urinary Biomarkers

A panel of three genes (LYVE1, REG1A and TFF1) were identified as potential biomarkers for pancreatic cancer after being shown to be present in significantly higher concentrations in the urine of PDAC patients (n = 192) compared to healthy individuals (n = 87) [56]. The REG1A gene belongs to a family of REG (regenerating) glycoproteins which are expressed in pancreatic acinar cells and act as both autocrine and paracrine growth factors. REG1A was later substituted in the panel for REG1B which enhanced the performance of the panel to detect resectable PDAC [57]. TFF1 belongs to a family of gastrointestinal secretory peptides which interact with mucins and are expressed at increased levels during reconstitution and repair of mucosal injury. In PDAC, TFF1 has been reported in both sporadic [58, 59] and familial PanINs [60] and it has been associated with early stages (I and II) of the disease. LYVE1 (lymphatic vessel endothelial hyaluronan receptor) binds hyaluronan (HA), an extracellular matrix mucopolysaccharide, and transports it across the lymphatic vessel wall, particularly in the lymph nodes, a site of HA degradation.

The PancRISK score was developed to utilise the biomarker panel within a risk stratification model for the earlier detection of PDAC [61]. PancRISK is a logistic regression model based on the 3 biomarkers, urine creatinine and age, which enables stratification of patients into those with 'normal' or 'elevated' risk for developing PDAC. In a study of the 590 urine specimens, 183 were from control individuals (control group) who had no known pancreatic conditions or malignancies or history of renal diseases at the time of collection, 208 were from patients with benign hepatobiliary diseases (benign group), and 199 were from PDAC patients [57]. Higher concentration of all 3 biomarkers were found in PDAC urine specimens at all stages (102 I–II and 97 III–IV), when compared with both benign and control samples though this difference was not found to be statistically significant in the earlier stages of PDAC. The main limitation of this study was that almost half of the PDAC cases (97) included were late-stage patients (Stage III – IV) owing to the difficulty of finding pancreatic cancer patients with early stage disease (Stage I – II).

All 3 biomarkers have been reported as upregulated in PDAC precursor lesions (i.e., PanINs) and involved in cancer progression and metastasis. Therefore, testing the urine samples from patients with pancreatic cystic lesions in this study could i) further validate the use of the 3 biomarkers and the PancRISK score in

differentiating risk of developing PDAC and ii) show that this method is a feasible, non-invasive way of determining prognosis in patients with precursor lesions.

Aims and Objectives

The primary aim of the study is to assess the accuracy of some existing protein markers (e.g., TF, AM) in the detection of early stages of pancreatic cancer. Patients with a known cancer diagnosis, compared to controls, will be used to determine whether a suitable cut-off for each assay can be found for accurate detection.

Secondary aims:

1. To ascertain whether the determined cut-off for each assay is effective in the classification of precancerous cystic lesions.
2. To compare specificity, sensitivity and diagnostic accuracy of TF, AM and other protein markers as they arise to current conventional assays performed on cystic fluid (i.e. CEA, mucin, amylase).
3. To assess the amount of fluid required for platform diagnostics (WGS and proteomics) and how many of the cysts are deemed suitable for this approach.
4. To generate a list of promising markers by analysing the data from platform based technologies on cystic fluid from a suitable cohort of patients and consider which of these have potential as genetic and protein markers.
5. To compare circulating levels of TF, AM and other protein markers as they arise from the platform technologies detected in serum from patients with cystic lesions to those in other groups (i.e. benign, early pancreatic, malignant).
6. To compare the urinary profile of these markers in benign vs malignant pathology.
7. To capture serial data of how many cysts come through the unit and how many of these cysts can be studied (to provide feasibility data to allow planning of later definitive study).
8. To examine the cyclical feedback between cancer cells and associated pancreatic stellate cells (from blood samples and pancreatic cancer tissue).
9. To analyse the urine samples from patients with pancreatic cystic lesions for three biomarkers (LYVE1, REG1B, and TFF1).

Study Design

This will be a prospective feasibility study based on the laboratory analysis of collected urine, blood and cystic fluid samples. Samples will be taken from 50 patients with pancreatic cysts on follow-up, 50 from localised (resectable and non-resectable) pancreatic cancers, and 80 age- and sex-matched control patients to include patients with benign hepatopancreatobiliary conditions (cholangitis/cholelithiasis/acute pancreatitis [non-resolving pseudocysts]) as well as normal controls. Samples for the index cases will be taken prior to commencement of any anti-cancer therapy.

The control population will comprise 20 patients with acute pancreatitis that have non-resolving pseudocysts, 20 undergoing cholecystectomy for stones, 20 undergoing cholecystectomy for inflammation,

and 20 patients undergoing endoscopy for dyspepsia. The latter will be classified as “normal controls” and will not be derived from any of the other benign groups.

Patients with cystic lesions:

For patients who have highly suspicious cystic lesions, cystic fluid will be obtained through cystic drainage of the IPMN/MCN, and blood samples will be obtained prior to the procedure. The group will comprise patients with lesions where a smaller amount of fluid is taken for diagnostic purposes, and patients with lesions already identified as suspicious, which will be totally drained during surgery and sent for analysis to look at histology.

Study Endpoints

The ELISAs and platform technologies will provide measurements of the markers (e.g. TF,AM) concentrations in patient urine, serum/blood and cystic fluid samples. This will then be immediately linked to information on the pancreatic cancer diagnosis where it is known (i.e. cancer and control groups) and, for patients with pancreatic cysts, linked to information obtained following diagnostic work-up (and over the follow-up period), to determine the accuracy of these markers in the potential early detection of pancreatic cancer within the Hull University Teaching Hospitals NHS Trust (HUTH) pancreatic cancer population.

Subject Selection

Patients will be recruited into 3 groups. A group of pancreatic cancer patients will be selected from those diagnosed with localised pancreatic cancer, including both those undergoing successful resection, and those undergoing biopsy only (localised, but radiologically inoperable) or where resection was attempted. A control group will be formed from age- and sex-matched patients receiving hepatobiliary surgery or endoscopic intervention (ERCP, PTCA, instrumentation of the biliary tree, endoscopic cystogastrostomy for pancreatic pseudocyst) for benign inflammatory conditions. A third group of patients will be derived from those with suspected pancreatic cancer who are undergoing follow-up for pancreatic cystic lesions. HUTH provides an EUS service that at this point investigates about 40 such cystic lesions annually with paracentesis and has a significant number of cystic lesions under close follow-up.

Inclusion and Exclusion Criteria

Inclusion Criteria (General)

- Capable of giving written informed consent
- Age ≥ 18 years

Exclusion Criteria (General)

- Inability to provide written informed consent
- Other known malignant condition, either active or in complete remission ≤ 5 years
- HIV, hepatitis C, or any other known communicable disease

Inclusion Criteria (Pancreatic Cancer Cohort)

- Diagnosed with localised pancreatic cancer amenable to resection (distal pancreatectomy, total pancreatectomy or Whipple’s procedure).

OR

- Diagnosed with inoperable localised pancreatic cancer and referred for further management (malignant control subgroup).

Inclusion Criteria (Pancreatic Cysts Cohort)

- Presence of cystic lesions where MDT have agreed further diagnostic intervention procedures (including FNA/EUS) necessary.

OR

- Patient the MDT have agreed have resectable lesions suspicious for pancreatic malignancy and going to surgery.

Inclusion Criteria (Benign Cohort)

- Referral for endoscopic cystogastrostomy for complicated acute pancreatitis characterised by peripancreatic fluid collections and pseudocysts in development or matured (non-resolving and requiring further intervention).

OR

- Referral for cholecystectomy for cholecystitis/cholelithiasis.

OR

- Patient planned to have endoscopy investigation for dyspepsia (normal control subgroup).

Subject Recruitment

Potential participants will be identified through the pancreatic multidisciplinary team (MDT) meetings or outpatient clinic. Once eligibility has been confirmed, they will be approached by a member of the research team. For those patients with cystic lesions, specialist time will include discussion of the study in their consultation relating to either further treatment plans (for patients who go to surgery) or further diagnostic plans (for patients who need further diagnostic investigation of cysts). All potential participants will be provided with a copy of the patient information leaflet outlining the purpose and exact nature of the study. This will give them ample time to consider and discuss their participation with family/friends/their GP, etc., and to contact the research team if necessary with any questions that may arise, to ensure they are fully informed on the conduct of the study.

The majority of patients with resectable pancreatic cancer will be inpatients and therefore will be approached by a member of the research team on the hospital ward. They will be given at least 24 hours to consider participation before consent is taken by the designated research nurse in accordance with Good Clinical Practice (GCP). Samples will be taken at the same time as phlebotomy for regular investigations.

Patients with non-resectable pancreatic cancer will be approached at their scheduled outpatient clinic appointment. For interested participants, consent will be taken at their pre-assessment appointment at the nurse-led chemotherapy clinic 1-2 weeks after the initial consultation. Blood and urine samples will be taken at the same time as their first bloods before commencing chemotherapy. Pancreatic tumour tissue will be taken as surplus to the patients' resected or biopsied tumour sample during the patients scheduled surgical procedure, study samples will be taken 'on table'.

Patients with complicated acute pancreatitis have a repeat CT scan at 6-8 weeks to determine whether the pseudocyst has resolved. Control patients with non-resolving pseudocysts will be approached with information about the study at their first clinic appointment after the repeat CT scan. Consent and study samples will be taken when they attend the EUS suite for endoscopic cystogastrostomy.

Control patients due to have cholecystectomy will be initially contacted by telephone with information about the study at least 1 week before they attend for their pre-assessment appointment. Consent will be taken by the designated research nurse at the pre-assessment appointment, and blood samples will be taken at the same time as pre-assessment bloods. Patients will be provided with a urine sample bottle at this appointment and asked to bring a urine sample when they attend for cholecystectomy.

Control patients with dyspepsia will initially be approached by a member of the research team during an appointment at the EUS suite for endoscopy. Consent will be taken by the designated research nurse at the follow up consultation in the gastric clinic 1-2 weeks after their endoscopy. Blood samples will be taken at the same time as scheduled follow-up bloods and patients will be asked to provide a urine sample at this appointment.

Patients with pancreatic cysts will initially be approached by a member of the research team during the consultation in which they are informed they need to have the cyst aspirated. Consent and study samples will then be taken either when they attend the EUS suite for the endoscopy procedure, which is generally 2-4 weeks later, or for cases who go directly to surgery, consent will be taken on the day of their scheduled appointment, and study samples will be taken 'on table'.

Pancreatic cyst patients that have already been recruited to the study will be re-consented by the study research nurse by telephone or by post, provided with the most up-to-date version of the patient information leaflet, and, if they provide consent to do so, an additional 'buffy coat' blood sample and a whole-blood sample will be taken at a scheduled clinic appointment. Due to the COVID-19 pandemic it is irresponsible to ask patients to attend the hospital to provide these blood samples if they do not have a scheduled appointment, thus samples will not be taken from these patients in this instance.

Retrospective samples from pancreatic cyst patients who provided their consent to participate in the TEM-PAC study and either 1) died before the TEM-PAC substantial amendment 002 (dated 15.01.21) was approved, or 2) died before they were able to be re-consented for WGS analysis, will be analysed via WGS without the participant's specific consent.

Patients from all patient cohorts that have already been recruited to the study will be re-consented by the study research nurse by telephone or by post, provided with the most up-to-date version of the patient information leaflet, and, if they provide consent, will have their already collected sample sent to Queen Mary University of London (QMUL) for laboratory analysis.

Retrospective urine samples from all patient cohorts from patients who provided their consent to participate in the TEM-PAC study and died before the TEM-PAC substantial amendment 005 (dated 12.10.22) was approved will be analysed by the laboratory at QMUL without the participant's specific consent.

All patients approached have the right to refuse participation without giving reasons, and without detriment to their subsequent treatment. Those patients still interested in participating in the study will then be provided with an informed consent form to sign to indicate their willingness to participate and to permit their enrolment in the study. Informed consent must be obtained from every patient prior to participation in the study.

Subject Follow-Up

Patients with pancreatic cysts but no confirmed cancer will be followed up for a period of 3 years to check for any subsequent diagnoses that may have been missed or occurred since the original diagnostic workup. This is based on current MRI recommendations where repeat imaging is performed at 2-3 years. Any results will be obtained through reference to patients' medical records only.

Withdrawal of Subjects

Patients have the right to withdraw from the study at any time without giving reason, and without this decision jeopardising their future care. Their reasons for withdrawal should be detailed on the relevant CRF where possible.

Safety Reporting

Patient participation will consist of the provision of a urine and serum sample for pancreatic cancer and benign patients, and also of a cystic fluid sample and whole blood sample for those with pancreatic lesions. The urine sample can be obtained non-invasively, while the blood samples will be obtained at the same time as routinely collected blood samples. The cystic fluid sample will be taken as excess from the surplus fluid remaining following a routine procedure, and therefore will not require any additional intervention.

Therefore we anticipate no safety-related issues during the conduct of the study and no adverse event data will be collected.

Samples

Urine samples: for each sample, about 40 ml will be collected in a clearly labelled container tube with no preservatives. Urine samples will be aliquoted equally into two fresh sterile bottles. All urine samples will be stored at -80°C prior to shipping. Samples (20 ml) will be transported on dry ice to a laboratory at the University of Hull and stored in a locked -80°C freezer prior to batch analysis. Samples (20 ml) will be transported on dry ice to a laboratory at the Centre for Cancer Biomarkers and Biotherapeutics, Barts Cancer Institute, Queen Mary University of London, London, UK.

Serum samples: 10 ml (2x yellow-top tubes) blood will be collected per patient. Samples will be centrifuged to separate out the serum fraction, prior to storage in a -80°C freezer. They will then be transported in batches to the University of Hull laboratory, where they will be stored in a locked -80°C freezer prior to batch analysis.

Buffy coat blood samples: 10 ml (2x purple-top EDTA tubes) blood will be collected per pancreatic cyst patient. Samples will be stored in a -80°C freezer. They will then be transported in batches to the University of Hull laboratory where they will be stored in a locked -80°C freezer prior to batch analysis. These samples will be collected only from pancreatic cyst patients that consent to genetic testing.

Whole-blood samples: 10 ml (2x purple-top EDTA tubes) blood will be collected per patient. Samples will be stored in a -80°C freezer. They will then be transported in batches to the University of Hull laboratory where they will be stored in a locked -80°C freezer prior to batch analysis. These samples will be collected only from pancreatic cyst patients that consent to genetic testing.

Pancreatic tumour tissue samples: If it is deemed that there is a sufficient surplus of tumour tissue available for research purposes by the pathologist, then a tissue sample will be collected from the Pathology Department after the pancreatic cancer patients' surgical procedure. The tissue will be snap-frozen and

stored in a -80°C freezer. They will then be transported in batches to the University of Hull laboratory where they will be stored in a locked -80°C freezer prior to analysis.

Cystic fluid samples: The top third of drained cystic fluid will be collected. The majority of cysts will have a volume of 30 cm³ or more, but there may also be smaller cysts with solid elements of concern. Cysts are expected to generate between 3 to 10 ml fluid for research purposes, which will be collected in a sterile tube. The cystic fluid samples will be stored at -80°C. They will then similarly be transported in batches to the University of Hull laboratory and stored in a locked -80°C freezer prior to batch analysis.

For genomic analysis, DNA will be extracted and subsequently tested by Novogene Company Limited, 25 Cambridge Science Park, Milton Road, Cambridge, UK.

For proteomic analysis, samples will be prepared at the University of Hull and then analysed by Target Discovery Institute, Nuffield Department of Medicine, Roosevelt Drive, University of Oxford, Oxford OX3 FZ, UK.

The University of Hull will be responsible for sending samples to Novogene and the Target Discovery Institute. On receipt, all samples will be stored at -80°C until required for analysis. All samples will be analysed anonymously.

Data Collection

All samples will be coded with a unique identifier prior to transport to the respective laboratories. Samples will be numbered consecutively, starting CHH 001, CHH 002, CHH 003, etc. Laboratory researchers will therefore be blinded to the nature of all samples received. All data reported will therefore be anonymous, identified by study number only.

Source Data

As a minimum, the following information will be recorded in patients' case notes for study visits or telephone contacts:

- Clearly written date of visit or contact, brief study title/acronym and visit number
- Date patient given patient information leaflet
- Date consent form signed
- Date of screening
- Medical history, concomitant diseases and medication

Case Report Forms

The following data will be collected on a Case Report Form (CRF) for each patient:

- Study identification number

For patients with cystic lesions only:

- Type of cyst
- Volume of fluid removed
- Final histological diagnosis and stage

Protocol Deviations/Serious Breaches

All deviations from the protocol or GCP will be recorded by investigators on the Protocol Deviation Form for the study available from HUTH R&D. A serious breach is likely to affect to a significant degree either the safety or physical or mental integrity of a study subject or the scientific value of the study. Major deviations or serious breaches will be reported by investigators to HUTH R&D by telephone (tel. 01482 461883) or in person within 24 hours of the deviation or breach being identified. HUTH R&D will notify the REC within 7 days of becoming aware of a serious breach. Investigators will take into account all protocol deviations and any serious breaches in the final study analysis and publication.

End of trial

The end of the study is the date of the last follow-up assessment of the last patient enrolled on the study.

An end of study declaration form (using the NRES form) will be submitted to the REC and HUTH R&D within 90 days from completion of the study and within 15 days if the study is discontinued prematurely. A summary of the study report/publication will be submitted to the REC and HUTH R&D within 1 year of the end of the study.

Sample size calculation

This is a feasibility study and therefore no formal power calculation has been performed.

Statistical analysis

Baseline clinical and demographic characteristics of the 50 pancreatic cancer patients and 80 benign control patients will be described and summarised. For potential markers of early pancreatic cancer (e.g., TF and AM) from urine and serum samples, the sensitivity, specificity, negative predictive value (NPV) and positive predictive value (PPV) of biomarkers will be calculated with different cut-off levels. The receiver operating characteristics (ROC) curves will be plotted with calculated areas under the curve (AUC). The optimal cut-off levels will be determined as the one maximising the value of the sum of sensitivity and specificity.

For the 50 pancreatic cyst patients, baseline clinical and demographic characteristics will also be described and summarised. ELISAs will measure the concentration of markers in patients' cystic fluid. With the usual pathological diagnosis (radiological features plus conventional markers) as the benchmark, at the end of three years follow-up, we will analyse the sensitivity, specificity, NPV and PPV of these markers with different cut-off levels. The ROC curves will be plotted with calculated AUC. The optimal cut-off levels will be determined as the one maximising the value of the sum of sensitivity and specificity. The markers in urine and serum samples will also be collected and analysed for comparisons.

For genomic data, the first steps of bioinformatics analysis will be conducted by the service provider (Novogene, Cambridge) and the rest will be done at the University of Hull using the High Performance Computer VIPER. Professor David Chang at the University of Glasgow, Glasgow will advise on the analysis of the data.

For proteomic analysis data, the first steps of bioinformatics analysis will be conducted by collaborators (Target Discovery Institute, Oxford) and the rest will be done at the University of Hull using the High Performance Computer VIPER.

Feasibility features of this study, such as the consent rate, retention rate, analysable rate (how many cysts come through the unit and how many of these cysts can be studied), will also be calculated for future definitive trial consideration.

Monitoring

The study may be monitored in accordance with HUTH R&D department's standard operating procedures to ensure compliance with the International Conference for Harmonisation of Good Clinical Practice (ICH GCP) and the Research Governance Framework 2005. All study-related documents will be made available upon request for monitoring by R&D monitors.

Ethical considerations

The patient samples required in this study are either surplus from routine samples already indicated (i.e. cystic fluid, tumour tissue), will be obtained at the same time as other routine tests (i.e. blood) or can be obtained easily and non-invasively (i.e. urine). Therefore the risks to patients will be minimal, and patient inconvenience can be avoided.

To ensure anonymity, all patients enrolled in the study will be allocated a unique patient identifier which will serve as the coding number for data collection, the CRF form and all samples, and also for the reporting of any results. A code sheet linking the patient to their code number will be held in a locked filing cabinet in the Queen's Centre for Oncology and Haematology Trials Office at Castle Hill Hospital, Hull. Only authorised members of the study team will have access to this information, and the researchers performing the laboratory analysis will be blinded to it.

Study Approvals

The study will be performed subject to Research Ethics Committee (REC) favourable opinion, Health Research Authority (HRA) approval, and confirmation of local HUTH R&D capacity and capability. In the event that a protocol amendment needs to be made that requires REC and HRA approval, the changes in the protocol will not be implemented until the amendment and revised study documentation have been reviewed and receive a favourable opinion/approval.

Research Governance

The study will be conducted in accordance with the ICH GCP guidelines and the Research Governance Framework for Health and Social Care.

Data handling and record keeping

All data will be stored on password-protected NHS computers, with user-restricted access and in adherence to the Trust Information Governance Policy.

Transfer of any data between the University of Hull or a commercial institution or the University of Glasgow and members of the research team at Castle Hill Hospital will be in an encrypted format over a secure network.

IT Services Department has a backup procedure approved by auditors for disaster recovery. Servers are backed up to disk media each night. The disks run on a 4 week cycle. Files stay on the server unless deleted by accident or deliberately. Anything deleted more than 4 weeks previously is therefore lost. Additional 'archive' backups are taken for archived data, so data should not be lost from this type of system e.g. FileVision which stores Medical Records. Disks are stored in a fireproof safe.

Study documents (paper and electronic) will be retained in a secure location during and after the trial has finished. All essential documents including source documents will be retained for a period of 5 years after

study completion. A sticker stating the date after which the documents can be destroyed will be placed on the inside front cover of the case notes of the study participants.

Data will be collected and retained in accordance with the Data Protection Act 2018 and the General Data Protection Regulation (GDPR).

Access to Source Data

Patient information is confidential and will only be disclosed to third parties as permitted by the informed consent form. Direct access to the source data and study documents will be made available by the Chief Investigator to authorised representatives from the Sponsor, host institution and regulatory inspection authorities if requested to permit monitoring, audits and/or review by the REC as appropriate.

Annual progress report

An annual progress report will be submitted to the main REC 12 months following HUTH Trust approval and thereafter until the end of the study.

Indemnity

This is an NHS-sponsored research study. If there is negligent harm during the study when the NHS body owes a duty of care to the person harmed, NHS indemnity covers NHS staff and medical academic staff with honorary contracts only when the trial has been approved by HUTH R&D department. NHS indemnity does not offer no-fault compensation and is unable to agree in advance to pay compensation for non-negligent harm.

Ownership

Patient-related data will remain within HUTH, where the analysis with patient diagnosis will be undertaken.

Reporting and Dissemination

The results of the study will be analysed as soon as possible after the completion of the study, and will be submitted for publication in a peer-reviewed journal, and presented at national and international conferences where possible.

References

1. CRUK. Pancreatic cancer statistics 2017 [Available from: <https://www.cancerresearchuk.org/health-professional/cancer-statistics/statistics-by-cancer-type/pancreatic-cancer?script=true>].
2. Ducreux M, Cuhna AS, Caramella C, Hollebecque A, Burtin P, Goere D, et al. Cancer of the pancreas: Esmo clinical practice guidelines for diagnosis, treatment and follow-up. *Annals of oncology : official journal of the European Society for Medical Oncology*. 2015;26 Suppl 5:v56-68.
3. NCRAS. National cancer registration and analysis service - stage breakdown by ccg 2014. London: CRAS: London; 2016.
4. CRUK. Pancreatic cancer incidence 2017 [Available from: <https://www.cancerresearchuk.org/health-professional/cancer-statistics/statistics-by-cancer-type/pancreatic-cancer#heading-Zero>].

5. Chari ST. Detecting early pancreatic cancer: Problems and prospects. *Seminars in oncology*. 2007;34(4):284-94.
6. Khorana AA, Fine RL. Pancreatic cancer and thromboembolic disease. *The Lancet Oncology*. 2004;5(11):655-63.
7. Cunningham D, Chau I, Stocken DD, Valle JW, Smith D, Steward W, et al. Phase iii randomized comparison of gemcitabine versus gemcitabine plus capecitabine in patients with advanced pancreatic cancer. *Journal of clinical oncology : official journal of the American Society of Clinical Oncology*. 2009;27(33):5513-8.
8. Conroy T, Desseigne F, Ychou M, Bouche O, Guimbaud R, Becouarn Y, et al. Folfirinox versus gemcitabine for metastatic pancreatic cancer. *N Engl J Med*. 2011;364(19):1817-25.
9. Von Hoff DD, Ervin T, Arena FP, Chiorean EG, Infante J, Moore M, et al. Increased survival in pancreatic cancer with nab-paclitaxel plus gemcitabine. *N Engl J Med*. 2013;369(18):1691-703.
10. Bhutani MS, Thosani N, Suzuki R, Guha S. Pancreatic cancer screening: What we do and do not know. *Clinical gastroenterology and hepatology : the official clinical practice journal of the American Gastroenterological Association*. 2013;11(6):731-3.
11. Greer JB, Brand RE. Screening for pancreatic cancer: Current evidence and future directions. *Gastroenterology & hepatology*. 2007;3(12):929-38.
12. Canto MI, Harinck F, Hruban RH, Offerhaus GJ, Poley JW, Kamel I, et al. International cancer of the pancreas screening (caps) consortium summit on the management of patients with increased risk for familial pancreatic cancer. *Gut*. 2013;62(3):339-47.
13. Laffan TA, Horton KM, Klein AP, Berlanstein B, Siegelman SS, Kawamoto S, et al. Prevalence of unsuspected pancreatic cysts on mdct. *AJR American journal of roentgenology*. 2008;191(3):802-7.
14. Robinson SM, Scott J, Oppong KW, White SA. What to do for the incidental pancreatic cystic lesion? *Surgical oncology*. 2014;23(3):117-25.
15. Nougaret S, Mannelli L, Pierredon MA, Schembri V, Guiu B. Cystic pancreatic lesions: From increased diagnosis rate to new dilemmas. *Diagnostic and interventional imaging*. 2016;97(12):1275-85.
16. Sharib J, Kirkwood K. Early and accurate diagnosis of pancreatic cancer? *Oncotarget*. 2016;7(52):85676-7.
17. Nougaret S, Reinhold C, Chong J, Escal L, Mercier G, Fabre JM, et al. Incidental pancreatic cysts: Natural history and diagnostic accuracy of a limited serial pancreatic cyst mri protocol. *European radiology*. 2014;24(5):1020-9.
18. Sahani DV, Kambadakone A, Macari M, Takahashi N, Chari S, Fernandez-del Castillo C. Diagnosis and management of cystic pancreatic lesions. *AJR American journal of roentgenology*. 2013;200(2):343-54.
19. Spinelli KS, Fromwiller TE, Daniel RA, Kiely JM, Nakeeb A, Komorowski RA, et al. Cystic pancreatic neoplasms: Observe or operate. *Annals of surgery*. 2004;239(5):651-7; discussion 7-9.
20. Wong JC, Lu DS. Staging of pancreatic adenocarcinoma by imaging studies. *Clinical gastroenterology and hepatology : the official clinical practice journal of the American Gastroenterological Association*. 2008;6(12):1301-8.

21. Early DS, Acosta RD, Chandrasekhara V, Chathadi KV, Decker GA, Evans JA, et al. Adverse events associated with eus and eus with fna. *Gastrointestinal endoscopy*. 2013;77(6):839-43.
22. Tarantino I, Fabbri C, Di Mitri R, Pagano N, Barresi L, Mocciaro F, et al. Complications of endoscopic ultrasound fine needle aspiration on pancreatic cystic lesions: Final results from a large prospective multicenter study. *Digestive and liver disease : official journal of the Italian Society of Gastroenterology and the Italian Association for the Study of the Liver*. 2014;46(1):41-4.
23. Kakkar AK, Lemoine NR, Scully MF, Tebbutt S, Williamson RC. Tissue factor expression correlates with histological grade in human pancreatic cancer. *The British journal of surgery*. 1995;82(8):1101-4.
24. Nitori N, Ino Y, Nakanishi Y, Yamada T, Honda K, Yanagihara K, et al. Prognostic significance of tissue factor in pancreatic ductal adenocarcinoma. *Clinical cancer research : an official journal of the American Association for Cancer Research*. 2005;11(7):2531-9.
25. Khorana AA, Ahrendt SA, Ryan CK, Francis CW, Hruban RH, Hu YC, et al. Tissue factor expression, angiogenesis, and thrombosis in pancreatic cancer. *Clinical cancer research : an official journal of the American Association for Cancer Research*. 2007;13(10):2870-5.
26. Echrish HH, Xiao Y, Madden LA, Allgar V, Cooke J, Wedgwood K, et al. Effect of resection of localized pancreaticobiliary adenocarcinoma on angiogenic markers and tissue factor related pro-thrombotic and pro-angiogenic activity. *Thromb Res*. 2014;134(2):479-87.
27. Tesselaar ME, Romijn FP, Van Der Linden IK, Prins FA, Bertina RM, Osanto S. Microparticle-associated tissue factor activity: A link between cancer and thrombosis? *Journal of thrombosis and haemostasis : JTH*. 2007;5(3):520-7.
28. Thaler J, Ay C, Mackman N, Bertina RM, Kaider A, Marosi C, et al. Microparticle-associated tissue factor activity, venous thromboembolism and mortality in pancreatic, gastric, colorectal and brain cancer patients. *Journal of thrombosis and haemostasis : JTH*. 2012;10(7):1363-70.
29. Zwicker JJ, Liebman HA, Neuberger D, Lacroix R, Bauer KA, Furie BC, et al. Tumor-derived tissue factor-bearing microparticles are associated with venous thromboembolic events in malignancy. *Clinical cancer research : an official journal of the American Association for Cancer Research*. 2009;15(22):6830-40.
30. Adamson AS, Francis JL, Roath OS, Witherow RO, Snell ME. Urinary tissue factor levels in transitional cell carcinoma of the bladder. *The Journal of urology*. 1992;148(2 Pt 1):449-52.
31. Lwaleed BA, Chisholm M, Francis JL. Urinary tissue factor levels in patients with breast and colorectal cancer. *The Journal of pathology*. 1999;187(3):291-4.
32. Lwaleed BA, Francis JL, Chisholm M. Urinary tissue factor levels in patients with bladder and prostate cancer. *European journal of surgical oncology : the journal of the European Society of Surgical Oncology and the British Association of Surgical Oncology*. 2000;26(1):44-9.
33. Collier ME, Ettelaie C. Regulation of the incorporation of tissue factor into microparticles by serine phosphorylation of the cytoplasmic domain of tissue factor. *The Journal of biological chemistry*. 2011;286(14):11977-84.
34. Ettelaie C, Elkeeb AM, Maraveyas A, Collier ME. P38alpha phosphorylates serine 258 within the cytoplasmic domain of tissue factor and prevents its incorporation into cell-derived microparticles. *Biochimica et biophysica acta*. 2013;1833(3):613-21.

35. Egorina EM, Sovershaev MA, Osterud B. Regulation of tissue factor procoagulant activity by post-translational modifications. *Thrombosis research*. 2008;122(6):831-7.
36. ElKeab AM, Collier ME, Maraveyas A, Ettelaie C. Accumulation of tissue factor in endothelial cells induces cell apoptosis, mediated through p38 and p53 activation. *Thrombosis and haemostasis*. 2015;114(2):364-78.
37. Ettelaie C, Collier ME, Featherby S, Greenman J, Maraveyas A. Oligoubiquitination of tissue factor on lys255 promotes ser253-dephosphorylation and terminates tf release. *Biochimica et biophysica acta*. 2016;1863(11):2846-57.
38. Nikitenko LL, Fox SB, Kehoe S, Rees MC, Bicknell R. Adrenomedullin and tumour angiogenesis. *British journal of cancer*. 2006;94(1):1-7.
39. Nikitenko LL, Leek R, Henderson S, Pillay N, Turley H, Generali D, et al. The g-protein-coupled receptor clr is upregulated in an autocrine loop with adrenomedullin in clear cell renal cell carcinoma and associated with poor prognosis. *Clinical cancer research : an official journal of the American Association for Cancer Research*. 2013;19(20):5740-8.
40. Larráyoiz IM, Martínez-Herrero S, García-Sanmartín J, Ochoa-Callejero L, Martínez A. Adrenomedullin and tumour microenvironment. *Journal of translational medicine*. 2014;12:339.
41. Aggarwal G, Ramachandran V, Javeed N, Arumugam T, Dutta S, Klee GG, et al. Adrenomedullin is up-regulated in patients with pancreatic cancer and causes insulin resistance in β cells and mice. *Gastroenterology*. 2012;143(6):1510-7.e1.
42. Keleg S, Kayed H, Jiang X, Penzel R, Giese T, Büchler MW, et al. Adrenomedullin is induced by hypoxia and enhances pancreatic cancer cell invasion. *International journal of cancer*. 2007;121(1):21-32.
43. Raman P, Maddipati R, Lim KH, Tozeren A. Pancreatic cancer survival analysis defines a signature that predicts outcome. *PLoS One*. 2018;13(8):e0201751.
44. McLatchie LM, Fraser NJ, Main MJ, Wise A, Brown J, Thompson N, et al. Ramps regulate the transport and ligand specificity of the calcitonin-receptor-like receptor. *Nature*. 1998;393(6683):333-9.
45. De Rubis G, Rajeev Krishnan S, Bebawy M. Liquid biopsies in cancer diagnosis, monitoring, and prognosis. *Trends in pharmacological sciences*. 2019;40(3):172-86.
46. Ravikanth VV. Next-generation sequencing (ngs) in the prediction of pancreatic malignancy: Does cell free mean error free? *Digestive diseases and sciences*. 2020;65(8):2153-5.
47. Laquière AE, Lagarde A, Napoléon B, Bourdariat R, Atkinson A, Donatelli G, et al. Genomic profile concordance between pancreatic cyst fluid and neoplastic tissue. *World J Gastroenterol*. 2019;25(36):5530-42.
48. Springer S, Masica DL, Dal Molin M, Douville C, Thoburn CJ, Afsari B, et al. A multimodality test to guide the management of patients with a pancreatic cyst. *Science translational medicine*. 2019;11(501).
49. Grant RC, Denroche R, Jang GH, Nowak KM, Zhang A, Borgida A, et al. Clinical and genomic characterisation of mismatch repair deficient pancreatic adenocarcinoma. *Gut*. 2020.

50. Aung KL, Fischer SE, Denroche RE, Jang GH, Dodd A, Creighton S, et al. Genomics-driven precision medicine for advanced pancreatic cancer: Early results from the compass trial. *Clinical cancer research : an official journal of the American Association for Cancer Research*. 2018;24(6):1344-54.
51. Ivry SL, Sharib JM, Dominguez DA, Roy N, Hatcher SE, Yip-Schneider MT, et al. Global protease activity profiling provides differential diagnosis of pancreatic cysts. *Clinical cancer research : an official journal of the American Association for Cancer Research*. 2017;23(16):4865-74.
52. Mann BF, Goetz JA, House MG, Schmidt CM, Novotny MV. Glycomic and proteomic profiling of pancreatic cyst fluids identifies hyperfucosylated lactosamines on the n-linked glycans of overexpressed glycoproteins. *Molecular & cellular proteomics : MCP*. 2012;11(7):M111.015792.
53. Britton D, Zen Y, Quaglia A, Selzer S, Mitra V, Löbner C, et al. Quantification of pancreatic cancer proteome and phosphorylome: Indicates molecular events likely contributing to cancer and activity of drug targets. *PLoS One*. 2014;9(3):e90948.
54. Pothula SP, Pirola RC, Wilson JS, Apte MV. Pancreatic stellate cells: Aiding and abetting pancreatic cancer progression. *Pancreatology : official journal of the International Association of Pancreatology (IAP) [et al]*. 2020;20(3):409-18.
55. Li C, Cui L, Yang L, Wang B, Zhuo Y, Zhang L, et al. Pancreatic stellate cells promote tumor progression by promoting an immunosuppressive microenvironment in murine models of pancreatic cancer. *Pancreas*. 2020;49(1):120-7.
56. Radon TP, Massat NJ, Jones R, Alrawashdeh W, Dumartin L, Ennis D, et al. Identification of a three-biomarker panel in urine for early detection of pancreatic adenocarcinoma. *Clinical cancer research : an official journal of the American Association for Cancer Research*. 2015;21(15):3512-21.
57. Debernardi S, O'Brien H, Algahmdi AS, Malats N, Stewart GD, Plješa-Ercegovac M, et al. A combination of urinary biomarker panel and pancrisk score for earlier detection of pancreatic cancer: A case-control study. *PLoS medicine*. 2020;17(12):e1003489.
58. Arumugam T, Brandt W, Ramachandran V, Moore TT, Wang H, May FE, et al. Trefoil factor 1 stimulates both pancreatic cancer and stellate cells and increases metastasis. *Pancreas*. 2011;40(6):815-22.
59. Prasad NB, Biankin AV, Fukushima N, Maitra A, Dhara S, Elkahloun AG, et al. Gene expression profiles in pancreatic intraepithelial neoplasia reflect the effects of hedgehog signaling on pancreatic ductal epithelial cells. *Cancer Res*. 2005;65(5):1619-26.
60. Crnogorac-Jurcevic T, Chelala C, Barry S, Harada T, Bhakta V, Lattimore S, et al. Molecular analysis of precursor lesions in familial pancreatic cancer. *PLoS One*. 2013;8(1):e54830.
61. Blyuss O, Zaikin A, Cherepanova V, Munblit D, Kiseleva EM, Prytomanova OM, et al. Development of pancrisk, a urine biomarker-based risk score for stratified screening of pancreatic cancer patients. *British journal of cancer*. 2020;122(5):692-6.

Appendix 2

List of amendment numbers and dates

- SA 001 (substantial amendment) 17/01/19
- NSA 001 (non-substantial amendment) 19/02/19
- NSA (unnumbered - HRA/REC submission not required) 02/04/19
- SA 002 15/01/21
- SA 003 19/03/21
- NSA 002 08/09/21
- SA 004 08/10/21
- SA 005 12/10/22